Characterising the molecular response of *Agaricus bisporus* to mushroom virus X infection

A thesis submitted to Maynooth University for the degree of Doctor of Philosophy

Eoin O'Connor, B.Sc.

October 2019

Supervisor

Dr. David Fitzpatrick

Department of Biology

Maynooth University

Co. Kildare

Ireland

Supervisor

Dr. Helen Grogan

Horticulture Development Department

Teagasc Food Research Centre

Ashtown, Dublin 8

Ireland

Head of Department

Prof. Paul Moynagh

Department of Biology

Maynooth University

Co. Kildare

Ireland

Table of Contents

Index of Figures

Chapter 1

Chapter 2

Chapter 3

Chapter 4

Chapter 5

Chapter 6

Index of Tables

Chapter 2

Chapter 3

Chapter 4

Chapter 5

Abbreviations

ΔE	Colour distance differential
µg	Microgram
µg	Microlitre
AA	Amino acid
AbV(N)	*Agaricus bisporus virus* (number)
AD	Anno domini
ANOVA	Analysis of variance
ARP	Agaricus Resource Program
BC	Before Christ
BGI	Beijing Genome Institute
BLAST	Basic Local Alignment Search Tool
BlastKOALA	BLAST-KEGG Orthology And Links Annotation
BLASTp	Protein Basic Local Alignment Search Tool
BSA	Bovine serum albumin
BSR	BLAST score ratio
BUSCO	Benchmarking Universal Single Copy Orthologs
BWA	Burrows-Wheeler Aligner
c.a.	Circa
CAZy	Carbohydrate-active enzyme
CEM	Compost extract media
CGN	Conserved gene neighbourhood
CRISPR	Clustered Regularly Interspaced Short Palindromic Repeats
CTCL	Compost proteome control
CTMC	Compost proteome MC-inoculated
CTMS	Compost proteome MS-inoculated
CWH	Commercial-wild hybrid
CYM	Complete yeast media
DAPI	4’,6-diamidino-2-phenylindole
DDR	DNA damage-responsive

DEG	Statistically significant differentially expressed genes
dsDNA	Double-stranded DNA
DTT	Dithiothreitol
EDTA	Ethylene diamine tetraacetic acid
EM	Electron microscopy
ER	Endoplasmic reticulum
ERAD	ER-associated degradation
ERV	Endogenous retroviruses
EST	Expressed sequence tag
FAOSTAT	Food and Agriculture Organization Statistics Division
FISH	Fluorescence in situ hybridisation
FITC	Fluorescein isothiocyanate
GH	Glycosyl hydrolase
GMC	Glucose-methanol-choline
GO	Gene ontology
GPD II	Glyceraldehyde-3- phosphate dehydrogenase
HCl	Hydrochloric acid
HMM	Hidden Markov Models
Hsp	Heat-shock protein
IAA	Indole-3-acetic acid
ICTV	International Committee for Taxonomy of Viruses
K_2HPO_4	Dipotassium phosphate
KEGG	Kyoto Encyclopaedia of Genes and Genomes
KH_2PO_4	Potassium dihydrogen phosphate
LC-MS/MS	Liquid chromatography mass spectrometry
LDA	Lignin degrading auxiliary
LFQ	Label-free quantification
LINE	Long interspersed nuclear elements
LSP	Leaderless-signal peptides
MAT	Mating-type

MBV	Mushroom Bacilliform Virus
MC	MVX-inoculation at the beginning of case run
$MgSO_4$	Magnesium sulphate
MS	MVX-inoculation at the beginning of spawn run
MTP	Mushroom and truffle production
MVX	Mushroom virus X
NCBI	National Centre of Biotechnology Information
NDGS	NADPH-dependant glutamate synthase
NGS	Next generation sequencing
NN	Neural networks
ORF	Open reading frame
OWC	Off-white commercial hybrid
PBS	Phosphate-buffered saline
Pfam	Protein family
PNA	Peptide nucleic acid
PPO	Polyphenol oxidase
RBD	RNA-binding domain
RdRp	RNA-dependant RNA polymerase
RH	Relative humidity
RIN	RNA integrity number
RNAi	RNA silencing/interference
RNase	Ribonuclease
RNA-seq	RNA sequencing
RNP	Ribonucleoprotein domain
ROS	Reactive oxygen species
rRNA	Ribosomal ribonucleic acid
SCC	Smooth-cap commercial hybrid
SDS	Sodium dodecyl sulphate
SINE	Short interspersed nuclear elements
siRNA	Small interfering RNA

SNP	Single nucleotide polymorphism
SOCs	Syntenic ortholog clusters
SP	Signal peptide
sRNA	Small noncoding RNA
ss(+)RNA	Positive-sense single-stranded RNA
SSDA	Statistically significant differentially abundant
SSH	Suppression subtractive hybridisation
TCA	Trichloroacetic acid
TE	Transposable elements
TF	Transcription factor
TFA	Trifluoroacetic acid
TM	Transmembrane membrane
TR	Tandem Repeats
Tr.	Translate
tRNA	Transfer ribonucleic acid
TSA	Transcriptome shotgun assembly
Vic	Vegetative incompatibility complex

Acknowledgements

Firstly, I want to thank my supervisors Dr. David Fitzpatrick and Dr. Helen Grogan. Dave, thank you for the time you have invested in me over the last five years. Your patience, guidance and friendship through my undergrad and postgrad have made the whole process both engaging and enjoyable. Helen, thank you for all your support over the last four years. Your passion for research will be a source of inspiration I'll carry with me for the rest of my career. Thank you both for the opportunities you've afforded me.

I'd like to extend my gratitude to my supervisory team, Dr. Paul Dowling and Prof. Sean Doyle, for the guidance and enthusiasm they've shown towards my PhD. In particular, I'd like to thank Prof. Sean Doyle for fostering me while I drained his lab of all its natural resources during my wet-lab work and all the advice and knowledge he shared with me in that time.

My sincerest thanks to Prof Dan Eastwood for hosting me for a summer in Swansea University and for keeping in touch with me afterwards too.

Thank you so much to the administrative and technical staff in the Biology department. Particularly, Trish, Emer, Michelle, Caroline and Francis, for all the help, chats, fun and general professionalism you all bring to the department.

I want to express my gratitude to the Teagasc Walsh Scholarship scheme (10564231) for funding my research.

Thanks to the no. 1 kwens Charley and Jamie. Many's the time they coaxed me out of bursting my head against the table during my dry-lab work. I enjoyed every breakdown with you both. Thanks also to the past participants of the lab, Rob, Sarah and Steve.

I had the opportunity to work from four different labs over the last few years and would like to give a big thanks to Keith Dunne, Brian McGuiness, Martin O'Donoghue, Anna Rawlings, Niall Conlon, Nicola Moloney and Rose Waldron for the help and conversations on those long days in the lab. There are too many names out of the Callan

Building to list so just know I really appreciate you all! It will be difficult to find another workplace where I can call every person there a good friend again.

To my parents, thank you both so much for the endless support in everything I do and for sitting through another four years' worth of mood swings. You have always been my role models for dedication and hard work.

Lastly and most importantly, I want to thank my partner Marc Tuffy. Without his love, care and encouragement, none of this would have been possible. Since the day you convinced me to "go for it", your support has never wavered and for that, I owe you a lifetime of gratitude.

This thesis is dedicated to Eva Mullally

Declaration

This thesis has not been submitted in whole or in part to this or any other university or tertiary institution and is the original work of the author except where otherwise specified. A full list of relevant information used throughout the text are supplied in bibliographies.

Signature:.....

Eoin O'Connor B. Sc.

Date:.....

Statement of Contributions

All computational and experimental work was solely carried out by the author with the exception of:

Chapter 2: Phylogenomic and syntenic analyses were carried out by Jamie McGowan and pangenomic analyses were carried out by Charley McCarthy.

Publications and Presentations

Publications

O'Connor, E., McGowan, J., McCarthy, C.G., Amini, A., Grogan, H. and Fitzpatrick, D.A., 2019. Whole Genome Sequence of the Commercially Relevant Mushroom Strain *Agaricus bisporus* var. *bisporus* ARP23. *G3: Genes, Genomes, Genetics*, *9*(10), pp.3057-3066.

O'Connor, E., Owens, R., Doyle, S., Amini, A., Grogan, H. and Fitzpatrick, D.A., 2020. Proteomic investigation of interhyphal interactions between strains of Agaricus bisporus. *Fungal Biology*.

O'Connor, E., Coates, C.J., Eastwood, D.C., Fitzpatrick, D.A. and Grogan, H., 2020. FISHing in fungi: Visualisation of mushroom virus X in the mycelium of *Agaricus bisporus* by fluorescence *in situ* hybridisation. *Journal of Microbiological Methods*, p.105913.

Publications not contributing to this thesis

Sipos, G., Prasanna, A.N., Walter, M.C., **O'Connor, E**., Balint, B., Krizsan, K., Kiss, B., Hess, J., Varga, T., Slot, J., Riley, R., Boka, B., Rigling, D., Barry, K., Lee, J., Mihaltcheva, S., LaButti, K., Lipzen, A., Waldron, R., Moloney, N.M., Sperisen, C., Kredics, L., Vagvolgyi, C., Patrignani, A., Fitzpatrick, D., Nagy, I., Doyle, S., Anderson, J.B., Grigoriev, I.V., Guldener, U., Munsterkotter, M., and Nagy, L.G. (2017) Genome expansion and lineage-specific genetic innovations in the forest pathogenic fungi Armillaria. *Nat Ecol Evol* **1**: 1931-1941.

Oral Presentations

O'Connor, E., Burton, K., Fitzpatrick, D., Grogan, H. (2016): Transmission of Mushroom Virus X in Different Strains of *Agaricus bisporus*. Department of Biology Seminar Series, Maynooth University, Maynooth, Ireland; 22nd November. Oral.

O'Connor, E., Burton, K., Fitzpatrick, D., Grogan, H. (2017). Genomics-directed approach to understanding the response of *Agaricus bisporus* to Mushroom Virus X Infection. 6th Biology Research Day, Maynooth University, Maynooth, Co. Kildare, Ireland; 6th June. Oral. (**awarded 2nd prize**)

O'Connor, E., Fitzpatrick, D., D., Eastwood, Grogan, H. (2018). Visualisation of MVX RNA in *Agaricus bisporus* mycelium by fluorescence *in situ* hybridisation. Microbiology Society Annual Meeting 2018, The Magic of Mushrooms, The International Convention Centre, Birmingham B1 2EA, UK; 13th April. Oral.

O'Connor, E., Fitzpatrick, D., D., Eastwood, Grogan, H. (2018). Visualisation of MVX RNA in *Agaricus bisporus* mycelium by fluorescence *in situ* hybridisation. Irish Plant Scientists' Association Meeting 2018, Agriculture and Food Science Centre, UCD, Dublin 4, Ireland; 12th June. Oral.

O'Connor, E., Fitzpatrick, D., D., Eastwood, Grogan, H. (2018). Visualisation of MVX RNA in *Agaricus bisporus* mycelium by fluorescence *in situ* hybridisation. 7th Biology Research Day, Maynooth University, Maynooth, Co. Kildare; 14th June. Oral. (**awarded 1st prize**)

O'Connor, E., Fitzpatrick, D., D., Eastwood, Grogan, H. (2018). Visualisation of MVX RNA in *Agaricus bisporus* mycelium by fluorescence *in situ* hybridisation. Irish Fungal Society Annual Scientific Meeting 2018, Maynooth University, Maynooth, Co. Kildare, Ireland; 18th June. Oral. (**awarded 1st prize**)

O'Connor, E., Fitzpatrick, D., D., Eastwood, Grogan, H. (2018). Visualisation of MVX RNA in *Agaricus bisporus* mycelium by fluorescence *in situ* hybridisation. Irish Plant Scientists' Association Meeting 2018, Agriculture and Food Science Centre, UCD, Dublin 4, Ireland; 12th June. Oral.

O'Connor, E., Fitzpatrick, D., D., Eastwood, Grogan, H. (2018). FISH for Fungi: Visualisation of viruses in the mycelium of the commercial mushroom *Agaricus bisporus.* Teagasc Walsh Fellowship Awards Seminar 2018, Johnstown Castle, Co. Wexford, Ireland; 5th October. Oral. (**awarded 1st prize**)

O'Connor, E., Fitzpatrick, D., Grogan, H. (2019). Host response of *Agaricus bisporus* to mushroom virus X infection. Microbiology Society Annual Meeting, Applied and Environmental Microbiology, ICC, Belfast, Northern Ireland, BT1 3WH; 11th April. Oral

O'Connor, E., Fitzpatrick, D., Grogan, H. (2019). Whole Genome Sequencing of a wild strain of *Agaricus bisporus*. Department of Biology Seminar Series, Maynooth University, Maynooth, Ireland; 28th May. Oral.

O'Connor, E., Fitzpatrick, D., Grogan, H. (2019). Transcriptomic and Proteomic response of *Agaricus bisporus to* Mushroom Virus X Infection. 8th Biology Research Day, Maynooth University, Maynooth, Co. Kildare; 5th June. Oral.

Poster Presentations

O'Connor, E., Burton, K., Fitzpatrick, D., Grogan, H. (2016). Determination of the Antiviral Genetic Attributes of *Agaricus bisporus*. 13th European Conference on Fungal Genetics - CS5: Applied genomics and biotechnology, Centre des congrès de la Villette – Cité des sciences et de l'Industrie 30 Avenue Corentin Cariou, 75019 Paris, France; 5th April. Poster.

O'Connor, E., Burton, K., Fitzpatrick, D., Grogan, H. (2016). Genomic, transcriptomic and proteomic analyses of *Agaricus bisporus* strains showing some tolerance/resistance to mushroom virus X. 5th Biology Research Day, Maynooth University, Maynooth, Ireland; 6th June. Poster.

O'Connor, E., Burton, K., Fitzpatrick, D., Grogan, H. (2017). Genomics-directed approach to understanding the response of *Agaricus bisporus* to Mushroom Virus X Infection. Irish Fungal Society Annual Scientific Meeting 2017, Limerick Institute of Technology, Co. Limerick, Ireland; 15th June. Poster.

O'Connor, E., Fitzpatrick, D., D., Eastwood, Grogan, H. (2017). Visualisation of MVX RNA in *Agaricus bisporus* mycelium by fluorescence *in situ* hybridisation. Society of Irish Plant Pathologists Annual Scientific Meeting 2017, O'Brien Centre for Science UCD, Dublin 4, Ireland; 6th December. Poster.

O'Connor, E., Fitzpatrick, D., Grogan, H. (2019). Host response of *Agaricus bisporus* to mushroom virus X infection. Genetics Society of America 30th Fungal Genetics Conference, Asilomar, Pacific Grove, CA, USA; 16th March. Poster

Abstract

Agaricus bisporus is a globally cultivated crop produced and consumed worldwide. This monoculture system and the advancement of consolidated growth of pre-colonised *A. bisporus* compost has coincided with the outbreak of a novel commercial disease, mushroom virus X (MVX). MVX constitutes a virome of 18 distinct single-stranded RNA viruses, of which select members cause detrimental disease phenotypes in infected mushrooms of *A. bisporus*. Scant focus has been placed on the molecular responses from the host during infection. The work presented herein provides novel genomic, transcriptomic, proteomic and cellular resources to help address the gaps in knowledge concerning MVX and *A. bisporus*.

The first whole genome sequencing and analysis of a wild *A. bisporus* var. *bisporus* was provided as a new resource for *A. bisporus* breeding research, revealing to be most closely related to the commercial white variety with a large accessory genome compared to other *A. bisporus* genomes. Dual-culture assays revealed the potential for MVX to transmit through hyphal fusion (anastomosis) into a variety of strains, whereas diagnostics of fruit bodies revealed different susceptibilities in certain strains with wild germ plasms. Mechanisms of anastomosis were revealed in varietal interactions and showed evidence of hyphae remodelling in compatible strains, metabolic starvation responses in competing interactions and antagonistic oxidative stresses in vegetative incompatible interactions. Molecular responses revealed increased regulation in gene expression, vesicle transport and ER-stress responses in virus infected fruit bodies, with less susceptible strains revealing increases of antiviral protein responses, general stress responses, lipid metabolism. The intracellular localisation of two of these viruses related to different symptomologies in infected fruit bodies revealed distinct patterns of virus distribution and characteristics related to persistent nature of infection. This work has provided novel insights into the molecular aspects of *A. bisporus* and MVX and the challenges they pose for the mushroom industry.

Preface

This thesis is presented in the form of a 'Thesis by publication'. The composition of this work includes four results chapters (2-5); one of which has been peer reviewed and published, two currently under review and one just at the point of journal submission. Results chapters are presented as the final documents that have been accepted or submitted for publication. Therefore, each results chapter has its own bibliography. Harvard style referencing is used in this thesis except for chapters submitted to research journals that use a different format. A review of the relevant literature is presented in Chapter 1 (Introduction), providing a general introduction to the research topic, which is focused in introductory sections of individual results chapters. Chapter 1 concludes with the aims and objectives of this work and provides over-arching hypotheses that guide the research. Chapter 1 has a standalone bibliography. Chapter 2 consists of a published work concerning the whole genome sequencing and analysis of *A. bisporus* var. *bisporus* (ARP23). Chapter 3 involves published work investigating the proteomic characterisation of anastomosis in *A. bisporus*. Chapter 4 focuses on the molecular characterisation of *A. bisporus* strains when challenged with MVX and will be submitted in November 2019. Chapter 5 is a published article that describes a novel approach to visualise MVX viruses *in situ*. The figure and table legends within results chapter begin from 1 for each chapter and will not be appended by the chapter number (e.g. the first figure of Chapter 3 will be Figure 1 and not Figure 3.1). The summarisation of Chapters 2-5 and critical analysis of findings and output are synthesised in Chapter 6 (Synthesis and Future Directions), this chapter also has a standalone bibliography associated with it.

Chapter 1:

General Introduction

1.0 General Introduction

1.1 A history of *Agaricus bisporus*

1.1.1 Ancient Mycophagy

Consumption of edible fungi in the wild can be mapped back as early as 11,000 BC to Chilean foragers, although the accounts are anomalous (Rojas and Mansur, 1995; Kumar and Sharma, 2011). Relics from the Neolithic Yangshoa culture (*c.a.* 5,000 BC – 4,000 BC) suggest that innocuous mushrooms were being consumed by ancient civilisations in China for dietary and medicinal purposes (Wang, 1987). Western writings show evidence of some the earliest records unambiguously describing fungi, albeit in adumbration, from Greek literature in the 5th century BC. Later, the first botanical considerations of fungi were made by the student of Aristotle, Theophrastus. In his natural history book *Historia Plantarum* (Enquiry into plants, c.a. 350 BC – *c.a.* 287 BC) he notes that fungi have

"*No root. They grow out of and near the root of oaks and other trees*"

He also noted that some fungi

"*grow on dung and have no bad smell*"

likely referring to the common meadow mushroom *Agaricus arvensis* (Buller, 1914). Based in Rome during the time of Nero, a pharmacologist by the name of Pedanios Dioscorides (*ca.* 40-90 AD) wrote of many macrofungi, including the àyapiKÒv (Agarikón or agaric) (Lu, 2014), a name derived from sites of procurement in the Agarum promontory of Samartia (Jones, 1958). Galen of Pergamům (*c.a.*131-199) also describes the apāviiai (anianitia or champignons) in his work *De Alimentorum Facultatibus* ('On the Property of Foodstuffs'; (Galen *et al*., 2003)).

Some of the earliest accounts of cultivation for mycophagy are by the Chinese, where the pharmacologist Tao Hongjing (456-536 AD) documented how villagers grew *Wolfiporia cocos* on pine logs (Lu, 2014). From the time of the Tang Dynasty (618-907), accounts referring to the cultivation of wood-ear fungus (*Auricularia auricula-juda*) on wood logs have been found (Liu, 1958). The shiitake mushroom (*Lentinula edodes*) has

also seen a long history of cultivation from Japan, China, Thailand and elsewhere in Asia, where it was cultivated on logs of the shii tree, a close relative to the oak tree, a process still practiced today (Leatham, 1981; Reid and Ainsworth, 1978).

1.1.2 The Baboon and the button mushroom

An essential item in one man's repast is largely responsible for the birth of the cultivation of *A. bisporus*. In the 17th century, King Louis XIV (the Baboon, the Sun King) of France had a particular taste for the Champignon de Paris (more commonly known now as the 'button mushroom'). The rarity of this mushroom and the demand set by the king led to Parisian champignonnistes creatively moving horse dung to the catacombs below the city where the temperate climate facilitated growth. Claude Aubriet, the Baboon King's botanical artist, created illustrations for the king in the *Jardin des Plantes* (botanical garden of France). Aubriet would go onto illustrate for Joseph Pitton de Tournefort, in the famous Élémens de Botanique (Tournefort, 1797), the key literature in plant taxonomy before the work of Linnaeus. Though Tournefort's earliest work focused heavily on plants, his interests progressively moved to fungi. After Bonnefons would allude to the cultivation of *A. bisporus* in his book *Le Jardinier Français* (1650), Tournefort went on to fully detail what would be considered the commercial production of the button mushroom in 1707 (Spencer, 1985). This was an impressive feat considering how little naturalists understood about the biology of *Agaricus* or even fungi themselves. The historical mentions of dung didn't end with Theophrastus, as the mysterious nature of fungi led Abercrombie to write about *Agaricus* in stating

"*the mushroom tribe has long afforded speculation to naturalists, with respect to being perfect or imperfect plants*"

and

"*their exceeding minuteness and obscurity*"

he continues perhaps with an air of frustration, to state that many believe they

"*owe their origin entirely to the putrefaction of earth and dung*" (Mawe, 1779).

1.1.3 Innovations preceding modern *A. bisporus* cultivation

As mentioned, cultivation of *A. bisporus* came from France, where horse manure was used to grow mushrooms in the foothills of Paris (Tournefort, 1707). The 19th century saw a move to cultivation in caves or growing houses (1810) where growing could occur all year round but the practice of gathering spawn from the wild continued. Mycelia sourced from horse dung would be introduced into compost beds, a practice which resulted in inadvertent cultivation of many pathogenic fungal and bacterial species also. It wasn't until the 20th century that axenic *A. bisporus* spawn started to be produced by the Pasteur Institute (Paris, France) in an attempt to grow disease-free mycelium that mushroom growers could use for their compost beds (Fritsche, 1978). By 1902, literature was published detailing cultivar propagation from spore-borne mycelium of *A. bisporus* (Ferguson, 1902). Two additional innovations came relatively soon after, with the development of using cereal grain to manufacture spawn (Sinden, 1932) and the characterisation of the composting process being distinguished in two distinct phases of Phase I (free heating) and Phase II (pasteurisation) These innovations are still very much applicable to modern *A. bisporus* cultivation.

1.2 Biology of *A. bisporus*

This section will provide an outline of the taxonomy, phenotype and life cycle of *A. bisporus* and what classifications it falls into in the wider context of fungi.

1.2.1 Taxonomy

The earliest fossil records for fungi date back 1,010 – 890 million years (Loron *et al.,* 2019*)*. Fungi originally formed one of five kingdoms; along with plants, animals, protists, and prokaryotes, largely based upon ecological function or trophic levels (Whittaker, 1969). Hierarchically, fungi later fell into one of three domains in Eukaryota (Woese *et al.*, 1990). Fungi were later assigned to monophyletic Opisthokonta along with the animal lineages (Adl *et al*., 2005). Fungal taxonomy is currently in a state of flux, with new phyla being suggested and older phyla being merged or split. Currently there are nine major divisions within the fungal kingdom; Ascomycota, Basidiomycota,

Blastocladiomycota, Chytridiomycota, Cryptomycota, Mucoromycota, Neocallimastigomycota, Zoopagomycota and the Microsporidia (Hibbett *et al.*, 2007). *A. bisporus* belongs to the Basidiomycota division and, more specifically to the homobasidiomycetes subdivision. Homobasidiomycetes, in contrast to the heterobasidiomycete, which contain septate basidia, contain single-celled aseptate basidia. They consist of the most conspicuous fruit body forming fungi as they form mushrooms and play major roles as wood-decayers and ectomycorrhizal symbionts to many species of forest tree (Rayner and Boddy, 1988). The filamentous forms of homobasidiomycetes rarely form single-celled phases and are segregated by septa with barrel-shaped dolipores traveling through the centre, with parenthesomes (pore caps) flanking either side. The hyphae are generally dikaryotic (two haploid nuclei within each cell: $n + n$).

1.2.2 Description of *Agaricus bisporus* (Lange) Imbach

In lay terms, the *A. bisporus* (Lange) Imbach commercial white-coloured varieties are named 'white button mushroom', 'Portobello mushroom', 'common mushroom', 'champignon mushroom' and in brown varieties the 'chestnut mushroom', 'heirloom mushroom', 'cremini mushroom' and 'Swiss brown mushroom'. The etymology for *Agaricus* comes from the Greek Agarikón, and as mentioned previously, which derives from the Agari people of ancient Sarmatia Europaea where the fungus 'Agaricum' was used to treat disease. Four-spored basidia are prevalent in most homobasidiomycetes. In contrast, the distinguishing feature of the button mushroom is found in their basidium where only two spores are present and is responsible for their nomenclature of '*bisporus*' ('bearing two spores'). *A. bisporus* belong to the class Agaricomycotina. They are a terricolous saprotrophic fungus, adapted to a humicolous niche environment. They differ to certain closely related species such as *Coprinopsis cinerea*, which are coprophilous, in that that they contain enzymatic repertoires tailored to primary degradation of plant material in humic-rich environments (Morin *et al*., 2012). The vegetative phase of growth consists of hyphae partitioned by septa, but no clamp-connections are found between adjacent cells. Abiotic stimuli (e.g. cooler temperatures in Autumn) trigger a switch to reproductive growth whereby mycelium congregates to more oxygen rich areas of the substrate (the surface) in the form of 'pins'. These pins become the primordia with an

increase in size to ultimately form a mature fruiting body. Grasslands in Europe and North America form the natural habitats of *A. bisporus* where fruit bodies are commonly found with grey/brown pilei. Other habitats include the leaf-litter of temperate forests and arid lands of Californian desert (Callac *et al*., 2002; Kerrigan, 1995).

1.2.3 The life cycle of *A. bisporus*

Thallism in fungi was first described in species from the Mucorales and can be segregated into two main types; heterothallism and homothallism (Blakeslee, 1904). Heterothallism involves syngamy where two haploid mycelia carry nuclei of heteroallelic mating-type (MAT) genes. A fertile mycelium capable of fruitification is produced from the successful pairing of heterogenous haploid nuclei. Isogamous mating types derived from only a single locus are considered as having unifactorial (bipolar) mating systems. Control of mating with a single locus may result with complete compatibility of a fruit body with a different allelic mating pair, as the only requirement for mating is the difference of a single mating locus. A bifactorial system (tetrapolar) requires compatible pairs of alleles for mating, where one mating gene has two loci and the complementary mating gene the same. With a unifactorial system there is a 50% chance of mating occurring between spores from the same fruit body and a 25% chance with bifactorial mating system (Hsueh *et al.*, 2008). Many mushroom forming fungi follow the standard bifactorial mating system. Homothallic fungi express both mating types and package both into a single spore (self-fertile). Certain homothallic fungi engage in mating-type switching, where mating-type identity can be swapped during vegetative growth, the frequency of which can be increased when sexual partners are scarce (Hadjivasiliou *et al.*, 2016; Lin and Heitman, 2007). A mycelium harbouring a single haploid nucleus of one mating-type is referred to as monokaryon. Uninucleate cells prevent the intracellular movement of nuclei within hypha through septal structures (Giesy and Day, 1965). Binucleated cells of compatible mating-type constitute the mycelium of a dikaryon.

A. bisporus has a unifactorial pseudo-homothallic or amphithallic life cycle, such that heterothallism and homothallism operate concurrently (Raper *et al.*, 1972; Elliott, 1972). Homothallism dominates in *A. bisporus*, where it is sometimes referred to as inbreeding or intramix. The spores of this system harbour two non-sister nuclei which are heterogenous at centromeric-linked loci, such as the MAT genes. Thallism in *A. bisporus*

is closely tied to spore number in basidia where the typical bisporic form manifests a pseudo-homothallic life cycle (Callac *et al*., 1996(b)). *Agaricus bisporus* var. *burnettii*, a tetrasporic variety found solely in the Sonoran Desert in California, USA, differs to the *bisporus* variety as it nearly exclusively produces spores for heterothallic mycelium (Kerrigan *et al.*, 1994). In the bisporic variety, nuclear fusion occurs in the basidium (Evans, 1959), followed by meiosis to produce four haploid nuclei (Elliott, 1985). Nuclei undergo random migration to the basidiospores, where two heterogenous meiotic nuclei occupy each basidiospore (Raper *et al.*, 1972; Summerbell *et al.*, 1989). Rarer occurrences of spore migration involve homokaryotic (*n* + *n*) nuclei in two spores, trisporic state (*n* + *n*, *n*, *n*), and the tetrasporic state (*n*, *n*, *n*, *n*) appearing less than 0.05 % naturally (Elliott, 1985; **Figure 1.1**). A haploid chromosome number of 13, was assigned to nuclei of *A. bisporus* through light microscopy (Evans, 1959). The two varieties var. *bisporus* and var. *burnettii* have unifactorial mating systems as they lack a functional B-mating type which differs to that of the model *Agaricomycete* mushroom-forming fungus *C. cinerea. C. cinerea* is a bifactorial species where the *A* and *B* mating types contain additional subloci of α- and β- subunits.

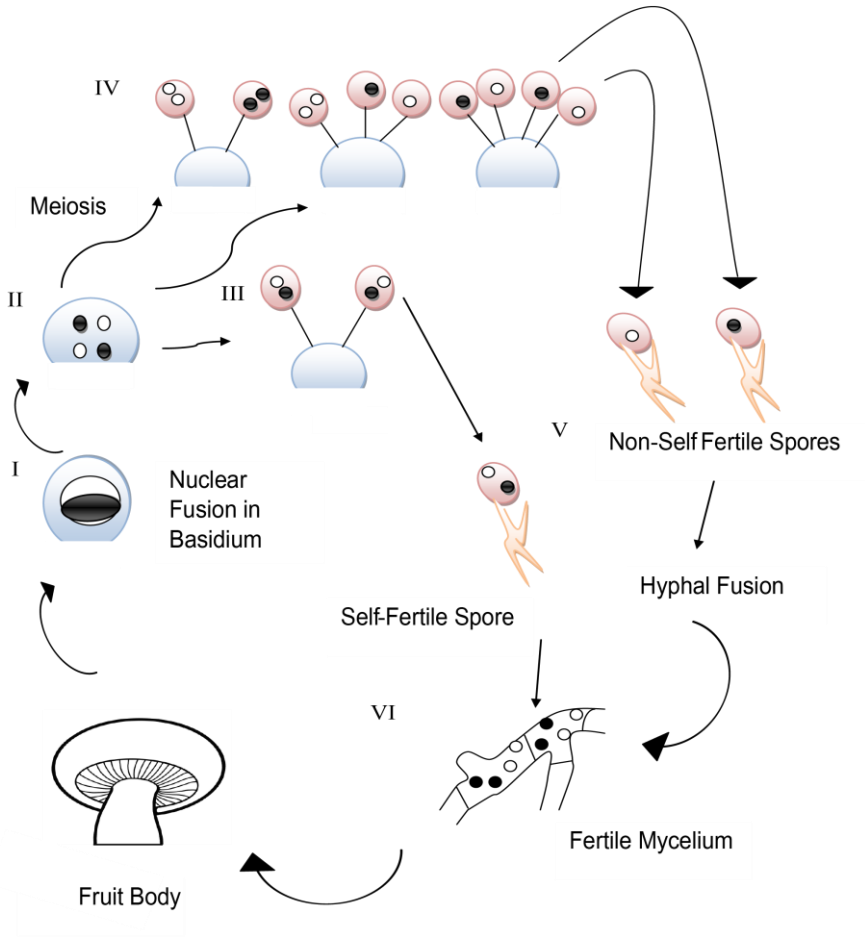

Figure 1.1: The life cycle of *Agaricus bisporus* var. *bisporus*. Basidia are located within the hymenophore of basidiocarps (fruit bodies). (I) Nuclear fusion occurs within the basidium. (II) Meiosis forms four haploid nuclei, which undergo randomised basidiospore migration. (III) The most common circumstance post spore migration is the bisporic form where two meiotic nuclei are contained in each basidiospore. These nucleic pairs are heteroallelic at their MAT loci (heterokaryon). (IV) A less common occurrence is random spore migration leading to a homokaryotic (homoallelic at their MAT loci) bisporic form, rarer than that a trisporic homokaryon and two mononkaryotic basidiospores, and the rarest a tetrasporic monokaryotic form. (V) Heterokaryotic basidiospores germinate to form a fertile mycelium. Homokaryotic basidiospores germinate to form a homokaryotic mycelium whereby fusion with a compatible mating type mycelium of the complementary MAT locus is needed to form fertile mycelium. Fertile mycelium can undergo the morphogenesis switch from vegetative growth to reproductive growth to produce fruit bodies where the process can repeat. Modified from Elliot (1985).

1.3 Commercial Mushroom Breeding

1.3.1 Methods in mushroom breeding

The ability of pseudo-homothallic varieties of *A. bisporus* to self-mate and produce fertile mycelium, potentially reduces genetic variation between generations by the inhibition of gene flow (Ullrich and Raper, 1977). Prior to many advances in breeding, single spore isolates (SSI) or multi-spore cultures were generated from existing cultivars (Elliott and Langton, 1981). This was an adequate way to repeatedly spawn the same cultivars but did not facilitate the breeding of novel cultivars as the spores retain almost all of the parental genotype (Kerrigan *et al.*, 1993). With improvements in methods (e.g. protoplasting) leading to the adoption of outcrossing of homokaryons, the first hybrid varieties reached markets in the early 1980's. Efforts to drive selective breeding in *A. bisporus* were accelerated with improvements of electrophoretic techniques allowing the identification of codominant (allozyme) genetic markers in mate crossings (May and Royse, 1982). While hybrid varieties can be generated with relative ease, the introduction of specific phenotypes into new cultivars is problematic due to linkage drag (Sonnenberg *et al.*, 2016). This results in unwanted genomic elements being unintentionally crossed into cultivars, a consequence of the life cycle of *A. bisporus* (**Figure 1.1**).

1.3.2 The hybrid varieties

The first white hybrid varieties were developed in a laboratory in Horst (Netherlands) and arrived to markets approximately in the year 1980. They were referred to as the "Horst" strains U1 and U3 and their pedigree was assigned to the older commercial cultivars, the off-white cultivar Somycel 9.2 and the white cultivar Somycel 53 (Imbernon *et al.*, 1996). The U1 cultivar became widely used in commercial cultivation as the choice white cultivar. The first whole genome sequencing project was completed for *A. bisporus* in 2011 from one of the constituent homokaryons of the U1 hybrid, H97 (Morin *et al.*, 2012). This was followed by the genome of the other constituent homokaryon (H39) along with further improvements to the reference genome (H97) (Sonnenberg *et al.*, 2016). With both genomes, the crossover landscape could be mapped for multiple SSIs revealing that recombination was very low between different

hybrid varieties (Sonnenberg *et al.*, 2016). This may explain the difficulties in introducing commercially desirable strains into outcrossings. U1 is still cultivated today, but to a much lesser extent and only in select locations. The strain "Sylvan" A15, a lineage group of U1 and U3 developed from vegetative clonal propagation, has largely replaced the use of U1 in commercial spawn production. The assignment of some of the contemporary white cultivars as 'hybrid' may be contested, as genotyping studies revealed that these cultivars are not just phenotypically identical to traditional cultivars, they appear to have originated from the selection of dikaryotic single spore isolates from the first white hybrids (Sonnenberg *et al.*, 2016). Furthermore, analysis of single nucleotide polymorphism (SNP) markers of these white hybrid cultivars showed a very low genetic variation when compared to isolates of wild populations (Sonnenberg *et al.*, 2017). The past few years have seen some advances into efforts to establish new hybrid varieties and importantly, hybrids that incorporate wild *A. bisporus* parental genotypes. This includes the new hybrid varieties J15987, J10102-s69, B12998-s39, J11500 (see patents assigned to Sylvan America Inc. www.patents.justia.com). One of the novel hybrid strains, J9277, is progeny to a white hybrid U1 and the wild tetrasporic strain *A. bisporus* var. *burnettii*. The full genome sequence of var. *burnettii* to which the full genome sequence was released alongside H97 (Morin *et al.*, 2012).

1.3.3 The *Agaricus* Resource Program (ARP)

The Agaricus Resource Program (ARP; Callac *et al.*, 1996(a)), which is referred to as the Agaricus Recovery Program in older publications (Kerrigan, 1991), was an initiative set up by Richard W. Kerrigan (Sylvan Spawn Laboratory, PA, USA) in 1988. The program sought to collect wild populations of *A. bisporus* from diverse geographical locations around the world. This was to address the lack of genetic diversity in the mushroom industry as there were believed to be fewer than 20 independent lines of *A. bisporus* in circulation for commercial purposes. This was speculated to be the fewest of any commercially important crop. ARP was a bounty driven scheme ('Dollars-for-Diversity') that called upon scientists or enthusiasts with adequate knowledge in fungal taxonomy to send isolates for submission. By 1995, of the 206 samples submitted, 58 novel genotypes were identified with one entirely new population discovered {Formatting Citation}. The isolates within the ARP were geographically distinct and found to be

genetically diverse (Callac *et al*., 2002; Kerrigan, 1995). For a time, it was debated among taxonomists whether wild isolates and commercial cultivars represented distinct species but ultimately, they were confirmed as conspecifics (Malloch *et al*., 1987). By the year 2000, reports from ARP noted up to 500 wild specimens had been collected and stored in liquid nitrogen (Callac *et al.*, 2002). Other collections of wild isolates have been gathered and characterised in France (Callac, 1995) and Greece (Callac *et al.*, 2002). At present, further growth of wild *Agaricus* germplasm collections will require funding incentives to continue (Sonnenberg *et al.*, 2017) however, there have been recent studies involving the use of new wild *A. bisporus* material (Halász *et al.*, 2014; Mata *et al.*, 2016; Navarro and Savoie, 2015; Prasad and Agarwal, 2013; Rokni *et al.*, 2016; Sobieralski *et al.*, 2010). **Chapter 2** of this thesis provides the description of the first whole genome sequencing of an isolate from the ARP collection, *Agaricus bisporus* var. *bisporus* (ARP23) (O'Connor *et al.*, 2019). ARP23, sometimes referred to as BP-1 in the industry, is one parent of the 'heirloom' (chestnut mushroom) commercial variety.

1.4 Mushroom Browning

The button mushroom market is dominated by white varieties (up to 80%) (Deakin *et al.*, 2015) due to consumer demand (Wejin *et al.*, 2011). Whiteness is a double-edged sword, as the visual appearance of the mushroom appeals to consumers and is associated with high quality but the uniformity and purity of white is easily affected by three main types of browning: genetic, mechanical-damage and pathogenesis.

1.4.1 Genetic basis of browning

The 'white' mushroom phenotype of commercial mushrooms is rarely found in the wild and is caused by a recessive allele of the Pilei-pellis Colour 1 gene - *PPC1* (Callac *et al.*, 1998). Early cultivated mushrooms were all a certain shade of brown. In the USA (1926), by chance a small cluster of white mushrooms grew on a compost bed surrounded by light-brown mushrooms in a commercial farm. This reoccurred decades later in Denmark (1960). Tissues were collected and retained from these mutant isolates and introduced into commercial breeding. Off-white varieties still derive parentage and the genetic basis for their phenotype from these original cultures today (Sinden, 1990).

Melanin is associated with many functions in adaptive fungal strategies (Krah *et al.*, 2019), one of which is defence from hydrolytic enzymes from antagonistic organisms (Bell and Wheeler, 1986). It is also responsible for brown pigmentation. Oxidative polymerisation of the two main polyphenol oxidases (PPOs) laccase and tyrosinase is responsible for melanin production. Recently the gene editing tool CRISPR-Cas9 was used to knock out one of six genes encoding for PPO, causing a 30% reduction in the enzyme's activity (Waltz, 2016). In doing so, researchers have created a genetically modified *A. bisporus* variety which is resistant to browning. These genetically modified mushrooms have also bypassed regulations in the US, as no transgenics were used in their formulation.

1.4.2 Mechanically induced browning

Browning induced from mechanical damage is a huge hurdle for the mushroom industry. One of the reasons the mushroom industry still harvests mushrooms by hand is the delicate nature of the fruit body. Picking by hand may be costly in terms of labour but it helps reduce bruising or mechanical damage to the product. Automation of mushroom harvesting is used in many countries, but these harvests are more often used for products where the visual quality of the mushroom is not as important (e.g. mushrooms used in canned goods). The browning from mechanical damage is caused by the biosynthesis of melanin, used to protect the organism against harmful external stimuli. Melanin is synthesised from a repertoire of at least 26 separate enzyme-coding genes (Weijn *et al.*, 2013). Post-harvest browning occurs at a much slower rate than bruising and occurs more uniformly over the mushroom (Burton and Noble, 1993). Bruising triggers a biochemical chain of reactions involving tyrosinases and quinones that result in the biosynthesis of melanin (Burton and Noble, 1993). In the same way, melanogenesis caused by the intramix of oxygen and cellular phenols and tyrosinase occurs from mechanically compromised intracellular membranes (Burton and Noble, 1993).

1.4.3 Pathogenesis induced browning

One of the most direct examples of a pathogen causing browning of the fruit body, is from the 'brown blotch' bacterium *Pseudomonas tolaasii* as this pathogen secretes a

lipodepsipeptide which causes mixing of cell contents by forming ion channels within cellular membranes (Brodey, 1991). Brown spots from the pathogenic fungus *Lecanicillium fungicola* are also well known to growers (Fletcher and Gaze, 2007). Browning is also associated with La France disease and mushroom virus X (MVX), albeit less localised than in the bacterial and fungal pathogens, with a more even discolouration over the entire cap of infected fruit bodies (Grogan *et al.*, 2003). The mechanisms for mycovirus browning are still unclear, but the cellular stress induced from high viral titres is a likely hypothesis. Additional information on mycopathogens is provided in **Section 1.6**.

1.5 Cultivation of *Agaricus bisporus*

1.5.1 The Mushroom Industry

Edible mushrooms from both the wild and commercial cultivation are consumed globally and have a market worth of US$42 billion per year (Prescott *et al.*, 2018). There has been a 30-fold increase in the production of cultivated, edible mushrooms to only a 1.7-fold increase in the world's population from 1978 to 2013, demonstrating the increase in demand for mushrooms in consumer diets (Royse *et* al., 2017) (**Figure 1.2A**). In the category of mushroom and truffle production (MTP), the top five countries rank in order of the Republic of China, Italy, USA, Netherlands and Poland. Ireland ranks at number 10 in MTP and belongs in the highest category of gross yield (**Figure 1.2B**). Data accumulated from the United Nations Food and Agriculture Organization Statistics Division (FAOSTAT) shows that Ireland produced 66,500 tonnes of mushroom biomass in 2017 in categories for mushrooms and truffles (where species other than the button mushroom make up only a small fraction) (FAOSTAT, 2019). Ireland has seen an increase in button mushroom production from records as far back as 1961 and the highest commercial production yet recorded in 2015. Mushroom cultivation saw a sharp increase in the 1990's and continuous growth with the exception of the beginning of the millennium, for reasons related to epidemic diseases (discussed later). (**Figure 1.2C**). *A. bisporus* is one of the most widely cultivated mushrooms globally and production accounted for US$38.13 M in 2017 (www.researchandmarkets.com). *A. bisporus* is one of the few horticultural outputs in Ireland that is primarily exported, with exports reaching a farmgate value of €91 M (77% of total product) in 2017 (www.bordbia.ie**).**

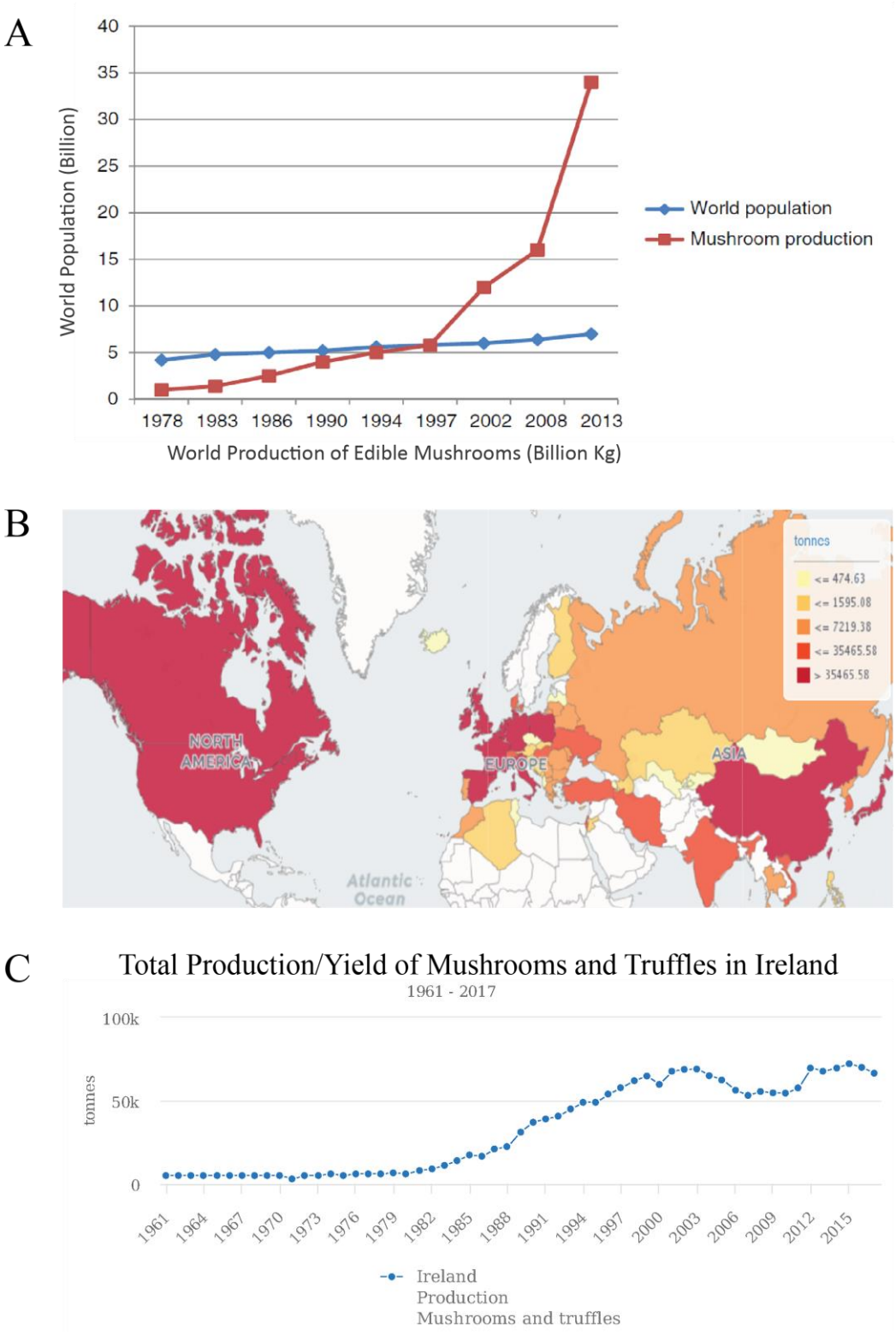

Figure 1.2: Worldwide and Irish production of mushrooms and truffles. (**A**) Comparison of the increase in production of cultivated, edible mushrooms to the increase of the world's population from 1978 to 2013, taken from Royse *et al*. (2017). (**B**) Map of North America, Europe and Asia representing gross mushroom production by colour (tonnes) for the year 2017. (**C**) Gross mushroom production/yield in Ireland from the earliest and latest records from the UN (1961-2017). Data for (**B**) and (**C**) collected from FAOSTAT (2019).

1.5.2 Commercial Cultivation

As outlined in the historical overview above, cultivation of *A. bisporus* has a long history with generational improvements and isolated discoveries revolutionising how growers cultivate this edible fungus. Technological advancements have taken growing strategies from caves in Paris (for example) to sophisticated growing houses capable of producing several thousand tonnes of button mushroom annually. However, the core principles for growing *Agaricus* on raw materials consisting of animal wheat straw, gypsum, mixed animal manure and water remain (Gerrits, 1988). In 1936, the addition of gypsum (calcium sulphate) was found to greatly reduce the greasiness of compost and enhance mycelial colonisation of substrate (Pizer and Thompson, 1938), its addition is still practised today. The highly abundant lignocellulosic polymers in straw acts as a carbon source for *A. bisporus,* through the breakdown of plant cell walls consisting of different polysaccharides such as cellulose, hemicellulose and aromatic lignin (Iiyama *et al.,* 1994; Jurak *et al.,* 2014). The manure is a rich source of nitrogen, so too are the bacterial communities within the compost microbiome (Fermor *et al*., 1991).

Compost for mushroom growing follows three key phases:

Phase I: In Ireland bales of wheat straw are prewet with water to ensure an even wetness then mixed with poultry manure and gyspsum. Wetting and mixing is sometimes referred to as phase 0. Homogenous mixes are filled into concrete bunkers with aerated floors. Solid-state fermentation begins whereby the wetness of compost triggers a plethora of microbial activity. This activity results in the generation of heat and influenced further by forced air retention where temperatures reach 80°C. This process takes between 11-13 days to complete.

Phase II: The phase I compost is transported to environmentally controlled tunnels where the compost temperature can reach 58°-60°C for 8 hours to allow for the process of pasteurisation to take place. After pasteurisation, the compost temperature is reduced to 45-48 degrees for about six days to facilitate aerobic thermophilic activity known as ‘conditioning’

Phase III: Cooled phase II substrate is transported to a spawning hall where it is inoculated with mushroom ‘spawn’ – a pure culture of *A. bisporus,* grown on rye or millet grain. The spawned compost is filled into a new environmentally controlled tunnel and incubated at

25°C, for 15-17 days until it is fully colonised with mushroom mycelium (bulk phase III). Bulk phase III compost is then removed from the tunnel using winches and conveyors, causing the mass of colonised substrate to break apart and fragment (the impacts in relation to disease are discussed in **Section 1.5.3**) . The bulk phase III compost is then loaded into specially designed trucks and transported to the growers (Fletcher and Gaze, 2007)

On mushroom farms, phase III compost is filled onto shelving units with a conveyor. Growers then add a layer of casing (peat neutralised with sugar beet lime to pH 7) over the colonised compost, ensuring an even depth across beds. Some mushroom growers will 'ruffle' the crop. This can be done using a ruffling machine, whereby a roller covered in tines is used to mix the compost casing interface to promote mycelial colonisation to the casing layer. Casing does not provide nutrition for the mycelium, rather, it is a medium that allows for the aerial growth and anchorage of hyphae, as well holding moisture to supply the growing mushrooms with water (Seaby, 1999). It is at the surface of the casing layer that the switch from vegetative growth of the mycelium to reproductive growth of fruit bodies occurs.

This triggering of reproductive growth occurs as a result of a process known as 'airing' (**Figure 1.3**). After the casing layer is added and the vegetative mycelium has grown to the surface (case-run) (**Figure 1.3 A**, **B**), environmental conditions are altered steadily over a three-day period. Temperatures are lowered from 25°C during case run to 18°C, the relative humidity is reduced from 95% to 88-90% and levels of CO_2 are reduced by bringing in fresh air. These changes trigger the vegetative mycelium to enter the reproductive phase with the initiation of fruiting (Eastwood *et al*., 2013). Airing is one of the most crucial steps in the cropping cycle, as if done incorrectly, will lead to a marked loss in fruit body formation and yield. 'Hyphal knots' (pins) begin to form in a process referred to as 'pinning' (**Figure 1.3 C**).

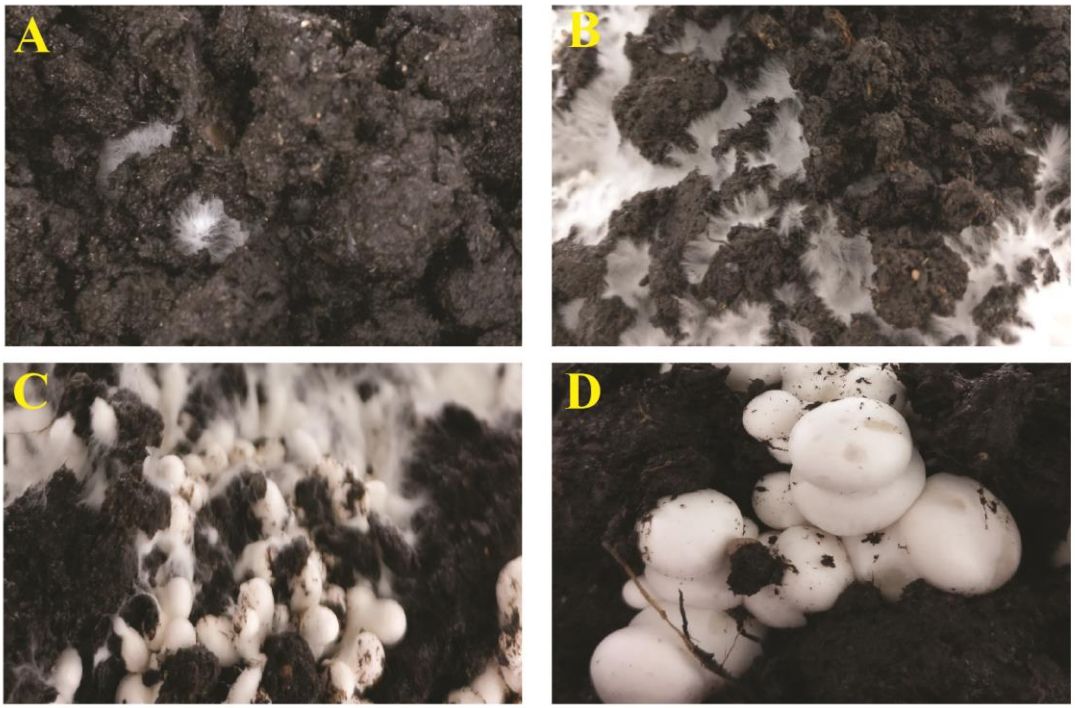

Figure 1.3: Phase change from vegetative growth to reproductive growth triggered by the process of 'airing' within the casing layer. (**A**) Casing layer where the mycelium is beginning to grow to the surface. (**B**) Taken 3 days after (**A**), Casing layer nearly entirely colonised with vegetative mycelium. (**C**) Pins forming from the mycelium during the airing process. (**D**) Primordia formation from pins nearing the stage of young fruit body. (Photo: E. O'Connor).

After pinning has been triggered the developing fruit bodies approximately double in diameter every 24 h. These are then harvested by trained picking staff. Depending on the supplier demand, a precise size/diameter of cap is selected for picking. Harvests generally occur over a window of two to four days with the initial harvest referred to as the 1st flush. Mushroom growers will harvest at least two flushes with many also taking a 3rd flush. Once all the mushrooms are harvested the crop is killed off by a steam 'cook-out', a process whereby growing rooms are filled with steam until the compost substrate reaches temperatures of 65-70°C for at least 8 h. The spent cooked-out substrate is then disposed of appropriately.

1.5.3 Bulk Phase III

The production of phase III compost is described above. Bulk phase III compost is delivered to growers as loose bulk-handled fragmented pieces of compost fully colonised with *A. bisporus* mycelium. Bulk phase III compost promotes both faster growth of mycelium and higher quality mushrooms and is the preferred choice of cultivation (primarily in Europe) for almost three decades. The move to use of bulk phase III compost is attributed to the consolidation of mushroom production in Ireland and other countries. Multiple small-scale growers have ceased production in recent decades with expansion of large-scale growers due to consolidation and rationalisation of the sector (Mushroom Sector Development Plan 2020, 2013). The use of bulk phase III means that fully colonised compost is open to contamination once it is emptied from the tunnel and delivered to growers. There is a significant risk of mycelium exposure to the bacteria, fungi, viruses and other potential mycopathogens. Moreover, fragmentation of compost and breakages in hyphae creates a large surface area otherwise less readily accessible to pathogens, potentially leading to exposure to intracellular virus infection and causes an initial stress to hyphae as they repair and restore the fungal mycelium architecture. This may result in the systemic spread of pathogens into new crops.

1.6 Pests and pathogens of *A. bisporus*

Some of the most well-known pathogens and pests of mushroom crops are discussed in this section, with a more in-depth review of the literature surrounding mycoviruses presented in later sections, particularly mushroom virus X as it is the focus of this thesis.

1.6.1 Pests

The more salient reasons for the proliferation of pests in crops would be the frugivorous activities and controlled climate environments. These environments are present in mushroom growing rooms where unbridled access to food and protection are not afforded to these pests in natural environments where conspecific competition and predation are much more prevalent (Van Lenteren, 1988). The most serious mushroom

pests are the Diptera (two-winged flies) and specifically members of three families encompassing the sciarids, phorids and cecids. Sciarids or fungus gnats include two species which dominate as pests, *Lycoriella castanescens* and *Lycoriella ingenua.* They are particularly troublesome to growers as their introduction can affect all stages beyond phase II production. The larvae produce faecal matter that coagulates in compost causing foul odours, they primarily feed on organic substrate, but when present in high numbers will feed on mushroom mycelium and can tunnel inside of stalks resulting in yield loss and post-harvest rejection (Fletcher and Gaze, 2007). Entomopathogenic nematodes can be introduced into casing as a biocontrol agent of sciarids, as they predate the larvae of the flies and do not participate in fungivory (Navarro and Gea, 2014). The most damaging member of the phorid family, *Megaselia halterata*, feeds primarily on the vegetative mycelium of *A. bisporus* in the crop, and can also tunnel inside stalks, reducing mushroom quality. Once the flies of both pests emerge, they can become vectors of pathogenic fungal spores and bacteria (*Lecanicillium, Mycogone and Trichoderma* spp.) which further exacerbates disease outbreaks. The introduction of nematodes can also act as a biocontrol of phorids as they predate their larvae (Scheepmaker *et al*., 1998). Cecid larvaes , of which *Heteropeza pygmaea* and *Mycophila speyeri* are the most common members, are bacterial vectors that feed on developing mushrooms (Fletcher and Gaze, 2007).

1.6.2 Fungi

Certain fungi are a source of disease in crops and others may compete with *Agaricus* for nutrients or surface area on crop beds. Disease causing fungi include *Mycogone perniciosa,* commonly referred to simple as ‘mycogone’ or ‘wet bubble’, due to the phenotypic sclerodermoid masses that form on diseased mushrooms. While this fungus is not known for major losses in crops, pathogenicity is linked to the colour of the fungus, with yellow and brown varieties showing greater virulence than white varieties (Li *et al*., 2019). In dry conditions, wet bubble can be confused with ‘dry bubble’. Wet bubble is found in every major mushroom growing country.

Dry bubble is caused by the fungus *Lecanicillium fungicola* predominately in Europe and the *Verticillium fungicola* var. *aleophilum* is more common in USA and warmer countries. Unlike, wet bubble, dry bubble is notoriously persistent in crops and found in every mushroom growing country. Depending on the developmental stage of the

mushroom when infection occurs, disease phenotypes vary from undifferentiated masses of undeveloped and clustered primordia, wart-like protuberances on caps and mushroom-like masses of tissues (Fletcher and Gaze, 2007). Spread of dry bubble is difficult to control as the sticky spores are easily spread by water splash as well as sticking to many vectors such as debris, mites, flies and personnel. Growers add a salt pile to cover infected areas as soon as detected in an attempt to physically prevent access of potential spore vectors. Few fungicides are available for use and so tackling fungal disease is a huge challenge for growers. Some studies have found the nascent microbiome of casing can hinder the advance and growth of dry bubble, but only to a particular threshold (Carrasco *et al*., 2019).

The common pathogen known as 'cobweb' is more of a collective term for a number of different fungi, but primarily refers to *Cladobotryum dendroides* and *C. mycophilum.* Genotyping of ITS regions from Irish and UK isolates have shown that *Cladobotryum mycophilum* is most commonly associated with this disease phenotype and that populations are clonal (McKay *et al*., 1999). White areas of cobweb-like mycelium appear on the crop surface and envelop mushrooms in its path.

Different strains of *Trichoderma* species are found in mushroom crops, with pathologies from members ranging from mild to severe. The most recognised disease phenotype is the green mould produced primarily from *Trichoderma aggressivum.* This fungus can reduce yield up to 100% and lead to brown spots and dry decay on mushrooms and is also known for its high secondary metabolite secretion activities such as peptaibols which are putative growth inhibitors of *Agaricus* mycelium (Marik *et al*., 2017). Bulk phase III compost has seen sporadic cases of severe *T. aggressivum* outbreaks in recent years, with the process of bulk handling believed to stimulate the growth of the fungus (O'Brien *et al*., 2017).

1.6.3 Bacteria

Bacterial pathogens of *Agaricus* are ubiquitous in countries where mushrooms are cultivated. 'Brown blotch' is the most prolific of the bacterial diseases and particularly troublesome in countries with warmer climates. Brown blotch is commonly associated with *Pseudomonas tolaasii.* As the name suggests, blotches or spots appear on infected caps. As this bacterium is found everywhere, its entry into growing houses is

unpreventable. However, effective control through ventilation and humidity in growing rooms can reduce the incidence of blotch. Quantitative trait loci analyses revealed a strong association between resistance to brown blotch and gene responsible for white mushroom phenotypes *PPC1* (Moquet *et al*., 1999).

A similar disease named 'ginger-blotch' is caused by *P. gingeri*, where a similar phenotype is observed to brown blotch, but affected areas appear with a paler colour.

1.7 Mycoviruses

Mycovirology is field that started almost 60 years ago, but in certain aspects can be considered in its infancy (Ghabrial *et al*., 2015). For many decades, information and focused research on mycoviruses was limited. This has changed in recent years through advances in technology and also the discovery that certain mycoviruses can induce hypovirulence (reducing the virus host's ability to cause disease) in phytopathogenic fungi (Nuss, 2005). The following section will describe key characteristics of mycoviruses and an up-to-date description of the ever-increasing diversity of mycoviruses. As an integral focus of this thesis, an independent segment on MVX will be provided at the end of this section.

1.7.1 Biology of mycoviruses

Viruses that infect fungi (mycoviruses) remained elusive to the scientific community until 1962, when the first mycovirus was discovered in *A. bisporus* (Hollings, 1962). The enigmatic biology of mycoviruses persisted for many decades following. Now, mycoviruses have been described in every major group of fungi, testament to their pervasiveness (Ghabrial *et al*., 2015). One of the factors leading to the lack of discovery for many years is that most mycoviruses have little impact or effect on their fungal host. This is reflected in the simplicity of some mycoviruses, including the simplest of all known virus families, the *Narnaviridae,* that have genomes that encode a single protein purely for their own replication, RNA-dependant RNA polymerase (RdRp)(Hillman and Cai, 2013). The majority of mycoviruses are obligate intracellular parasites, which rely on a range of host systems for transmission and movement (Son *et al*., 2015). Unlike

many plant and animal viruses that use 'movement proteins', mycoviruses traverse their fungal hosts vertically (within spores), horizontally (hyphal fusion) or simply through plasma streaming whereby the progressive extension of a hypha facilitates the movement of intracellular mycoviruses, although whether the movement is passive or active is unknown (Sasaki *et al*., 2006).

1.7.2 Mycovirus diversity

The latest release from the International Committee for Taxonomy of Viruses (ICTV; (Lefkowitz *et al*., 2018)) reports the identification of dsRNA virus families; *Partitiviridae, Totiviridae, Chrysoviridae, Endornaviridae, Megabirnaviridae, Reoviridae* and *Quadriviridae*. The report also includes six positive-sense single stranded RNA (ss(+)RNA) families; *Alphaflexiviridae, Narnaviridae, Barnaviridae, Deltaflexiviridae, Gammaflexiviridae* and *Hypoviridae*. A new family of (ss(+)RNA) viruses not yet incorporated into ICTV is the *Ambsetviridae* (Deakin *et al*., 2017). A single negative-sense ssRNA virus family has been described, *Mymonaviridae* (Liu *et al*., 2014). No dsDNA mycoviruses have yet been described, with only a single ssDNA virus described in the literature belonging to the family *Genomoviridae* (Yu *et al*., 2010), but these are predicted to be widespread in the environment (Krupovic *et al*., 2016). The majority of characterised mycoviruses contain dsRNA genomes (approximately 70%) and the remaining are predominantly (ss(+)RNA) genomes (Ghabrial *et al*., 2015).

1.7.3 Double-stranded RNA mycoviruses

Partitiviridae

Viruses of this family have dsRNA genomes which are small in size and bisegmented (1.3 to 2.2 Kbp). They are non-enveloped and segments are encapsidated. An RdRp is generally encoded by the larger segment and a capsid protein from the smaller segment. An additional segment is sometimes found and believed to be a satellite RNA, like that of the tripartite *Penicilium stoloniferum virus F, Pleurotus ostreatus virus 1* and *Fusarium poae virus 1* (Compel *et al*., 1999; Kim *et al*., 2005; Nogawa *et al*., 1996). One of the virus members of MVX, *Agaricus bisporus virus 4*, is classified as a partitivirus. Causal viruses for the brown disease phenotype in *A. bsiporus*, MVX dsRNA

molecules of 1.8 kbp and 2.0 kbp, were speculated as being members of Partitivirus based on the size of the molecules (Eastwood *et al*., 2015)

Chrysoviridae

These viruses currently comprise only a single genus, the *Chrysovirus*. They infect ascomyscetes and basidiomycetes exclusively, with some chrysovirus-related viruses found to infect plants through their seeds (Zhang *et al*., 2017). *Chrysovirus* members are multipartite with four dsRNA segment genomes in sizes of 2.5 to 3.6 kpb and each segment is encapsidated (Ghabrial *et al*., 2018). The causative agent for disease phenotype in La France disease, *Agaricus bisporus* virus 1 (AbV1), is thought to be a member of this family due to protein sequences showing significant similarity to other *Chrysoviridae* family members (Urayama *et al*., 2016). Although, AbV1 has an atypical genome composition for this genus with nine segments.

Megabirnaviridae

This genus contains a single assigned member, the *Rosellinia ceactrix megabirnavirus 1*. This virus has had much investigation applied to it as it is a hypovirulence-inducing mycovirus in phytopathogenic fungi (Chiba *et al*., 2009; Salaipeth *et al*., 2014). This virus has been found to persistently infect filamentous fungi *in vitro* via horizontal transmission (Chiba *et al*., 2009; Yaegashi *et al*., 2011). The genome of this virus is bisegmented with RNA 1 at 8.9 kbp and RNA 2 at 7.2 kbp (Sato *et al*., 2019).

Quadriviridae

A single genus for this family is recognised, the *Quadrivirus.* There are two reported members, the *Rosellinia necatrix quadrivirus 1* and *Leptodphaeria biglobosa quadrivirus 1* (Shah *et al*., 2018). As the family name implies, they have quadripartite dsRNA genomes (3.5-5.0 kbp). They infect filamentous fungi although pathogenicity has not been reported (Chiba *et al*., 2018). They have structurally unique virions when compared to other dsRNA viruses (Chiba *et al*., 2018).

Botybirnaviridae

A newly reported dsRNA family of viruses consisting of six members of bipartite genomes, included the new addition of *Bipolaris maydis botybirnavirus 1* which confers

hypovirulence in the phytopathogenic fungus *Botryosphaeria dothidea* (Zhai *et al*., 2019).

Totiviridae

Among dsRNA virus groups, *Totiviridae* are the best characterised (Ghabrial *et al*., 2015). These viruses are monopartite dsRNA genome viruses with a single 5'-uncapped end, linear, non-segmented dsRNA molecule within an isometric virion (Sahin and Akata, 2018). A large number of recently described virus species likely belong to this family from preliminary phylogenetic analyses, but they have not yet fully validated by the ICTV (de Lima *et al*., 2019).

Reoviridae

This family include viruses with highly segmented dsRNA genomes (as high as 12). Their icosahedral shape is due in part to the single or multi-layered concentric layers of capsid proteins (Trask *et al*., 2012). Host range of viruses from this family are broad and members which infect fungi belong to the genus *Mycoreovirus*. These viruses are monocistronic and encapsidated and three different members are tied to induction of hypovirulence in the chestnut blight fungus *Cryphoneectria parasitica* and also *Rosellinia necatrix,* a pathogen responsible for white-rot in different varieties of fruit (Turína and Rostagno, 2007; Wei *et al*., 2004).

1.7.4 Single-stranded RNA mycoviruses

Hypoviridae

Interest in mycovirology has expanded in recent years due to its application in biocontrol of phytopathogenic fungi through mycoviral-triggering of hypovirulent states in the fungal hosts (Pearson *et al*., 2009). The *Hypoviridae* name originally derives from the discovery that the earliest identified members induced hypovirulence in the chestnut blight fungus, *C. parasitica* (Peever *et al*., 2000). They have ss(+)RNA genomes and are capsidless, unable to for virions. However, not all members induce hypovirulence in hosts (Suzuki *et al*., 2018).

Narnaviridae

Narniviridae are the simplest of all mycoviruses and replicate within either the mitochondria (*Mitovirus*) or the cytosol (*Narnavirus*). They have linear ss(+)RNA genomes (2.2 kpb to 4.4 kbp) and do not code for a capsid, having only a single open reading frame (ORF) encoding an RdRp (King, 2012). Two members of this family are found in symptomless interactions with yeast, *Saccharomyces cerevisiae narnavirus 20S* and *23S* (Solórzano *et al*., 2000). A novel virus that infects the phytopathogenic fungus *Magnaporthe oryzae* has shown high sequence similarity to ourmiaviruses but distinct from *Narnaviridae*, possibly representing an intermediate between the plant virus and mycovirus (Li *et al*., 2019)

Endornaviridae

This family includes viruses with host ranges spanning fungi, oomycetes and plants. They encompass two genera, the *Alphaendornavirus* and *Betaendornavirus* separated by associated hosts and genome size, ranging from 9.7 kbp to 17.6 kbp (Sahin and Akata, 2018). Members do not form virions, with linear ss(+)RNA genomes. They are not attributed to disease phenotypes but members have been noted to minimally induce hypovirulence in fungal hosts (Osaki *et al*., 2006). Plants harbouring members of this family have been recorded to produce larger seeds in shorter period of times, an interesting pathology considering these viruses are noted to vertically transmit in plants from seeds (Khankhum and Valverde, 2018). Isolation of an endornavirus in *A. bisporus, Agaricus bisporus endornavirus 1,* has been characterised from the MVX complex (Maffettone, 2007).

Alphaflexiviridae/Deltaflexiviridae/Gammaflexiviridae

The *Alphaflexiviridae, Deltaflexiviridae* and *Gammaflexiviridae* families belong to the *Tymovirales* order. This order primarily infects plants, consists of monopartite ss(+)RNA genomes with filamentous virions (hence the flexivirus grouping). Some examples of viruses in this order include *Botrytis virus x* (*Alphaflexiviridae*), *Botrytis virus F* (*Gammaflexiviridae*) and *Fusarium graminearum deltaflexivirus 1* (*Deltaflexiviridae*) (Chen *et al*., 2016).

Barnaviridae

The only known member of this family is a virus that infects *A. bisporus* and is characterised by its bacilliform virions, *Mushroom Bacilliform Virus* (MBV). This virus is commonly found in co-infection with the *La France Isometric virus* and the RNA sequences of both are non-homologous (Romaine, 2000). MBV has an RNA genome that is 4,009 nt in length.

Ambsetviridae

The *Ambsetviridae* is a new family and contains *Agaricus bisporus* V16, although, is not yet recognised by the ICTV. AbV16 RNA 1 was grouped into its own clade and shares no homolog with any entry into the EST or TSA databases, leading the authors to propose this new family (Deakin *et al*., 2017). AbV16 is causal for *A. bisporus* mushroom cap browning (Deakin *et al*., 2017; Eastwood *et al*., 2015; Fleming-Archibald *et al*., 2015; Grogan *et al*., 2003).

1.8 Mycoviruses of *A. bisporus*

1.8.1 La France Disease

The first mycoviruses were detected as virus particles from a crop displaying the La France Isometric virus disease phenotype in the mushrooms of *A. bisporus* (J.E. Lange) Imbach. Discovery of La France disease arose from reports of dieback in mushrooms from the growing houses of the La France brothers in Pennsylvania, USA in 1948 (Sinden and Hauser, 1950), with later discovery of what was believed to be the causal particles, relating to viruses (virus-like particles) of which two were isometric (25 nm and 29 nm) and the other bacilliform (19 nm × 50 nm) (Hollings, 1962). However, these same particles would soon be isolated from healthy *A. bisporus* fruit bodies (van Zaayan, 1979). So began the field of mycovirology and many more discoveries of viruses associated with a range of fungi and oomycetes were documented (Banks *et al*., 1969; Hollings and Stone, 1969, 1971; Hollings, 1978). In the earlier years prior to much characterisation of this disease, the sporadic and widespread outbreaks of the disease on in different growing houses led to the accumulation of a variety of names, unbeknownst

to the growers, describing the same disease. These names illustrate the diversity of disease phenotypes witnessed by the growers in these times, names included; die-back (earliest name), brown disease, X-disease and watery stipe (Ghabrial, 1980; van Zaayen, 1979). Characterisation of La France greatly improved with the advent of dsRNA extraction methods, whereby a dsRNA banding pattern could be observed for diseased and healthy individuals and not rely solely upon older methods of electron microscopy (EM) (Marino *et al*., 1976; Morris, 1979). EM was an invaluable tool for identifying components of the disease such as the virus-like particles, but the resolution for distinguishing morphologically similar virus molecules is almost unobtainable, furthermore, EM may identify two morphologically similar yet genetically variant viruses as synonymous. A decade later and multiple outbreaks of La France in the Netherlands allowed a more in-depth analysis of dsRNA profiles using cross-hybridization (Harmsen *et al*., 1989). Ten novel major dsRNA molecules were described from diseased material and annotation provided corresponding to the lanes of the dsRNA gel, of which six were major dsRNAs; L1 (3.8 kbp), L2 (3.1 kbp), L3 (3.0 kbp), L4 (2.8 kbp), L5 (2.6 kpb) and M2 (1.3 kpb). Three minor dsRNAs were also reported; M1 (1.7 kbp), S1 (0.9 kbp) and S2 (0.8 kbp) with lower associations (Harmsen *et al*., 1989). A 36 nm isometric virus-like particle was co-purified with nine associated dsRNA elements and was named La France isometric virus (LIV)(Goodin, 1992). This was later changed to AbV1, as the former name was too suggestive that the virus had conclusively been considered causal forLa France disease (Van Der Lende *et al*., 1996). Although many hypothesise it is causal and constitutes a single virus, the composition of this virus is disputed. One hypothesis is that it's a single virion of nine segments, while others suggest that it is a 'multiparticle system' as nine segments seemed too large for a single particle of 34-36 nm (Ghabrial, 1998). From the time of its identification, La France has gone on to be the most commercially detrimental pathogen of *A. bisporus*, with cases of periodic outbreaks in different countries (Borodynko *et al*., 2010; Elibuyuk and Bostan, 2010).

1.8.3 Mushroom Virus X

This section will provide a broad overview of the findings related to MVX in the past two decades. A more focused review of the relevant literature can be found in **Chapter 4**.

Mushroom virus X (MVX) first appeared in mushroom crops in the UK (1996) and manifested what was referred to at the time as ‘die-back’ or bare patch disease phenotype, whereby the surfaces of the crop bed exhibited discrete barren areas surrounded by regular mushroom growth. In the following years, an increased number of farms began to report the same sightings, and this led to a notable economic loss in the UK (Gaze, 1999). As La France disease and MVX share many similarities, initial assumptions were that these curious defects in crops were from La France infections, but EM and gel-based dsRNA profiling for AbV1 showed an absence of the virus. Gel-based diagnostics did however reveal completely unrelated double-stranded RNA (dsRNA) elements (Gaze *et al*., 2000). Empirical evidence pointed to a novel disease, the enigmatic origins and properties of which have resulted in the etymology of ‘virus X’ (Gaze *et al*., 2000), a name still used to collectively describe the symptoms produced from infections. MVX began to spread throughout the UK, the Netherlands and Ireland. The range of disease symptoms expanded to include crop delay, premature veil opening, fruit body malformations and discolouration of the cap ranging from off-white, pale brown to deep browning (**Figure 1.4**) (Grogan *et al*., 2003).

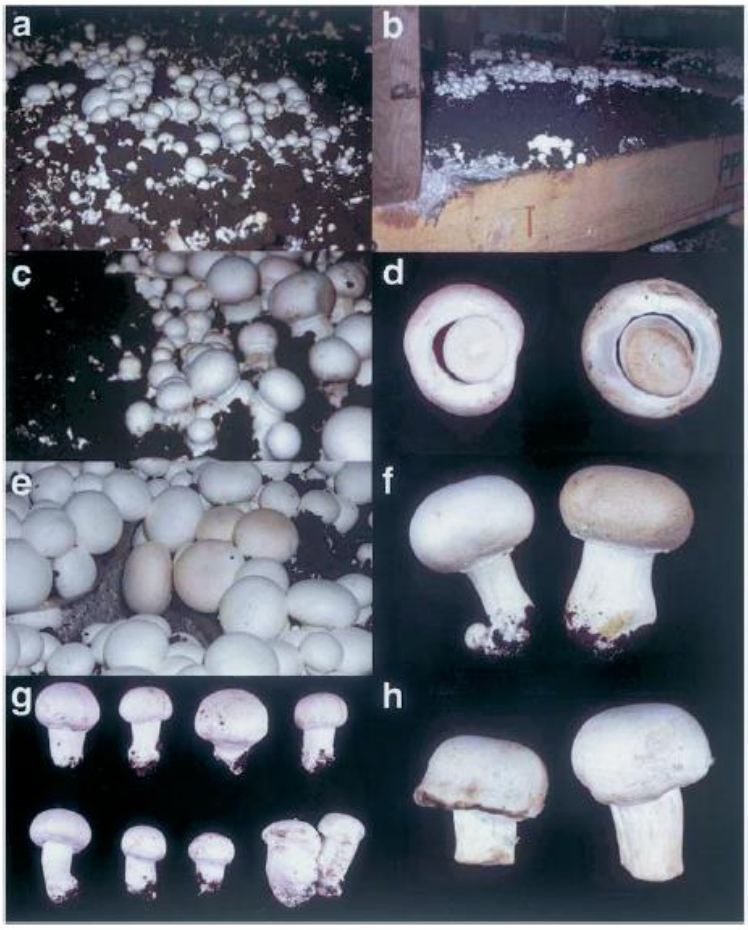

Figure 1.4: The range of MVX symptoms originally observed in *A. bisporus*: (A) Localised pinning suppression where areas of the crop do not form fully matured fruit bodies. (B) Bare patches (dieback) on crop beds of barren growth (C) A gradient from no growth areas to regular growth of mushrooms from left to right. (D) Premature veil opening. (E) Browning of mushrooms surrounded by seemingly 'healthy' white mushrooms. (F) Comparison of a healthy mushroom (left) and diseased brown mushroom (right) also showing an irregular thickened stipe. (G and H) A range in malformations in diseased mushrooms. Taken from Grogan *et al*. (2003).

It is the browning of caps that mainly distinguishes MVX infection from La France disease. Disease symptoms differed between some countries, with 'bare patches' being more prevalent in the UK while cap browning prevailed in Ireland, the Netherlands (Sonnenberg and Lavrijssen, 2004), Belgium and Poland, suggesting that geographical symptom variability may reflect variable viral composition from different locations (Burton *et al*., 2011; Deakin *et al*., 2017). In terms of MVX infection, the year 2000 was the worst for the UK, where losses were estimated at £50 M (Adie *et al*., 2004). Grogan *et al* (2003) went on to isolate dsRNA from 320 mushroom samples consisting of healthy mushrooms and mushrooms from symptomatic crops and examined and compared dsRNA banding patterns on gels. Given the range of symptoms, dsRNA banding patterns, numbers of dsRNAs and their varying sizes, it was concluded that MVX likely represented a complex of multiple viruses. The dsRNA banding profiles of symptomatic mushrooms revealed 26 distinct dsRNA molecules ranging in sizes between 0.64 Kbp and 20.2 Kbp (Grogan *et al*., 2003). Of the 26, three dsRNA bands (16.2 Kbp, 9.4 Kbp and 2.4 Kbp) were identified in 'healthy' mushrooms from farms having never reported symptoms linked to MVX. Interestingly, the 26 dsRNA bands represent the total profile, with 17 being the total number of dsRNAs being identified in a given infected isolate (Grogan *et al*., 2003). Of 26, three dsRNA bands (16.2 Kbp, 9.4 Kbp and 2.4 Kbp) were attributed to 'healthy' mushrooms from farms having never reported symptoms linked to MVX. Interestingly, the 26 dsRNA bands represent the total profile as the presence of certain bands generally results in the absence of other bands and vice versa, with 17 being the total number of bands being identified in a given infected isolate (Grogan *et al*., 2003). Furthermore, the constitution of certain bands is not random. The most characteristic and important symptomologies consistently produce the same groups of dsRNA bands. The browning phenotype consistently presented four low molecular weight bands, two larger bands at 2.0 and 1.8 Kbp and two smaller bands at 0.8 Kbp and 0.6 Kbp (Grogan *et al*., 2003). Although, banding profiles for other symptomologies were inconsistent compared to La France disease where a continuous pattern is known. Reappearing bands began to adopt names corresponding to their molecular weights, such as the largest dsRNA molecule with 'Band 1', bands found in 'healthy' fruit bodies designated 'H-1','H-2','H-3', the four bands affiliated with the brown disease phenotype 'Band 18', 'Band 19', 'Band 21', 'Band 22' and the band frequently found from bare patch disease phenotypic crops 'Band 15' (Grogan *et al*., 2004). Further research identified significant increases of transcripts, viral in origin, from white, infected, non-symptomatic mushrooms and brown,

infected mushrooms (Eastwood *et al*., 2015). It is now understood that MVX represents multiple viruses in a virus complex or virome of *A. bisporus*, composed of 18 ss(+)RNA viruses and 8 ORFans based on the presence of RdRp domains (Deakin *et al*., 2017). The change in virus characterisation from dsRNA to ss(+)RNA was made due to the similarities of the amino acid sequences to the RdRp domains of ss(+)RNA viruses (Deakin *et al*., 2017). As the authors suggest, the long and successful use in detecting these viruses with methods tailored to dsRNA, may suggest the inclusion of secondary and tertiary structures in the life cycles of these viruses. Standardised nomenclature has also been applied to these viruses, based on sequential integer values (*N*) appended to '*Agaricus bisporus virus (N)*', to proceed on from the original nomenclature for the La France disease-associated virus, AbV1. The virus causal for the brown cap disease phenotype is now referred to as AbV16 (MVX $^{2.0, 1.8, 0.8, 0.6}$formerly Band 18, 19) and the virus commonly associated with diseased crops exhibiting the bare patch disease phenotype is known as AbV6 (formerly MVX $^{3.6}$ Band 15). AbV16 was shown to be a multipartite virus consisting of four segments of RNA and AbV6 a bipartite segmented virus composed of two RNAs (Deakin *et al*., 2017). Of the 18 distinct viruses in the MVX virome, constituents showed significant homologies to sequences from a range of taxonomical families; Benyviridae (ss(+)RNA viruses of plants (Gilmer and Ratti, 2017), Narniviridae (mycovirus), Hypoviridae (mycovirus (Suzuki *et al*., 2018)), the order Tymovirales (ss(+)RNA primarily with plant hosts). AbV16 formed its own clade and was assigned to the novel mycovirus family Ambsetviridae. Original dsRNA banding profile and functional characterisation of the 18 viruses in MVX can be seen in **Figure 1.5**.

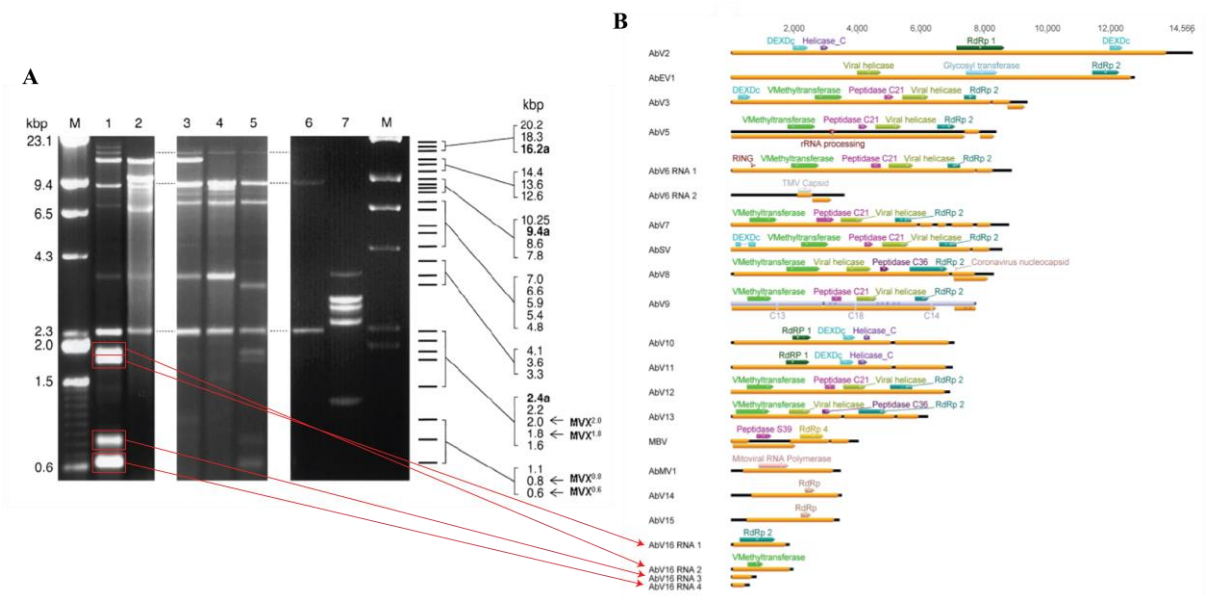

Figure 1.5: Characterisation of the viruses from MVX: (A) The original dsRNA banding profiles from multiple MVX-infected fruit bodies. Lanes 1-5 represent a range of samples symptomatic for MVX. Lane 6 is from an asymptomatic mushroom. Lane 7 is from a mushroom infected with La France disease. The schematic next to the gel image represents their band sizes (Kbp). Values in bold text designate bands found in healthy mushrooms (H1, H2, H3). (B) Illustration of the 18 viruses in the MVX complex and their genome organisation and functional protein domains. Red boxes and arrows are drawn to show which bands correspond to the multipartite RNA of AbV16. (A) is adapted from Grogan *et al*. (2003) and (B) is adapted from Deakin *et al*. (2017).

1.8.4 Modes of MVX Transmission

Members of MVX, like other ss(+)RNA viruses, are unencapsidated with no identified extracellular route of transmission. Viruses utilise modes of both vertical transmission (through sexual spores) and horizontal transmission (hyphal fusion/ anastomosis), although anastomosis appears to be the dominant route of transmission for MVX viruses (Grogan *et al*., 2004). It takes only a few segments of compost colonised with virus-infected mycelium to introduce a virus infection into a new batch of phase III compost. Additionally, research suggests that regarding AbV16, symptomatic off-coloured mushrooms are more likely to occur if the virus is introduced later in te crop cycle , such as at casing time, compared to infection at an earlier stage such as at

spawning time (Eastwood *et al*., 2015; Fleming-Archibald *et al*., 2015). With La France disease, the introduction of a vegetative incompatible strain such as *A. bitorquis*, acted as a 'virus breaker' crop due to lack of anastomoses occurring with virus-infected *A. bisporus* mycelia (Fletcher and Gaze, 2007) although, this practise is not a viable solution for commercial growers today.

1.8.5 Origins of Mushroom Virus X

The numerous members of the MVX virome and their taxonomical distributions/diversity point to multiple ancient infection events in *A. bisporus* likely prior to their cultivation in the 17th century (Deakin *et al*., 2017). As *A. bisporus* is found in terrestrial environments that span a wide geographical range (Morin *et al*., 2012), the opportunity for mycoviral diversity and adaption to this host is high. This is highlighted by the recent description of a new family of viruses within MVX alone (Deakin *et al*., 2017), the advent of new discoveries of mycoviruses in a broad range of ecosystems should shed further light onto the origins of more of these viruses. In the last year alone, metatranscriptomic analyses of soil microbiome have already grouped novel mycoviruses with the *Ambsetviridae via* RdRp homology (Starr *et al*., 2019).

The origins of the introduction of MVX into commercial practise are also enigmatic. One general hypothesis is that the development of the bulk phase III compost production system, along with the associated bulk-handling and delivery of vulnerable fully-colonised mushroom compost, may have facilitated the entry of viruses in wild populations of *A. bisporus* into commercial phase III. . This is due to the timing of MVX outbreaks which coincide with the industry's adoption and expansion of bulk phase III production. Additionally, as cultivation of *A. bisporus* is carried out *via* clonal vegetative propagation and due to only very few novel varieties being bred into production over the past three decades, *A. bisporus* is considered a monoculture crop (Sonnenberg *et al*., 2017). The monoculture situation is a platform for the outbreak of many diseases due to the scale of *A. bisporus* fungiculture and facilitates pathogen distribution from national to international ranges.

1.8.6 Other mycoviruses that infect edible fungi

Mycoviruses have been described in 14 species of edible fungi, seven of which are commercially cultivated; *Agaricus bisporus*, *Pleurotus ostreatus*, *Flammulina velutipes*, *Lentiluna edodes*, *Agrocybe aegerita*, *Boletus edulis* and *Volvariella volvacea*, and seven which are from wild populations; *Tuber aestivum*, *Tuber excavatum*, *Laccaria laccata*, *Laccaria amethystina*, *Craterellus tubaeformis*, *Lactarius rufus* and *Lactarius tabidus* (Sahin and Akata, 2018). Two dsRNA viruses have been characterised from the edible mushroom Enoki, *Flammulina velutipes*, and assigned to the *Partitiviridae* (Magae and Sunagawa, 2010). Similar to the MVX symptomologies, these viruses also cause browning in their host and are appropriately named *Flammulina velutipes browning virus*. The first segmented ss(-)RNA virus (*Lentinula edodes negative-strand RNA virus 2)* was recently described in the shiitake mushroom, *Lentinula edodes*, with an additional monopartite ss(-)RNA genome (*Lentinula edodes negative-strand RNA virus 1)* (Lin *et al*., 2019).

1.9 Host mycoviral defence

Many mycoviruses persist within fungal hosts and do not manifest deducible phenotypes or pathologies (Koloniuk *et al*., 2014; Pearson *et al*., 2009; Wang *et al*., 2013; Xie *et al*., 2011; Yaegashi *et al*., 2012). When latency transitions to acute infection and host symptom expression, this may trigger fungal defence strategies to curtail further virus replication, modulate genes of antiviral compounds and prevent further spread of virus to neighbouring hyphae.

1.9.1 RNA silencing/interference

RNA silencing/interference (RNAi) is an evolutionary conserved mechanism in eukaryotes whereby the regulation of both transcriptional and posttranscriptional processes are mediated by small noncoding RNA (sRNA) (Castel and Martienssen, 2013). There are three classes of sRNA; microRNA (miRNA), PIWI-interacting RNA (piRNA) and small interfering RNA (siRNA) (Kim *et al*., 2009; Moazed, 2009; Thomson and Lin, 2009). RNAi is also a part of the fungal innate immunity towards mycoviruses,

as virus infection can prompt the production siRNA which is initiated by the cleavage of the dsRNA of virus genomes or replicative intermediates (Chang *et al*., 2012). Cleavage is carried out by an RNase III family enzyme (Dicer) resulting in virus-derived small RNA (vsRNA) ranging in lengths of 21 – 25 nucleotides (Ding and Lu, 2011). A multiprotein effector RNA-induced silencing complex (RISC) is formed and the vsRNA is shuttled by an Argonaute protein (Ding, 2010). The passenger strand from the vsRNA is removed leaving a guide strand to direct the RISC complementary of the virus dsRNA sequence resulting in cleavage via the Argonaute protein (Ding and Lu, 2011). RNAi is further amplified by host RNA polymerases (Ding, 2010). Mycovirus mediated suppression is a counter defence whereby genes encode proteins that perform as viral suppressors of RNAi (VSR; reviewed in (Wu *et al*., 2010)). This process has been detailed in only a few instances in mycoviruses, such as CHPV-1 infections of *Aspergillus* species (Dang *et al*., 2011; Hammond *et al*., 2008). VSR is mediated by the mycovirus-encoded p29 protein which functions as an inhibitor of hairpin RNA-induced silencing (Segers *et al*., 2006). Deletion of p29 genes in CHV1 clones resulted in almost an 80% reduction in viral titre of the infected host (Suzuki and Nuss, 2002). The antiviral role these types of systems was first was first demonstrated in higher plants with the expression of viral RNA from transgenic *Nicotiana tabacum* aided in the prevention of infection from other similar viruses (Lindbo and Dougherty, 1992). RNAi has been demonstrated in many plants and lower eukaryotes, with the core processes of these systems being shared amongst diverse eukaryotes (Csorba *et al*., 2009).

Cryphonectria hypovirus 1 (CHV-1) infection in the phytopathogenic fungus responsible for chestnut blight *Cryphonectria parasitica*, is a successful biological control agent that induces hypovirulence. Studies have shown *C. parasitica* elicits the response of two genes for Dicer and Argonuate activity, *dcl2* and *agl2*, as a defensive RNA-silencing response to CHV-1 (Zhang *et al*., 2014). *Fusarium graminearum* features four RNAi genes responsive to mycoviral infection, *rdr1*, *dcl1*, *dcl2* and *agl2* (Lee *et al*., 2014). However, two separate viruses elicit distinct responses to infection. *Fusarium graminearum virus 1* (FGV1) induces the down-regulation of *dcl2* and *agl2*, whereas *Fusarium graminearum virus 2-4* (FGV2-4) causes an increase of abundance in transcripts for these genes (Lee *et al*., 2014). RNAi systems have not been actively linked as a mechanistic response to MVX in *A. bisporus*. In contrast, genes identified with

related functions in RNAi were downregulated during MVX infection in the commercial hybrid strain A15 (Deakin, 2015).

1.9.2 Antiviral Proteins

There are proteins which directly interact with mycoviruses to hamper their activities within cells. An example of antiviral proteins include the SKI (superkiller) proteins that are encoded and well characterised in *S. cerevisiae* (Widner and Wickner, 1993). SKI1/XRN1complex contains an RNA helicase module which performs 3'-mRNA degradation activity while SKI2, 3 and 8 prevent virus replication by blocking translation through the recognition of the absence of CAP or poly(A) tails (Benard *et al*., 1998).

1.9.3 Vegetative incompatibility

The life cycles of mycoviruses, with very few exceptions (Yu *et al*., 2013), occur entirely intracellularly. The successful transmission of virus within hyphae depend on transmission through sexual spores or by the more commonly reported route of anastomosis with neighbouring hyphae (Ghabrial *et al*., 2015). Somatic exchange or plasmogamy must occur and if viruses have not moved past hyphal compartments from the apices of hyphae, post-fusion programmed cell death is detrimental to their survival (Leslie and Zeller, 1996). The vegetative incompatibility system is governed by specific *vic* genes and pheromone receptors (Pál *et al*., 2007). This system is a source of nonself allorecognition, which is widely used in fungi as a virus attenuating system.

1.10 Functional analyses of the *A. bisporus* genome

This section details the initial genome sequencing of *A. bisporus* and a selection of the transcriptomic and proteomic analyses that were made possible through the availability of a reference genome.

1.10.1 Sequencing

As mentioned in **Section 1.3.2**, the first whole genome sequencing of *A. bisporus* was completed in 2012 for the genome of H97, a constituent homokaryon of the hybrid variety U1 (Morin *et al*., 2012). This was accompanied with genome sequencing of the tetrasporic variety*A. bisporus* var. *burnettii*. The *A. bisporus* genome sequence revealed similarities to wood decomposing fungi in relation to enzymatic repertoires of polysaccharide-degrading enzymes. The transcriptome was also used to decipher the regulation of genes in commercial substrates and revealed niche adaptions to environments with high levels of humic acid through the expansion of heme-thiolate peroxidases and β-etherases. A common motif was identified in promoter regions of the most highly regulated genes in compost. This motif was also found in orthologous genes of *C. cinerea* and *L. bicolor*, but the frequency of this motif is much higher in *A. bisporus*. These motifs were found in both H97 and var. *burnettii*. This distinguishes the *A. bisporus* genome from that of other wood decomposers and leaf litter saprobes as an adapted niche of humicolous environments (Morin *et al*., 2012). With the sequencing of the second constituent homokaryon of U1, H39, the representative genomes of both nuclear types were made available (Sonnenberg *et al*., 2016). The SNPs of 139 SSIs homokaryotic offspring were mapped to areas of chromosomal crossovers from U1. The information gleaned from two high quality genomes showed that although parental genomes are highly heterozygous, this heterozygosity is carried over to offspring and rates of recombination are low and localised within 100 Kb of chromosome ends (Sonnenberg *et al*., 2016). These studies highlight the potential that high quality genomes possess for molecular studies in *A. bisporus* research.

1.10.2 Transcriptomic studies

The genome sequencing of *A. bisporus* allows for the analysis of gene expression patterns in *A. bisporus*, exemplified in studies relating to MVX, drought-tolerance and fruit body biology. The design of microarrays to investigate gene regulation and a reference genome for mapping transcripts from RNA-seq experiments have been made from the availability of the genome. These examples relate solely to studies focusing on the gene expression for *A. bisporus* genes.

Researchers have used suppression subtractive hybridisation (SSH; the targeted sequencing of amplified cDNA that differ from a treatment transcriptome to a control transcriptome) and microarray technologies to sequence non-host viral transcripts of MVX (Eastwood *et al*., 2015). Host transcripts were additionally deciphered in diseased, brown fruit bodies which were up-regulated in relation to amino acid metabolism, transcription and vesicle transport and down-regulated for multiple ribosomal proteins, protein turnover and cell signalling (Eastwood *et al*., 2015). Initiation responses for fruitification in *A. bisporus* were studied in relation to the roles of the two crucial stimuli, 1-octen-3-ol and CO_2 (Eastwood *et al*., 2013). SSH was used to target a subset of 45 genes important for the switch from vegetative growth to reproductive growth and promoter regions mapped from the *A. bisporus* genome to reveal the crucial motifs located in specific gene cluster (Eastwood *et al.*, 2013). Another group have used high-density microarray hybridisation was used to assess the function of drought stress-responsive genes to reveal the protective role of riboflavin (Guhr *et al*., 2017). Gene expression revealed detoxification and stress-priming response in drought inducing treatments, a process previously only investigated in plants (Guhr *et al*., 2017). The high resolution of RNA-seq was demonstrated in a study examining the nucleus-specific mRNA expression and functional impact between heterologous nuclei typically found in dikaryotic cells of *A. bisporus* (Gehrmann *et al*., 2018). Gene expression revealed the differential roles that individual genotypes play during physiological development in *A. bisporus*, particularly in the fruit body compared to the mycelium (Gehrmann *et al*., 2018). The transcription factor, C_2H_2, was identified for its potential as role in fruit body formation (Pelkmans *et al*., 2016). *Agrobacterium*-mediated transformation was adapted to over-express this transcription factor, resulting in early formation of fruit bodies. RNA-seq was used to reveal the differential regulation of genes in early stages of primordia formation to mature fruit bodies of transformants (Pelkmans *et al*., 2016).

1.10.3 Proteomic studies

Studies identifying protein products of *A. bisporus* have ranged from mushroom quality studies, medicinal proteins and pathology of fungal pathogens. A targeted proteomics approach was used to underline the biochemical response of "browning" to *A. bisporus* fruit bodies post-harvest (Chen *et al*., 2017). This approach facilitated

analyses where temporal findings were overlapped in four time-points to deduce proteins common in each phase of post-harvest maturation, and revealed reoccurring functional processes relating to signal transduction, DNA binding, and endopeptidase activities. An analysis of fruit body low molecular weight proteins and their antihypertensive activities in people with high blood pressure, has demonstrated that the applications of proteomic technologies on *A. bisporus* can extend beyond understanding the biology of *A. bisporus* and into human health (Lau *et al*., 2012). Proteomics has been used to characterise the interaction of *A. bisporus* with a prominent fugal pathogen (O'Brien *et al*., 2014). The virulence of *Trichoderma aggressivum* was studied in *A. bisporus* tissue through proteomic characterisation of infected cellular contents, revealing proteins functioning in oxidative stress tolerance, cell integrity and constituents of cystoskeletal structures.

1.10.4 Combination transcriptomic proteomic studies

To the authors knowledge, to date, there have been two published studies which combined transcriptomic and proteomic analyses for *A. bisporus* (Patyshakuliyeva *et al*., 2015; Pontes *et al*., 2018). The first examined the breakdown of plant biomass throughout the life cycle of *A. bisporus*. Gene expression analysis revealed that ligninolytic enzymes were most active during spawning and the secretome were highly represented by cellulose-degrading enzymes (Patyshakuliyeva *et al*., 2015). The second study focused on the physiological roles of different wild strains of *A. bisporus* to break down compounds that are poorly utilised by the commercial A15 strain, such as xylosyl and glucosyl residues (Pontes *et al*., 2018). RNA-seq revealed the most highly expressed genes related to carbohydrate-active enzymes and LC-MS/MS profiled these enzymes within fruit bodies. These techniques revealed a conserved molecular machinery between wild strains and A15 for the breakdown of an array of compost carbohydrates (Pontes *et al*., 2018). These systematic approaches demonstrate the strengths of combing the transcriptomic and proteomic responses of complicated molecular systems in *A. bisporus*. These state-of-the-art omics-based techniques are significantly enhanced with the availability of high-quality genomes for *A. bisporus.*

1.11 Aims and Objectives

Since the first reports of MVX in commercial cultivation over two decades ago, research has been conducted on the description of causative agents of disease and symptomologies of MVX (Eastwood *et al*., 2015; Fleming-Archibald *et al*., 2015; Grogan *et al*., 2003; Gaze *et al*., 2000) and characterisation of the viruses (Burton *et al*., 2011; Deakin *et al*., 2017; Eastwood *et al*., 2015; Green, 2011; Deakin, 2015; Maffettone, 2007). Yet knowledge of the host response to these viruses is limited. One published study exists which identified a small number of differentially regulated genes from MVX-infected fruit bodies from the susceptible strain, A15, but the focus of that particular work was primarily placed upon the non-*Agaricus* transcripts (Eastwood *et al*., 2015). The strategy through which transmission of the viruses into healthy hosts has been identified as anastomosis (Grogan, 2003), but no molecular studies exist for the process of anastomosis in *A. bisporus.* Additionally, no study has ever demonstrated the behaviour of these viruses in the mycelium or provided much evidence for their intracellular transport.

The main overarching hypotheses which have driven the work detailed in this thesis include the following:

Hypothesis 1: Vegetative incompatibility acts as a barrier to virus transmission. Therefore, the key to MVX-resistance is cultivation of strains which do not readily anastomose with the susceptible commercial strain A15.

Hypothesis 2: The introduction of infectious MVX material at a later point in the cropping cycle results in a greater level of disease in the fruit bodies. This is due to an inability of the host to mount a response to infection whilst undergoing the morphogenic switch from vegetative growth to reproductive growth.

Hypothesis 3: The current commercially cultivated monoculture (strain A15) is susceptible to infection by MVX. The establishment of wild germ plasm into commercial breeding may be a valuable reservoir of resistance attributes to MVX.

These hypotheses were tested with a combination of the following main experiments constituting the work of **Chapters 2-5**:

(I) Sequence and assemble the first genome of a commercially-relevant wild strain of *A. bisporus* var *bisporus*. (**Chapter 2**)

(II) Characterise the process of anastomosis between different strains of *A. bisporus* using a proteomic approach. (**Chapter 3**)

(III) Document the transmission of MVX in the vegetative mycelium and into the fruit bodies of a variety of *A. bisporus* strains. (**Chapter 4**)

(IV) Characterise the transcriptomes and proteomes of these varietal strains upon MVX infection. (**Chapter 4**)

(V) Adapt and develop a method to visualise the key viruses in the MVX complex. (**Chapter 5**)

Literature Cited

Adl, S.M., Simpson, A.G.B., Farmer, M.A., Andersen, R.A., Anderson, O.R., Barta, J.R., Bowser, S.S., Brugerolle, G., Fensome, R.A., Fredericq, S., James, T.Y., Karpov, S., Kugrens, P., Krug, J., Lane, C.E., Lewis, L.A., Lodge, J., Lynn, D.H., Mann, D.G., McCourt, R.M., Mendoza, L., Moestrup, O., Mozley-Standridge, S.E., Nerad, T.A., Shearer, C.A., Smirnov, A. V, Spiegel, F.W., Taylor, M.F.J.R., 2005. The new higher level classification of eukaryotes with emphasis on the taxonomy of protists. J. Eukaryot. Microbiol. 52, 399–451.

Adie, B., Choi, I., Soares, A., Holcroft, S., Eastwood, D. C., Mead, A., Grogan, H. M., Kerrigan, R. W., Challen, M., and Mills, P. R. (2004). MVX disease and double-stranded RNA elements in Agaricus bisporus. Mushroom Sci. 16: 411-420.

Banks, G.T., Buck, K.W., Chain, E.B., Darbyshire, J.E., Himmel Weit, F., 1969. Virus-like Particles in Penicillin producing Strains of Penicillium chrysogenum. Nature 222, 89–90.

Bell, A.A., Wheeler, M.H., 1986. Biosynthesis and Functions of Fungal Melanins. Annu. Rev. Phytopathol. 24, 411–451.1

Benard, L., Carroll, K., Valle, R.C.P., Wickner, R.B., 1998. Ski6p Is a Homolog of RNA-Processing Enzymes That Affects Translation of Non-Poly(A) mRNAs and 60S Ribosomal Subunit Biogenesis. Mol. Cell. Biol. 18, 2688–2696.

Blakeslee, A.F., 1904. Sexual Reproduction in the Mucorineae. Proc. Am. Acad. Arts Sci. 40, 205.

Bord Bia (2019). Irish food board. https://bordbia.ie/industry/sector-profiles/irish-horticulture-industry

Borodynko, N., Hasiow-Jaroszewska, B., Rymelska, N., Pospieszny, H., 2010. La France disease of the cultivated mushroom Agaricus bisporus in Poland. Acta Virol. 54, 217–219.

Brodey, C.L., 1991. Research Notes Bacterial Blotch Disease of the Cultivated Mushroom Is Caused by an Ion Channel Forming Lipodepsipeptide Toxin. Mol. Plant-Microbe Interact. 4, 407.

Burton, K., Green, J., Baker, A., Eastwood, D. a N., Grogan, H., 2011. Mushroom Virus X – the Identification of Brown Cap Mushroom Virus and a New Highly Sensitive Diagnostic Test for Phase Iii Compost. Proc. 7th Int. Conf. Mushroom Biol. Mushroom Prod. 466–473.

Burton, K.S., Noble, R., 1993. The influence of flush number, bruising and storage temperature on mushroom quality. Postharvest Biol. Technol. 3, 39–47.

Callac, P., 1995. Breeding of edible fungi with emphasis on the variability among French genetic resources of Agaricus bisporus. Can. J. Bot. 73, 980–986.

Callac, P., Imbernon, M., Kerrigan, R.W. and Olivier, J.M., 1996. The two life cycles of Agaricus bisporus. Mushroom biology and mushroom products, pp.57-66.

Callac, P., Billette, C., Imbernon, M., Kerrigan, R.W., 1993. Morphological, Genetic, and Interfertility Analyses Reveal a Novel, Tetrasporic Variety of Agaricus

bisporus from the Sonoran Desert of California. Mycologia 85, 835.

Callac, P., Moquet, F., Imbernon, M., Guedes-Lafargue, M.R., Mamoun, M., Olivier, J.-M., 1998. Evidence forPPC1, a Determinant of the Pilei-Pellis Color of Agaricus bisporus Fruitbodies. Fungal Genet. Biol. 23, 181–188.

Callac, P., Theochari, I., Kerrigan, R.W., 2002. The germplasm of Agaricu bisporus: Main results after ten years of collecting in France, in Greece, and in North America.. Acta Hortic. 49–55.

Callac, P., Xu, J., Desmerger, C., 2002. Fine-scale genetic analyses reveal unexpected spatial-temporal heterogeneity in two natural populations of the commercial mushroom Agaricus bisporus. Microbiology 148, 1253–1262.

Carrasco, J., Tello, M.L., de Toro, M., Tkacz, A., Poole, P., Pérez-Clavijo, M., Preston, G., 2019. Casing microbiome dynamics during button mushroom cultivation: implications for dry and wet bubble diseases. Microbiology 165, 611–624.

Castel, S.E., Martienssen, R.A., 2013. RNA interference in the nucleus: roles for small RNAs in transcription, epigenetics and beyond. Nat. Rev. Genet. 14, 100–112.

Chang, S.-S., Zhang, Z., Liu, Y., 2012. RNA Interference Pathways in Fungi: Mechanisms and Functions. Annu. Rev. Microbiol. 66, 305–323.

Chen, M., Liao, J., Li, H., Cai, Z., Guo, Z., Wach, M.P., Wang, Z., 2017. iTRAQ-MS/MS Proteomic Analysis Reveals Differentially Expressed Proteins During Post-harvest Maturation of the White Button Mushroom Agaricus bisporus. Curr. Microbiol. 74, 641–649.

Chen, X., He, H., Yang, X., Zeng, H., Qiu, D., Guo, L., 2016. The complete genome sequence of a novel Fusarium graminearum RNA virus in a new proposed family within the order Tymovirales. Arch. Virol. 161, 2899–2903

Chiba, S., Castón, J.R., Ghabrial, S.A., Suzuki, N., 2018. ICTV Virus Taxonomy Profile: Quadriviridae. J. Gen. Virol. 99, 1480–1481.

Chiba, S., Salaipeth, L., Lin, Y.-H., Sasaki, A., Kanematsu, S., Suzuki, N., 2009. A Novel Bipartite Double-Stranded RNA Mycovirus from the White Root Rot Fungus Rosellinia necatrix: Molecular and Biological Characterization, Taxonomic Considerations, and Potential for Biological Control. J. Virol. 83, 12801–12812.

Compel, P., Papp, I., Bibó, M., Fekete, C., Hornok, L., 1999. Genetic interrelationships and genome organization of double-stranded RNA elements of Fusarium poae. Virus Genes.

Csorba, T., Pantaleo, V., Burgyán, J., 2009. RNA Silencing: An Antiviral Mechanism, in: Advances in Virus Research. pp. 35–230.

Dang, Y., Yang, Q., Xue, Z., Liu, Y., 2011. RNA Interference in Fungi: Pathways, Functions, and Applications. Eukaryot. Cell 10, 1148–1155.

de Lima, J.G.S., Teixeira, D.G., Freitas, T.T., Lima, J.P.M.S., Lanza, D.C.F., 2019. Evolutionary origin of 2A-like sequences in Totiviridae genomes. Virus Res. 259, 1–9.

De Tournefort, J.P., 1797. Élémens de Botanique, ou méthode pour connoître les plantes (Vol. 1). chez Pierre Bernuset et comp..

Deakin, G., Dobbs, E., Bennett, J.M., Jones, I.M., Grogan, H.M., Burton, K.S., 2017. Multiple viral infections in Agaricus bisporus - Characterisation of 18 unique RNA viruses and 8 ORFans identified by deep sequencing. Sci. Rep. 7, 2469.

Deakin G, 2015. Understanding the Biology of Mushroom Virus X by Molecular Characterisation of Viral RNAs and their Role in Disease Epidemiology. PhD dissertation, East Malling Research.

Ding, S.-W., 2010. RNA-based antiviral immunity. Nat. Rev. Immunol. 10, 632–644.

Ding, S.-W., Lu, R., 2011. Virus-derived siRNAs and piRNAs in immunity and pathogenesis. Curr. Opin. Virol. 1, 533–544.

Eastwood, D., Green, J., Grogan, H., Burton, K., 2015. Viral Agents Causing Brown Cap Mushroom Disease of Agaricus bisporus. Appl. Environ. Microbiol. 81, 7125–7134.

Eastwood, D.C., Herman, B., Noble, R., Dobrovin-Pennington, A., Sreenivasaprasad, S., Burton, K.S., 2013. Environmental regulation of reproductive phase change in Agaricus bisporus by 1-octen-3-ol, temperature and CO2. Fungal Genet. Biol. 55, 54–66.

Elibuyuk, I. O. and Bostan, H. (2010). Detection of a virus disease on white button mushroom (Agaricus bisporus) in Ankara, Turkey. Int. J. Agric. Biol. 12: 597-600.

Elliott, T.J., Langton, F.A., 1981. Strain improvement in the cultivated mushroom Agaricus bisporus. Euphytica 30, 175–182.

Elliott T.J. (1972). Sex and the single spore. Mush. Sci. 8: 11-18.

Elliott, T.J., 1985. Genetics and breeding of species of Agaricus. Biology and technology of the cultivated mushroom/edited by PB Flegg, DM Spencer, and DA Wood.

Evans, H.J., 1959. Nuclear behaviour in the cultivated mushroom. Chromosoma.

FAOSTAT (2019). Food and Agriculture Organization Statistics Division (United Nations) http://faostat.fao.org/site/567/default.aspx#ancor.

Ferguson, Margaret C. " A preliminary study of the germination of the spores of Agaricus campestris and other Basidiomycetous fungi." Bull. U.S. Bur. PI. Ind. No. 16 (1902).

Fermor, T.R., Wood, D.A., Lincoln, S.P., Fenlon, J.S., 1991. Bacteriolysis by Agaricus bisporus. J. Gen. Microbiol. 137, 15–22.

Flegg, P.B. & Wood, D.A. (1985) Growth and fruiting, in The Biology and Technology of the Cultivated Mushroom (eds P.B. FJegg, D.M. Spencer & D.A. Wood), John Wiley & Sons, chichester, New York, pp. 141-78.

Fleming-Archibald, C., Ruggiero, A., Grogan, H.M., 2015. Brown mushroom symptom expression following infection of an Agaricus bisporus crop with MVX associated dsRNAs. Fungal Biol. 119, 1237–1245.

Fletcher T., Gaze, H., 2007. Mushroom Pest and Disease Control, A Colour Handbook. CRC Press.

Fritsche, GE, 1978. Breeding work. The biology and cultivation of edible mushrooms, pp.239-248.

Galen, Powell, O., Wilkins, J., 2003. Galen: On the Properties of Foodstuffs, Galen: On the Properties of Foodstuffs. Cambridge University Press, Cambridge.

Gaze, R.H. (1999). Virus in disguise? Mushroom J. 590, 17–19.

Gehrmann, T., Pelkmans, J.F., Ohm, R.A., Vos, A.M., Sonnenberg, A.S.M., Baars, J.J.P., Wösten, H.A.B., Reinders, M.J.T., Abeel, T., 2018. Nucleus-specific expression in the multinuclear mushroom-forming fungus Agaricus bisporus reveals different nuclear regulatory programs. Proc. Natl. Acad. Sci. U. S. A.

Gerrits, J., 1988. Nutrition and compost. In: van Griensven, L. (Ed.), The Cultivation of Mushrooms. Darlington Mushroom Laboratories Ltd., UK, pp. 29–72.

Ghabrial, S.A., 1998. Origin, adaptation and evolutionary pathways of fungal viruses. Virus Genes.

Ghabrial, S.A., 1980. Effects of Fungal Viruses on Their Hosts. Annu. Rev. Phytopathol. 18, 441–461.

Ghabrial, S.A., Castón, J.R., Coutts, R.H.A., Hillman, B.I., Jiang, D., Kim, D.-H., Moriyama, H., 2018. ICTV Virus Taxonomy Profile: Chrysoviridae. J. Gen. Virol. 99, 19–20.

Ghabrial, S.A., Castón, J.R., Jiang, D., Nibert, M.L., Suzuki, N., 2015. 50-plus years of fungal viruses. Virology 479–480, 356–368.

Giesy, R.M., Day, P.R., 1965. The Septal Pores of Coprinus lagopus in Relation to Nuclear Migration. Am. J. Bot.

Goodin, M.M., 1992. Encapsidation of the La France Disease-Specific Double-Stranded RNAs in 36-nm Isometric Viruslike Particles. Phytopathology.

Green JM, 2010. Investigating gene expression and brown colour development in the edible mushroom Agaricus bisporus during Mushroom Virus X infection. PhD dissertation, Warwick University.

Grogan, H.M., Adie, B.A.T., Gaze, R.H., Challen, M.P., Mills, P.R., 2003. Double-stranded RNA elements associated with the MVX disease of Agaricus bisporus. Mycol. Res. 107,

Grogan, H.M., Tomprefa, N., J., M., Holcroft, S., Gaze, R., 2004. Transmission of Mushroom Virus X Disease in crops. Mushroom Sci. XVI - Sci. Cultiv. Edible Med. Fungi (eds Romaine, C. P., Keil, C. B., Rinker, D. J. Royse, D. J.) 489–498.

Guhr, A., Horn, M.A., Weig, A.R., 2017. Vitamin B 2 (riboflavin) increases drought tolerance of Agaricus bisporus. Mycologia 109, 860–873.

Hadjivasiliou, Z., Pomiankowski, A., Kuijper, B., 2016. The evolution of mating type switching. Evolution.

Halász, K., Geösel, A., Szarvas, J., Virágh, N., Hajdú, C., Lukács, N., 2014. Occurrence

of double-stranded RNA species in champignon and their relation to Mushroom Virus X symptoms. Acta Aliment. 43, 592–603.

Hammond, T.M., Andrewski, M.D., Roossinck, M.J., Keller, N.P., 2008. Aspergillus Mycoviruses Are Targets and Suppressors of RNA Silencing. Eukaryot. Cell 7, 350–357.

Harmsen, M.C., van Griensven, L.J.L.D., Wessels, J.G.H., 1989. Molecular Analysis of Agaricus bisporus Double-stranded RNA. J. Gen. Virol. 70, 1613–1616.

Harris, C. R. (1986). Pure white mushrooms - how were they developed? Mushroom News 34: 10-12.

Hibbett, D.S., Binder, M., Bischoff, J.F., Blackwell, M., Cannon, P.F., Eriksson, O.E., Huhndorf, S., James, T., Kirk, P.M., Lücking, R., Thorsten Lumbsch, H., Lutzoni, F., Matheny, P.B., McLaughlin, D.J., Powell, M.J., Redhead, S., Schoch, C.L., Spatafora, J.W., Stalpers, J.A., Vilgalys, R., Aime, M.C., Aptroot, A., Bauer, R., Begerow, D., Benny, G.L., Castlebury, L.A., Crous, P.W., Dai, Y.-C., Gams, W., Geiser, D.M., Griffith, G.W., Gueidan, C., Hawksworth, D.L., Hestmark, G., Hosaka, K., Humber, R.A., Hyde, K.D., Ironside, J.E., Kõljalg, U., Kurtzman, C.P., Larsson, K.-H., Lichtwardt, R., Longcore, J., Miądlikowska, J., Miller, A., Moncalvo, J.-M., Mozley-Standridge, S., Oberwinkler, F., Parmasto, E., Reeb, V., Rogers, J.D., Roux, C., Ryvarden, L., Sampaio, J.P., Schüßler, A., Sugiyama, J., Thorn, R.G., Tibell, L., Untereiner, W.A., Walker, C., Wang, Z., Weir, A., Weiss, M., White, M.M., Winka, K., Yao, Y.-J., Zhang, N., 2007. A higher-level phylogenetic classification of the Fungi. Mycol. Res. 111, 509–547.

Hillman, B.I., Cai, G., 2013. The Family Narnaviridae, in: Advances in Virus Research. pp. 149–176.

Hollings, M., 1978. Mycoviruses: Viruses that Infect Fungi, in: Advances in Virus Research. pp. 1–53.

Hollings, M., 1962. Viruses Associated with A Die-Back Disease of Cultivated Mushroom. Nature 196, 962–965.

Hollings, M., Stone, O.M., 1971. Viruses that Infect Fungi. Annu. Rev. Phytopathol. 9, 93–118.

Hollings, M., Stone, O.M., 1969. Viruses in fungi. Sci. Prog.

Hort, A. 1916. Theophrastus: Enquiry into Plants. (English transl.). London: Heinemann. 2 vols.: 475, 499 pp.

Hsueh, Y.-P., Fraser, J.A., Heitman, J., 2008. Transitions in Sexuality: Recapitulation of an Ancestral Tri- and Tetrapolar Mating System in Cryptococcus neoformans. Eukaryot. Cell 7, 1847–1855.

Iiyama, K., Stone, B.A., Macauley, B.J., 1994. Compositional Changes in Compost during Composting and Growth of Agaricus bisporus. Appl. Environ. Microbiol. 60, 1538–46.

Imbernon, M., Callac, P., Gasqui, P., Kerrigan, R.W., Velcko, A.J., 1996. BSN, the Primary Determinant of Basidial Spore Number and Reproductive Mode in Agaricus bisporus, Maps to Chromosome I. Mycologia 88, 749.

Jones, D.M., 1958. Hjalmar Frisk: Griechisches etymologisches Wörterbuch. Lieferung 4. Pp. 289–384. Heidelberg: Winter, 1956. Paper, DM. 8.60. Classical Rev. 8, 186–186.

Jurak, E., Kabel, M.A., Gruppen, H., 2014. Carbohydrate composition of compost during composting and mycelium growth of Agaricus bisporus. Carbohydr. Polym. 101, 281–

Kerrigan, R.W., 1995. Global genetic resources for Agaricus breeding and cultivation. Can. J.

Kerrigan, R.W., 1991. What on earth is the Agaricus recovery program? Mycologist 5, 22.

Kerrigan, R.W., Horgen, P.A., Anderson, J.B., 1993. The California Population of Agaricus bisporus Comprises at Least Two Ancestral Elements. Syst. Bot. 18, 123.

Kerrigan, R.W., Imbernon, M., Callac, P., Billette, C., Olivier, J.-M., 1994. The Heterothallic Life Cycle of Agaricus bisporus var. burnettii and the Inheritance of Its Tetrasporic Trait. Exp. Mycol. 18, 193–210.

Kerrigan, R.W., Royer, J.C., Baller, L.M., Kohli, Y., Horgen, P.A., Anderson, J.B., 1993. Meiotic behavior and linkage relationships in the secondarily homothallic fungus Agaricus bisporus. Genetics 133, 225–36.

Khankhum, S., Valverde, R.A., 2018. Physiological traits of endornavirus-infected and endornavirus-free common bean (Phaseolus vulgaris) cv Black Turtle Soup. Arch. Virol. 163, 1051–1056.

Kim, J.W., Choi, E.Y., Lee, J. Il, 2005. Genome Organization and Expression of the Penicillium stoloniferum Virus F. Virus Genes 31, 175–183.

Kim, V.N., Han, J., Siomi, M.C., 2009. Biogenesis of small RNAs in animals. Nat. Rev. Mol. Cell Biol. 10, 126–139. h

King, A., 2012. Narnaviridae, in: Virus Taxonomy. Elsevier, pp. 1055–1060.

Koloniuk, I., El-Habbak, M.H., Petrzik, K., Ghabrial, S.A., 2014. Complete genome sequence of a novel hypovirus infecting Phomopsis longicolla. Arch. Virol. 159, 1861–1863.

Krah, F.-S., Büntgen, U., Schaefer, H., Müller, J., Andrew, C., Boddy, L., Diez, J., Egli, S., Freckleton, R., Gange, A.C., Halvorsen, R., Heegaard, E., Heideroth, A., Heibl, C., Heilmann-Clausen, J., Høiland, K., Kar, R., Kauserud, H., Kirk, P.M., Kuyper, T.W., Krisai-Greilhuber, I., Norden, J., Papastefanou, P., Senn-Irlet, B., Bässler, C., 2019. European mushroom assemblages are darker in cold climates. Nat. Commun. 10, 2890.

Krupovic, M., Ghabrial, S.A., Jiang, D., Varsani, A., 2016. Genomoviridae: a new family of widespread single-stranded DNA viruses. Arch. Virol. 161, 2633–2643.

Kumar S and Sharma Y, 2011. Diversity of wild mushrooms from Jammu and Kashmit (India). Proceedings of the 7th International Conference on Mushroom Biology and Mushroom Products (ICMBMP7) Section: Economical and societal features.

Lau, C.-C., Abdullah, N., Shuib, A.S., Aminudin, N., 2012. Proteomic Analysis of

Antihypertensive Proteins in Edible Mushrooms. J. Agric. Food Chem. 60, 12341–12348.

Leatham, G.F., 1981. Cultivation of shiitake, the Japanese forest mushroom, on logs: a potential industry for the United States. Forest Products Laboratory

Lee, K.-M., Cho, W.K., Yu, J., Son, M., Choi, H., Min, K., Lee, Y.-W., Kim, K.-H., 2014. A comparison of transcriptional patterns and mycological phenotypes following infection of Fusarium graminearum by four mycoviruses. PLoS One 9, e100989.

Lefkowitz, E.J., Dempsey, D.M., Hendrickson, R.C., Orton, R.J., Siddell, S.G., Smith, D.B., 2018. Virus taxonomy: the database of the International Committee on Taxonomy of Viruses (ICTV). Nucleic Acids Res. 46, D708–D717.

Leslie, J.F., Zeller, K.A., 1996. Heterokaryon incompatibility in fungi—more than just another way to die. J. Genet. 75, 415–424.

Li, C., Zhu, J., Gao, B., Zhu, H., Zhou, Q., Zhong, J., 2019. Characterization of a Novel Ourmia-Like Mycovirus Infecting Magnaporthe oryzae and Implications for Viral Diversity and Evolution. Viruses 11, 223.

Li, D., Sossah, F.L., Yang, Y., Liu, Z., Dai, Y., Song, B., Fu, Y., Li, Y., 2019. Genetic and Pathogenic Variability of Mycogone perniciosa Isolates Causing Wet Bubble Disease on Agaricus bisporus in China. Pathogens 8, 179.

Lin, Y.-H., Fujita, M., Chiba, S., Hyodo, K., Andika, I.B., Suzuki, N., Kondo, H., 2019. Two novel fungal negative-strand RNA viruses related to mymonaviruses and phenuiviruses in the shiitake mushroom (Lentinula edodes). Virology 533, 125–136.

Lin X, Heitman J. 2007. Mechanisms of Homothallism in Fungi and Transitions between Heterothallism and Homothallism, p 35-57. In Heitman J, Kronstad J, Taylor J, Casselton L (ed), Sex in Fungi. ASM Press, Washington, DC.

Lindbo, J.A., 1992. Pathogen-Derived Resistance to a Potyvirus: Immune and Resistant Phenotypes in Transgenic Tobacco Expressing Altered Forms of a Potyvirus Coat Protein Nucleotide Sequence. Mol. Plant-Microbe Interact. 5, 144.

Liu, B., 1958. The primary investigation on utilization of the fungi by ancient Chinese. Shansi Normal College Journal, 1, pp.49-67.

Liu, L., Xie, J., Cheng, J., Fu, Y., Li, G., Yi, X., Jiang, D., 2014. Fungal negative-stranded RNA virus that is related to bornaviruses and nyaviruses. Proc. Natl. Acad. Sci. 111,

Loron, C.C., François, C., Rainbird, R.H., Turner, E.C., Borensztajn, S., Javaux, E.J., 2019. Early fungi from the Proterozoic era in Arctic Canada. Nature.

Lu, D., 2014. Ancient Chinese people's knowledge of macrofungi as medicinal material during the period from 581 to 979 AD. Int. J. Med. Mushrooms 16, 189–204.

Maffettone E, 2007. Characterization of a novel virus associated with the MVX disease of Agaricus bisporus, PhD dissertation, Cranfield University.

Magae, Y., Sunagawa, M., 2010. Characterization of a mycovirus associated with the

brown discoloration of edible mushroom, Flammulina velutipes. Virol. J. 7, 342.

Malloch, D., Castle, A., Hintz, W., 1987. Further Evidence for Agaricus brunnescens Peck as the Preferred Name for the Cultivated Agaricus. Mycologia 79, 839.

Marik, T., Urbán, P., Tyagi, C., Szekeres, A., Leitgeb, B., Vágvölgyi, M., Manczinger, L., Druzhinina, I.S., Vágvölgyi, C., Kredics, L., 2017. Diversity Profile and Dynamics of Peptaibols Produced by Green Mould Trichoderma Species in Interactions with Their Hosts Agaricus bisporus and Pleurotus ostreatus. Chem. Biodivers. 14, e1700033.

Marino, R., Saksena, K.N., Schuler, M., Mayfield, J.E., Lemke, P.A., 1976. Double-stranded ribonucleic acid in Agaricus bisporus. Appl. Environ. Microbiol. 31, 433–8.

Mata, G., Medel, R., Callac, P., Billette, C., Garibay-Orijel, R., 2016. Primer registro de Agaricus bisporus (Basidiomycota, Agaricaceae) silvestre en Tlaxcala y Veracruz, México. Rev. Mex. Biodivers. 87, 10–17.

Mawe, T., 1797. The Universal Gardener and Botanist: Or, A General Dictionary of Gardening and Botany.The Second Edition. Carefully Revised and Very Much Enlarged, Etc. GG & J. Robinson; T. Cadell jun. & W. Davies.

May, B., Royse, D.J., 1982. Confirmation of crosses between lines of Agaricus brunnescens by isozyme analysis. Exp. Mycol. 6, 283–292.

McKay, G.J., Egan, D., Morris, E., Scott, C., Brown, A.E., 1999. Genetic and morphological characterization of Cladobotryum species causing cobweb disease of mushrooms. Appl. Environ. Microbiol. 65, 606–10.

Moazed, D., 2009. Small RNAs in transcriptional gene silencing and genome defence. Nature 457, 413–420.

Moquet, F., Desmerger, C., Mamoun, M., Ramos-Guedes-Lafargue, M., Olivier, J.-M., 1999. A Quantitative Trait Locus of Agaricus bisporus Resistance to Pseudomonas tolaasii Is Closely Linked to Natural Cap Color. Fungal Genet. Biol. 28, 34–42.

Morin, E., Kohler, A., Baker, A.R., Foulongne-Oriol, M., Lombard, V., Nagye, L.G., Ohm, R. a., Patyshakuliyeva, A., Brun, A., Aerts, A.L., Bailey, A.M., Billette, C., Coutinho, P.M., Deakin, G., Doddapaneni, H., Floudas, D., Grimwood, J., Hilden, K., Kues, U., LaButti, K.M., Lapidus, A., Lindquist, E.A., Lucas, S.M., Murat, C., Riley, R.W., Salamov, A. a., Schmutz, J., Subramanian, V., Wosten, H. a. B., Xu, J., Eastwood, D.C., Foster, G.D., Sonnenberg, A.S.M., Cullen, D., de Vries, R.P., Lundell, T., Hibbett, D.S., Henrissat, B., Burton, K.S., Kerrigan, R.W., Challen, M.P., Grigoriev, I. V., Martin, F., 2012. Genome sequence of the button mushroom Agaricus bisporus reveals mechanisms governing adaptation to a humic-rich ecological niche. Proc. Natl. Acad. Sci. 109, 17501–17506.

Morris, T.J., 1979. Isolation and Analysis of Double-Stranded RNA from Virus-Infected Plant and Fungal Tissue. Phytopathology 69, 854.

Mushroom Sector Development Plan 2020 (2013). Teagasc Mushroom Stakeholder Consultative Group. https://www.teagasc.ie/media/website/publications/2013/Mushroom_-Conference_-Proceedings_web

Navarro, M.J., Gea, F.J., 2014. Entomopathogenic nematodes for the control of phorid and sciarid flies in mushroom crops. Pesqui. Agropecuária Bras. 49, 11–17.

Navarro, P., Savoie, J.-M., 2015. Selected wild strains of Agaricus bisporus produce high yields of mushrooms at 25°C. Rev. Iberoam. Micol. 32, 54–58.

Nogawa, M., Kageyama, T., Nakatani, A., Taguchi, G., Shimosaka, M., Okazaki, M., 1996. Cloning and Characterization of Mycovirus Double-stranded RNA from the Plant Pathogenic Fungus, Fusarium solani f. sp. robiniae. Biosci. Biotechnol. Biochem. 60, 784–788.

Nuss, D.L., 2005. Hypovirulence: Mycoviruses at the fungal–plant interface. Nat. Rev. Microbiol. 3, 632–642.

O'Brien, M., Grogan, H., Kavanagh, K., 2014. Proteomic response of Trichoderma aggressivum f. europaeum to Agaricus bisporus tissue and mushroom compost. Fungal Biol. 118, 785-791

O'Brien, M., Kavanagh, K., Grogan, H., 2017. Detection of Trichoderma aggressivum in bulk phase III substrate and the effect of T. aggressivum inoculum, supplementation and substrate-mixing on Agaricus bisporus yields. Eur. J. Plant Pathol. 147, 199–209.

O'Connor, E., McGowan, J., McCarthy, C.G.P., Amini, A., Grogan, H., Fitzpatrick, D.A., 2019. Whole Genome Sequence of the Commercially Relevant Mushroom Strain Agaricus bisporus var. bisporus ARP23. G3 (Bethesda). g3.400563.2019.

Osaki, H., Nakamura, H., Sasaki, A., Matsumoto, N., Yoshida, K., 2006. An endornavirus from a hypovirulent strain of the violet root rot fungus, Helicobasidium mompa. Virus Res. 118, 143–149.

Pál, K., van Diepeningen, A.D., Varga, J., Hoekstra, R.F., Dyer, P.S., Debets, A.J.M., 2007. Sexual and vegetative compatibility genes in the aspergilli. Stud. Mycol. 59, 19–30.

Patyshakuliyeva, A., Post, H., Zhou, M., Jurak, E., Heck, A.J.R., Hildén, K.S., Kabel, M.A., Mäkelä, M.R., Altelaar, M.A.F., de Vries, R.P., 2015. Uncovering the abilities of A garicus bisporus to degrade plant biomass throughout its life cycle. Environ. Microbiol. 17, 3098–3109.

Pearson, M.N., Beever, R.E., Boine, B., Arthur, K., 2009. Mycoviruses of filamentous fungi and their relevance to plant pathology. Mol. Plant Pathol. 10, 115–128.

Peever, T.L., Liu, Y.-C., Cortesi, P., Milgroom, M.G., 2000. Variation in Tolerance and Virulence in the Chestnut Blight Fungus-Hypovirus Interaction. Appl. Environ. Microbiol. 66, 4863–4869.

Pelkmans, J.F., Vos, A.M., Scholtmeijer, K., Hendrix, E., Baars, J.J.P., Gehrmann, T., Reinders, M.J.T., Lugones, L.G., Wösten, H.A.B., 2016. The transcriptional regulator C2H2 accelerates mushroom formation in Agaricus bisporus. Appl. Microbiol. Biotechnol. 100, 7151–7159.

Pizer, N.H., Thompson, A.J., 1938. Investigations into the environment and nutrition of the cultivated mushroom (Psalliota campestris): II. The effect of calcium and phosphate on growth and productivity. J. Agric. Sci. 28, 604–617.

Pontes, M.V.A., Patyshakuliyeva, A., Post, H., Jurak, E., Hildén, K., Altelaar, M., Heck, A., Kabel, M.A., de Vries, R.P., Mäkelä, M.R., 2018. The physiology of Agaricus bisporus in semi-commercial compost cultivation appears to be highly conserved among unrelated isolates. Fungal Genet. Biol. 112, 12–20.

Prasad, M.P., Agarwal, K., 2013. DNA fingerprinting of commercial mushrooms by ISSR and SSR markers for genetic discrimination. Int. J. Pharma Bio Sci. 4, 1243–1249.

Prescott, T., Wong, J., Panaretou, B., Boa, E., Bond, A., Chowdhury, S., Davies, L., Ostergaard, L., 2018. Useful fungi, in: Willis, K. (Ed.), State of the World's Fungi. Report. Royal Botanic Gardens, Kew. pp. 24–31.

Raper, C.A., Raper, J.R., Miller, R.E., 1972. Genetic Analysis of the Life Cycle of Agaricus bisporus. Mycologia 64, 1088.

Rayner, A. D. M. and Boddy, L. 1988. Fungal decomposition of wood: its biology and ecology. John Wiley and Sons, Chichester.

Research and Markets (2019). The world's largest market and research store. https://researchandmarkets.com/research/zsckhw/global_mushroom?w=5

Reginald Buller, A.H., 1914. The fungus lore of the Greeks and Romans. Trans. Br. Mycol. Soc. 5, 21-66

Reid, D.A., Ainsworth, G.C., 1978. Introduction to the History of Mycology. Kew Bull.

Rojas, C. & Mansur, E. 1995. Ecuador: informaciones generales sobre productos non madereros en Ecuador. In Memoria, consulta de expertos sobre productos forestales no madereros para America Latina y el Caribe, pp. 208–223.

Rokni, N., Goltapeh, E.M., Shafeinia, A., Safaie, N., 2016. Evaluation of genetic diversity among some commercial cultivars and Iranian wild strains of Agaricus bisporus by microsatellite markers. Botany 94, 9–13.

Romaine, C.P. (2000). Family Barnavirida: In Virus Taxonomy-Classifcation and nomenclature of viruses (van Regenmortel, M. H. V., Fauquet, C. M., Bishop, D. H. L., Carstens, E. B., Estes, M. K., Maniloff, J., Mayo, M. A., McGeoch, D. J., Pringle, C. R. and Wickner, R. B. eds). Academic Press, NY.

Royse, D.J., Baars, J., Tan, Q., 2017. Current Overview of Mushroom Production in the World, in: Edible and Medicinal Mushrooms. John Wiley & Sons, Ltd, Chichester, UK, pp. 5–13.

Sahin, E., Akata, I., 2018. Viruses infecting macrofungi. VirusDisease 29, 1–18.

Salaipeth, L., Chiba, S., Eusebio-Cope, A., Kanematsu, S., Suzuki, N., 2014. Biological properties and expression strategy of rosellinia necatrix megabirnavirus 1 analysed in an experimental host, Cryphonectria parasitica. J. Gen. Virol. 95, 740–750.

Sasaki, A., Kanematsu, S., Onoue, M., Oyama, Y., Yoshida, K., 2006. Infection of Rosellinia necatrix with purified viral particles of a member of Partitiviridae (RnPV1-W8). Arch. Virol. 151, 697–707.

Sato, Y., Miyazaki, N., Kanematsu, S., Xie, J., Ghabrial, S.A., Hillman, B.I., Suzuki, N., 2019. ICTV Virus Taxonomy Profile: Megabirnaviridae. J. Gen. Virol. 100,

1269–1270.

Scheepmaker, J.W.A., Geels, F.P., Van Griensven, L.J.L.D., Smits, P.H., 1998. Susceptibility of larvae of the mushroom fly Megaselia halterata to the entomopathogenic nematode Steinernema feltiae in bioassays. BioControl. 43, 201-214

Seaby, D., 1999. The Influence on Yield of Mushrooms (Agaricus bisporus) of the Casing Layer Pore Space Volume and Ease of Water Uptake. Compost Sci. Util. 7, 56–65.

Segers, G.C., van Wezel, R., Zhang, X., Hong, Y., Nuss, D.L., 2006. Hypovirus Papain-Like Protease p29 Suppresses RNA Silencing in the Natural Fungal Host and in a Heterologous Plant System. Eukaryot. Cell 5, 896–904.

Shah, U., Kotta-Loizou, I., Fitt, B., Coutts, R., 2018. Identification, Molecular Characterization, and Biology of a Novel Quadrivirus Infecting the Phytopathogenic Fungus Leptosphaeria biglobosa. Viruses 11, 9.

Sinden, J. W. (1990). Developments in spawn production. Mushroom News 38: 6-10.

Sinden Aug. 2, 1932 2,262,851 Lescarboura Nov. 18, 1941 Encyclopedia of Food" by Ward, New York, Number 50, Union Square, 1923, 333-334.

Sinden, J.W., Hauser, E., 1950. Report of two new mushroom diseases. Mushroom Sci. 1, 96–100.

Sobieralski, K., Siwulski, M., Frużyńska-Jóźwiak, D., Błaszczyk, L., Sas-Golak, I., Jasińska, A., 2010. Impact of Infections with two Trichoderma aggressivum f. europaeum Isolates on the Yielding of Some Wild Strains of Agaricus bisporus (Lange) Imbach. J. Plant Prot. Res. 50, 501–504.

Solórzano, A., Rodríguez-Cousiño, N., Esteban, R., Fujimura, T., 2000. Persistent Yeast Single-stranded RNA Viruses Exist in Vivo as Genomic RNA·RNA Polymerase Complexes in 1:1 Stoichiometry. J. Biol. Chem. 275, 26428–26435.

Son, M., Yu, J., Kim, K.-H., 2015. Five Questions about Mycoviruses. PLOS Pathog. 11, e1005172.

Sonnenberg, A.S.M., Baars, J.J.P., Gao, W., Visser, R.G.F., 2017. Developments in breeding of Agaricus bisporus var. bisporus: progress made and technical and legal hurdles to take. Appl. Microbiol. Biotechnol. 101, 1819–1829.

Sonnenberg, A.S.M., Gao, W., Lavrijssen, B., Hendrickx, P., Sedaghat-Tellgerd, N., Foulongne-Oriol, M., Kong, W.-S., Schijlen, E.G.W.M., Baars, J.J.P., Visser, R.G.F., 2016. A detailed analysis of the recombination landscape of the button mushroom Agaricus bisporus var. bisporus. Fungal Genet. Biol. 93, 35–45.

Sonnenberg, A. S. M. and Lavrijssen, B. (2004). Browning and the presence of viral double-stranded RNA in Dutch mushrooms. Mushroom Sci. 16: 541-546.

Spencer DM, 1985. The Mushroom, Its History and Importance. In: Flegg PB, Spencer DM and Wood DA(eds), The Biology and Technology of the Cultivated Mushroom. Chichester, John Wiley & Sons, pp. 1-22.

Starr, E.P., Nuccio, E.E., Pett-Ridge, J., Banfield, J.F., Firestone, M.K., 2019.

Metatranscriptomic reconstruction reveals RNA viruses with the potential to shape carbon cycling in soil. bioRxiv.

Summerbell, R.C., Castle, A.J., Horgen, P.A., Anderson, J.B., 1989. Inheritance of restriction fragment length polymorphisms in Agaricus brunnescens. Genetics 123, 293–300.

Suzuki, N., Ghabrial, S.A., Kim, K.-H., Pearson, M., Marzano, S.-Y.L., Yaegashi, H., Xie, J., Guo, L., Kondo, H., Koloniuk, I., Hillman, B.I., 2018. ICTV Virus Taxonomy Profile: Hypoviridae. J. Gen. Virol. 99, 615–616.

Suzuki, N., Nuss, D.L., 2002. Contribution of Protein p40 to Hypovirus-Mediated Modulation of Fungal Host Phenotype and Viral RNA Accumulation. J. Virol. 76,

Thomson, T., Lin, H., 2009. The Biogenesis and Function of PIWI Proteins and piRNAs: Progress and Prospect. Annu. Rev. Cell Dev. Biol. 25, 355–376.

Tournefort, J., 1707. Observations sur la naissance et sur la culture des champignons.Memoires de l'Acad. Royale (Paris), pp.58-65

Trask, S.D., McDonald, S.M., Patton, J.T., 2012. Structural insights into the coupling of virion assembly and rotavirus replication. Nat. Rev. Microbiol. 10, 165–177.

Turína, M., Rostagno, L., 2007. Virus-induced hypovirulence in Cryphonectria Parasitica: Still an unresolved conundrum. J. Plant Pathol. 165-178

Ullrich, R.C., Raper, J.R., 1977. Evolution of genetic mechanisms in fungi. Taxon.

United States Patents Number Name Date Re. 22,202 Stoller Oct. 13, 1942 1,869,517

Urayama, S., Kimura, Y., Katoh, Y., Ohta, T., Onozuka, N., Fukuhara, T., Arie, T., Teraoka, T., Komatsu, K., Moriyama, H., 2016. Suppressive effects of mycoviral proteins encoded by Magnaporthe oryzae chrysovirus 1 strain A on conidial germination of the rice blast fungus. Virus Res. 223, 10–19.

Van Der Lende, T.R., Duitman, E.H., Gunnewijk, M.G.W., YU, L., Wessesl, J.G.H., 1996. Functional Analysis of dsRNAs (L1, L3, L5, and M2) Associated with Isometric 34-nm Virions ofAgaricus bisporus(White Button Mushroom). Virology 217, 88–96.

Van Lenteren, J., 1988. Biological And Integrated Pest Control In Greenhouses. Annu. Rev. Entomol. 33, 239–269.

van Zaayen, A. (1979). Mushroom viruses. In Viruses and plasmids in fungi, pp. 239-324. Edited by P. A. Lemke. New York: Marcel Dekker.

Waltz, E., 2016. Gene-edited CRISPR mushroom escapes US regulation. Nature 532, 293–293.

Wang, S., Kondo, H., Liu, L., Guo, L., Qiu, D., 2013. A novel virus in the family Hypoviridae from the plant pathogenic fungus Fusarium graminearum. Virus Res. 174, 69–77.

Wang, Y.-C., 1987. Mycology in ancient China. Mycologist 1, 59–61.

Wei, C.Z., Osaki, H., Iwanami, T., Matsumoto, N., Ohtsu, Y., 2004. Complete nucleotide sequences of genome segments 1 and 3 of Rosellinia anti-rot virus in

the family Reoviridae. Arch. Virol. 149, 773–777.

Weijn, A., Bastiaan-Net, S., Wichers, H.J., Mes, J.J., 2013. Melanin biosynthesis pathway in Agaricus bisporus mushrooms. Fungal Genet. Biol. 55, 42–53.

Weijn, A., Tomassen, M., Bastiaan-Net, S., Hendrix, E., Baars, J., Sonnenberg, A., *et al*. (2011). Browning sensitivity of button mushrooms. Proceedings of the 7th international conference

Whittaker, R.H., 1969. New concepts of kingdoms or organisms. Evolutionary relations are better represented by new classifications than by the traditional two kingdoms. Science (80-.).

Widner, W.R., Wickner, R.B., 1993. Evidence that the SKI antiviral system of Saccharomyces cerevisiae acts by blocking expression of viral mRNA. Mol. Cell. Biol. 13, 4331–4341.

Woese, C.R., Kandler, O., Wheelis, M.L., 1990. Towards a natural system of organisms: Proposal for the domains Archaea, Bacteria, and Eucarya. Proc. Natl. Acad. Sci. U. S. A.

Wu, Q., Wang, X., Ding, S.-W., 2010. Viral Suppressors of RNA-Based Viral Immunity: Host Targets. Cell Host Microbe 8, 12–15.

Wu, S., Cheng, J., Fu, Y., Chen, T., Jiang, D., Ghabrial, S.A., Xie, J., 2017. Virus-mediated suppression of host non-self recognition facilitates horizontal transmission of heterologous viruses. PLOS Pathog. 13, e1006234.

Xie, J., Xiao, X., Fu, Y., Liu, H., Cheng, J., Ghabrial, S.A., Li, G., Jiang, D., 2011. A novel mycovirus closely related to hypoviruses that infects the plant pathogenic fungus Sclerotinia sclerotiorum. Virology 418, 49–56.

Yaegashi, H., Kanematsu, S., Ito, T., 2012. Molecular characterization of a new hypovirus infecting a phytopathogenic fungus, Valsa ceratosperma. Virus Res. 165, 143–150.

Yaegashi, H., Sawahata, T., Ito, T., Kanematsu, S., 2011. A novel colony-print immunoassay reveals differential patterns of distribution and horizontal transmission of four unrelated mycoviruses in Rosellinia necatrix. Virology 409, 280–289.

Yu, X., Li, B., Fu, Y., Jiang, D., Ghabrial, S.A., Li, G., Peng, Y., Xie, J., Cheng, J., Huang, J., Yi, X., 2010. A geminivirus-related DNA mycovirus that confers hypovirulence to a plant pathogenic fungus. Proc. Natl. Acad. Sci. 107, 8387–8392.

Yu, X., Li, B., Fu, Y., Xie, J., Cheng, J., Ghabrial, S.A., Li, G., Yi, X., Jiang, D., 2013. Extracellar transmission of a DNA mycovirus and its use as a natural fungicide. Proc. Natl. Acad. Sci. 110, 1452–14

Zhai, L., Yang, M., Zhang, M., Hong, N., Wang, G., 2019. Characterization of a Botybirnavirus Conferring Hypovirulence in the Phytopathogenic Fungus Botryosphaeria dothidea. Viruses 11, 266.

Zhang, D.-X., Spiering, M.J., Nuss, D.L., 2014. Characterizing the Roles of Cryphonectria parasitica RNA-Dependent RNA Polymerase-Like Genes in

Antiviral Defense, Viral Recombination and Transposon Transcript Accumulation. PLoS One 9, e108653.

Zhang, J., Zhao, Z., Hu, R., Guo, L., Zheng, L., Du, Z., Wu, Z., Fang, S., Zhang, S., Liu, Y., 2017. The genome sequence of Brassica campestris chrysovirus 1, a novel putative plant-infecting tripartite chrysovirus. Arch. Virol. 162, 1107–1111.

Chapter 2:

Whole Genome Sequence of the Commercially Relevant Mushroom Strain *Agaricus bisporus* var. *bisporus* ARP23

2.0 Whole Genome Sequence of the Commercially Relevant Mushroom Strain *Agaricus bisporus* var. *bisporus* ARP23

Eoin O'Connor[*,§], Jamie McGowan[*,†], Charley GP McCarthy[*,†], Aniça Amini[‡], Helen Grogan[§] & David A. Fitzpatrick[*,†]

[*]Genome Evolution Laboratory, Department of Biology, Maynooth University, Maynooth, Co. Kildare, Ireland

[†] Human Health Research Institute, Maynooth University, Maynooth, Co. Kildare, Ireland

[‡] Sylvan-Somycel (ESSC - Unité 2), ZI SUD, rue Lavoisier, BP 25, 37130 Langeais, France

[§] Teagasc Food Research Centre, Ashtown, Dublin 15, D15 KN3K, Ireland

This paper was accepted for publication in the journal G3: Genes, Genomes, Genetics (August 2019)

Citation:

O'Connor, E., McGowan, J., McCarthy, C.G., Amini, A., Grogan, H. and Fitzpatrick, D.A., 2019. Whole Genome Sequence of the Commercially Relevant Mushroom Strain Agaricus bisporus var. bisporus ARP23. *G3: Genes, Genomes, Genetics*, *9*(10), pp.3057-3066.

Keywords: Button mushroom, *Agaricus bisporus*, Genome report, Agaricus Resource Program, Agaricus *bisporus* mating locus, Agaricus pangenome

Abstract

Agaricus bisporus is an extensively cultivated edible mushroom. Demand for cultivation is continuously growing and difficulties associated with breeding programmes now means strains are effectively considered monoculture. While commercial growing practices are highly efficient and tightly controlled, the over-use of a single strain has led to a variety of disease outbreaks from a range of pathogens including bacteria, fungi, and viruses. To address this, the Agaricus Resource Program (ARP) was set up to collect wild isolates from diverse geographical locations through a bounty-driven scheme to create a repository of wild *Agaricus* germplasm. One of the strains collected, *Agaricus bisporus* var. *bisporus* ARP23, has been crossed extensively with white commercial varieties leading to the generation of a novel hybrid with a dark brown pileus commonly referred to as 'Heirloom'. Heirloom has been successfully implemented into commercial mushroom cultivation. In this study the whole genome of *Agaricus bisporus* var. *bisporus* ARP23 was sequenced and assembled with Illumina and PacBio sequencing technology. The final genome was found to be 33.49 Mb in length and have significant levels of synteny to other sequenced *Agaricus bisporus* strains. Overall, 13,030 putative protein coding genes were located and annotated. Relative to the other *A. bisporus* genomes that are currently available, *Agaricus bisporus* var. *bisporus* ARP23 is the largest *A. bisporus* strain in terms of gene number and genetic content sequenced to date. Comparative genomic analysis shows that the *A. bisporus* mating loci is unifactorial and unsurprisingly highly conserved between strains. The lignocellulolytic gene content of all *A. bisporus* strains compared is also very similar. Our results show that the pangenome structure of *A. bisporus* is quite diverse with between 60-70% of the total protein coding genes per strain considered as being orthologous and syntenically conserved. These analyses and the genome sequence described herein are the starting point for more detailed molecular analyses into the growth and phenotypical responses of *Agaricus bisporus* var. *bisporus* ARP23 when challenged with economically important mycoviruses.

2.1 Introduction

The global market for edible mushrooms is estimated to be worth US$42 billion per year (Prescott *et al.* 2018). Due to its high yielding potential and appealing morphology the mushroom industry has relied solely on a single white variety of *A. bisporus*. However, the over-use of a single cultivar has led to a variety of disease outbreaks from a variety of pathogens (Hussey and Wyatt 1960; Fletcher 1992; North and Wuest 1993; Soler-Rivas 1999; Grogan *et al.* 2003). One approach to increase disease resistance profiles in important crops is the use of desirable traits from wild germplasms (Arora *et al.* 2019). However, breeding of new strains in the mushroom industry has been difficult. Notwithstanding these difficulties the introduction of desirable traits to novel cultivars and the need for genomic biorepositories of wild germplasms of closely related or ancestral agricultural crops remains crucial for the protection of low diversity crops (Dempewolf *et al.* 2017).

A. bisporus has effectively been considered a monoculture crop for a considerable amount of time (Royse and May 1982). To this end, the *Agaricus* Resource Program (ARP) (Callac *et al.* 1996) was set up to collect wild isolates from diverse geographical locations. The focus of this genome report is a wild isolate from the ARP collection referred to as *A. bisporus* var. *bisporus* ARP23. Crosses of homokaryons of U1 and old-fashioned brown led to an intermediate hybrid that was subsequently crossed with ARP23 to produce a novel commercially productive hybrid referred to as 'Heirloom'. Wild strains are also a promising resource for the introduction of disease-resistant traits for common commercial mushroom diseases. It has been shown that the wild tetrasporic *A. bisporus* var. *burnettii* has heightened resistance to the pathogen that causes bacterial blotch (*Pseudomonas tolaasii*) through genetic markers linked to the *PPC1* allele (Moquet *et al.* 1999). Polygenic inheritance of resistance attributes has been described (Kerrigan 2000) and so the consideration of the introduction of wild *A. bisporus* germplasm into breeding novel strains must be considered on the basis of careful selection of screened wild strains with distinct mechanisms pertaining to disease resistance (Foulongne-Oriol *et al.* 2011).

To date, two genomes of the constituent homokaryons of Horst U1 have been sequenced, H97 (Morin *et al.* 2012) and H39 (Sonnenberg *et al.* 2016). This represents the genome of the first commercially cultivated white hybrid strain. The manuscript that reported the H97 genome sequence also described the genome of *Agaricus bisporus* var.

burnettii (JB137-S8), a strain exclusively native to the Sonoran Desert of California. That study uncovered the genetic and enzymatic mechanisms that favour *A. bisporus* to a humic-rich environment by primary degradation of plant material. A gene arsenal of compost-induced carbohydrate enzymes (heme-thiolate peroxidase, β-etherases, multicopper oxidase) and CYP450 oxidoreductases for example, together with high protein degradation and nitrogen-scavenging abilities were determined to be crucial to the challenges posed by complex composts (Morin *et al.* 2012).

The genome presented herein, represents the first commercially relevant genome for a wild cultivar of *Agaricus bisporus* var. *bisporus*, and is an invaluable tool for future efforts in mushroom breeding. Furthermore, the genome sequence described will act as the starting point for more detailed OMIC based studies into the growth and phenotypical responses of *Agaricus bisporus* var. *bisporus* ARP23 when challenged with economically important mycoviruses.

2.2 Methods

2.2.1 Strain, culture conditions and homokaryon genotyping

A. bisporus var. *bisporus* ARP23 cultures were grown on compost extract agar (aqueous extract of phase II mushroom compost, double-autoclaved for sterility) for three weeks at 25 ºC in the dark. 10 ml of protoplasting medium (50 mM maleic acid, 0.6 M saccharose, 1 M NaOH pH 5.8) containing 10 g Glucanex (Sigma Aldrich cat. no. L1412) (Kerrigan *et al.* 1994) was added to established mycelium and incubated for 5 hours at 25 ºC in the dark with occasional shaking. Resulting protoplasts were grown on a saccharose-enriched compost extract medium and incubated for two weeks at 25ºC in the dark. To assess whether protoclones were homokaryons or heterokaryons, growth tests, hyphal morphology, and nuclear type were conducted. Cultures that had an average diameter of 54 mm (Kerrigan *et al.* 1994) or less after this time, were isolated as putative-homokaryons. A total of 86 out of 100 isolated protoplasts were assigned as putative homokaryons due to their delayed growth. Hyphae of homokaryons tend to be more 'thread-like' with far fewer branching hyphae. To confirm that protoplasts were homokaryons, the presence of a single MAT locus was assessed using the 39Tr 2/5-2/4 primer sets for targeting MAT loci and amplification was carried out as previously described (Gao *et al.* 2013). Genotype-validated homokaryons were grown on complete yeast media (2 g proteose peptone, 2 g yeast extract, 20 g glucose, 0.5 $MgSO_4$, 0.46 g KH_2PO_4, 1 g K_2HPO_4, 10 g agar in 500 ml dH_20) for 3 weeks in the dark, at 25 ºC. 7 mm agar plugs were excised from the growing hyphal edges of homokaryons of MAT2 genotype (the MAT1 genotype was not recovered) and shaken at 30 Hz for 7 minutes in 500 µL malt extract and the resulting homogenate added to 50 ml malt extract liquid medium (10 g malt extract in 600 ml of dH_2O) in a 500 ml Erlenmeyer flask. Liquid cultures were grown for 12 days at 25ºC in the dark at 150 rpm.

2.2.2 DNA isolation and libraries

Fungal mycelium was isolated in Miracloth and washed with sterile PBS. The mycelium was flash frozen and ground in liquid nitrogen using a mortar and pestle. DNA isolation was carried out immediately on ground material with the Wizard® Genomic DNA Purification Kit (Promega) following the plant tissue method with minor

modifications. Nuclei lysis buffer was supplemented with 0.5 M EDTA and 0.1 mg/mL Proteinase K and cell lysis was carried out at 37 ºC for 30 min. The remainder of the DNA isolation was as per manufacturer's guidelines. An Illumina paired-end sequencing library with insert size of 270 bp (80 X coverage) and a Pacbio RSII mate pair library of 20 Kb insert size were generated for a hybrid assembly approach. Sequencing on HiSeq 4000 and Pacbio RSII generated 5.90 GB and 57.64 GB of raw sequence data, respectively. DNA library construction and sequencing on the Pacbio (RSII) and Illumina (HiSeq 4000) platforms was carried out by BGI Tech Solutions Co., Ltd. (Hong Kong, China).

2.2.3 Fruit-body material, RNA isolation and sequencing

ARP23 mycelia was added to mushroom compost in crates (n = 3) and incubated at 25°C, 90-95 % relative humidity (spawn-run phase) for 17 days. A layer of peat was added to the surfaces of the colonised compost (case-run phase) and incubated for another 7 days. Temperatures and relative humidity were lowered to 18°C and 85-90 % and fruit-bodies were harvested after 7 days of development. All cropping procedures were as per standard mushroom growing practices. Fruit-bodies were flash-frozen, freeze-dried and material was crushed in liquid N_2. RNA was isolated using the RNeasy plant minikit (Qiagen) as per manufacturers guidelines. DNA digestion was done with DNase I (Invitrogen). RNA quantity and quality was assessed with an RNA6000 Nano Assay (Agilent 2100 Bioanalyzer, Agilent Technologies, USA). High-quality RNA was sent to BGI Tech Solutions Co., Ltd. (Hong Kong, China) for RNA sequencing (RNA-seq).

2.2.4 Genome assembly and gene calling

Short-read libraries had adaptor removal (Martin 2011) and quality trimming performed using Trim Galore! (https://github.com/FelixKrueger/TrimGalore). A minimum phred score cut-off of 25 and a minimum read length of 90 nt was applied to short-read libraries. Long-read libraries were corrected using short reads using Proovread (Hackl *et al.* 2014). Corrected long reads were then self-corrected with additional adaptor trimming using Canu (Koren *et al.* 2017). Canu was then used for genome assembly with an error rate of 2.5 %. Scaffolding of assembled contigs was performed by scaffolding

with corrected long reads using SSPACE long-read hybrid assembler (Boetzer and Pirovano 2014). This primary assembly was then processed using Purge Haplotigs (Roach *et al.* 2018) for removal of duplicated haplotypes, with default parameters. These steps were carried out as a precaution to remove potential areas of heterozygosity in the assembly introduced by sequencing data collected from different MAT2 homokaryon protoplasts, which were pooled for DNA isolation, due to their excessively slow growth rates in culture. Levels of heterozygosity were not explicitly examined however. Jellyfish v. 1.1.12 (Marçais and Kingsford 2011) was used to generate histograms of the frequency distribution of kmers from Illumina reads which were fed into GenomeScope (Vurture *et al.* 2017) for estimation of genome size. Synteny between the genome assemblies of ARP23, JB137-S8 and H97 was assessed by performing global whole genome alignments using BWA (Li and Durbin 2010) and visualised with Jupiter Plot (Chu 2018). The H39 assembly wasn't included as it has been shown to have almost complete synteny to H97 (Sonnenberg *et al.* 2016).

For gene calling purposes, RNAseq data from fruitbodies with a read length of 100 nt (phred score > 25) were aligned to the final genome assembly using Bowtie 2 (Langmead and Salzberg 2012). Resulting alignment files were used to train AUGUSTUS using Braker2 (Stanke *et al.* 2006; Hoff *et al.* 2016). The completeness of the predicted gene models were assessed using BUSCO with the Basidiomycota BUSCO dataset (Simão *et al.* 2015).

2.2.5 Genome functional annotation and characterisation

Putative open reading frames (ORFs) were assigned protein family (PFam) domains using funannotate (https://github.com/nextgenusfs/funannotate) using default settings of Interproscan 5 (Jones *et al.* 2014). Gene ontology (GO) IDs (Ashburner *et al.* 2000) were assigned where available and a corresponding GO term map was obtained using YeastMine (Balakrishnan *et al.* 2012). Information on the pathways associated with different genes were analysed with KEGG (Kyoto Encyclopaedia of Genes and Genomes) (Ogata *et al.* 1999) by assigning KO (KEGG ontology) through BlastKOALA (Kanehisa *et al.* 2016). A search for repetitive elements was done by identifying tandem repeats (TR) and transposable elements (TE). TRs were identified over the entire assembly with Tandem Repeats Finder (TRF 4.07) (Benson 1999). Classification of the

different categories of TE in the genome were conducted using RepeatMasker 4.06 with the modified version of NCBI Blast for RepeatMasker, RMBLAST (http://www.repeatmasker.org/RMBlast.html). Simple single repeats were also determined using RepeatMasker with the default settings. tRNAs were identified across all scaffolds using tRNAscan-SE v 2.0 (Lowe and Chan 2016) and rRNAs were also identified with RNAmmer 1.2 (Lagesen *et al.* 2007).

2.2.6 Carbohydrate-Active Enzymes

Translated ORFs were used to search dbCAN2 (Zhang *et al.* 2018) for presence of Carbohydrate Active Enzymes (CAZys) (Lombard *et al.* 2014). For comparative purposes 32 fungal genomes consisting of a variety of Ascomycota and Basidiomycota species (**Table S1**) were also searched to catalogue their CAZy content. As well as including brown rot and white rot fungi, genomes for 7 of the top 10 most highly cultivated mushrooms are also included in this dataset (**Table S1**).

2.2.7 Mating Locus

The locus coding for homeodomain proteins typical for the A mating type in *Coprinopsis cinerea* was used to locate the unifactorial *A. bisporus* mating-type locus. The homeodomain proteins as well as flanking proteins were individually searched using BLASTP (Altschul *et al.* 1997) (evalue 10^{-3}) against the predicted proteomes of *A. bisporus* ARP23, H97 and JB137-S8 respectively. Top hits from these gene sets were then searched back against the *C. cinerea* gene set to locate reciprocal best BLAST hits which were then considered orthologs.

2.2.8 Phylogenomic reconstruction

Orthologous gene families were identified with OrthoFinder2 (Emms and Kelly 2015), using BLASTp (Altschul *et al.* 1997) as the search algorithm, an inflation value of 2.0 for MCL clustering (Enright *et al.* 2002) and the command-line parameter "-msa". 71 gene families were ubiquitously present and single copy and used for phylogenomic analysis. Each family was individually aligned using MUSCLE (Edgar 2004) and trimmed using trimAl (Capella-Gutierrez *et al.* 2009) with the parameter "-automated1"

to remove poorly aligned regions. Trimmed alignments were concatenated together resulting in a final supermatrix alignment of 27,861 amino acids. Phylogenomic analyses were performed using both Maximum likelihood and Bayesian inference. IQ-TREE (Nguyen *et al.* 2015) was used to perform maximum likelihood analysis under the LG+F+R5 model, which was the best fit model according to ModelFinder (Kalyaanamoorthy *et al.* 2017), and 1,000 ultrafast bootstrap replicates (Hoang *et al.* 2018). Bayesian analyses were carried out using PhyloBayes with the CAT model (Lartillot *et al.* 2009). Two independent chains were run for 8,000 cycles and convergence was assessed using bpcomp and tracecomp. A consensus Bayesian phylogeny was generated with a burn-in of 10%. Support values represent posterior probabilities. The phylogeny was visualised and annotated using the Interactive Tree of Life (iTOL) (Letunic and Bork 2007).

2.2.9 *Agaricus bisporus* pangenome dataset assembly

Genome assembly data for three *Agaricus bisporus* strains (H97, JB137 and H39) were obtained from NCBI. Gene sequence and genomic location datasets were generated for each of the three strains through the pangenome analysis pipeline Pangloss; a gene prediction strategy using a combination of HMM-dependent gene prediction with GeneMark-ES and PWM-dependent long ORF prediction was chosen (McCarthy and Fitzpatrick 2019b). Combined with data from *A. bisporus* ARP23, a total of 42,264 *A. bisporus* gene sequences and their corresponding genomic locations were predicted. An all-vs.-all BLASTp search was performed on the *A. bisporus* dataset using an e-value cutoff of $1e^{-4}$ (Camacho *et al.* 2009).

Data availability

The Bioproject designation for this project is PRJNA544931. This Whole Genome Shotgun project has been deposited at DDBJ/ENA/GenBank under the accession VCNO00000000. The version described in this paper is version VCNO01000000.

Supplemental material is available at Figshare. **Table S1** shows the genomes, taxonomy and download links for the 32 genomes used in the phylogenomic and CAZy studies. **Table S2** shows the presence of lignocellulolytic genes in the 32 fungal genomes. **Figure S1:** Macrosynteny between *A. bisporus* H97 chromosomes and all *A. bisporus* ARP23 scaffolds. Only regions larger than 10,000bp are connected with links. Macrosynteny visualised with Jupiter Plot.

2.3 Results and Discussion

2.3.1 Whole-genome assembly

The genome of the monokaryotic *A. bisporus* var. *bisporus* strain ARP23 (ARP23 herein) was sequenced using a hybrid approach of short (Illumina Hiseq 4000) paired-end reads and long-reads (Pacbio RSII). A total of 8,861,726 reads representing a cumulative size of 4.074 GB were generated including 8,424,105 and 437,621 reads from Illumina and PacBio sequencing platforms respectively. Upon trimming adaptors, error-correction and hybrid-assembly of both short and long-read libraries, a 33.49Mb genome with a GC content of 46.33% was generated. The assembly is comprised of 169 contigs, the longest being 1.5Mb with an N50 of 350,711 and an L50 of 26 (**Table 1**). The average length of contigs is 198,204.6 bp. Kmer-analyses conducted with GenomeScope (Vurture *et al.* 2017) suggest a genome size of 34.02Mb indicating that the 169 scaffolds of this assembly cover 98.44% of the entire genome. The completeness of the assembly was quantified by determining the presence/absence of the 1,315 fungal orthologs found in the Basidiomycete BUSCO set. A total of 1,170 (87.6%) complete BUSCO genes were located in the ARP23 assembly, this is comparable to what is observed in A. *bisporus* H97 (1,172 or 87.8%) and *A. bisporus* JB137-S8 (1,179 or 88.3%) strains (H97 and JB137-S8 respectively herin) (**Table 1**). Macrosynteny between the ARP23 assembly and the 13 complete H97 chromosomes was visualised with Jupiter Plot. Overall high levels of synteny are observed with the vast majority of ARP23 scaffolds mapping directly to individual H97 chromosome **(Figure 1 & Figure S1).** There are a number of scaffolds that have hits to multiple chromosomes indicating low levels of genome rearrangements have occurred (**Figure 1 & Figure S1**). There are no scaffolds in the ARP23 that do not map to the H97 assembly. Scaffold 74 was found to be 137,116 nucleotides in length and contains all 17 mitochondrial genes previously described in the mitochondrion of H97 (Férandon *et al.* 2013). Furthermore, it is also of a comparable length to the H97 mitochondrial genome (135,005 bp), therefore scaffold 74 corresponds to the full length ARP23 mitochondrial genome.

Table 1. Genome statistics for *A. bisporus* strains ARP23, H97 and JB137-S8.

Feature	ARP23	H97	JB137-S8
Number of Scaffolds	169	29	2016
Largest Contig	1,506,893	3,343,696	2,973,556
Total Size of Scaffolds (Mb)	33.49	30.23	31.20
N50	350,711	2,334,609	1,225,131
L50	26	6	8
GC content (%)	46.33	46.48	46.59
Number of Introns	70,261	50,356	53,337
Complete BUSCOs (C)[a]	87.6%	87.8%	88.3%
Number of protein coding genes	13,030	10,863	11,289
Proteins with a signal peptide	750	717	734
Number of tRNA	200	160	215
Number of rRNA	10	22	3
Number of sRNA	93	90	87
Repetitive regions (%)	0.79	0.79	0.75
Number of tandem repeats	2,287	2,353	2,480
Simple repeat sequences (%)	0.54	0.54	0.53
Low complexity regions (%)	0.13	0.13	0.12
Non-LTR transposons	250	240	134
LTR transposons	1	2	2

[a] BUSCO analysis conducted with the Basidiomycota (odb9) lineage

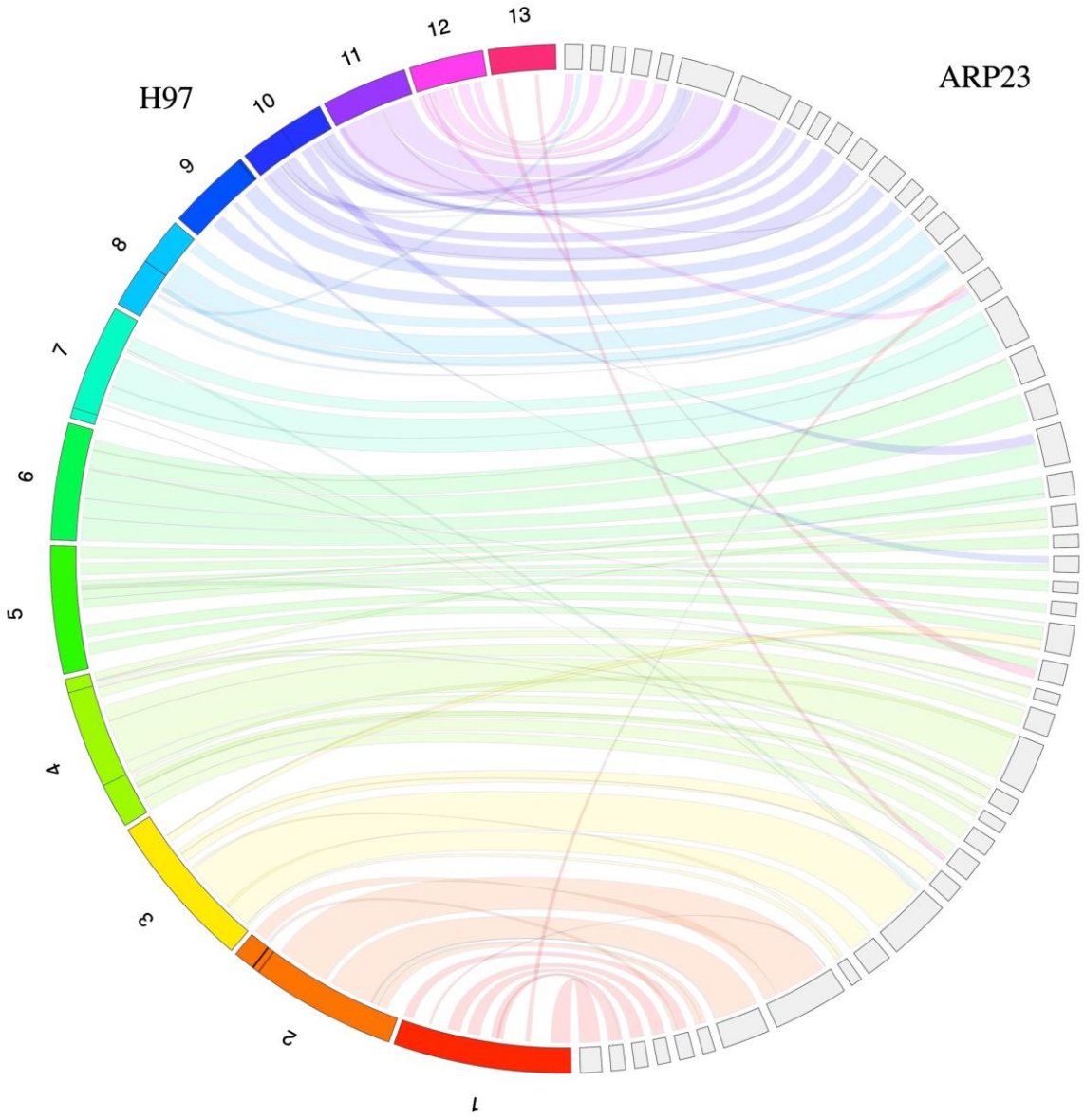

Figure 1: Macrosynteny between *A. bisporus* H97 chromosomes and *A. bisporus* ARP23 scaffolds. Only regions larger than 10,000bp are connected with links. Macrosynteny visualised with Jupiter Plot. For display purposes only the largest scaffolds that correspond to 75% of the ARP23 assembly are incorporated. When all scaffolds are included higher levels of coverage are observed particularly with respect to H97 chromosomes 1 and 13 (**Figure S1**).

2.3.2 Genome annotation

The total length of repetitive elements in *A. bisporus* strain ARP23 amounted to 264,404 bp (0.79 % of the total assembly) this is similar to what is observed for both H97 and JB137-S8 (**Table 1**). The number of tandem repeat regions across the 169 scaffolds of the assembled genome was 2,287, with 'scaffold00003' containing the greatest number at 321 repeat regions. Simple sequence repeats (SSRs) amounted to 180,995 bp (0.54%) and low complexity regions covered 44,108 bp (0.13 %) (**Table 1**). We searched for the two sub-types of Non-LTR retrotransposons; long interspersed nuclear elements (LINEs) and short interspersed nuclear elements (SINEs). Of the 241 LINE-type elements; 17 belonged to L1, 69 to L2 and 78 to L3. For the 30 regions designated to SINES; 9 belonged to the MIRs and none were classified as ALUs. A single LTR retrotransposon was found for the endogenous retroviruses (ERV) class I. A single hAT-Charlie family DNA transposon and 7 DNA/TcMar-Tiggers were found out of a total of 55 DNA elements. Overall the ARP23 assembly contains 200 tRNAs, 10 rRNAs and 93 sRNAs (**Table 1**).

In total 13,030 putative protein-coding genes were called for ARP23. Of these 7,725 (59.3%) were annotated with PFam domains. An analysis of the presence of the BUSCO set of orthologous genes for Basidiomycetes in the ARP23 gene set revealed that it is missing 40 (3%) of the BUSCO genes. This is comparable to the predicted proteomes of H97 and JB137-S8 which are both missing 39 (2.9%) of the BUSCO genes. ARP23 gene calling incorporated RNAseq data from fruitbodies, the final gene set showed evidence that 775 (5.95%) of protein coding genes are alternatively spliced. Overall, the number of genes predicted for ARP23 is larger than that for H97 (10,863) and JB137-S8 (11,289) (**Table 1**). The average number of introns per ORF for the ARP gene set is 5.4, this number is larger than that observed in H97 (4.6) and JB137-S8 (4.7) respectively (**Table 1**). High-level functional annotations were assigned for predicted genes using BlastKOALA (Kanehisa *et al.* 2016). Of the 13,030 predicted ARP23 genes, KO assignments were made for 3,808 (29.22 %). General functions and protein families relating to genetic information processing accounted for the majority of KEGG annotation with 1,693 (45.46%) of proteins falling into these categories. Other pathways highly represented were carbohydrate metabolism with 313 (8%) and environmental information processing with 176 (5%). A total of 750 secreted proteins were predicted by

assigning signal peptides in SignalP v. 5. Putatively secreted proteins with a transmembrane domain downstream of the N-terminus signal peptide were excluded (Sonnhammer *et al.* 1998), with the subsequent prediction of 606 proteins. Secreted proteins involved in hydrolysis of glycoside (*n* = 54, GO:0004553), oxidation-reduction processes (*n* = 82, GO:0055114), and fungal hydrophobins (*n* = 20, PF01185) were highly represented.

2.3.3 Genome phylogeny

The availability of whole genomes permits the reconstruction of phylogenomic trees. From our dataset of 32 fungal genomes we located 71 ubiquitously distributed gene families. These were individually aligned and concatenated to give a supermatrix of 27,861 amino acids. Using this supermatrix, phylogenomic reconstruction analyses were performed using both Maximum likelihood and Bayesian inference (**Figure 2**). The resultant phylogeny successfully resolved strongly supported monophyletic clades for the Ascomycota and Basidiomycota phyla. It also resolved monophyletic clades for the Agaricales, Boletales and Polyporales orders within the Basidiomycota clade (**Figure 2**). Within in the Agaricales order a strongly supported monophyletic Marasmioid clade containing *Schizophyllum commune*, *Moniliophthora roreri*, *Gymnopus luxurians* and *Lentinula* species is present. A monophyletic Agaricoid clade containing *Laccaria bicolor, Coprinopsis cinerea* and *Agaricus bisporus* is also present (**Figure 2**). The single Tricholomatoid clade species, *Hypsizygus marmoreus* is grouped beside the Agaricoid clade in agreement with previous studies (Matheny *et al.* 2006). However the two Pluteoid clade species, *Pleurotus ostreatus* and *Volvariella volvacea* are not grouped together, however it has been suggested that the Pluteoid clade may not be monophyletic (Matheny *et al.* 2006).

With respect to the phylogenetic relationships between the *A. bisporus* strains, our phylogeny groups all three strains in a monophyletic clade with maximum Bayesian posterior probability (BPP) and bootstrap support (BP). Furthermore, H97 and ARP23 are grouped as sister taxa with relatively strong BPP and BP (**Figure 2**). This phylogenetic relationship infers that ARP23 is more closely related to H97 that it is to JB137-S8.

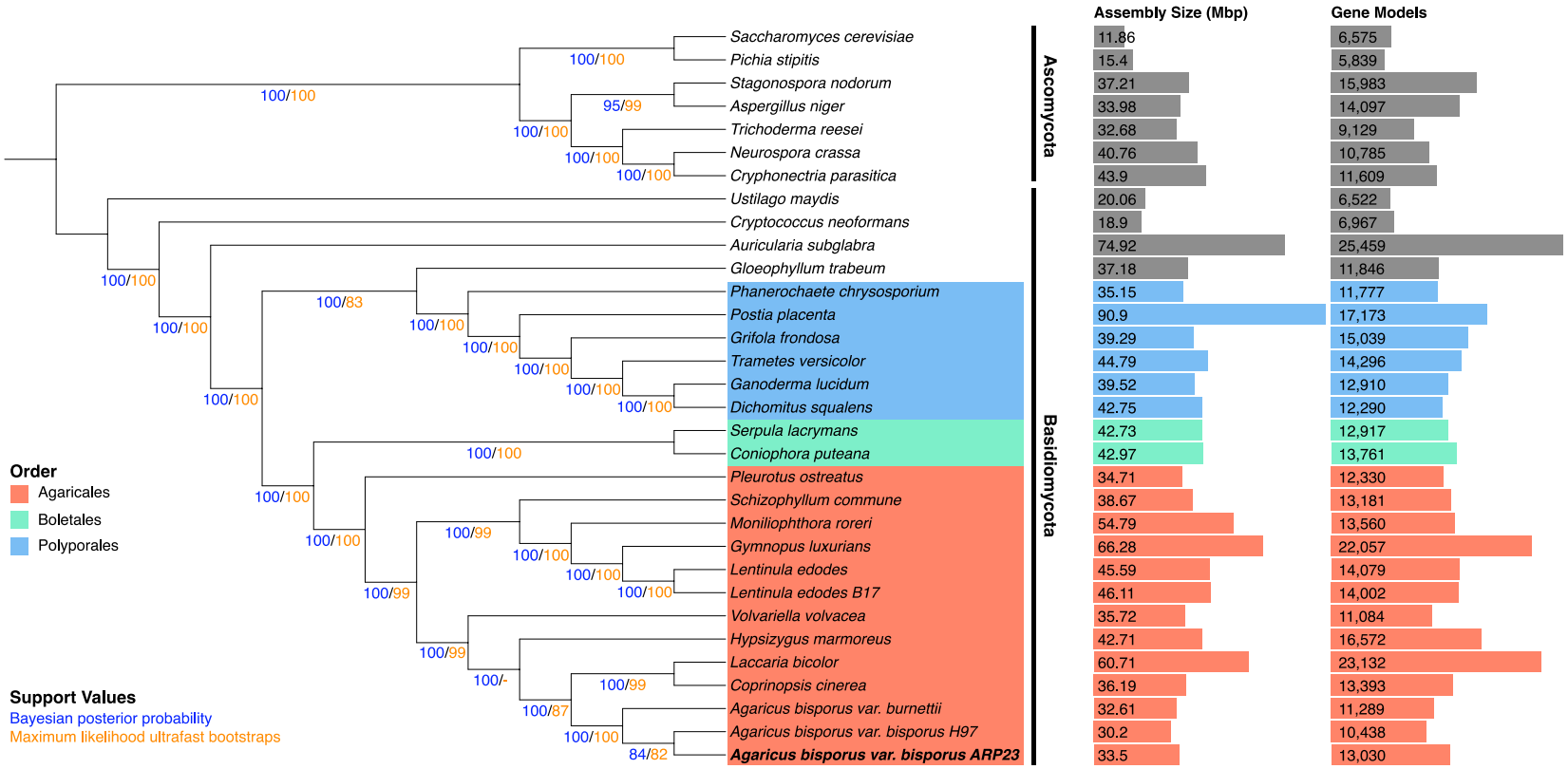

Figure 2: Supermatrix phylogeny of 32 fungal species (71 ubiquitous fungal gene families, 27,861 characters). Phylogenomic analyses were performed using both maximum likelihood (IQ-TREE with LG+F+R5 model) and Bayesian inference (PhyloBayes with the CAT model). Both phylogenies were identical except the maximum likelihood phylogeny grouped *V. volvacea* and *H. marmoreus* as sister taxa while the Bayesian phylogeny did not. Bayesian posterior probabilities and ultrafast bootstrap supports are indicated at all nodes. For comparative purposes the assembly size and number of gene models for each species are also shown.

2.3.4 Carbohydrate-Active Enzymes (CAZys)

A. bisporus is adapted to growth in a humic-rich, leaf-litter environment. The genome of H97 has a carbohydrate-active enzyme gene (CAZyme) (Lombard *et al.* 2014) repertoire more similar to that of white- and brown-rot basidiomycetes as opposed to closer taxonomically-related species such as *C. cinerea* and *L. bicolor* (**Figure 2**) (Morin *et al.* 2012). Similar results were replicated in our analyses of the genomes of *A. bisporus* H97, JBS137-S8 and ARP23 (**Table S2**). A total of 411 putative CAZymes were found in the genome of ARP23 including 176 glycoside hydrolases, 60 glycosyl transferases and 14 carbohydrate-binding modules. In terms of lignocellulolytic genes the three strains of *A. bisporus* have very similar repertoires with ARP23, JB137-S8 and H39 having 149, 142 and 136 genes respectively. Specifically, ARP23 was found to contain 48 cellulases, 19 hemicellulases, 12 pectinases, 17 lignin oxidases and 53 lignocellulolytic auxiliary enzymes (**Table S2**).

2.3.5 Mating Locus

Agaricus bisporus has a pseudo-homothallic life cycle with a unifactorial mating system (Miller 1971; Raper *et al.* 1972). Pseudo-homothallism is a particular system in which automixis is forced, as two haploid nuclei from one meiotic tetrad are packaged together into one spore, therefore self-fertility is the result of the packaging of two independent and opposite mating type nuclei within a single spore (Wilson *et al.* 2015). This lifestyle not only enables the fungus to reproduce without finding a compatible partner, but also to cross with any compatible mate it may encounter (Grognet and Silar 2015). To date this type of reproduction in Basidiomycetes has only been observed in Agaricomycetes (Nieuwenhuis *et al.* 2013). It is possible that pseudo-homothallics benefit from both homothalism, which allows the possibility to self-cross when no compatible partner is present and heterothallism, which favors the creation of genetic variation through recombination during outbreeding (Grognet and Silar 2015).

The locus encoding the homeodomain proteins has previously been located on Chromosome 1 of *A. bisporus* H97 (Morin *et al.* 2012). Our analysis of the mating-type locus of *A. bisporus* ARP23, H97 and JB137-S8 shows they are all very similar to the A mating-type locus of the model species *Coprinopsis cinerea* and are located on scaffold

16, chromosome 1 and scaffold 1 respectively. The locus contains a pair of homeodomain transcription factor genes orthologous to b1-2 and a1-2 from *C. cinerea* (**Figure 3**). The mitochondrial intermediate peptidase (MIP) gene and a Beta-flanking gene which typically accompany the mating A locus are also found in the genomic vicinity (**Figure 3**). Interestingly, all three *A. bisporus* strains have an additionally copy of the Beta-flanking gene relative to *C. cinerea*. Levels of synteny with respect to other flanking genes are also very high (**Figure 3**). The JB137-S8 assembly contains six ORFs between the homeodomain proteins, sequence analysis leads us to believe that this is a misassembly artefact, furthermore all ORFs have homologs in H97 and ARP23 but are located on different scaffolds. Relative to the other mating loci of the other two assemblies, H97 has an additional putative ORF (**Figure 3**). A homolog for this gene is absent for the assemblies of both ARP23 and JB137-SB, furthermore it does not contain any known Pfam domains and a BLASTP search against GenBank retrieves a single significant hit to another Agaricales species (*Leucoagaricus* sp) therefore it may be dubious.

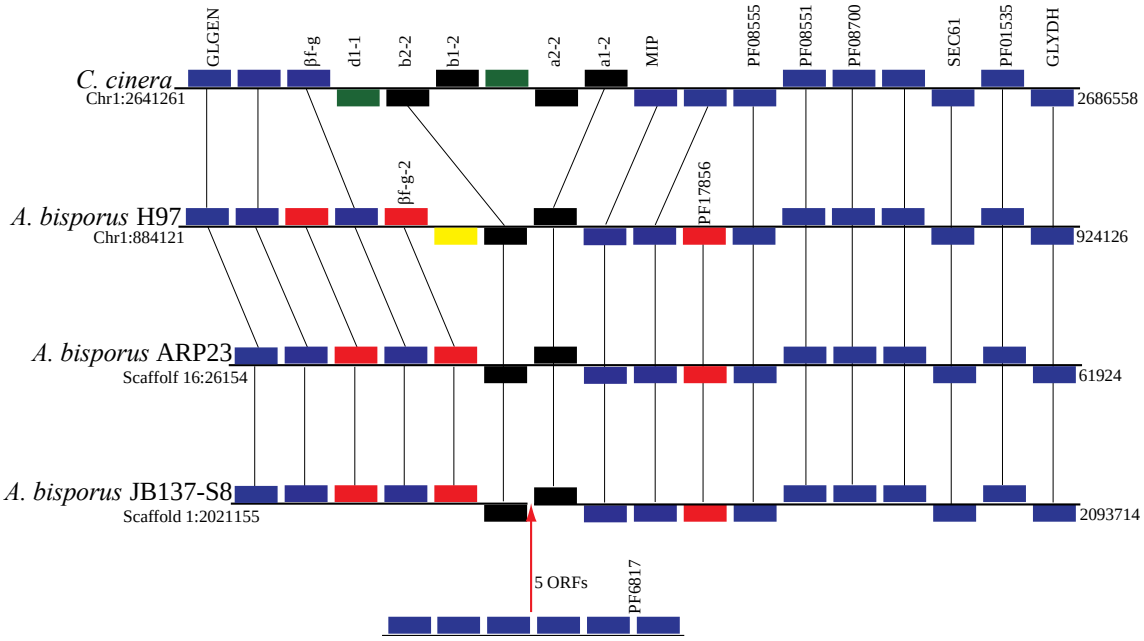

Figure 3: Distribution of genes in the mating type locus of *A. bisporus* H97, ARP23 and JB137-S8. For comparative purposes the mat A locus of the model species C. *cinerea* is also displayed. Chromosome or scaffold and relative genomic position of loci are indicated. Genes that are coloured blue are orthologous in all four genomes and syntenically conserved. Red genes indicate syntenically conserved orthologs in *A. bisporus* strains but missing from *C. cinerea*. *A. bisporus* has a single pair of homeodomain genes (coloured black) while *C. cinerea* has two pairs. Green genes in *C. cinerea* are absent from *A. bisporus* strains. *A. bisporus* H97 has a unique gene (coloured yellow). Six ORFs are located between the homoedomain genes of *A. bisporus* JB137-S8 but are most likely the result of misassembly.

2.3.6 Pangenome analysis of *Agaricus bisporus*

Individual reference genomes do not and cannot contain all genetic information for a species due to genetic and genomic variation between individuals within a species. To account for such variation, it has become increasingly common to refer to species with multiple genomes sequenced in terms of their Pangenome, which is defined as the union of all genes observed across all isolates/strains of a species. A species pangenome for *A. bisporus* was constructed using the synteny-dependent PanOCT method implemented in Pangloss with the default parameters (Fouts *et al.* 2012; McCarthy and Fitzpatrick 2019a, 2019b). PanOCT clusters homologous sequences into syntenic orthologs clusters (SOCs) based on BLAST score ratio (BSR) assessment of sequence similarity and on proportions of relative synteny (conserved gene neighbourhood, CGN) between potential orthologs (Rasko *et al.* 2005; Fouts *et al.* 2012). SOCs with syntenic orthologs from all four *A. bisporus* strain genomes in our dataset were classified as "core" SOCs, and clusters missing an ortholog from ≥1 strain genome were classified as "accessory" SOCs. After initial construction with PanOCT, the *A. bisporus* pangenome was refined by merging accessory SOCs based on reciprocal strain best hits between all members of a given pair of accessory SOCs (McCarthy and Fitzpatrick 2019a, 2019b). In total, we identified 7,732 core SOCs and 8,478 accessory SOCs within our *A. bisporus* dataset (16,120 in total) (**Figure 4**). The proportion of core SOCs relative to the total number of protein coding genes per genome ranged from a low of ~60% in ARP23 to a high of 71% in H97. This proportion of core to accessory genes is lower than we have previously observed in a number of model fungal species (McCarthy and Fitzpatrick 2019a). Analysis of the distribution of SOCs within the *A. bisporus* accessory genome was performed within Pangloss using UpSetR, which is an R implementation of the UpSet method for visualization of set intersections and occurrences within a dataset using matrix representation. The UpSetR plot in **Figure 4** shows that singleton SOCs (i.e. singleton genes) are the most common within the accessory genome, with 2,161 singleton SOCs from ARP23 alone and 6,574 in total (~78% of all syntenic SOCs in the accessory genome). The distribution of the remaining 1,904 non-singleton SOCs within the *A. bisporus* accessory genome appears to follow evolutionary history (**Figure 2**), for example H97 and ARP23 share 727 accessory SOCs either exclusively or along with one other strain, while JB137 and ARP23 only share 615 accessory SOCs exclusively or with another strain (**Figure 4**).

Selection analysis of the core and accessory genomes was performed using the Yang & Nielsen method as implemented in yn00 with the default parameters for yn00. 680 of 7,732 core SOCs (~9% of core SOCs) and 172 of 1,904 non-singleton accessory SOCs (~9% of non-singleton accessory SOCs, ~2% of all accessory SOCs) showed evidence of at least 1 pairwise alignment under positive selection where $d_N/d_S \geq 1$ and $d_N/d_S \neq \infty$ (Yang and Nielsen 2000).

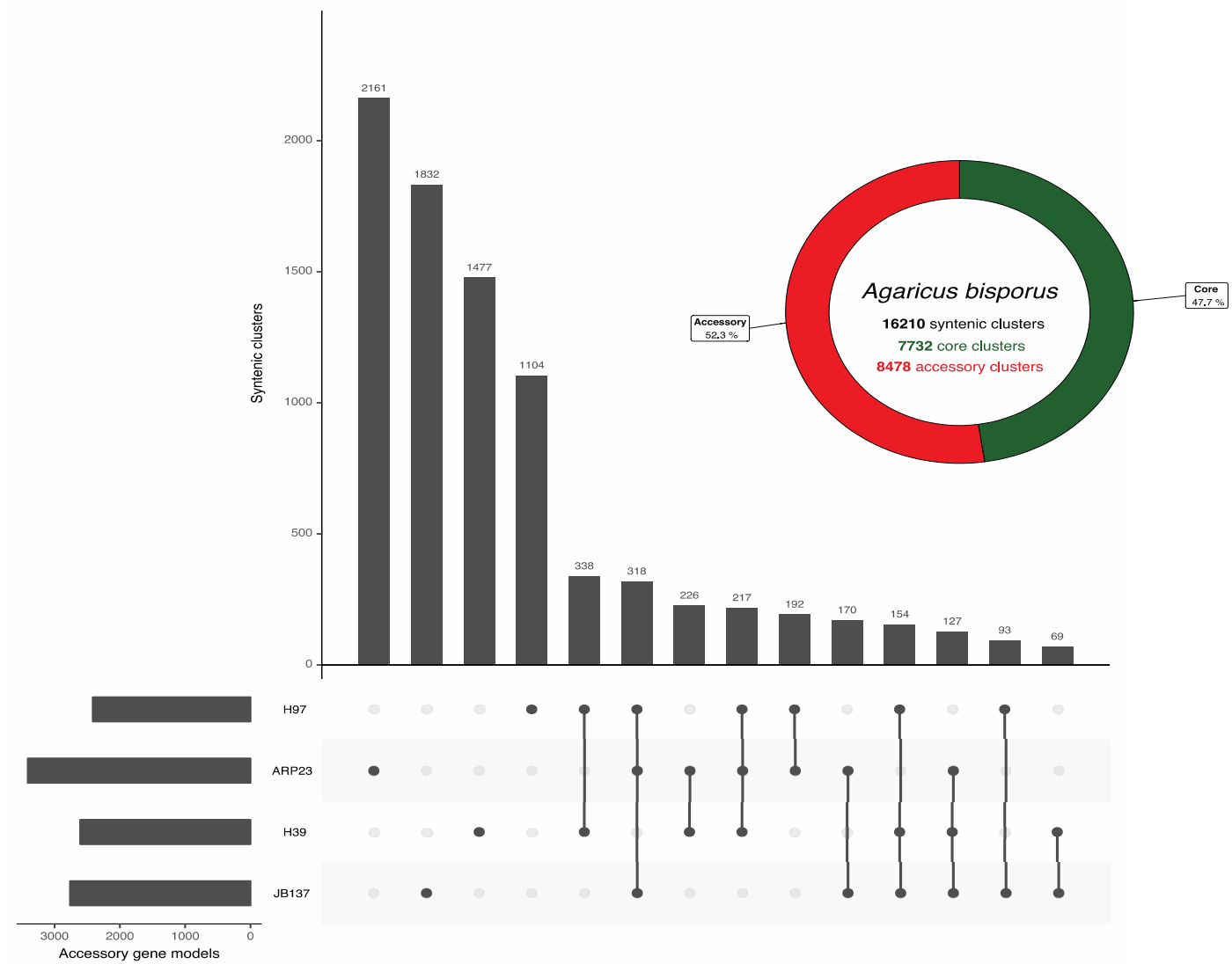

Figure 4: UpSetR plot of the distribution of syntenic clusters within the accessory genome of *Agaricus bisporus*. Inset: The pangenome of *Agaricus bisporus* constructed from four strain genomes. Core genome proportion in green, accessory genome proportion in red.

2.4 Conclusion

In this analysis, we have presented the high-quality genome sequence of *A. bisporus* var. *bisporus* ARP23, a commercially relevant genome. In total the genome was found to be 33.49 Mb in length, have high levels of synteny to H39 and contain 13,030 putative protein coding genes. Relative to the other two *A. bisporus* genomes that are currently available, ARP23 is the largest *A. bisporus* strain sequenced to date. Our analyses show that phylogenetically speaking ARP23 is more closely related to H97 than JB137-SB. Furthermore, all three strains have highly conserved mating loci. The lignocellulolytic gene content of all three *A. bisporus* strains is very similar. The pangenome of *A. bisporus* is quite diverse with between 60 – 70 % of genes considered as core SOCs depending on isolate under consideration. The above analyses and genome sequence are the starting point for more detailed molecular analyses into the growth and phenotypical responses of ARP23 when challenged with economically important mycoviruses.

Acknowledgments

EOC is funded by a Teagasc Walsh Scholarship Scheme (grant reference number 10564231). JM and CGPM are funded by postgraduate scholarships from the Irish Research Council, Government of Ireland (grant numbers GOIPG/2016/1112 and GOIPG/2015/2242). We acknowledge the DJEI/DES/SFI/HEA Irish Centre for High-End Computing (ICHEC) for the provision of computational facilities and support.

Literature Cited

Altschul, S. F., T. L. Madden, A. A. Schäffer, J. Zhang, Z. Zhang *et al.*, 1997 Gapped BLAST and PSI-BLAST: a new generation of protein database search programs. Nucleic Acids Res. 25: 3389–402.

Arora, S., B. Steuernagel, K. Gaurav, S. Chandramohan, Y. Long *et al.*, 2019 Resistance gene cloning from a wild crop relative by sequence capture and association genetics. Nat. Biotechnol. 37: 139–143.

Ashburner, M., C. A. Ball, J. A. Blake, D. Botstein, H. Butler *et al.*, 2000 Gene Ontology: tool for the unification of biology. Nat. Genet. 25: 25–29.

Balakrishnan, R., J. Park, K. Karra, B. C. Hitz, G. Binkley *et al.*, 2012 YeastMine-An integrated data warehouse for Saccharomyces cerevisiae data as a multipurpose tool-kit. Database 2012: bar062.

Benson, G., 1999 Tandem repeats finder: A program to analyze DNA sequences. Nucleic Acids Res. 27: 573–580.

Boetzer, M., and W. Pirovano, 2014 SSPACE-LongRead: scaffolding bacterial draft genomes using long read sequence information. BMC Bioinformatics 15: 211.

Callac, P., M. Imbernon, R. W. Kerrigan, and J.-M. Olivier, 1996 The Two Life Cycles of Agaricus bisporus, Callac, 1996.pdf, pp. 57–66 in *Mushroom Biology and Mushroom Products*,.

Camacho, C., G. Coulouris, V. Avagyan, N. Ma, J. Papadopoulos *et al.*, 2009 BLAST+: architecture and applications. BMC Bioinformatics 10: 421.

Capella-Gutierrez, S., J. M. Silla-Martinez, and T. Gabaldon, 2009 trimAl: a tool for automated alignment trimming in large-scale phylogenetic analyses. Bioinformatics 25: 1972–1973.

Chu, J., 2018 Jupiter Plot: A Circos-based tool to visualize genome assembly consistency.

Dempewolf, H., G. Baute, J. Anderson, B. Kilian, C. Smith *et al.*, 2017 Past and future use of wild relatives in crop breeding. Crop Sci. 57: 1070–1082.

Edgar, R. C., 2004 MUSCLE: Multiple sequence alignment with high accuracy and high throughput. Nucleic Acids Res. 32: 1792–1797.

Emms, D. M., and S. Kelly, 2015 OrthoFinder: solving fundamental biases in whole genome comparisons dramatically improves orthogroup inference accuracy. Genome Biol. 16: 157.

Enright, A. J., S. Van Dongen, and C. A. Ouzounis, 2002 An efficient algorithm for large-scale detection of protein families. Nucleic Acids Res. 30: 1575–84.

Férandon, C., J. Xu, and G. Barroso, 2013 The 135 kbp mitochondrial genome of Agaricus bisporus is the largest known eukaryotic reservoir of group I introns and plasmid-related sequences. Fungal Genet. Biol. 55: 85–91.

Fletcher, J. T., 1992 Disease resistance in protected crops and mushrooms. Euphytica 63: 33–49.

Foulongne-Oriol, M., A. Rodier, T. Rousseau, M. Largeteau, and J. M. Savoie, 2011 Quantitative genetics to dissect the fungal-fungal interaction between Lecanicillium verticillium and the white button mushroom Agaricus bisporus. Fungal Biol. 115: 421–431.

Fouts, D. E., L. Brinkac, E. Beck, J. Inman, and G. Sutton, 2012 PanOCT: Automated clustering of orthologs using conserved gene neighborhood for pan-genomic analysis of bacterial strains and closely related species. Nucleic Acids Res. 40: e172–e172.

Gao, W., J. J. P. Baars, O. Dolstra, R. G. F. Visser, and A. S. M. Sonnenberg, 2013 Genetic Variation and Combining Ability Analysis of Bruising Sensitivity in Agaricus bisporus (C. Schönbach, Ed.). PLoS One 8: e76826.

Grogan, H. M., B. A. T. Adie, R. H. Gaze, M. P. Challen, and P. R. Mills, 2003 Double-stranded RNA elements associated with the MVX disease of

Agaricus bisporus. Mycol. Res. 107: 147–154.

Grognet, P., and P. Silar, 2015 Maintaining heterokaryosis in pseudo-homothallic fungi. Commun. Integr. Biol. 8: e994382.

Hackl, T., R. Hedrich, J. Schultz, and F. Förster, 2014 Proovread: Large-scale high-accuracy PacBio correction through iterative short read consensus. Bioinformatics 30: 3004–3011.

Hoang, D. T., O. Chernomor, A. von Haeseler, B. Q. Minh, and L. S. Vinh, 2018 UFBoot2: Improving the Ultrafast Bootstrap Approximation. Molecular biology and evolution. Mol. Biol. Evol. 35: 518–522.

Hoff, K. J., S. Lange, A. Lomsadze, M. Borodovsky, and M. Stanke, 2016 BRAKER1: Unsupervised RNA-Seq-based genome annotation with GeneMark-ET and AUGUSTUS. Bioinformatics 32: 767–769.

Hussey, N. W., and I. J. Wyatt, 1960 Insecticidal control of paedogenetic cecid larvae in mushroom beds. Ann. Appl. Biol. 48: 347–351.

Jones, P., D. Binns, H.-Y. Chang, M. Fraser, W. Li *et al.*, 2014 InterProScan 5: genome-scale protein function classification. Bioinformatics 30: 1236–40.

Kalyaanamoorthy, S., B. Q. Minh, T. K. F. Wong, A. von Haeseler, and L. S. Jermiin, 2017 ModelFinder: fast model selection for accurate phylogenetic estimates. Nat. Methods 14: 587–589.

Kanehisa, M., Y. Sato, and K. Morishima, 2016 BlastKOALA and GhostKOALA: KEGG Tools for Functional Characterization of Genome and Metagenome Sequences. J. Mol. Biol. 428: 726–731.

Kerrigan, R. W., 2000 A brief history of marker assisted selection in Agaricus bisporus. Sci. Cultiv. edible fungi. Proc. 15th Int. Congr. Sci. Cultiv. Edible Fungi, Maastricht, Netherlands, 15-19 May, 2000. 183–189.

Kerrigan, R. W., M. Imbernon, P. Callac, C. Billette, and J.-M. Olivier, 1994 The Heterothallic Life Cycle of Agaricus bisporus var. burnettii and the

Inheritance of Its Tetrasporic Trait. Exp. Mycol. 18: 193–210.

Koren, S., B. P. Walenz, K. Berlin, J. R. Miller, N. H. Bergman *et al.*, 2017 Canu: Scalable and accurate long-read assembly via adaptive κ-mer weighting and repeat separation. Genome Res. 27: 722–736.

Lagesen, K., P. Hallin, E. A. Rødland, H.-H. Stærfeldt, T. Rognes *et al.*, 2007 RNAmmer: consistent and rapid annotation of ribosomal RNA genes. Nucleic Acids Res. 35: 3100–3108.

Langmead, B., and S. L. Salzberg, 2012 Fast gapped-read alignment with Bowtie 2. Nat. Methods 9: 357–359.

Lartillot, N., T. Lepage, and S. Blanquart, 2009 PhyloBayes 3: a Bayesian software package for phylogenetic reconstruction and molecular dating. Bioinformatics 25: 2286–2288.

Letunic, I., and P. Bork, 2007 Interactive Tree Of Life (iTOL): An online tool for phylogenetic tree display and annotation. Bioinformatics 23: 127–128.

Li, H., and R. Durbin, 2010 Fast and accurate long-read alignment with Burrows-Wheeler transform. Bioinformatics 26: 589–595.

Lombard, V., H. Golaconda Ramulu, E. Drula, P. M. Coutinho, and B. Henrissat, 2014 The carbohydrate-active enzymes database (CAZy) in 2013. Nucleic Acids Res. 42: D490-5.

Lowe, T. M., and P. P. Chan, 2016 tRNAscan-SE On-line: integrating search and context for analysis of transfer RNA genes. Nucleic Acids Res. 44: W54–W57.

Marçais, G., and C. Kingsford, 2011 A fast, lock-free approach for efficient parallel counting of occurrences of k-mers. Bioinformatics 27: 764–770.

Martin, M., 2011 Cutadapt removes adapter sequences from high-throughput sequencing reads. EMBnet.journal 17: 10.

Matheny, P. B., J. M. Curtis, V. Hofstetter, M. C. Aime, J.-M. Moncalvo *et al.*,

2006 Major clades of Agaricales: a multilocus phylogenetic overview. Mycologia 98: 982–95.

McCarthy, C. G. P., and D. A. Fitzpatrick, 2019a Pan-genome analyses of model fungal species. Microb. Genomics 5:.

McCarthy, C. G. P., and D. A. Fitzpatrick, 2019b Pangloss: A Tool for Pan-Genome Analysis of Microbial Eukaryotes. Genes (Basel). 10: 521.

Miller, R. E., 1971 Evidence of Sexuality in the Cultivated Mushroom, Agaricus bisporus. Mycologia 63: 630.

Moquet, F., C. Desmerger, M. Mamoun, M. Ramos-Guedes-Lafargue, and J. M. Olivier, 1999 A quantitative trait locus of Agaricus bisporus resistance to Pseudomonas tolaasii is closely linked to natural cap color. Fungal Genet. Biol. 28: 34–42.

Morin, E., A. Kohler, A. R. Baker, M. Foulongne-Oriol, V. Lombard *et al.*, 2012 Genome sequence of the button mushroom Agaricus bisporus reveals mechanisms governing adaptation to a humic-rich ecological niche. Proc. Natl. Acad. Sci. 109: 17501–17506.

Nguyen, L. T., H. A. Schmidt, A. Von Haeseler, and B. Q. Minh, 2015 IQ-TREE: A fast and effective stochastic algorithm for estimating maximum-likelihood phylogenies. Mol. Biol. Evol. 32: 268–274.

Nieuwenhuis, B. P. S., S. Billiard, S. Vuilleumier, E. Petit, M. E. Hood *et al.*, 2013 Evolution of uni- and bifactorial sexual compatibility systems in fungi. Heredity (Edinb). 111: 445–55.

North, L. H., and P. J. Wuest, 1993 The infection process and symptom expression of verticillium disease of agaricus bisporus. Can. J. Plant Pathol. 15: 74–80.

Ogata, H., S. Goto, K. Sato, W. Fujibuchi, H. Bono *et al.*, 1999 KEGG: Kyoto Encyclopedia of Genes and Genomes. Nucleic Acids Res. 27: 29–34.

Prescott, T., J. Wong, B. Panaretou, E. Boa, A. Bond *et al.*, 2018 Useful fungi, pp. 24–31 in *State of the World's Fungi. Report. Royal Botanic Gardens, Kew.*, edited by K. Willis.

Raper, C. A., J. R. Raper, and R. E. Miller, 1972 Genetic Analysis of the Life Cycle of Agaricus bisporus. Mycologia 64: 1088.

Rasko, D. A., G. S. A. Myers, and J. Ravel, 2005 Visualization of comparative genomic analyses by BLAST score ratio. BMC Bioinformatics 6: 2.

Roach, M., S. Schmidt, and A. Borneman, 2018 Purge Haplotigs: Synteny Reduction for Third-gen Diploid Genome Assemblies. bioRxiv 286252.

Royse, D. J., and B. May, 1982 Genetic Relatèdness and Its Application in Selective Breeding of Agaricus brunnescens. Mycologia 74: 569–575.

Simão, F. A., R. M. Waterhouse, P. Ioannidis, E. V. Kriventseva, and E. M. Zdobnov, 2015 BUSCO: Assessing genome assembly and annotation completeness with single-copy orthologs. Bioinformatics 31: 3210–3212.

Soler-Rivas, C., 1999 Biochemical and physiological aspects of brown blotch disease of Agaricus bisporus. FEMS Microbiol. Rev. 23: 591–614.

Sonnenberg, A. S. M., W. Gao, B. Lavrijssen, P. Hendrickx, N. Sedaghat-Tellgerd *et al.*, 2016 A detailed analysis of the recombination landscape of the button mushroom Agaricus bisporus var. bisporus. Fungal Genet. Biol. 93: 35–45.

Sonnhammer, E. L., G. von Heijne, and A. Krogh, 1998 A hidden Markov model for predicting transmembrane helices in protein sequences. Proceedings. Int. Conf. Intell. Syst. Mol. Biol. 6: 175–82.

Stanke, M., O. Schöffmann, B. Morgenstern, and S. Waack, 2006 Gene prediction in eukaryotes with a generalized hidden Markov model that uses hints from external sources. BMC Bioinformatics 7: 62.

Vurture, G. W., F. J. Sedlazeck, M. Nattestad, C. J. Underwood, H. Fang *et al.*,

2017 GenomeScope: fast reference-free genome profiling from short reads (B. Berger, Ed.). Bioinformatics 33: 2202–2204.

Wilson, A. M., P. M. Wilken, M. A. van der Nest, E. T. Steenkamp, M. J. Wingfield *et al.*, 2015 Homothallism: an umbrella term for describing diverse sexual behaviours. IMA Fungus 6: 207–14.

Yang, Z., and R. Nielsen, 2000 Estimating Synonymous and Nonsynonymous Substitution Rates Under Realistic Evolutionary Models. Mol. Biol. Evol. 17: 32–43.

Zhang, H., T. Yohe, L. Huang, S. Entwistle, P. Wu *et al.*, 2018 DbCAN2: A meta server for automated carbohydrate-active enzyme annotation. Nucleic Acids Res. 46: W95–W101.

Chapter 3:

Proteomic investigation of interhyphal interactions between strains of *Agaricus bisporus*

3.0 Proteomic investigation of interhyphal interactions between strains of *Agaricus bisporus*

Eoin O'Connor[1,4], Rebecca Owens[1,2], Sean Doyle[1], Aniça Amini[3], Helen Grogan[4] & David A. Fitzpatrick[1,2]

[1]Department of Biology, Maynooth University, Maynooth, Co. Kildare, Ireland

[2] Human Health Research Institute, Maynooth University, Maynooth, Co. Kildare, Ireland

[3] Sylvan-Somycel (ESSC - Unité 2), ZI SUD, rue Lavoisier, BP 25, 37130 Langeais, France

[4] Teagasc Food Research Centre, Ashtown, Dublin 15, D15 KN3K, Ireland

This paper was accepted for publication in the journal Fungal Biology (February 2020)

Citation:

O'Connor, E., Owens, R., Doyle, S., Amini, A., Grogan, H. and Fitzpatrick, D.A., 2020. Proteomic investigation of interhyphal interactions between strains of Agaricus bisporus. *Fungal Biology*.

Keywords: *Agaricus bisporus*, hypha-hypha proteomics, anastomosis, hyphal-fusion, vegetative incompatibility.

Abstract

Hyphae of filamentous fungi undergo polar extension, bifurcation and hyphal fusion to form reticulating networks of mycelia. Hyphal fusion or anastomosis, a ubiquitous process among filamentous fungi, is a vital strategy for how fungi expand over their substrate and interact with or recognise self- and non-self hyphae of neighbouring mycelia in their environment. Morphological and genetic characterisation of anastomosis has been studied in many model fungal species, but little is known of the direct proteomic response of two interacting fungal isolates. *Agaricus bisporus*, the most widely cultivated edible mushroom crop worldwide, was used as an *in vitro* model to profile the proteomes of interacting cultures. The globally cultivated strain (A15) was paired with two distinct strains; a commercial hybrid strain and a wild isolate strain. Each co-culture presented a different interaction ranging from complete vegetative compatibility (self), lack of interactions, and antagonistic interactions. These incompatible strains are the focus of research into disease-resistance in commercial crops as the spread of intracellular pathogens, namely mycoviruses, is limited by the lack of interhyphal anastomosis. Unique proteomic responses were detected between all co-cultures. An array of cell wall modifying enzymes, plus fungal growth and morphogenesis proteins were found in significantly ($P < 0.05$) altered abundances. Nitrogen metabolism dominated in the intracellular proteome, with evidence of nitrogen starvation between competing, non-compatible cultures. Changes in key enzymes of *A. bisporus* morphogenesis were observed, particularly via increased abundance of glucanosyltransferase in competing interactions and certain chitinases in vegetative compatible interactions only. Carbohydrate-active enzyme arsenals are expanded in antagonistic interactions in *A. bisporus*. Pathways involved in carbohydrate metabolism and genetic information processing were higher in interacting cultures, most notably during self-recognition. New insights into the differential response of interacting strains of *A. bisporus* will enhance our understanding of potential barriers to viral transmission through vegetative incompatibility. Our results suggest that a differential proteomic response occurs between *A. bisporus* at strain-level and findings from this work may guide future proteomic investigation of fungal anastomosis.

3.1 Introduction

Unicellular fungi from the Ascomycota phylum, such as the yeasts *Candida albicans* and *Saccharomyces cerevisiae*, form adhesions for cell-cell communication, biofilm formation, pathogenesis, commensalisms and primary phases of saprophytic interactions composed of mannoproteins covalently bound to the cell wall (Lipke, 2018). Adhesion and signalling domains are critical for the innovation from unicellularity to complex multicellularity (CM). Phylogenomic and genomic evidence suggests that CM has independently evolved in five eukaryotic groups including the fungi (Knoll, 2011). Within the fungi it occurs in most major clades and displays at least 8 and perhaps as many as 11 independent origins (Nagy et al., 2018). A variety of complex micropore structures bridge intracellular connections of multicellular ascomycete and basidiomycete hyphae (Markham, 1994). Hyphae are the structural units, segmented by septa (Harris, 2001), of vegetative growth in filamentous fungi. They are tubular in shape and have polarised extensions through apical growth mediated by high pressure and vesical transport of a multitude of important enzymes for cell wall biosynthesis. These enzymes remain inactive in cytoplasmic transit until buried in the transmembrane of apical regions, whereby the synthesis of β-1-3-glucan and chitin can occur and recruitment of cytosolic-derived glycoproteins from the endoplasmic reticulum-to-Golgi pathway for cell wall biogenesis (Riquelme *et al*., 2016). In fast growing hyphal tips, a cytoskeletal-derived structure known as the Spitzenkörper, both fuses and extends the cell wall of the apex by recruitment of transport vesicles (Bartnicki-Garcia *et al*., 1989) and is responsible for the directionality of hyphal growth (Reynaga-Pena et al., 1997). Hyphae both extend at their apex and form sub-apical growth of branching hyphae commonly in a bifurcating fashion (Girbardt, 1957, 1969; Lopez-Franco and Bracker, 1996; Riquelme and Bartnicki-Garcia, 2004). Anastomosis (hyphal fusion) of branching and apical hyphae takes place to form the reticulating network architecture known as the mycelium (**Figure 1**).

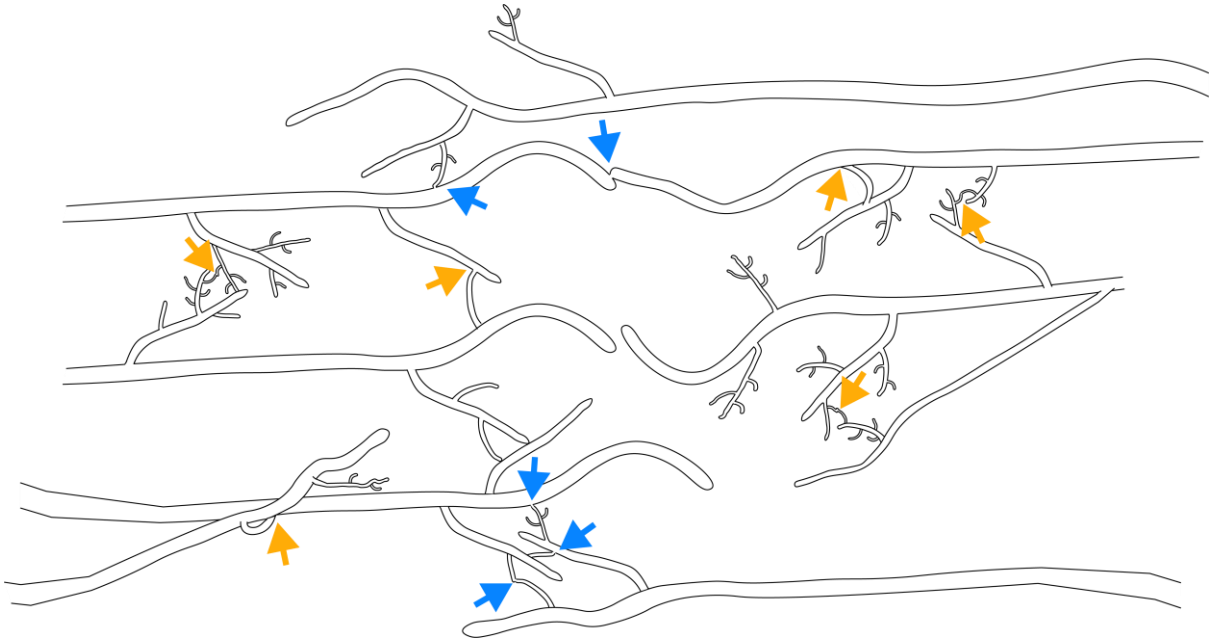

Figure 1: Representation of the demarcation zone between two neighbouring vegetative-compatible strains of *A. bisporus* mycelia originating from opposite directions. The substrate area is covered by the apical extension of a main/leading hypha which continuously generates primary branches which may be subtended by secondary branches. Anastomoses are most frequently observed in branching hyphae but may occasionally be seen in leading hyphae. Orange arrows represent self-anastomoses and blue arrows represent non-self anastomoses.

The process of anastomosis allows the mycelium to form large single-unit colonies for purposes of heightening exocytosis coverage for chemotactic activity and hydrolysing proteins allowing for physical expansions in ecosystems. Mating of combinations of different cultures was first evaluated when it was found that mixing cultures of the model fungus *Aspergillus nidulans* created parasexual recombinants (Pontecorvo *et al*., 1953). Parasexuality in filamentous fungi allows heterokaryons with different genotypes to undergo anastomosis and form a new hybrid heterokaryotic mycelium with cytoplasmic exchange (plasmogamy) and novel nuclear types, conferring genetic advantages to species, particularly those that may have low rates of meiosis or recombination (Glass and Fleissner, 2006; Pontecorvo, 1956; Swart et al., 2001). To

prevent anastomoses of incompatible hyphae or hyphae that may incur deleterious interactions, a vegetative incompatibility complex (*vic*) and a sexual incompatibility (*het*) system, mediated by mating loci, are found in filamentous fungi. Incompatible fusions of fungal hyphae can trigger inhibited growth and even programmed cell death (Biella et al., 2002; Garnjobst and Wilson, 1956; Labarere and Bernet, 1977; Sarkar, 2002). These systems can act as protective mechanisms where anastomosis with non-self hyphae could be disadvantageous. An example of such is fusion with a foreign mycelium harbouring infectious intracellular mycoviruses (Chu et al., 2002; Grogan et al., 2004; Kashif et al., 2019; Romaine et al., 1993; van Diepeningen et al., 1998).

Agaricus bisporus is the most cultivated mushroom worldwide and is grown commercially on a pasteurised compost substrate most commonly composed of wheat straw, horse and/or poultry manure and gypsum (Van Griensven, 1987; Vedder, 1978). In commercial practice, two main phases precede the formation of mushrooms; the spawn run phase and casing phase. Focusing on the former, the success of the spawn run phase is dependent on the compost substrate being heavily colonised by *A. bisporus* hyphae (Kabel et al., 2017), a process that involves mass breakdown of aromatic lignins, cellulose, hemicellulose and nitrogen sources (including bacterivorous nutrient acquisition (Fermor et al., 1991)). To begin this process, pasteurised compost is 'seeded' with *A. bisporus*-coated spawn that instigates the process of compost colonisation. These isolated colonies must undergo self-recognition and anastomose with other colonies. While studies have focused on molecular mechanisms governing how *A. bisporus* breaks down commercial compost (Pontes et al., 2018; Wood and Thurston, 1991; Yague et al., 1997), little attention has been paid to the impact of colony recognition/anastomosis in this process. To address this, we have analysed the proteomic response of three different strains of *A. bisporus in-vitro* to build an understanding of the molecular mechanisms governing inter-hyphal interactions. Particular focus is paid to the globally cultivated commercial white mushroom strain A15, as this strain has been almost exclusively used in commercial mushroom industries for nearly three decades due to its commercial appeal (Arce-Cervantes et al., 2015). Furthermore, this strain is susceptible to disease-causing mycoviruses, the transmission of which is governed by anastomosis of infected mycelium with healthy mycelium (Grogan et al., 2003). Breeding research has focused attention on novel hybrids that have vegetative incompatibility with A15, as strains which do not readily form hyphal fusions are a tool for disease-resistance. This is exemplified by the

method of introducing a "virus-breaker variety" to a diseased crop, as the latter introduced mycelium can prevent further transmission of mycoviruses in the compost bed (Fletcher and Gaze, 2007). One such strain is a novel commercial white and brown wild strain hybrid referred herein as CWH, known for its heightened resistance to mushroom virus X (data unpublished). Another strain used in this study is ARP23, a wild isolate of the ARP collection (Callac et al., 1996). Wild strains of *A. bisporus* have also shown promise in terms of disease resistance (Glass et al., 2000; Glass and Kuldau, 1992; Leslie, 1993) for their lack of vegetative compatibility (in heterokaryotic terms) with commercial white strains.

Inter-hyphal fusion in the commercial button mushroom fungus *A. bisporus* is a key area of interest due to its importance in successful compost substrate colonisation and the roles it plays in the spread of deleterious mycoviral diseases. In this study, phenotypic evidence shows A15 anastomoses more readily with itself than with strains CWH or ARP23. By using a combination of three distinct strains of *A. bisporus*, an untargeted approach was taken to elucidate the proteomic response of anastomosis.

3.2 Methods

3.2.1 Strains and culture conditions

Three strains of *A. bisporus* were used in this study: (1) commercial strain A15, (2) a novel experimental hybrid strain CWH from a cross between a commercial white and a wild-type brown, and (3) a wild strain ARP23 from the *Agaricus* Resource Program (ARP) collection (Callac et al., 1996), all obtained from Sylvan Inc., France. All strains were grown on complete yeast media (CYM) containing 2 g proteose peptone, 2 g yeast extract, 20 g glucose, 0.5 g $MgSO_4$, 0.46 g KH_2PO_4, 1 g K_2HPO_4, 10 g agar in 500 ml dH_20. Once molten media had solidified and cooled, a sterile sheet of cellophane, the same circumference as the petri dish was added to the surface of the CYM. CYM was either inoculated with a single agar plug for monoculture preparations or two agar plugs placed either end of the petri dish for co-culture preparations. Cultures were grown for two weeks in the dark, at 25 ºC. Two weeks allows enough time for ample hyphal interaction of co-cultures. The following samples were prepared: monocultures of A15, CWH and ARP23; co-cultures of A15-A15, A15-CWH and A15-ARP23.

3.2.2 Extracellular and secreted protein extraction

Equal numbers of monocultures (n = 8) to co-cultures were used to minimize quantity bias of starting materials for any particular strain. The entire mycelial mass was subject to protein isolation, as opposed to targeting growing edges of monocultures or growing edge and interaction zones of co-cultures, so as to capture the broadest suite of secreted and extracellular proteins present. Cellophane coated with fungal hyphae was carefully removed with sterile forceps and added to 50 ml 50 mM potassium phosphate pH 7.5, 1 µg/ml Pepstatin A, 1 mM PMSF, 1 mM EDTA to allow for detachment of the mycelial sheet from the cellophane. Mycelium/buffer mix was gently agitated for 24 h on a daisywheel at 4°C. Hyphal suspensions were filtered through Miracloth and filtrates were clarified by centrifuging at 25,000 x g for 30 min (4°C), twice. Supernatants were brought to 15% (v/v) trichloroacetic acid (TCA) using 100% TCA. TCA suspensions were agitated overnight using a daisywheel (4°C). Protein precipitate was centrifuged at 1700 x g for 45 min (4°C) and pellets were washed with 20% (v/v) 50 mM Tris-base in acetone with two additional Tris-buffered acetone washes and one additional acetone

wash. Dried-protein pellets were resuspended in 6 M urea, 2 M thiourea and 100 mM Tris-HCl pH 8.0. Protein concentrations were calculated using the Qubit Protein assay kit (ThermoFisher, Waltham, Massachusetts, USA), measurements were performed using the Qubit Fluorometer 1.0 (ThermoFisher, Waltham, Massachusetts, USA) and resuspended protein concentrations were normalised for each sample. Urea concentration was adjusted to 1 M by addition of 50 mM ammonium bicarbonate. Proteins were reduced and alkylated by addition of 0.5 M DTT and 0.55 M IAA, with an incubation for 15 min in the dark at room temperature (Collins et al., 2013). Protein digestion was performed using ProteaseMAX at a concentration of 0.01% (w/v) followed by addition of sequencing-grade trypsin. Tryptic peptides were acidified with trifluoroacetic acid (TFA) and desalted using C_{18} Ziptips (Millipore® Ziptips C18) (Dolan et al., 2014; Moloney et al., 2016; O'Keeffe et al., 2014; Owens et al., 2015; Sipos et al., 2017).

3.2.3 LC-MS/MS analysis of *A. bisporus* proteins

LC-MS/MS identification of *A. bisporus* proteins was carried out on tryptic peptide mixtures using a Q-Exactive (ThermoFisher Scientific, U.S.A) coupled to a Dionex RSLCnano. LC gradients from 3-45% B were run over 2 h and data were collected using a Top15 method for MS/MS scans. Spectra were analysed using the predicted protein databases of *Agaricus bisporus* var. *bisporus* (H97) v2.0 (Morin et al., 2012) for the main protein data set and functional analysis. Spectra were also analysed against the predicted proteome of *Agaricus bisporus* var. *bisporus* (ARP23;O'Connor *et al.*, 2019) for analysis of ARP23 specific hits. This was done by concatenating the H97 and ARP23 genomes and considering protein hits to the ARP23 genome alone. MaxQuant (version 1.6.2.3) with integrated Andromeda was used for database searching (Cox and Mann, 2008). MaxQuant parameters are as previously described (Owens et al., 2015). Removal of reverse hits and contaminant sequences, filtering of protein hits found in only a single replicate (n = 3), and Log_2 transformation of LFQ intensities was performed using Perseus (version 1.4.1.3; (Tyanova et al., 2016)).

3.2.4 Bioinformatics analyses

Peptides mapped to translated open reading frames (ORFs) in the genome of *A. bisporus* were functionally annotated with known protein family (Pfam) domains and domains allocated from the Interpro consortium using InterproScan 5 (Jones *et al.*, 2014). Gene ontology (GO; Ashburner *et al.*, 2000) IDs were assigned with Interoscan5 and a term map generated for functional descriptions with the Yeastmine resource (Balakrishnan et al., 2012). The proteomes of monocultures and co-cultures were analysed using KEGG (Kyoto Encyclopaedia of Genes and Genomes; Ogata *et al.*, 1999) with pathway annotations assigned by BlastKOALA (Kanehisa *et al*., 2016). Identification of putatively secreted proteins was done using SignalP v3 (Dyrløv Bendtsen et al., 2004). SignalP v3 was chosen over newer versions (v4 and v5) as studies have established it is an effective prediction tool for fungal secretomes (Sperschneider et al., 2015). Criteria for putatively secreted proteins in SignalP v3 were as follows; NN D score of ≥0.5, HMM S probability value of ≥0.9 and NN Y_{max} score of ≥0.5. TMHMM was used to predict transmembrane (TM) domains (Sonnhammer *et al*., 1998). Proteins containing TM domains after the signal peptide (SP) cleavage site are embedded in the membrane and so normally TMHMM is used as a filtering tool to remove proteins that are not secreted into extracellular space (Käll *et al*., 2007). However, as these proteins may be embedded in the outer membrane of cells, they were not removed for the purposes of this study. SecretomeP was also used to predict leaderless signal peptides (LSPs) of secreted proteins that do not contain classical SignalP domains (Bendtsen *et al.*, 2004). A cut-off of NN-score/SecP ≥0.6 was applied.

Comparative quantitative proteomics was carried out with particular focus on proteins which were statistically significant differentially abundant (SSDA; $P < 0.05$, fold change ≥ 1.5) between pairwise comparisons of samples. Each monoculture and co-culture proteome was searched against the dbCAN2 (Zhang et al., 2018) to identify Carbohydrate Active Enzymes (CAZys; Cantarel *et al.*, 2009). All gene accession IDs listed in this text are preceded by the Joint Genome Institute (JGI) identifier 'jgi|Agabi_varbisH97_2'.

3. Results

3.3.1 Interactions of three strains of *A. bisporus*

Observations were made between anastomoses of A15 with A15 (A15-A15), A15 with CWH (A15-CWH) and A15 with ARP23 (A15-ARP23). A clear distinction is evident between the interactions of A15-A15 (self) and the other combinations**.** When A15 is paired with itself, a plethora of hypha-hypha fusion ensues almost immediately upon interaction of the two colonies growing in the same trajectory (positive tropism) (**Figure 2A**). However, a characteristic demarcation zone of interaction is still evident pertaining to a level of recognition between cultures from different sources. The interaction of A15 with CWH is less prominent, with a distinct zone where hyphal extension is halted (negative tropism) and evidence of hyphal fusion between colonies can only be observed microscopically (data not shown) (**Figure 2B**). Although there is evidently more interaction between A15 and ARP23, a more defined barrier of interaction is established between the two colonies (combination of positive and negative tropism) (**Figure 2C**). Interestingly, A15 formed hyphal plumes of aerial growth in every interaction replicate with ARP23. Aerial or 'fluffy' growth of mycelium *in vitro* can be an indication of stress (Beites et al., 2015; Flärdh and Buttner, 2009; Hansberg and Aguirre, 1990). Aerial growth occurs as polar extension of apical hyphae attempt non-planar growth from the current substrate surface to a new area. Each strain/interaction was grown on CYM, a media commonly used for culturing *A. bisporus* (De La Bastide et al., 1997; Kaur et al., 2011; Li et al., 1994; Masoumi et al., 2015). A thin layer of cellophane was applied to the media prior to inoculation with *A. bisporus* cultures to allow for careful removal of mycelium prior to protein capture and exclusion of any proteins originating from the constituents of CYM. Acquisition of nutrients and normal growth from the cellophane membrane-coated CYM is exemplified through growth rate measurements (data not shown).

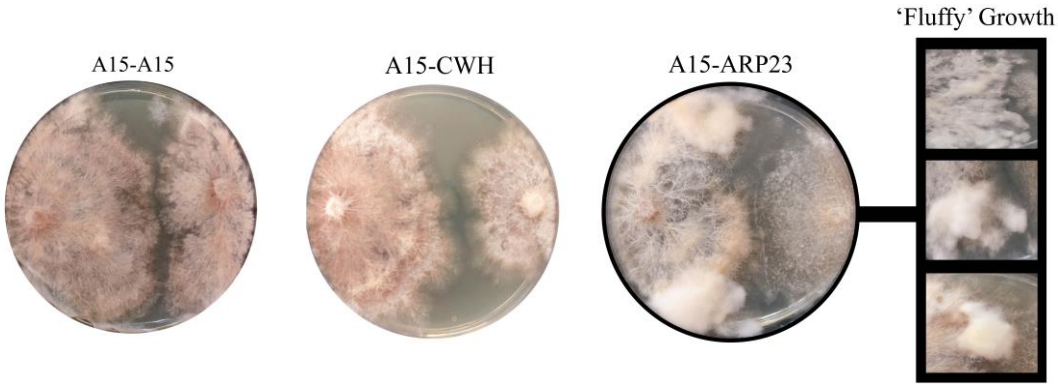

Figure 2: Interactions between different strains of *A. bisporus* grown on cellophane membranes on CYM. A15 paired with A15: Note areas where hyphae cross culture boundaries primarily at the top and bottom of the interaction zones. A15 (left colony) paired with CWH (right colony): Cultures appear to repel one another, with no visible hyphal crossover. A15 (left colony) interacting with ARP23 (right colony): A highly defined zone of interaction is clear. Formation of 'fluffy' growth in plumes of hyphae can be seen at the top and bottom of A15 and in the three panels from other A15-ARP23 replicate plates.

3.3.2 Monoculture and co-culture proteomes

For the purpose of this investigation, the methods used to extract proteins were tailored to extracellular and secreted protein acquisition from hyphae to minimise cell lysis. However, intracellular proteins were also considered as they may also play key roles in inter-hyphal interactions, due to fact that the process from recognition to anastomosis can often result in levels of cell lysis via apoptosis and necrosis leading to release of cytosolic proteins into extracellular spaces (Bourges et al., 1998; Paoletti and Clavé, 2007). The total number of unique unambiguously-detected proteins, for all monoculture and co-culture comparisons, was 1,500 when aligned to the predicted proteome of *A. bisporus* (H97; commercial cultivar) and 1,510 when aligned to the predicted proteome of *A. bisporus* (ARP23; wild strain). By concatenating the two genomes a total number of 1,829 proteins were detected, indicating that certain proteins are uniquely identified or absent in the concomitant strain genomes (see **Table 1**). This is unsurprising as pangenome analyses of *A. bisporus* strains have shown high levels of

gene variability between individual strains (O'Connor et al., 2019). Qualitative and quantitative data for the whole proteome were combined to assess the proteomic response of anastomosing strains versus axenic cultures (**Figure 3)**. Proteins were then classified as secreted if they contained a signal peptide; *n* = 292 (SignalP v.3). Proteins with transmembrane domains were not filtered out of the extracellular/secretome dataset as they may represent proteins on cellular surfaces that play a role in inter-hyphal contact. Finally, proteins containing atypical signal peptides or LSPs were also included. Proteins with LSPs may also play pivotal roles in the proteomic response of anastomosis, although confidence in assignment as 'secreted proteins' is disputable (Lonsdale et al., 2016). Overall, 529 SSDA proteins which had a high probability of a SP, SP and TM, or LSP, were in all three interactions (see supplementary **Table_S1**). In all three strains, 204 proteins are uniquely expressed in monocultures and 242 are found only in co-culture interactions, where 1,106 proteins are common to both. KEGG analyses revealed key differences in the pathways of proteomes between monoculture and co-cultures (**Figure 4**). Higher levels of carbohydrate metabolism and genetic information processing are found in all co-cultures. Interestingly, A15-A15 has the greatest levels of carbohydrate metabolism and genetic information processing with A15-CWH having the lowest levels (**Figure 4**). This may reflect the lack of interaction evident between A15 and CWH. MS data was searched in a concatenated database comprising the genomes of H97 and ARP23 to see which peptides might exclusively map to the wild *A. bisporus* ARP23 genome. As per **Table 1**, a variety of carbohydrate metabolic enzymes is seen in the ARP23 monoculture, and stress-related, heat shock proteins and nitrogen metabolism enzymes in the ARP23 co-culture. Exclusive mapping to the ARP23 genome and protein detection in ARP23 monocultures and co-cultures have generated a list of proteins of functional annotation (**Table 2**) which play important roles in interactions (e.g. Hsp70, glutamate enzymes), as discussed below.

Table 1: Proteins found exclusively in ARP23 monoculture and co-culture. Proteins were unambiguously mapped to the genome of *A. bisporus var. bisporus* (ARP23) only, with none mapping to *A. bisporus var. bisporus* (H97) after peptide scoring of the ARP23 and H97 concatenated database. Proteins found exclusively in sample replicates (*n* =2/3) of ARP23 or A15-ARP23 were considered.

	Accession No.[a]	Pfams	Description[b]	GO Description	Unique peptides	Sequence coverage [%]	Mol. weight [kDa]
ARP23 - Monoculture	**08516**	PF01263	Aldose 1-epimerase	GO:0016853: Isomerase activity; GO:0005975: Carbohydrate metabolic process	2	59.3	42.13
	09378	No Pfam	-	No GO Terms	9	50.2	22.288
	00967	PF00561	Alpha/beta hydrolase fold	No GO Terms	2	63.7	35.265
	01587	PF13561	Enoyl-reductase	No GO Terms	3	27.6	27.077
	02545	PF07249	Cerato-platanin	No GO Terms	2	47.4	16.514
	03883	PF00734, PF01341	GH6	GO:0030248: Cellulose binding; GO:0005975: Carbohydrate metabolic process; GO:0030245: Cellulose catabolic process; GO:0005576: Extracellular region; GO:0004553: Hydrolase activity, hydrolyzing O-glycosyl compounds	4	75.6	46.168
	05644	No Pfam	na	No GO Terms	1	46.7	31.729
	07238	PF01915, PF00933	GH3	GO:0004553: Hydrolase activity, hydrolyzing O-glycosyl compounds; GO:0005975: Carbohydrate metabolic process	1	58.1	95.432
	07366	PF00108, PF02803	Thiolase	GO:0016747: Transferase activity, transferring acyl groups other than amino-acyl groups	1	56.9	28.53
	10146	PF13363, PF10435,	Beta-galactosidase/GH35	No GO Terms	3	44.5	106.14

		PF13364 PF01301					
	10232	No Pfam	-	No GO Terms	6	35.1	39.876
	11520	PF01764	Lipase	GO:0006629: Lipid metabolic process	1	35.6	31.11
	12240	PF01423	LSM domain	No GO Terms	3	18.7	17.898
A15-ARP23 Co-culture	**01577**	PF00795	Carbon-nitrogen hydrolase	GO:0006807: Nitrogen compound metabolic process	2	54.1	35.293
	02924	PF00208	Glutamate/Leucine/Phenylalanine/Valine dehydrogenase	GO:0016491: Oxidoreductase activity; GO:0006520: Cellular amino acid metabolic process; GO:0055114: Oxidation-reduction process	1	63.9	29.122
	05228	PF00012	Hsp70 protein	No GO Terms	4	55.6	73.502
	09093	PF00012	Hsp70 protein	No GO Terms	2	64.5	88.11
	09149	PF03556, PF14555	Cullin binding	No GO Terms	2	8.7	37.661
	10633	PF00248	Aldo/keto reductase family	No GO Terms			
	01577	PF00795	Carbon-nitrogen hydrolase	GO:0006807: Nitrogen compound metabolic process	2	8.7	37.661
	02924	PF00208	Glutamate/Leucine/Phenylalanine/Valine dehydrogenase	GO:0016491: Oxidoreductase activity; GO:0006520: Cellular amino acid metabolic process; GO:0055114: Oxidation-reduction process	2	37.2	39.248

[a] Gene ID are preceded by >AgAr|ABP

[b] Descriptions relate to Pfam of main protein function. Anchoring domains, for example, are not included but can be deduced from full list of Pfams provided.

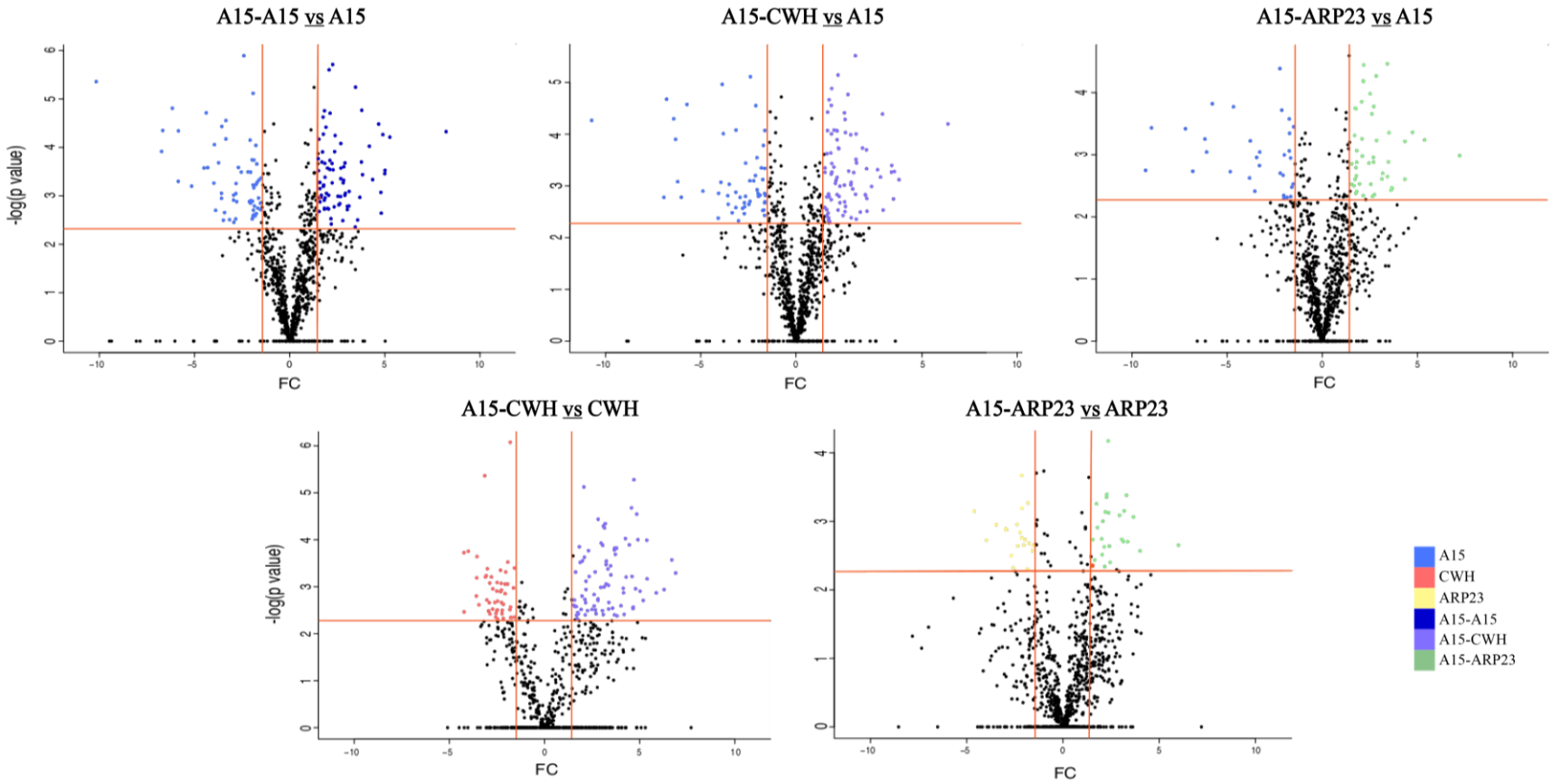

Figure 3: SSDA proteins from the whole proteome of each monoculture and co-culture. Non-axial horizontal lines represent -$\log_{10}$ *P* cut-off ($P < 0.05$ prior to transformation) and non-axial vertical lines represent $\log_2$ fold change (FC) ±1.5. Data points which are coloured in the top left quadrant are significantly increased in abundance in monocultures and data points coloured in the top right quadrant are significantly increased in abundance in co-culture.

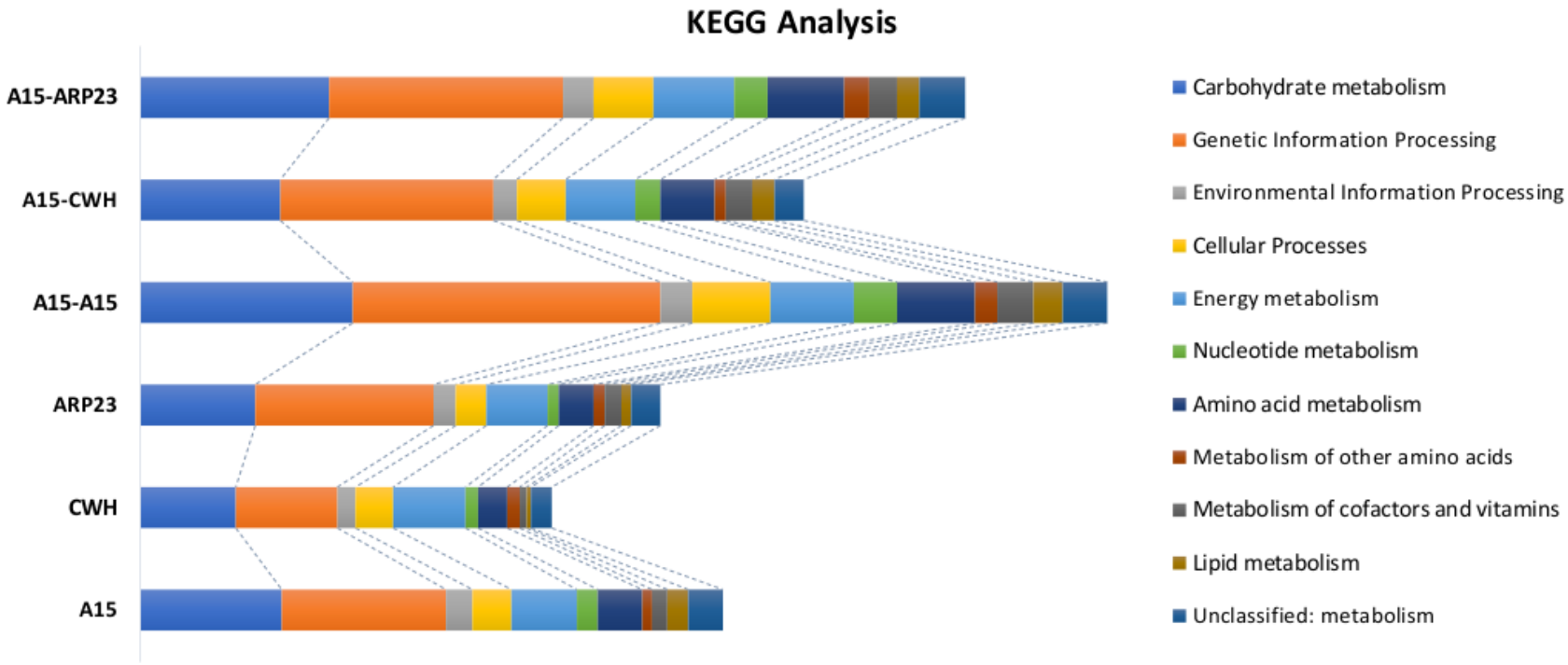

Figure 4: **KEGG analysis of whole proteomes from each monoculture and co-culture.** Functional annotation of each proteome was made through aligning protein sequences to known KEGG genes and categories were formed based on high-level functionality.

3.3.3 Changes in secreted and extracellular proteomes during anastomosis

The total number of proteins predicted to be secreted was 337. A total of 463 proteins were SSDA when all treatments were considered (**Table_S1**) and 247 of these were non-redundant (**Table_S1**). Putatively secreted proteins with significantly differential abundances were assessed for their possible roles in fungal anastomosis.

Glucose-methanol-choline (GMC) oxidoreductase exhibited increased abundance in most co-cultures compared to monoculture preparations (**Figure 5**). GMC oxidoreductase forms a diverse family of lignin-degrading auxiliary (LDA) enzymes and contains a signature flavin adenine dinucleotide (FAD) cofactor. **Figure 5** shows an interesting pattern where the levels of GMC oxidoreductase are higher in A15-CWH to A15 than to A15-CWH to CWH pairwise comparisons. The same pattern is evident in A15-ARP23 to A15 and A15-ARP23 to ARP23. Extracellular H_2O_2 is produced by GMC oxidoreductase and used as the overall oxidiser of lignin and polysaccharides in brown- and white-rot fungi (Ferreira et al., 2015). A database search of the amino acid sequence showed a closest non-*Agaricus sp.* hit as an alcohol oxidase from the 'splash cup' fungus *Crucibulum laeve* (Query cover: 89%; Identity: 56.84%). Extracellular alcohol oxidases generally fall into two classes; aromatic alcohol oxidases and secondary alcohol oxidases, whereas intracellular alcohol oxidases form another two distinct classes; short chain alcohol oxidases and long chain alcohol oxidases. A protein from the whole proteome SSDA dataset (see supplementary **Table_S2**) in A15-A15 for GMC oxidoreductase has the largest reduced abundance of any protein ($\log_2$ -10.17-fold). While the exact type of alcohol oxidase cannot be deduced, a possible compensatory mechanism whereby the sharp increase in numbers of one alcohol oxidase from a particular gene results in the downregulation of another alcohol oxidase gene may explain the opposing trends in abundance of these functionally indistinct proteins.

Profilin is observed in greater amounts in all A15 co-cultures, particularly in A15-A15 showing that the more compatible the interaction the higher the levels of profilin are found. Profilin has high affinity for actin and replaces ADP for ATP in G-actin resulting in a profilin-ATP-actin complex that accelerates rates of actin filament elongation and nucleation (Babich *et al.*, 1996; Kovar *et al.*, 2006; Rangamani *et al*., 2014).

Shikimate kinase is up-regulated in A15-A15 to A15 and A15-ARP23 to ARP23 comparisons (**Figure 5**). The shikimate pathway has a multitude of functions but

primarily forms the crossover from metabolism of carbohydrates to the biosynthesis of aromatic compounds (Herrmann and Weaver, 1999).

Glucanosyltransferase has known functions in cell wall expansion and hyphal growth by the splitting of β-1-3-glucan and joining of the newly exposed reducing end to the non-reducing end of another β-1-3-glucan (Hartland et al., 1996). This protein has pivotal roles in apical growth and morphogenesis (Saporito-Irwin et al., 1995). Abundance elevations of this protein were observed in A15-A15 to A15 and A15-CWH to A15 (**Figure 5**), possibly an indication of the competition for hyphal growth when paired with a neighbouring mycelium. In contrast, the inverse is observed for A15-CWH to CWH where a high degree of reduced abundance is observed (log_2 -3.03-fold change), which suggests CWH represses growth of hyphae in the presence of A15. A15-ARP23 to A15 and A15-ARP23 to ARP23 show no significant change in the levels of glucanosyltransferase.

A fundamental enzyme in the process of cell wall formation through the rearrangement of 1,3-β-glucanase is glycosyl transferase family 1. Quantities of this enzyme increase for all A15 co-cultures, but no significant amount is detected when CWH and ARP23 are compared to A15 in co-culture (**Figure 5**).

Strong molecular evidence supports the observation that A15 and ARP23 pairing creates biotic stress due to the high abundance of heat-shock protein 70 (Hsp70) in both A15-ARP23 to A15 and A15-ARP23 to ARP23 (**Figure 5**). Hsp70 protects against aberrant aggregation of proteins by binding to hydrophobic residues of proteins partially unfolded by thermal or oxidative stress (Mogk et al., 2003), although, Hsps are also involved in many fundamental biological processes ranging from transcription to post-translational modifications (Tiwari *et al*., 2015). It has been shown that Hsp70 has known functions in translation by assisting nascent polypeptides through ribosomal channels (Nelson et al., 1992). The combination of Hsp70 and Hsp90 play important roles in fungal morphogenesis (Tiwari *et al*., 2015). Hsp90 does not appear in the secreted and extracellular SSDA datasets, however, a Hsp90 ATPase appears in similar patterns to Hsp70 in A15-ARP23 to A15 and A15-ARP23 to ARP23 with an additional finding of reduced abundance in A15-CWH to CWH (log_2 -4.71-fold; **Figure 5**). This cochaperone of the Hsp90 system stimulates the ATPase activity of Hsp90 and loss of function results in heightened sensitivity to conditions of elevated stress (Panaretou et al., 2002).

Hydrophobins were also up-regulated when comparing A15 to A15-ARP23 (**Figure 5**). Hydrophobins are implicated in stress-response due to their importance in the structural integrity of aerial hyphae and evasion to of biotic stressors through coating the extremities of hyphae (Mikus et al., 2009; Mosbach et al., 2011; Templeton, 1994).

An additional protein detected in higher abundance is a laccase-5 (Pfam description as multi-copper oxidase) which is elevated in both A15 to A15-ARP23 and ARP23 to A15-AP23 (**Figure 5**). Laccases have been found to increase during interspecific interactions in white-rot fungi (Baldrian, 2004; Freitag and Morrel, 1992; Zhong et al., 2018) and are implicated with oxidation of xenobiotic compounds and general detoxification (Kües, 2007). ARP23 is a wild isolate strain with a brown phenotype in its fruiting bodies and highly melanised hyphae compared to most commercial cultivar mycelium. Laccase is involved in the melanin synthesis (Nagai, 2003). Cell wall integrity is heightened by melanin (Brush and Money, 1999).

An interesting observation is that the comparison of ARP23 to A15-ARP23 has heightened levels of a protein relating to the *het* system (*het*erokaryon incompatibility; Glass and Kuldau, 1992). Het-C plays a role in the recognition of self and non-self (Wu et al., 1998). This finding shows that A15 and ARP23 are sufficiently divergent to trigger a system designed to maintain colony individuality.

When comparing the whole proteomes of A15 co-cultures (**Figure 5** and **Table_S2**), a NADPH-dependant glutamate synthase (NDGS) exhibited the highest fold increase in all anastomosing cultures. NDG are broadly involved in housekeeping through activities in nitrogen metabolism by catalysing assimilation of ammonia into glutamine and glutamate (Ahmad and Hellebust, 1991). Some studies hypothesise that NDGS plays a role in bridging a connection in carbohydrate and nitrogen metabolism in yeast, the former acting as a producer of energy and the latter for biomass production by means of cytosol and mitochondria shuttling (Guillamon *et al.*, 2001), just as in other known redox shuttles in yeast (Bakker, 2001).

Another intracellular protein related to nitrogen metabolism at significantly high levels, is urease (**Table_S2**). This is a nickel-containing enzyme associated with breakdown of urea. Urea is found in high concentrations in *A. bisporus* fruit-bodies, particularly the primordia (Wagemaker et al., 2006). Increased urease abundance was the highest in A15-ARP23 to ARP23 comparisons ($\log_2$ 6.0-fold). This might reflect the use

of internal urea as a nitrogen source for generating energy for hyphal growth (Baars et al., 1994; Mobley and Hausinger, 1989).

The SSDA protein with the most elevated levels (log_2 4.23-fold) in A15-CWH to CWH comparisons was a protein containing a domain annotation for ferritin-like (**Table_S2**). Ferritins are found in plants, animals, bacteria and some zygomycetes and are involved in sequestering free iron for subsequent iron storage. Ferritin-like proteins have only been described in a few of the ascomycetes (Sashidhar and Deshpande, 2005a; Sashidhar and Deshpande, 2005b; Vakdevi *et al*., 2009; Validandi *et al.*, 2009). To date, only *in silico* predictions of ferritin-like genes have been made in basidiomycetes (Canessa and Larrondo, 2013).

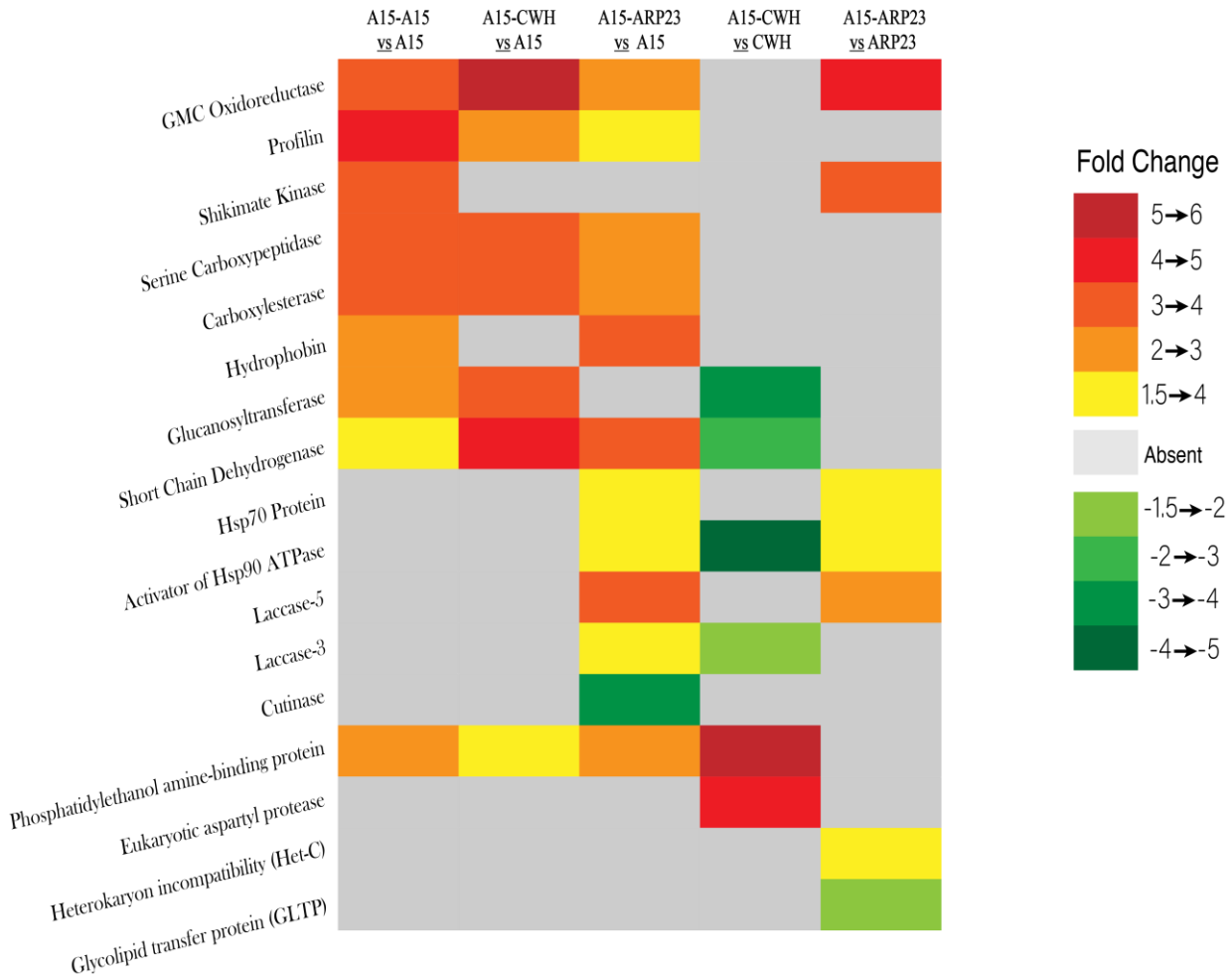

Figure 5: Secreted and extracellular SSDA proteins of comparisons of monoculture to co-culture interactions that potentially play important roles in anastomosis. Fold change ranges are of $\log_2$ transformed LFQ intensities. Grey tiles indicate proteins which did not fall within SSDA criteria or may not have been detected.

3.3.4 Secreted and extracellular proteins of carbohydrate metabolism in comparisons of A15 monocultures to A15 co-cultures

Proteins relating to carbohydrate metabolism and the possible roles of these proteins in the breakdown of nutrient substrate, but also fungal cell wall modifications, were examined between A15 monocultures and corresponding co-culture interactions

(**Table 2)**. Overall, a pattern of reduced levels of carbohydrate-active SSDA proteins is observed in anastomosing cultures when compared to individual constituent monocultures, regardless of the levels of vegetative compatibility observed (**Table 2**).

Cellulose is degraded during mycelial growth and levels of cellulase peak during periods of fruitification in *A. bisporus* (Manning and Wood, 1984), with fresh peaks of the enzyme evident in subsequent mushroom harvests (Claydon *et al*., 1988). Levels of cellulase are significantly lower in anastomosing cultures of A15-15, A15-CWH and A15-ARP23 (log_2 -6.67-fold, log_2 -5.78-fold and -6.79-fold, respectively; **Table 2**). *β*-Glucanase (GH16) levels are not observed in significantly differential abundances in either A15-A15 or A15-CWH,but are increased in A15-ARP23 (**Table 2**). In the context of *A. bisporus, β*-glucanase is normally studied for its antagonistic relationship by means of cell-wall degradation by the pathogen *Trichoderma aggressivum* (Abubaker et al., 2013). Two polysaccharide deacetylases (PD), members of the carbohydrate esterase family 4 (CE4 according to the CAZy database), show high levels in A15-A15 and A15-CWH for both proteins and high levels for one protein in A15-ARP23 (**Table 2**). A BLASTP database search against the NR database of GenBank of both proteins independantly showed the closest hit outside of the *Agaricus* genus is to a chitin deacetylase from *Leucoagaricus sp. SymC.cos* (Query cover: 69%, Identity: 67.85%). Intracellular chitin deacetylase has been implicated in cell wall formation in *Mucor rouxii* (Davis and Bartnicki-Garcia, 1984) while extracellular/secreted chitin deacetylases are known for their roles in pathogenicity of *Colletotrichum lindemuthianum* through aiding in evasion of host plant immunity by modifications of chitin on penetrating hyphae (Tsigos and Bouriotis, 1995). It is unclear whether the role of this protein in the different interactions may be a result of competition for fungal growth or as a protective role against a potentially incompatible fungal neighbour. Another enzyme of interest is β-*N*-acetylhexosaminidase (GH20). Levels of GH20 are increased in A15-A15 and reduced in A15-CWH and A15-ARP23. β-*N*-acetylhexosaminidase is a chitinase attributed to the degradation of chitin by hydrolysis of N-acetyl-hexosaminyl residues (**Table 2**). Chitinases are also known for their roles in hyphal growth by remodelling the cell wall during horizontal growth (Takaya *et al.*, 1998; Takaya *et al.*, 2005). Another chitinase protein, GH18, is in lower levels in A15-A15 and A15-ARP23. A protein identified as an esterase PHB depolymerase which shows similarities to an acetyl xylan esterase in *Leucoagaricus gongylophorus* (Query cover:100%, Identity: 70.87%) is in significantly

low abundance in A15-CWH only (log_2 -6.32-fold; **Table 2**). In combination with other xylanolytic enzymes, acetyl xylan esterase is involved in the breakdown of the hemicellulose-backbone (Zhang et al., 2011).

Table 2: SSDA secreted and extracellular proteins relating to carbohydrate metabolism of A15 monocultures compared to A15 co-cultures. Proteins considered; $P < 0.05$, $\log_2$ fold-change ≥ 1.5.

Description			A15-A15		A15-CWH		A15-ARP23	
Accession No.[a]	Pfams	Description[b]	p-value	FC (log2)	p-value	FC (log2)	p-value	FC (log2)
229390	PF00150	Cellulase (GH5)	4.47E-05	↓6.67	2.11E-05	↓6.79	1.51E-04	↓5.78
114473	PF01522	Polysaccharide deacetylase	2.96E-03	↑2.17	1.03E-04	↑2.88	2.49E-02	↑1.55
194656	PF01522	Polysaccharide deacetylase	3.05E-02	↑1.69	1.75E-02	↑2.72	np	np
195052	PF00933, PF01915, PF14310	GH3/Fibronectin type III-like	7.08E-05	↓2.08	4.50E-04	↓1.82	1.91E-04	↓2.13
194280	PF01670	GH12	2.66E-04	↓4.50	1.39E-03	↓4.06	1.50E-02	↓2.71
70106	PF17801, PF16499	Alpha galactosidase A	1.55E-05	↓6.17	2.66E-05	↓5.72	1.69E-04	↓4.67
194630	PF01263	Aldose 1-epimerase	1.21E-04	↓6.73	8.06E-03	↓3.69	5.99E-04	↓3.78
193587	PF00278	GH20	2.59E-04	↑1.51	7.98E-04	↓2.42	1.01E-03	↓2.00
217305	PF00933, PF01915, PF14310	GH3/Fibronectin	4.71E-04	↓1.61	np	np	6.52E-03	↓2.10
194297	PF00722	GH16	5.86E-04	np	np	np	2.15E-02	↑1.86
192455	PF00723, PF00686	GH15/starch binding domain	6.82E-04	↓1.89	np	np	3.33E-03	↓1.60
194940	PF00295	GH28	6.32E-04	↓5.16	np	np	9.06E-04	↓3.28
211936	PF00704	GH18	9.09E-05	↓1.78	np	np	4.52E-03	↓2.03
190944	PF01055, PF13802, PF16863	GH31/Galactose mutarotase-like	1.82E-04	↓1.88	np	np	6.85E-03	↓1.52
79914	PF00450	Serine carboxypeptidase	2.49E-03	↓1.51	2.99E-03	↓1.74	np	np

227191	PF00704	GH18	5.60E-03	↓2.66	2.70E-03	↓2.80	np	np
203798	PF17678, PF07971	GH92	3.00E-03	↓2.83	3.44E-03	↓2.71	np	np
136707	PF00734, PF01083	Fungal Cellulose binding/Cutinase	2.22E-03	↓3.42	2.63E-03	↓3.16	np	np
191333	PF16862	GH79	1.72E-02	↓3.53	3.30E-03	↓3.35	np	np
217231	PF01979	Amidohydrolase family	3.23E-04	↓2.05	2.81E-05	↓2.11	np	np
199426	PF00316	Fructose-1-6-bisphosphate	1.32E-02	↑1.82	np	np	np	np
136775	PF00704	GH18	1.42E-03	↑1.54	np	np	np	np
194179	PF01532	GH47	1.38E-02	↓1.70	np	np	np	np
64273	PF16863, PF13802, PF01055	GH31	5.24E-04	↓1.71	np	np	np	np
211936	PF00704	GH18	9.09E-05	↓1.78	np	np	np	np
194180	PF01532	GH47	np	np	2.97E-02	↑1.95	np	np
188016	PF02055	GH30	np	np	3.64E-04	↓2.64	np	np
190841	PF07470	GH88	np	np	9.74E-03	↓2.69	np	np
196213	PF00734, PF10503	Fungal cellulose binding domain/Esterase PHB depolymerase	np	np	1.26E-04	↓6.32	np	np
230096	PF17678, PF07971	GH92	np	np	np	np	1.01E-02	↓3.26
133541	PF00331	GH10	np	np	np	np	1.85E-03	↓6.80
191440	PF00331	GH10	np	np	np	np	3.70E-04	↓8.97
194521	PF00840, PF00734	GH7/Fungal cellulose binding domain	np	np	np	np	1.78E-03	↓9.28
185916	PF02782, PF00370	FGGY family of carbohydrate kinases	np	np	np	np	1.55E-02	↓1.54

[a] Gene ID from JGI are preceded by >jgi|Agabi_varbisH97_2| [b] Descriptions limited to Pfam relating to main protein function. Anchoring domains, for example, are not included but can be deduced from full list of Pfams provided.

Qualitative analysis revealed distinct differences between the CAZyme arsenals of monocultures versus A15 co-cultures (**Figure 6A**). Monocultures had a comparably similar array of CAZymes. A15-CWH has fewer CAZymes (*n* = 72) compared to a largest expansion observed in A15-ARP23 (*n* = 127) and A15-A15 with the lowest (*n* = 69) (**6A** and **Table_S3**). This suggests that the diversity of CAZymes is lower in compatible interactions or repressed interactions but expand in antagonistic/stress inducing interactions. **Figure 6A** shows that the biggest expansion (*n* = 24) in A15-ARP23 is with LDA enzymes. LDA are attributed with the accumulation of H_2O_2 which is required for lignolytic peroxidases during lignolysis and can also aid in the prevention of reformation of lignin polymers. Laccases are also found in this group of enzymes and act as oxidisers of phenolic compounds and aromatic diamines (Leonowicz et al., 2001; Mayer, 2002). Previous studies have implicated them in detoxification of antagonistic interaction zones (Baldrian, 2004; Hiscox et al., 2010). Furthermore, A15-A15 shows a drop in LDA enzymes in co-culture (*n* = 8) compared to A15 monoculture (*n* = 15). The accumulation of reactive oxygen species (ROS) is attributed with contact zones of antagonistic interactions between fungi and high levels of oxidative stress (Silar, 2005). **Figure 6A** suggests that regulation of LDA enzymes is considerably altered in the compatible and incompatible interactions. **Figure 6C** shows that the expansions in different CAZyme classes in A15-ARP23 are not simply a consequence of the two different strains having distinct enzymatic arsenals, as their monoculture CAZyme profiles indicate no unique CAZys are found (no addition of unique CAZymes). Specific CAZymes in A15-CWH co-cultures are the lowest (*n* = 5; **Figure 6B**).

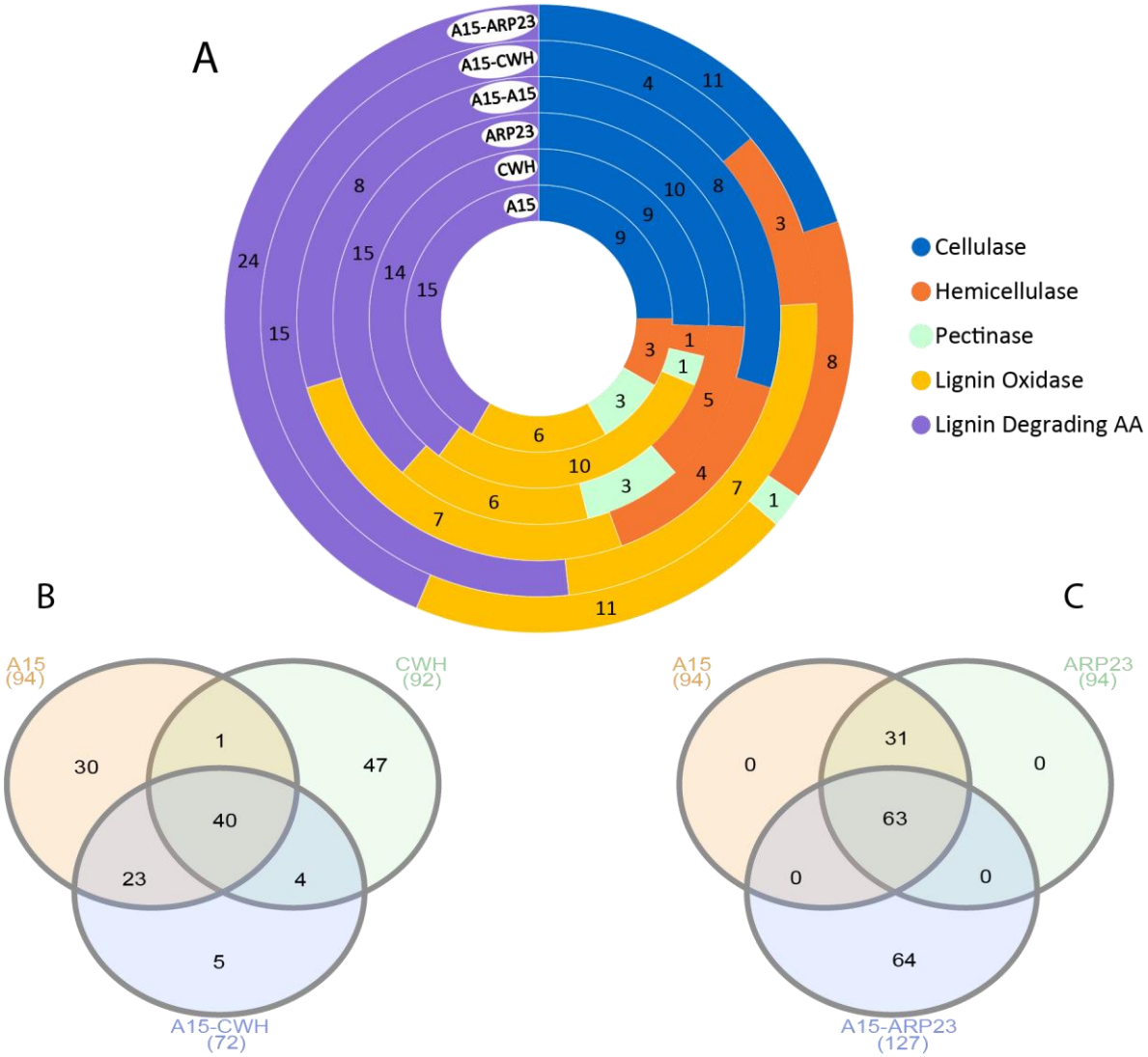

Figure 6: Selected CAZymes from monoculture and strain A15 co-cultures. **A**: Comparisons of the number of proteins found in each CAZyme class in monocultures and co-cultures. **B**: Shared and unique CAZymes in A15-CWH co-culture and respective monocultures. **C**: Shared and unique CAZymes in A15-ARP23 co-culture and respective monocultures.

3.3.5 Unique co-culture proteomic profiles

Comparisons of SSDA proteins were made between the three co-cultures to decipher if the three different interactions induce a distinct proteomic response to one another that is not found in A15 monocultures (**Figure 7**). 95 proteins are common to all interactions (not strain specific). A15-A15 and A15-CWH share the greatest number of unique proteins between two co-cultures (n = 71). The A15-ARP23 interaction is the most distinct interaction sharing the lowest number of proteins in pairwise-comparisons and having the greatest number of unique proteins overall (n = 43). Three putative laccases are found as SSDA in A15-ARP23 (**Table_S4)**. The presence of three different laccases found only in A15-ARP23 may be an indicator that these enzymes play an important role in the antagonism observed between the two strains. A septin and oxysterol-binding protein are found exclusively in A15-A15 (**Table_S4)**. Septins are involved in polarised growth of hyphae by acting as a scaffold during fungal morphogenesis (Khan *et al*., 2015) and oxysterol-binding proteins are implicated in vesicular-trafficking among other functions (Raychaudhuri and Prinz, 2010). These are examples of proteins that are likely beneficial in an interaction where anastomosis is advantageous to the neighbouring mycelia, such as that in A15-A15. The A15-CWH has a member of the arginase family in the unique set of proteins (**Table_S4)**. Arginase is involved in nitrogen remobilisation through the activation of urease (Cao et al., 2010). **Figure 7** exemplifies the key differences found between these three strains during anastomosis.

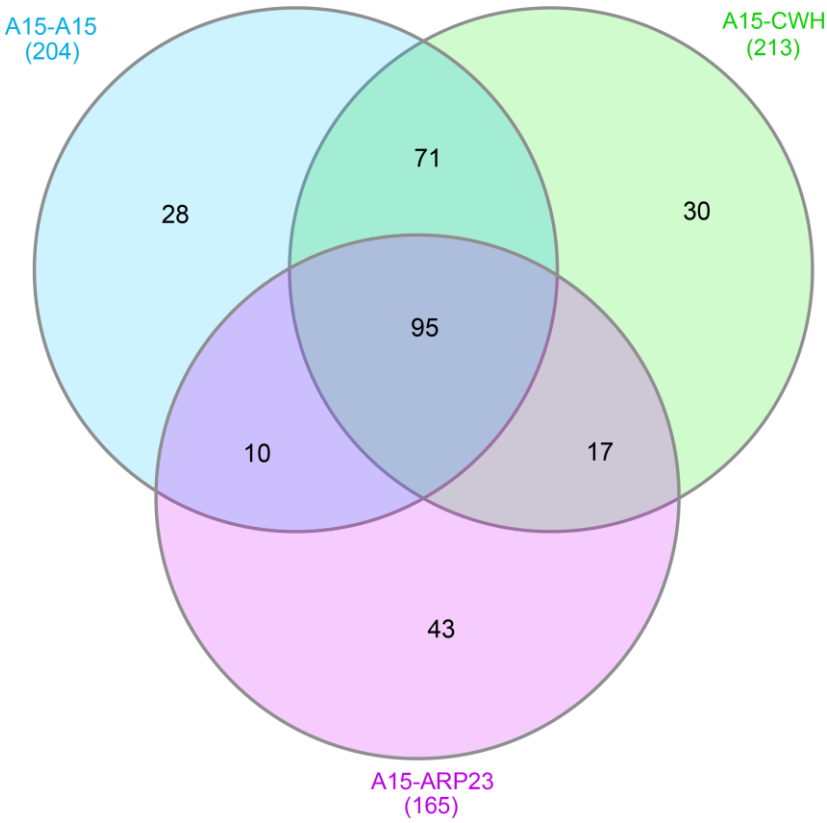

Figure 7: **Differentially abundant proteins (SSDA) detected in co-cultures.** Comparisons are made between co-cultures (A15-A15, A15-CWH, A15-ARP23) and the A15 monoculture.

3.4 Discussion

Many studies into the outcomes of fungal interactions and anastomosis have been carried out in the ascomycetes and basidiomycetes, ranging from biocontrol of economically-damaging plant pathogens to understanding wood decomposition fungal community structures (Ainsworth and Rayner 1986; Mccabe *et al*., 1999; Boddy, 2000; Donnelly and Boddy, 2001; Wells and Boddy, 2002; Wald, Pitkänen and Boddy, 2004; Hynes *et al.*, 2007; Evans *et al.*, 2008; Van Bael *et al.*, 2009; Ferreira *et al.*, 2010; ABear *et al.*, 2013; Hiscox, Savoury, Vaughan, *et al.*, 2015; Schöneberg *et al.*, 2015; Hiscox, Savoury, Müller, *et al.*, 2015; El Ariebi *et al.*, 2016; Hiscox *et al.*, 2016, 2017; Morón-Ríos *et al.*, 2017; Laur *et al.*, 2018; Moody *et al.*, 2018; O'Leary *et al.*, 2019). Many studies have also been conducted into the hyphal fusion process fungi undertake to form a mycelium (as reviewed by (Glass, 2004)) and the genes that govern recognition processes mitigating anastomosis (Smith *et al.*, 2006). To date, only one other study examining the proteomic response of antagonistic white rot fungi *in vitro* has been done (Zhong et al., 2018). Until now, no studies aimed specifically at the proteomic response during the process of anastomosis in a range of vegetative compatibilities have been done. Our use of three different strains of *A. bisporus* is an effective model to study such a response for the following reasons 1) they are conspecific and so interactions will represent a more conserved system of recognition and interaction compared to a study that focuses on different species of fungi. 2) Findings have applied value as anastomosis is a key element of the mushroom cropping process, and disease control of virus-breaking varieties. 3) Concerning the commercial strain A15, the three strains pose a distinct variety of interactions from full vegetative compatibility, lack of interaction of receding/repelling cultures, and levels of vegetative incompatibility (evidence of stress; **Figure 2**). Due to the current commercial use of A15 and the concept of different *A. bisporus* strains as breaker-varieties to A15, co-culture interactions and monoculture counterparts were established for proteomic analyses of the varying interactions.

Anastomosis is a crucial process in fungi regarding nutrition acquisition, hyphae morphogenesis, and recognition between neighbouring mycelia. Outcomes of gene-regulation reflected in the comparisons of protein profiles in the extracellular/secreted proteomes during the process of anastomosis were elucidated. A15 dominated the experimental setup and subsequent data analysis as the primary dual-culture partner (**Figure 2**). This was decided due to A15 being the contemporary-cultivated strain in

mushroom crops and CWH and ARP23 being recognised as good dual-culture partners in terms of vegetative incompatibility strains as virus-breaker varieties.

As very little is known of the proteomic mechanisms governing anastomosis, lists of up- and down-regulated proteins were separated into potentially important proteins involved in anastomosis (**Figure 5**) and carbohydrate metabolism (**Table 2**). An important step in the cropping cycle preceding mushroom formation is the spawn run phase, whereby mycelium colonizes and breaks down the mushroom compost substrate; rich in carbon (wheat) and nitrogen (generally horse and/or chicken manure)(Gerrits, 1985). Mycelium growth over the compost bed involves anastomosis en masse, as isolated colonies begin to come into contact. Proteins relevant to carbohydrate metabolism can be involved in the restructuring of self or non-self hyphae architectures and therefore, were also considered, based on functional annotations, as possible players in the process of anastomosis and not solely for nutrient acquisition. Proteins which may not necessarily directly contribute to anastomosis may still be relevant to the competition for substrate between two neighbouring mycelia.

The more obvious candidates warranting examination for this study are proteins involved in biosynthesis of hyphal components and polymerisation of the cell wall. After refining the proteomic datasets through statistical significance tests and cut-offs in minimum relative abundances, many key proteins involved in hyphal morphogenesis were still highly represented in the interaction cultures (**Table 2**), including profilin, glucanosyltransferase, chitin deacetylase, glycosyl transferase 1, N-acetylhexosaminidase (GH20) and GH18. The vegetative-compatible interaction (A15-A15) showed the greatest increase in hyphae remodelling proteins in terms of profilin and GH20. Proteins that are involved in the splitting of monomer components of hyphae however do not seem to dominate in A15-A15, as per chitin deacetylase, GH18 and glucanosyltransferase. However, intracellular levels of glycosyl transferase 1 relating to hyphal extension are high in all A15 co-cultures regardless of the interaction partner (**Table S_2**). Production of extracellular ROS is high in anastomosing cultures due to the peaks in GMC oxidoreductase found in all comparisons with the exception of A15-CWH to CWH (**Figure 5**). Similarity based searches showed closest hits to the alcohol oxidase class. Alcohol oxidases supply H_2O_2 as a co-oxidant to peroxidases for lignin and cellulose degradation. Production of ROS may also serve as a protective agent against competing microbes (for example in rhizospheres; Monti *et al.*, 2011) and so could be

considered as a competitive strategy in fungal interactions. LDA enzymes include enzymes that allow oxidative action to generate extracellular H_2O_2 in the breakdown of complex lignin structures. The broad substrate range of certain members of the LDA enzymes can expand to xenobiotic compounds with similar recalcitrant structures to lignin and so these enzymes play roles in detoxification (Wang et al., 2018). This may help explain the expansion of this CAZyme class in A15-ARP23 co-cultures and reduction in the A15-A15 co-cultures (**Figure 6**).

The interaction of A15-ARP23 showed signs of biotic stress. The fluffy plumes of aerial hyphae were evident in all A15 cultures when paired with ARP23, which is phenotypic evidence of stress (**Figure 2**). Proteomic analyses reinforced this in capturing up-regulation of secreted stress-response associated proteins Hsp70 and Hsp90 ATPase (**Figure 5**). Further evidence of stress-response is captured in heightened abundances of hydrophobins for A15-ARP23 (**Figure 5**). Hydrophobins are implicated in stress-response due to their importance in the production of aerial hyphae growth, as they confer hydrophobicity to aerial hyphae and prevent collapse through the weight of ambient moistures etc. (Mikus et al., 2009; Mosbach et al., 2011). The heightened levels of hydrophobins may play a role in the uncharacteristic fluffy growths observed in the A15-ARP23 co-culture, although it should be noted that hydrophobin levels in A15-A15 were also high, albeit, not to the same degree as A15-ARP23 (**Figure 5**). Heterokaryon incompatibility system (*Het*) was also induced during the interaction of A15 and ARP23. Nitrogen metabolism was highly represented through some of the highest abundances of proteins found in the intracellular proteome (**Table_S2**). While typical filamentous fungal nitrogen metabolism through glutamate was observed in most interactions, the finding of high levels of urease in A15-CWH to CWH comparisons may be evidence of nitrogen starvation by classical nitrogen assimilation means. Urease enzymes are induced in times of nitrogen starvation (Beckers et al., 2004). As A15 and CWH do not readily anastomose, it is possible that they do not readily 'fuse into a single colony' *in vitro* as seen for other vegetative-compatible dual-culture interactions. Evidence of nitrogen starvation mechanism may contribute to this idea, as nitrogen metabolism may be subverted to internal urea as a new nitrogen source. Moreover, many SSDA proteins found in high amounts in A15-A15 and A15-ARP23 are either absent in A15-CWH or in significantly lower amounts. A possible reason for this may be that both strains are effective at not interacting with one another. In terms of anastomosis, A15-CWH and A15-ARP23

interactions are not dissimilar, however, the A15-ARP23 interaction goes beyond lack of anastomosis and into antagonism as reflected in their proteomic profiles (**Figure** 5) and phenotypic evidence of uncharacteristic fluffiness of hyphal growth (**Figure 2**). The effects of vegetative compatibility versus incompatibility can be seen in **Figure 4**. Fundamental housekeeping processes and substrate metabolism are all highest when A15 is paired with itself. By comparing co-culture SSDA protein sets, a number of proteins were captured as common to all interactions (not a strain-level) and unique to certain interactions (strain-level), although the strain-specific assignments of proteins cannot be made **Figure 7**. From **Figure 7**, we see that greatest similarities are evident between A15-A15 and CWH-A15. The antagonistic interaction of ARP23-A15 represents the most distinct proteomic response.

In summary, proteomic responses of interhyphal interactions between the three strains of *A. bisporus* were investigated using an *in vitro* co-culture interaction design and a label-free/nontargeted approach of proteomic profiling. Even at the strain-level, a variety of changes are observed in interacting cultures ranging from proteins pertinent to hyphal morphology, carbohydrate metabolism, stress responses, *vic* system-related proteins and nitrogen metabolism.

3.5 Conclusion

This is the first study to characterise the proteomic response of three interacting *A. bisporus* strains ranging from full vegetative compatibility to incompatibility. New insights into pathways and candidate proteins vital to anastomosis have been discussed in detail. Our analysis shows that vegetative compatible interactions are represented by high levels of carbohydrate metabolism but evidently in the form of cell wall biogenesis, modification, and expansion. With respect to co-cultures, A15-CWH represents less of an antagonistic interaction and more of a competitive interaction for substrate, reflected by high levels of oxidoreductase activity and nitrogen-starvation responses. In terms of hyphal interaction, comparative protein abundances to the other interactions suggest A15 and CWH are likely interacting mush less. Conversely, the A15-ARP23 interaction is most highly representative of a vegetative incompatibility and antagonism, represented by high levels of LDA enzymes, hydrophobins, and oxidation of xenobiotic compounds. This study has provided insight into the how the proteomic response of different strains of *A. bisporus* can lead to vegetative incompatible interactions and therefore, reinforce the use of these strains as disease-breakers in commercial mushroom crops. Additionally, new insights have been gained into the proteomic response of a range of vegetative compatibilities during inter-hyphal interactions of this filamentous fungus that may guide future studies relating to anastomosis.

Acknowledgments

EOC is funded by a Teagasc Walsh Scholarship Scheme (grant reference number 10564231). We acknowledge the DJEI/DES/SFI/HEA Irish Centre for High-End Computing (ICHEC) for the provision of computational facilities and support. Mass spectrometry facilities were funded by Science Foundation Ireland (SFI 12/RI/2346(3)).

Literature Cited

A′Bear, A.D., Murray, W., Webb, R., Boddy, L., Jones, T.H., 2013. Contrasting Effects of Elevated Temperature and Invertebrate Grazing Regulate Multispecies Interactions between Decomposer Fungi. PLoS One 8, e77610.

Abubaker, K.S., Sjaarda, C., Castle, A.J., 2013. Regulation of three genes encoding cell-wall-degrading enzymes of Trichoderma aggressivum during interaction with Agaricus bisporus. Can. J. Microbiol. 59, pp. 417–424.

Ahmad, I., Hellebust, J.A., 1991. 7 Enzymology of Nitrogen Assimilation in Mycorrhiza, in: Methods in Microbiology. pp. 181–202.

Ainsworth, A.M., Rayner, A.D.M., 1986. Responses of Living Hyphae Associated with Self and Non-self Fusions in the Basidiomycete Phanerochaete velutina. Microbiology 132, pp. 191–201.

Arce-Cervantes, O., Saucedo-García, M., Leal Lara, H., Ramírez-Carrillo, R., Cruz-Sosa, F., Loera, O., 2015. Alternative supplements for Agaricus bisporus production and the response on lignocellulolytic enzymes. Sci. Hortic. (Amsterdam). 192, pp. 375–380.

Ashburner, M., Ball, C.A., Blake, J.A., Botstein, D., Butler, H., Cherry, J.M., Davis, A.P., Dolinski, K., Dwight, S.S., Eppig, J.T., Harris, M.A., Hill, D.P., Issel-Tarver, L., Kasarskis, A., Lewis, S., Matese, J.C., Richardson, J.E., Ringwald, M., Rubin, G.M., Sherlock, G., 2000. Gene Ontology: tool for the unification of biology. Nat. Genet. 25, pp. 25–29.

Baars, J.J.P., Op den Camp, H.J.M., Hermans, J.M.H., Mikes, V., van der Drift, C., Van Griensven, L.J.L.D., Vogels, G.D., 1994. Nitrogen assimilating enzymes in the white button mushroom Agaricus bisporus. Microbiology 140, pp. 1161–1168.

Babich, M., Foti, L.R.P., Sykaluk, L.L., Clark, C.R., 1996. Profilin Forms Tetramers That Bind to G-Actin. Biochem. Biophys. Res. Commun. 218, pp. 125–131.

Bakker, B., 2001. Stoichiometry and compartmentation of NADH metabolism in Saccharomyces cerevisiae. FEMS Microbiol. Rev. 25, pp. 15–37.

Balakrishnan, R., Park, J., Karra, K., Hitz, B.C., Binkley, G., Hong, E.L., Sullivan, J., Micklem, G., Michael Cherry, J., 2012. YeastMine—an integrated data warehouse for Saccharomyces cerevisiae data as a multipurpose tool-kit. Database 2012.

Baldrian, P., 2004. Increase of laccase activity during interspecific interactions of white-rot fungi. FEMS Microbiol. Ecol. 50, pp. 245–253.

Bartnicki-Garcia, S., Hergert, F., Gierz, G., 1989. Computer simulation of fungal morphogenesis and the mathematical basis for hyphal (tip) growth. Protoplasma 153, pp. 46–57.

Beckers, G., Bendt, A.K., Kramer, R., Burkovski, A., 2004. Molecular Identification of the Urea Uptake System and Transcriptional Analysis of Urea Transporter- and Urease-Encoding Genes in Corynebacterium glutamicum. J. Bacteriol. 186, pp. 7645–7652.

Beites, T., Oliveira, P., Rioseras, B., Pires, S.D.S., Oliveira, R., Tamagnini, P.,

Moradas-Ferreira, P., Manteca, Á., Mendes, M. V., 2015. Streptomyces natalensis programmed cell death and morphological differentiation are dependent on oxidative stress. Sci. Rep. 5, 12887.

Bendtsen, J.D., Jensen, L.J., Blom, N., von Heijne, G., Brunak, S., 2004. Feature-based prediction of non-classical and leaderless protein secretion. Protein Eng. Des. Sel. 17, pp. 349–356.

Biella, S., Smith, M.L., Aist, J.R., Cortesi, P., Milgroom, M.G., 2002. Programmed cell death correlates with virus transmission in a filamentous fungus. Proc. R. Soc. London. Ser. B Biol. Sci. 269, pp. 2269–2276.

Boddy, L., 2000. Interspecific combative interactions between wood-decaying basidiomycetes. FEMS Microbiol. Ecol. 31, pp. 185–194.

Bourges, N., Groppi, A., Barreau, C., Clavé, C., Bégueret, J., 1998. Regulation of gene expression during the vegetative incompatibility reaction in Podospora anserina. Characterization of three induced genes. Genetics 150, pp. 633–41.

Brush, L., Money, N.P., 1999. Invasive Hyphal Growth in Wangiella dermatitidis Is Induced by Stab Inoculation and Shows Dependence upon Melanin Biosynthesis. Fungal Genet. Biol. 28, pp. 190–200.

Callac, P., Imbernon, M., Kerrigan, R.W., Olivier, J.-M., 1996. A summary of allelic diversity and geographical distribution at six allozyme loci of Agaricus bisporus. Mushroom Biol. Mushroom Prod. pp. 57–66.

Canessa, P., Larrondo, L.F., 2013. Environmental responses and the control of iron homeostasis in fungal systems. Appl. Microbiol. Biotechnol. 97, 939–955.

Cantarel, B.L., Coutinho, P.M., Rancurel, C., Bernard, T., Lombard, V., Henrissat, B., 2009. The Carbohydrate-Active EnZymes database (CAZy): an expert resource for Glycogenomics. Nucleic Acids Res. 37, D233–D238.

Cao, F.-Q., Werner, A.K., Dahncke, K., Romeis, T., Liu, L.-H., Witte, C.-P., 2010. Identification and Characterization of Proteins Involved in Rice Urea and Arginine Catabolism. Plant Physiol. 154, pp. 98–108.

Chu, Y.-M., Jeon, J.-J., Yea, S.-J., Kim, Y.-H., Yun, S.-H., Lee, Y.-W., Kim, K.-H., 2002. Double-Stranded RNA Mycovirus from Fusarium graminearum. Appl. Environ. Microbiol. 68, pp. 2529–2534.

Claydon, N., Allan, M., Wood, D.A., 1988. Fruit body biomass regulated production of extracellular endocellulase during periodic fruiting by Agaricus bisporus. Trans. Br. Mycol. Soc. 90, pp. 85–90.

Collins, C., Keane, T.M., Turner, D.J., O'Keeffe, G., Fitzpatrick, D.A., Doyle, S., 2013. Genomic and Proteomic Dissection of the Ubiquitous Plant Pathogen, Armillaria mellea : Toward a New Infection Model System. J. Proteome Res. 12, pp. 2552–2570.

Cox, J., Mann, M., 2008. MaxQuant enables high peptide identification rates, individualized p.p.b.-range mass accuracies and proteome-wide protein quantification. Nat. Biotechnol. 26, pp. 1367–1372.

Davis, L.L., Bartnicki-Garcia, S., 1984. Chitosan synthesis by the tandem action of

chitin synthetase and chitin deacetylase from Mucor rouxii. Biochemistry 23, pp. 1065–1073.

De La Bastide, P.Y., Sonnenberg, A., Van Griensven, L., Anderson, J.B., Horgen, P.A., 1997. Mitochondrial Haplotype Influences Mycelial Growth of Agaricus bisporus Heterokaryons. Appl. Environ. Microbiol. 63, pp. 3426–31.

Dolan, S.K., Owens, R.A., O'Keeffe, G., Hammel, S., Fitzpatrick, D.A., Jones, G.W., Doyle, S., 2014. Regulation of Nonribosomal Peptide Synthesis: bis-Thiomethylation Attenuates Gliotoxin Biosynthesis in Aspergillus fumigatus. Chem. Biol. 21, pp. 999–1012.

Donnelly, D.P., Boddy, L., 2001. Mycelial dynamics during interactions between Stropharia caerulea and other cord-forming, saprotrophic basidiomycetes. New Phytol. 151, pp. 691–704.

Dyrløv Bendtsen, J., Nielsen, H., von Heijne, G., Brunak, S., 2004. Improved Prediction of Signal Peptides: SignalP 3.0. J. Mol. Biol. 340, pp. 783–795.

El Ariebi, N., Hiscox, J., Scriven, S.A., Müller, C.T., Boddy, L., 2016. Production and effects of volatile organic compounds during interspecific interactions. Fungal Ecol. 20, pp. 144–154.

Evans, J.A., Eyre, C.A., Rogers, H.J., Boddy, L., Müller, C.T., 2008. Changes in volatile production during interspecific interactions between four wood rotting fungi growing in artificial media. Fungal Ecol. 1, pp. 57–68.

Fermor, T.R., Wood, D.A., Lincoln, S.P., Fenlon, J.S., 1991. Bacteriolysis by Agaricus bisporus. J. Gen. Microbiol. 137, pp. 15–22.

Ferreira, P., Carro, J., Serrano, A., Martinez, A.T., 2015. A survey of genes encoding H_2O_2-producing GMC oxidoreductases in 10 Polyporales genomes. Mycologia 107, pp. 1105–1119.

Ferreira, V., Gonçalves, A.L., Pratas, J., Canhoto, C., 2010. Contamination by uranium mine drainages affects fungal growth and interactions between fungal species and strains. Mycologia 102, pp. 1004–1011.

Flärdh, K., Buttner, M.J., 2009. Streptomyces morphogenetics: dissecting differentiation in a filamentous bacterium. Nat. Rev. Microbiol. 7, pp. 36–49.

Fletcher T., Gaze, H., 2007. Mushroom Pest and Disease Control, A Colour Handbook. CRC Press.

Freitag, M., Morrel, J.J., 1992. Changes in selected enzyme activities during growth of pure and mixed cultures of the white-rot decay fungus Trametes versicolor and the potential biocontrol fungus Trichoderma harzianum. Can. J. Microbiol. 38, pp. 317–323.

Garnjobst, L., Wilson, J.F., 1956. Heterocaryosis and protoplasmic incompatability in *Neurospora crassa*.. Proc. Natl. Acad. Sci. 42, pp. 613–618.

Gerrits, J.P.G., 1985. Preparation of compost for the production of mushrooms in the Netherlands. Acta Hortic. pp. 253–254.

Girbardt, M., 1969. Die Ultrastruktur der Apikalregion von Pilzhyphen. Protoplasma

67, pp. 413–441.

Girbardt, M., 1957. Der Spitzenkörper von Polystictus versicolor (L.). Planta 50, 47–59.

Glass, N., 2004. Hyphal homing, fusion and mycelial interconnectedness. Trends Microbiol. 12, pp. 135–141.

Glass, N.L., Fleissner, A., 2006. Re-Wiring the Network: Understanding the Mechanism and Function of Anastomosis in Filamentous Ascomycete Fungi, in: Growth, Differentiation and Sexuality. Springer-Verlag, Berlin/Heidelberg, pp. 123–139.

Glass, N.L., Jacobson, D.J., Shiu, P.K.T., 2000. The Genetics of Hyphal Fusion and Vegetative Incompatibility in Filamentous Ascomycete Fungi. Annu. Rev. Genet. 34, pp. 165–186.

Glass, N.L., Kuldau, G.A., 1992. Mating Type and Vegetative Incompatibility in Filamentous Ascomycetes. Annu. Rev. Phytopathol. 30, pp. 201–224.

Grogan, H.M., Adie, B.A.T., Gaze, R.H., Challen, M.P., Mills, P.R., 2003. Double-stranded RNA elements associated with the MVX disease of Agaricus bisporus. Mycol. Res. 107, pp. 147–154.

Grogan, H.M., Tomprefa, N., J., M., Holcroft, S., Gaze, R., 2004. Transmission of Mushroom Virus X Disease in crops. Mushroom Sci. 16, pp. 489–498.

Guillamon, J., Vanriel, N., Giuseppen, M., Verrips, C., 2001. The glutamate synthase (GOGAT) of plays an important role in central nitrogen metabolism. FEMS Yeast Res. 1, pp. 169–175.

Hansberg, W., Aguirre, J., 1990. Hyperoxidant states cause microbial cell differentiation by cell isolation from dioxygen. J. Theor. Biol. 142, pp. 201–221.

Harris, S., 2001. Septum formation in Aspergillus nidulans. Curr. Opin. Microbiol. 4, pp. 736–739.

Hartland, R.P., Fontaine, T., Debeaupuis, J.-P., Simenel, C., Delepierre, M., Latgé, J.-P., 1996. A Novel β-(, ,)-Glucanosyltransferase from the Cell Wall of Aspergillus fumigatus. J. Biol. Chem. 271, pp. 26843–26849.

Herrmann, K.M., Weaver, L.M., 1999. The Shikimate Pathway. Annu. Rev. Plant Physiol. Plant Mol. Biol. 50, pp. 473–503.

Hickey, P.C., Jacobson, D.J., Read, N.D., Louise Glass, N., 2002. Live-cell imaging of vegetative hyphal fusion in Neurospora crassa. Fungal Genet. Biol. 37, pp. 109–119.

Hiscox, J., Baldrian, P., Rogers, H.J., Boddy, L., 2010. Changes in oxidative enzyme activity during interspecific mycelial interactions involving the white-rot fungus Trametes versicolor. Fungal Genet. Biol. 47, pp. 562–571.

Hiscox, J., Clarkson, G., Savoury, M., Powell, G., Savva, I., Lloyd, M., Shipcott, J., Choimes, A., Amargant Cumbriu, X., Boddy, L., 2016. Effects of pre-colonisation and temperature on interspecific fungal interactions in wood. Fungal Ecol. 21, pp. 32–42.

Hiscox, J., Savoury, M., Müller, C.T., Lindahl, B.D., Rogers, H.J., Boddy, L., 2015a.

Priority effects during fungal community establishment in beech wood. ISME J. 9, pp. 2246–2260.

Hiscox, J., Savoury, M., Toledo, S., Kingscott-Edmunds, J., Bettridge, A., Waili, N. Al, Boddy, L., 2017. Threesomes destabilise certain relationships: multispecies interactions between wood decay fungi in natural resources. FEMS Microbiol. Ecol. 93.

Hiscox, J., Savoury, M., Vaughan, I.P., Müller, C.T., Boddy, L., 2015b. Antagonistic fungal interactions influence carbon dioxide evolution from decomposing wood. Fungal Ecol. 14, pp. 24–32.

Hynes, J., Müller, C.T., Jones, T.H., Boddy, L., 2006. Changes in Volatile Production During the Course of Fungal Mycelial Interactions Between Hypholoma fasciculare and Resinicium bicolor. J. Chem. Ecol. 33, pp. 43–57.

Jacobson, D.J., Beurkens, K., Klomparens, K.L., 1998. Microscopic and Ultrastructural Examination of Vegetative Incompatibility in Partial Diploids Heterozygous athetLoci inNeurospora crassa. Fungal Genet. Biol. 23, pp. 45–56.

Jones, P., Binns, D., Chang, H.-Y., Fraser, M., Li, W., McAnulla, C., McWilliam, H., Maslen, J., Mitchell, A., Nuka, G., Pesseat, S., Quinn, A.F., Sangrador-Vegas, A., Scheremetjew, M., Yong, S.-Y., Lopez, R., Hunter, S., 2014. InterProScan 5: genome-scale protein function classification. Bioinformatics 30, pp. 1236–40.

Kabel, M.A., Jurak, E., Mäkelä, M.R., de Vries, R.P., 2017. Occurrence and function of enzymes for lignocellulose degradation in commercial Agaricus bisporus cultivation. Appl. Microbiol. Biotechnol. 101, pp. 4363–4369.

Kall, L., Krogh, A., Sonnhammer, E.L.L., 2007. Advantages of combined transmembrane topology and signal peptide prediction--the Phobius web server. Nucleic Acids Res. 35, W429–W432.

Kanehisa, M., Sato, Y., Morishima, K., 2016. BlastKOALA and GhostKOALA: KEGG Tools for Functional Characterization of Genome and Metagenome Sequences. J. Mol. Biol. 428, pp.726–731.

Kashif, M., Jurvansuu, J., Vainio, E.J., Hantula, J., 2019. Alphapartitiviruses of Heterobasidion Wood Decay Fungi Affect Each Other's Transmission and Host Growth. Front. Cell. Infect. Microbiol. 9, 64.

Kaur, L., Dhanda, S., Sodhi, H.S., Kapoor, S., Khanna, P.K., 2011. Storage and Preservation of Temperate Mushroom Cultures, Agaricus Bisporus and Pleurotus Florida. Indian J. Microbiol. 51, pp. 234–238.

Khan, A., McQuilken, M., Gladfelter, A.S., 2015. Septins and Generation of Asymmetries in Fungal Cells. Annu. Rev. Microbiol. 69, pp. 487–503.

Knoll, A.H., 2011. The Multiple Origins of Complex Multicellularity. Annu. Rev. Earth Planet. Sci. 39, pp. 217–239.

Kovar, D.R., Harris, E.S., Mahaffy, R., Higgs, H.N., Pollard, T.D., 2006. Control of the Assembly of ATP- and ADP-Actin by Formins and Profilin. Cell 124, pp. 423–435.

Kües, U. (Ed.), 2007. Wood production, wood technology, and biotechnological

impacts, Wood production, wood technology, and biotechnological impacts. Göttingen University Press, Göttingen 635 p.

Labarere, J., Bernet, J., 1977. Protoplasmic Incompatibility and Cell Lysis in PODOSPORA ANSERINA. I. Genetic Investigations on Mutations of a Novel Modifier Gene That Suppresses Cell Destruction. Genetics 87, pp. 249–57.

Laur, J., Ramakrishnan, G.B., Labbé, C., Lefebvre, F., Spanu, P.D., Bélanger, R.R., 2018. Effectors involved in fungal-fungal interaction lead to a rare phenomenon of hyperbiotrophy in the tritrophic system biocontrol agent-powdery mildew-plant. New Phytol. 217, pp. 713–725.

Leonowicz, A., Cho, N., Luterek, J., Wilkolazka, A., Wojtas-Wasilewska, M., Matuszewska, A., Hofrichter, M., Wesenberg, D., Rogalski, J., 2001. Fungal laccase: properties and activity on lignin. J. Basic Microbiol. 41, pp. 185–227.

Leslie, J.F., 1993. Fungal Vegetative Compatibility. Annu. Rev. Phytopathol. 31, 127–150.

Li, A., Begin, M., Kokurewicz, K., Bowden, C., Horgen, P.A., 1994. Inheritance of Strain Instability (Sectoring) in the Commercial Button Mushroom, Agaricus bisporus. Appl. Environ. Microbiol. 60, pp. 2384–8.

Lipke, P., 2018. What We Do Not Know about Fungal Cell Adhesion Molecules. J. Fungi 4, 59.

Lonsdale, A., Davis, M.J., Doblin, M.S., Bacic, A., 2016. Better Than Nothing? Limitations of the Prediction Tool SecretomeP in the Search for Leaderless Secretory Proteins (LSPs) in Plants. Front. Plant Sci. 7, 1451.

Löpez-Franco, R., Bracker, C.E., 1996. Diversity and dynamics of the Spitzenkörper in growing hyphal tips of higher fungi. Protoplasma 195, pp. 90–111.

Manning, K., Wood, D.A., 1984. Cellulase production and regulation byAgaricus bisporus. Appl. Biochem. Biotechnol. 9, pp. 385–386.

Marek, S.M., Wu, J., Louise Glass, N., Gilchrist, D.G., Bostock, R.M., 2003. Nuclear DNA degradation during heterokaryon incompatibility in Neurospora crassa. Fungal Genet. Biol. 40, pp. 126–137.

Markham, P., 1994. Occlusions of septal pores in filamentous fungi. Mycol. Res. 98, pp. 1089–1106.

Masoumi, F., Pourianfar, H.R., Masoumi, A., Mendi, E.M., 2015. A study of mycelium characterization of several wild genotypes of the button mushroom from Iran. Int. J. Adv. Res. Journalwww.journalijar.com Int. J. Adv. Res. 3, pp. 236–246.

Mayer, A., 2002. Laccase: new functions for an old enzyme. Phytochemistry 60, 551–565.

Mccabe, P.M., Gallagher, M.P., Deacon, J.W., 1999. Microscopic observation of perfect hyphal fusion in Rhizoctonia solani. Mycol. Res. 103, pp. 487–490.

Mikus, M., Hatvani, L., Neuhof, T., Komon-Zelazowska, M., Dieckmann, R., Schwecke, T., Druzhinina, I.S., von Dohren, H., Kubicek, C.P., 2009. Differential Regulation and Posttranslational Processing of the Class II Hydrophobin Genes

from the Biocontrol Fungus Hypocrea atroviridis. Appl. Environ. Microbiol. 75, pp. 3222–3229.

Mobley, H.L., Hausinger, R.P., 1989. Microbial ureases: significance, regulation, and molecular characterization. Microbiol. Rev. 53, pp. 85–108.

Mogk, A., Deuerling, E., Vorderwülbecke, S., Vierling, E., Bukau, B., 2003. Small heat shock proteins, ClpB and the DnaK system form a functional triade in reversing protein aggregation. Mol. Microbiol. 50, pp. 585–595.

Moloney, N.M., Owens, R.A., Meleady, P., Henry, M., Dolan, S.K., Mulvihill, E., Clynes, M., Doyle, S., 2016. The iron-responsive microsomal proteome of Aspergillus fumigatus. J. Proteomics 136, pp. 99–111.

Monti, D., Ottolina, G., Carrea, G., Riva, S., 2011. Redox Reactions Catalyzed by Isolated Enzymes. Chem. Rev. 111, pp. 4111–4140.

Moody, S.C., Dudley, E., Hiscox, J., Boddy, L., Eastwood, D.C., 2017. Interdependence of Primary Metabolism and Xenobiotic Mitigation Characterizes the Proteome of Bjerkandera adusta during Wood Decomposition. Appl. Environ. Microbiol. 84.

Morin, E., Kohler, A., Baker, A.R., Foulongne-Oriol, M., Lombard, V., Nagye, L.G., Ohm, R. a., Patyshakuliyeva, A., Brun, A., Aerts, A.L., Bailey, A.M., Billette, C., Coutinho, P.M., Deakin, G., Doddapaneni, H., Floudas, D., Grimwood, J., Hilden, K., Kues, U., LaButti, K.M., Lapidus, A., Lindquist, E.A., Lucas, S.M., Murat, C., Riley, R.W., Salamov, A. a., Schmutz, J., Subramanian, V., Wosten, H. a. B., Xu, J., Eastwood, D.C., Foster, G.D., Sonnenberg, A.S.M., Cullen, D., de Vries, R.P., Lundell, T., Hibbett, D.S., Henrissat, B., Burton, K.S., Kerrigan, R.W., Challen, M.P., Grigoriev, I. V., Martin, F., 2012. Genome sequence of the button mushroom Agaricus bisporus reveals mechanisms governing adaptation to a humic-rich ecological niche. Proc. Natl. Acad. Sci. 109, pp. 17501–17506.

Morón-Ríos, A., Gómez-Cornelio, S., Ortega-Morales, B.O., De la Rosa-García, S., Partida-Martínez, L.P., Quintana, P., Alayón-Gamboa, J.A., Cappello-García, S., González-Gómez, S., 2017. Interactions between abundant fungal species influence the fungal community assemblage on limestone. PLoS One 12, e0188443.

Mosbach, A., Leroch, M., Mendgen, K.W., Hahn, M., 2011. Lack of evidence for a role of hydrophobins in conferring surface hydrophobicity to conidia and hyphae of Botrytis cinerea. BMC Microbiol. 11, 10.

Nagai, M., 2003. Important role of fungal intracellular laccase for melanin synthesis: purification and characterization of an intracellular laccase from Lentinula edodes fruit bodies. Microbiology 149, pp. 2455–2462.

Nelson, R.J., Ziegelhoffer, T., Nicolet, C., Werner-Washburne, M., Craig, E.A., 1992. The translation machinery and 70 kd heat shock protein cooperate in protein synthesis. Cell 71, pp. 97–105.

O'Connor, E., McGowan, J., McCarthy, C.G.P., Amini, A., Grogan, H., Fitzpatrick, D.A., 2019. Whole Genome Sequence of the Commercially Relevant Mushroom Strain Agaricus bisporus var. bisporus ARP23. G3 (Bethesda). g3.400563.2019.

O'Keeffe, G., Hammel, S., Owens, R.A., Keane, T.M., Fitzpatrick, D.A., Jones, G.W., Doyle, S., 2014. RNA-seq reveals the pan-transcriptomic impact of attenuating the

gliotoxin self-protection mechanism in Aspergillus fumigatus. BMC Genomics 15, 894.

O'Leary, J., Hiscox, J., Eastwood, D.C., Savoury, M., Langley, A., McDowell, S.W., Rogers, H.J., Boddy, L., Müller, C.T., 2019. The whiff of decay: Linking volatile production and extracellular enzymes to outcomes of fungal interactions at different temperatures. Fungal Ecol. 39, pp. 336–348.

Ogata, H., Goto, S., Sato, K., Fujibuchi, W., Bono, H., Kanehisa, M., 1999. KEGG: Kyoto Encyclopedia of Genes and Genomes. Nucleic Acids Res. 27, pp. 29–34.

Owens, R.A., O'Keeffe, G., Smith, E.B., Dolan, S.K., Hammel, S., Sheridan, K.J., Fitzpatrick, D.A., Keane, T.M., Jones, G.W., Doyle, S., 2015. Interplay between Gliotoxin Resistance, Secretion, and the Methyl/Methionine Cycle in Aspergillus fumigatus. Eukaryot. Cell 14, pp. 941–957.

Panaretou, B., Siligardi, G., Meyer, P., Maloney, A., Sullivan, J.K., Singh, S., Millson, S.H., Clarke, P.A., Naaby-Hansen, S., Stein, R., Cramer, R., Mollapour, M., Workman, P., Piper, P.W., Pearl, L.H., Prodromou, C., 2002. Activation of the ATPase Activity of Hsp90 by the Stress-Regulated Cochaperone Aha1. Mol. Cell 10, pp. 1307–1318.

Paoletti, M., Clavé, C., 2007. The Fungus-Specific HET Domain Mediates Programmed Cell Death in Podospora anserina. Eukaryot. Cell 6, pp. 2001–2008.

Pontecorvo, G., 1956. The Parasexual Cycle in Fungi. Annu. Rev. Microbiol. 10, pp. 393–400.

Pontecorvo, G., Roper, J.A., Forbes, E., 1953. Genetic Recombination without Sexual Reproduction in Aspergillus niger. J. Gen. Microbiol. 8, pp. 198–210.

Pontes, M.V.A., Patyshakuliyeva, A., Post, H., Jurak, E., Hildén, K., Altelaar, M., Heck, A., Kabel, M.A., de Vries, R.P., Mäkelä, M.R., 2018. The physiology of Agaricus bisporus in semi-commercial compost cultivation appears to be highly conserved among unrelated isolates. Fungal Genet. Biol. 112, pp. 12–20.

Rangamani, P., Xiong, G.Y., Iyengar, R., 2014. Multiscale modeling of cell shape from the actin cytoskeleton. Prog. Mol. Biol. Transl. Sci. 123, pp. 143–67.

Raychaudhuri, S., Prinz, W.A., 2010. The Diverse Functions of Oxysterol-Binding Proteins. Annu. Rev. Cell Dev. Biol. 26, pp. 157–177.

Reynaga-Pena, C.G., Gierz, G., Bartnicki-Garcia, S., 1997. Analysis of the role of the Spitzenkorper in fungal morphogenesis by computer simulation of apical branching in Aspergillus niger. Proc. Natl. Acad. Sci. 94, pp. 9096–9101.

Riquelme, M., Bartnicki-Garcia, S., 2004. Key differences between lateral and apical branching in hyphae of Neurospora crassa. Fungal Genet. Biol. 41, pp. 842–851.

Riquelme, M., Reynaga-Peña, C.G., Gierz, G., Bartnicki-García, S., 1998. What Determines Growth Direction in Fungal Hyphae? Fungal Genet. Biol. 24, pp. 101–109.

Riquelme, M., Roberson, R.W., Sánchez-León, E., 2016. 3 Hyphal Tip Growth in Filamentous Fungi, in: Growth, Differentiation and Sexuality. Springer International Publishing, Cham, pp. 47–66.

Romaine, C.P., Ulhrich, P., Schlagnhaufer, B., 1993. Transmission of La France Isometric Virus during Basidiosporogenesis in Agaricus bisporus. Mycologia 85, 175.

Saporito-Irwin, S.M., Birse, C.E., Sypherd, P.S., Fonzi, W.A., 1995. PHR1, a pH-regulated gene of Candida albicans, is required for morphogenesis. Mol. Cell. Biol. 15, pp. 601–613.

Sarkar, S., 2002. Nonself recognition is mediated by HET-C heterocomplex formation during vegetative incompatibility. EMBO J. 21, pp. 4841–4850.

Schöneberg, A., Musa, T., Voegele, R.T., Vogelgsang, S., 2015. The potential of antagonistic fungi for control of Fusarium graminearum and Fusarium crookwellense varies depending on the experimental approach. J. Appl. Microbiol. 118, pp. 1165–1179.

Shashidhar, J., Sashidhar, R.B., Deshpande, V., 2005a. Purification and characterization of mycoferritin from Aspergillus parasiticus (255). FEMS Microbiol. Lett. 245, pp. 287–293.

Shashidhar, J., Sashidhar, R.B., Deshpande, V., 2005b. Role of mycoferritin from Aspergillus parasiticus (255) in secondary metabolism (aflatoxin production). FEMS Microbiol. Lett. 251, pp. 113–117.

Silar, P., 2005. Peroxide accumulation and cell death in filamentous fungi induced by contact with a contestant. Mycol. Res. 109, pp. 137–149.

Sipos, G., Prasanna, A.N., Walter, M.C., O'Connor, E., Bálint, B., Krizsán, K., Kiss, B., Hess, J., Varga, T., Slot, J., Riley, R., Bóka, B., Rigling, D., Barry, K., Lee, J., Mihaltcheva, S., LaButti, K., Lipzen, A., Waldron, R., Moloney, N.M., Sperisen, C., Kredics, L., Vágvölgyi, C., Patrignani, A., Fitzpatrick, D., Nagy, I., Doyle, S., Anderson, J.B., Grigoriev, I. V., Güldener, U., Münsterkötter, M., Nagy, L.G., 2017. Genome expansion and lineage-specific genetic innovations in the forest pathogenic fungi Armillaria. Nat. Ecol. Evol. 1, pp. 1931–1941.

Smith, M.L., Gibbs, C.C., Milgroom, M.G., 2006. Heterokaryon incompatibility function of barrage-associated vegetative incompatibility genes (vic) in Cryphonectria parasitica. Mycologia 98, pp. 43–50.

Sonnhammer, E.L., von Heijne, G., Krogh, A., 1998. A hidden Markov model for predicting transmembrane helices in protein sequences. Proceedings. Int. Conf. Intell. Syst. Mol. Biol. 6, pp. 175–82.

Sperschneider, J., Williams, A.H., Hane, J.K., Singh, K.B., Taylor, J.M., 2015. Evaluation of Secretion Prediction Highlights Differing Approaches Needed for Oomycete and Fungal Effectors. Front. Plant Sci. 6, 1168.

Swart, K., Debets, a J., Bos, C.J., Slakhorst, M., Holub, E.F., Hoekstra, R.F., 2001. Genetic analysis in the asexual fungus Aspergillus niger. Acta Biol. Hung. 52, pp. 335–43.

Takaya, N., Yamazaki, D., Horiuchi, H., Ohta, A., Takagi, M., 1998. Intracellular chitinase gene from Rhizopus oligosporus: molecular cloning and characterization. Microbiology 144, pp. 2647–2654.

Takaya, N., Yamazaki, D., Horiuchi, H., Ohta, A., Takagi, M., 1998. Cloning and Characterization of a Chitinase-encoding Gene (chiA) from Aspergillus nidulans , Disruption of Which Decreases Germination Frequency and Hyphal Growth. Biosci. Biotechnol. Biochem. 62, pp. 60–65.

Templeton, M.D., 1994. Small, Cysteine-Rich protenins and Recognition in Fungal-Plant Interactions. Mol. Plant-Microbe Interact. 7, 320.

Tiwari, S., Thakur, R., Shankar, J., 2015. Role of Heat-Shock Proteins in Cellular Function and in the Biology of Fungi. Biotechnol. Res. Int. 2015, pp. 1–11.

Tsigos, I., Bouriotis, V., 1995. Purification and Characterization of Chitin Deacetylase from Colletotrichum lindemuthianum. J. Biol. Chem. 270, pp. 26286–26291.

Tyanova, S., Temu, T., Sinitcyn, P., Carlson, A., Hein, M.Y., Geiger, T., Mann, M., Cox, J., 2016. The Perseus computational platform for comprehensive analysis of (prote)omics data. Nat. Methods 13, pp. 731–740.

Vakdevi, V., Sashidhar, R.B., Deshpande, V., 2009. Purification and characterization of mycoferritin from Aspergillus flavus MTCC 873. Indian J. Biochem. Biophys. 46, 360–5.

Validandi, V., Rupula, K., Beedu, S.R., Deshpande, V., 2009. Purification and characterization of mycoferritin from Fusarium verticillioides MRC 826. BioMetals 22, pp. 1063–1073.

Van Bael, S.A., Fernández-Marín, H., Valencia, M.C., Rojas, E.I., Wcislo, W.T., Herre, E.A., 2009. Two fungal symbioses collide: endophytic fungi are not welcome in leaf-cutting ant gardens. Proc. R. Soc. B Biol. Sci. 276, pp. 2419–2426.

van Diepeningen, A.D., Debets, A.J.M., Hoekstra, R.F., 1998. Intra- and Interspecies Virus Transfer in Aspergilli via Protoplast Fusion. Fungal Genet. Biol. 25, pp. 171–180.

Van Griensven, L.J.L.D., 1987. The Cultivation of Mushrooms: Its Present Status and Future Developments. Outlook Agric. 16, pp. 131–135.

Vedder, P.J.C., 1978. Modern mushroom growing. Educaboek.

Wagemaker, M.J.M., Eastwood, D.C., van der Drift, C., Jetten, M.S.M., Burton, K., Van Griensven, L.J.L.D., Op den Camp, H.J.M., 2006. Expression of the urease gene of Agaricus bisporus: a tool for studying fruit body formation and post-harvest development. Appl. Microbiol. Biotechnol. 71, pp. 486–492.

Wald, P., Pitkkänen, S., Boddy, L., 2004. Interspecific interactions between the rare tooth fungi Creolophus cirrhatus, Hericium erinaceus and H. coralloides and other wood decay species in agar and wood. Mycol. Res. 108, pp. 1447–1457.

Wang, X., Yao, B., Su, X., 2018. Linking Enzymatic Oxidative Degradation of Lignin to Organics Detoxification. Int. J. Mol. Sci. 19, 3373.

Wells, J.M., Boddy, L., 2002. Interspecific carbon exchange and cost of interactions between basidiomycete mycelia in soil and wood. Funct. Ecol. 16, pp. 153–161.

Wood, D.A., Thurston, C.F., 1991. Progress in the molecular analysis of Agaricus enzymes. Genet. Breed. Agaricus. Proc. First Int. Semin. Mushroom Sci.

Mushroom Exp. Station. Horst, Netherlands, 14-17 May 1991. pp. 81–86.

Wu, J., Saupe, S.J., Glass, N.L., 1998. Evidence for balancing selection operating at the het-c heterokaryon incompatibility locus in a group of filamentous fungi. Proc. Natl. Acad. Sci. 95, pp. 12398–12403.

Yague, E., Mehak-Zunic, M., Morgan, L., Wood, D.A., Thurston, C.F., 1997. Expression of CEL2 and CEL4, Two Proteins from Agaricus Bisporus with Similarity to Fungal Cellobiohydrolase I and -mannanase, Respectively, is Regulated by the Carbon Source. Microbiology 143, pp. 239–244.

Zhang, H., Yohe, T., Huang, L., Entwistle, S., Wu, P., Yang, Z., Busk, P.K., Xu, Y., Yin, Y., 2018. dbCAN2: a meta server for automated carbohydrate-active enzyme annotation. Nucleic Acids Res. 46, W95–W101.

Zhang, J., Siika-aho, M., Tenkanen, M., Viikari, L., 2011. The role of acetyl xylan esterase in the solubilization of xylan and enzymatic hydrolysis of wheat straw and giant reed. Biotechnol. Biofuels 4, 60.

Zhong, Z., Li, N., Liu, L., He, B., Igarashi, Y., Luo, F., 2018. Label-free differentially proteomic analysis of interspecific interaction between white-rot fungi highlights oxidative stress response and high metabolic activity. Fungal Biol. 122, pp. 774–784.

Chapter 4:

Transmission of Mushroom Virus X and the impact of virus infection on the transcriptomes and proteomes of different strains of *Agaricus bisporus*

4.0 Transmission of Mushroom Virus X and the impact of virus infection on the transcriptomes and proteomes of different strains of *Agaricus bisporus*

Eoin O'Connor[*,§], Sean Doyle[*],Helen Grogan[§] & David A. Fitzpatrick[*,†]

Affiliations:

[*]Department of Biology, Maynooth University, Maynooth, Co. Kildare, Ireland

[†] Human Health Research Institute, Maynooth University, Maynooth, Co. Kildare, Ireland

[§] Teagasc Food Research Centre, Ashtown, Dublin 15, D15 KN3K, Ireland

To be submitted

Keywords: *Agaricus bisporus*, commercial mushroom, mushroom virus X, MVX, mycovirus, transcriptomics, proteomics

Abstract

Cultivation of *Agaricus bisporus* is a large horticultural industry for many countries worldwide, where a single variety is almost grown exclusively. Mushroom virus X (MVX), a complex of multiple positive-sense single stranded RNA (ss(+)RNA) viruses, is a major pathogen of typical *A. bisporus* crops. MVX can manifest a variety of symptoms in crops and is highly infective and difficult to eradicate once established in host mycelium. Currently our knowledge regarding the molecular response of how *A. bisporus* fruit bodies respond to MVX infection is limited. To study the response of strains with different susceptibilities to MVX, we designed a model system to evaluate the *in-vitro* transmission of viruses in different *A. bisporus* hyphae over a time-course, the infection potential of fruit bodies in a crop when inoculated with MVX at two crucial phases in the crop cycle, the symptom expression of MVX in these varieties, the transcriptomic and proteomic response of fruit bodies to infection and the proteomic response of a susceptible strain mycelium to MVX-infection. Transmission studies revealed the high potential for MVX to spread to uninfected mycelium yet not into the fruit bodies of certain strains in a crop. MVX affected colour and quality of multiple fruit bodies. Gene expression is significantly altered in all strains and between times of inoculation in the crop. Genes related to transcription factors and a variety of stress responses were considerably regulated in each strain. Proteomic responses revealed restriction of cellular signalling and vesicle transport mechanism in infected fruit bodies. The MVX-infected mycelial networks contained within the composts revealed heightened abundances of proteins related to a variety of metabolic processes.

This in-depth analysis examining many factors relevant to MVX infection in different *A. bisporus* strains, will provide key insight into host responses to help guide future breeding research into improved disease-resistance varieties for this commercially important food crop.

4.1 Introduction

Mushroom virus X (MVX) first appeared in mushroom crops in the UK (1996) as a disease that exhibited certain symptoms reminiscent of La France disease. The earliest records noted discrete areas of pinning suppression and bare patches in crops. Initial assumptions were that these curious defects in crops were from La France infections, but diagnostics revealed completely unrelated double-stranded RNA (dsRNA) elements (Gaze *et al*., 2000). Empirical evidence pointed to a novel disease, the enigmatic origins and properties of which have resulted in the etymology of 'virus X' (Gaze *et al*., 2000), a name still used to collectively describe the symptoms produced from infections. Over the next four to six years, MVX became endemic in the UK, the Netherlands, Ireland and other countries with large mushroom industries. Disease phenotypes were inconsistent between some countries, where 'bare patch' was most prevalent in the UK and cap browning prevailed in Ireland, the Netherlands, Belgium and Poland, as geographical symptom variability, reflected viral composition from different locations (Burton *et al.*, 2011; Deakin *et al.*, 2017). The dsRNA banding profiles of symptomatic mushrooms revealed 26 distinct dsRNA molecules (Grogan *et al.*, 2003). Further research identified significant increases of transcripts, viral in origin, from white, infected, non-symptomatic mushrooms and brown, infected mushrooms (Eastwood *et al.*, 2015). A link between viral load and the extent of browning in infected mushrooms was also observed (Eastwood *et al.*, 2015). It is now understood that MVX represents multiple viruses in a virus complex or virome of *A. bisporus*. Next generation sequencing (NGS) techniques shed new insight on the characterisation of the virus within the MVX complex (Deakin *et al.*, 2017). Characterisation has led to the sequencing of viral RNA, the taxonomic distribution of viruses, viral genome composition, the number of individual viruses, the discrete RNAs they consist of and finally the new assignment of ss(+)RNA (Deakin *et al.*, 2017). Furthermore, the AbV16 virus, causal for the brown cap disease phenotype, was shown to be a multipartite virus consisting of four segments of RNA and AbV6, more affiliated with the bare patch phenotype, a bipartite segmented virus composed of two RNAs (Deakin *et al.*, 2017). 18 individual viruses are now known to belong to the MVX complex, of which constituent viruses show significant homologies to sequences from a range of taxonomical families; *Benyviridae* (ss(+)RNA viruses of plants (Gilmer and Ratti, 2017), *Narniviridae* (mycovirus), *Hypoviridae* (mycovirus (Suzuki *et al.*, 2018)), the order *Tymovirales*

(ss(+)RNA primarily with plant hosts) and the new virus family, *Ambsetviridae*. Furthermore, the dynamism of the MVX complex and constituent viruses along with their disparate homologies to different phylogenetic sources is suggestive of multiple ancient infection events of wild populations of *Agaricus* (Deakin *et al.*, 2017). Viruses have previously been identified in other edible mushrooms such as a dsRNA virus in *Flammulina velutipes* (Magae and Sunagawa, 2010), dsRNA virus in *Lentinula edodes* (Magae, 2012; Kim *et al.*, 2013) and a ss(+)RNA virus in *Pleurotus ostreatus* (Kim *et al.*, 2008). There is a paucity of findings for mycoviruses with DNA genomes, with only a single identification of a ssDNA virus of the phytopathogenic fungus *Sclerotinia sclerotiorum* (Yu *et al.*, 2010)

MVX first appeared during a period of technological advancement in many major *Agaricus* cultivating countries, namely, the use of bulk phase III compost. Phase III compost consists of compost fully colonised with *Agaricus* mycelium. Prior to being filled into growing house units, the mycelium binding the phase III compost must be broken apart for transportation. This process leads to *en-masse* breakages of the mycelium and subsequent repair by new growth and anastomosis. This activity is hypothesised to greatly promote the transmission and replication of MVX, as hyphae are more exposed, temporarily damaged (stress), and cell division is greatly increased (Eastwood *et al.*, 2015). The mushroom industry contends with a great variety of crop pathogens from fungi, bacteria, invertebrates and viruses (Fletcher and Gaze, 2007). One of the causes for the persistence of certain pathogens and the ease of spread of novel diseases from farm-to-farm, is due in part to the lack of genetic variation through use of homogenous populations in commercial cultivation. A single variety has dominated the commercial *Agaricus* industry for decades, resulting in what is essentially a monoculture crop. The lack of new varieties being introduced to mushroom market is due in part to difficulties in breeding arising from the life cycle of *A. bisporus* (Sonnenberg *et al.*, 2017). The use of novel hybrids and wild isolates of *A. bisporus* in cultivation or breeding would therefore prove useful in introducing resistance to MVX outbreaks. Off-white and brown varieties (wild) have already been shown to have heightened resistance to mycovirus infection, likely through vegetative incompatibility with commercial white strains (Sonnenberg *et al.*, 1995; Fletcher and Gaze, 2007). This study makes use of a range of strains of *A. bisporus* to understand different MVX susceptibilities/degree of resistance, symptom expression in a crop, transcriptomic and

proteomic response to MVX infection. The strains used in this study include A15 (globally cultivated white button strain), CWH (a novel commercial-wild hybrid strain), ARP23 (commercially-relevant wild strain isolate (O'Connor *et al.*, 2019)), SCC (smooth cap white hybrid variety) and OWC (off-white hybrid variety). This is the first study to evaluate the transcriptomic and proteomic response of multiple strains of *A. bisporus* to a commercially important pathogen. Here, for the first time, we aim to elucidate the transcriptomic and proteomic response of different *A. bisporus* strains fruit bodies, when the mycelium is inoculated with MVX. Inoculations were done at two crucial points in the crop:

1) When uninfected mycelium begins to colonise the compost.
2) Close to the time when transformation from vegetative growth to reproductive growth begins (pinning).

Information from this work is intended to highlight the host responses upon exposure to MVX and guide future breeding research with the determinants of MVX-resistant traits.

4.2 Methods

4.2.1 Strains and culture conditions

Five strains of *A. bisporus* were used for this study, with the exception of the transcriptomic work where three strains were selected from the five. The three strains used in every aspect of this study included: the most widely used contemporary commercial strain A15, a novel hybrid strain of commercial and wild strain parentage denoted as commercial-wild hybrid (CWH), a wild strain used in commercial breeding from the *Agaricus* resource program known as ARP23. The remaining two strains used in all analyses bar the transcriptomics were commercial hybrid strains that are not as readily commercially cultivated as they were in the past but still used in commercial breeding; strains smooth cap commercial hybrid (SCC) and off-white commercial hybrid (OWC).

The MVX-infected inoculum (MVX-1153) used was isolated from mushrooms showing brown-cap disease phenotype from an Irish mushroom farm in October 2016. Transects were cut from diseased mushrooms and tissue with no outer-surface area were cultured on compost extract media (CEM; aqueous extract of phase II mushroom compost, double-autoclaved for sterility) for two weeks at 25 ºC in the dark. Vegetative hyphae were sub-cultured to 30 g of autoclaved mushroom compost in 250 ml Duran flasks and incubated for three weeks at 25 ºC in the dark. Compost colonised with MVX-infected mycelium was used as an inoculum for all experiments.

4.2.2 *In-vitro* MVX-transmission setups

Dual-culture interactions were set up to assess the *in-vitro* transmission potential of MVX from the MVX-infected donor strain to a non-infected recipient strain over a time-course. Agar plugs containing hyphae from the donor and recipient strains were placed 10 mm apart on CEM and incubated at 25°C (n = 3). Cultures were monitored during initial colony growth and the first time-point (T_0) hyphae were extracted upon initial anastomosis of donor and recipient strains (3 days for all dual-culture interactions). T_1 hyphae were collected 6 days after T_0 and T_2 hyphae were taken 12 days after T_0. Time-point hyphae were excised as two agar plugs (7 mm Ø) from the top and bottom outer periphery of the growing edge of donor and recipient strain hyphae

(**Figure 1A)** and sub-cultured onto complete yeast media (CYM) containing 2 g proteose peptone, 2 g yeast extract, 20 g glucose, 0.5 g $MgSO_4$, 0.46 g KH_2PO_4, 1 g K_2HPO_4, 10 g agar in 500 ml dH_20 coated with a 9 cm sheet of cellophane. Sub-cultures were incubated at 25°C in the dark for 3 weeks after which mycelia was carefully removed from the cellophane, flash-frozen, freeze-dried and stored at -80°C for subsequent MVX diagnostics.

4.2.3 Cropping Experiment

A semi-commercial cropping experiment was set up to assess the transmission potential of MVX-1153 at two different infection times with the five strains of *A. bisporus*; A15, CWH, ARP23, SCC and OWC, respectively. The three treatments used for each strain were; MVX-1153 inoculation at the beginning of spawn run (MS; early infection), MVX-1153 inoculation at the beginning of case run (MC; late infection), and control uninfected plots. Treatments are described in detail below. Each treatment (n = 3) in all strains (n =5) were prepared in triplicate (n = 3). To prepare mushroom spawn prior to the beginning of the crop, rye grain was sterilised by autoclaving for 1 hr. Agar plugs with hyphae from each strain were added to 180g of sterilised grain in 500ml Duran flasks for each of the five strains. Grain was incubated at 25°C for four weeks in the dark, with gentle agitation of grains once a week to ensure homogeneity of hyphal growth.

Cropping was carried out as per industry standards in an environmentally controlled growing unit (Fancom 765 computer system). The *Agaricus* spawn was added and gently mixed throughout 18 Kg of pasteurised mushroom compost at a rate of 1.0% for each plot, which was then used to fill pre-cleaned polypropylene crates (0.6 × 0.4 × 0.24 m, 45 L). The first infection treatment (MS) was carried out at this point by addition of MVX-1153 at a rate of 0.01% to the assigned plots. This was done by leaving approximately 50 mm of the plot unfilled, sprinkling MVX-1153 compost fragments evenly on the surface and continuing to fill to the final weight of 18 Kg. Plots were incubated (spawn run) at 25°C, 90-95% RH, with high levels of ambient CO_2 (>6,000 ppm) for 17 d to allow for full colonisation of compost with *A. bisporus* hyphae. The second infection treatment (MC) was added at this point for the assigned plots with the same method described for (MS). Plots were then covered with 50 mm of pre-wetted peat 'casing' soil (Harte Peat, Clones, Co. Monaghan, Ireland). Plots were incubated under the

same conditions for an additional 7 d to allow for mycelium from the compost layer to grow to the surface of the casing layer. At this point, temperature and humidity were lowered steadily over a 3 d period from 25°C to 18°C and 90-95% RH to 85-90% RH and CO_2 levels were lowered through ventilation of filtered air. These environmental conditions were maintained to allow for primordia initiation ('pinning') and ultimate mushroom formation. Mushrooms were harvested after 7 d (1st flush) and 14 d (2nd flush). Two mushrooms either end of each plot were picked and immediately flash-frozen, freeze-dried and stored at -80°C for subsequent molecular analyses. All other mushrooms were weighed to record yield. Additional plots (n = 3 x 3), with control, MS and MC treatments, were also cultivated in the same manner as above for strain A15. These additional plots had 500 g of compost taken from the centre of the compost substrate layer during 1st flush, flash-frozen, freeze-dried and stored at -80°C.

4.2.4 Colour measurements

Data on mushroom colour was collected for every mushroom picked over two harvests (flushes). Colour measurements were recorded with a Minolta CR-400 chroma meter (Konica Minolta Inc., UK; illuminant D65, measurement aperture area ø=8mm). Measurements were taken in accordance to the CIE L*a*b* colour space (Luo, 2015). Calibrations were made using a white calibration plate (CR-A43) prior to colour recordings. A colour distance differential (ΔE) was calculated for each mushroom (Ajlouni, 1991;Fleming-Archibald *et al*., 2015). Statistical significance quoted within the treatments of each strain are based on single factor ANOVA ($P < 0.05$).

2.5 Diagnostics of disease-associated viruses AbV6 and AbV16

MVX diagnostics performed for mycelia from dual-culture transmission experiments and fruit bodies were identical with the exception of starting material, where all vegetative hyphae material available was used and fruit body material was limited to 100 mg. Although new insights into the characterisation of the MVX viruses suggests they are ss(+)RNA viruses (Deakin *et al.*, 2017), a standardised dsRNA isolation is used in current diagnostics as an established technique (Fleming-Archibald *et al*.,, 2015). dsRNA isolation, CF11 column purification, Super-Script® VILO™ cDNA

synthesis and PCR amplification of AbV16, AbV6 and GPD II (quality control) cDNAs were as described in detail (Fleming-Archibald *et al*., 2015).

4.2.6 RNA isolation, sequencing and data processing

RNA sequencing was carried out on mushroom isolates from strains A15, CWH and ARP23 to assess changes in gene expression of the fruit-bodies formed from hyphae exposed to MVX from two inoculation timepoints (MS and MC). Triplicate mushroom samples for the three strains and conditions from the 1st flush were used. The freeze-dried mushroom samples were crushed in liquid N_2. RNA was isolated using the RNeasy plant minikit (Qiagen) as per the manufacturer's guidelines. DNA digestion was done with DNase I (Invitrogen). RNA quantity and quality was assessed with an RNA6000 Nano Assay (Agilent 2100 Bioanalyzer, Agilent Technologies, USA). High-purity RNA isolations (RIN ≥ 8.5) were sent to BGI Tech Solutions Co., Ltd. (Hong Kong, China) for cDNA library construction and RNA sequencing (BGISEQ-500, PE100). Paired-end reads (100 nt) from each sample (n = 27) were filtered to remove low-quality regions (phred score < 20) using Trim Galore! (https://github.com/FelixKrueger/TrimGalore) and artefactual adaptors from sequencing runs with Cutadapt (Martin, 2011). Trimmed reads were aligned to the genome of *Agaricus bisporus* var. *bisporus* (H97) v2.0 (Morin *et al.*, 2012) using Hisat2 (Kim, Langmead and Salzberg, 2015). Transcripts were quantified using Salmon (Patro *et al.*, 2017). Transcript counts were normalised and significantly differentially expressed genes (DEGs) were assessed between samples using DESEQ2 (Love *et al*., 2014). DEGs were filtered by significance ($P < 0.05$) and a $\log_2$ fold change greater than or less than ± 1.5. A stricter criterion was not set due to the experimental design, as treatment replicates were based on plots and not diagnostics (i.e. some replicates may have manifested AbV16-infection and others may have been diagnosed as virus-free). A stricter filtering parameter may have resulted in reduced sensitivity.

4.2.7 Whole cell lysate protein extraction and LC-MS/MS analyses

Proteomic analyses were carried out on mushrooms of all five strains and A15 compost samples. The protein extractions for mushrooms and compost samples were

carried out in an identical manner, with the exception of the starting material; 100 mg of starting material was used for mushrooms and 50 mg of material was used with compost samples. Freeze-dried samples were crushed in liquid N_2. Ground material was added to a lysis buffer (100 mM Tris-HCl, 50 mM NaCl, 20 mM EDTA, 10%(v/v) glycerol, 1 mM PMSF and 1 μg ml^{-1} Pepstatin A pH 7.5) and subjected to sonication (Bandelin Sonoplus HD2200, Bandelin Elec.) three times, with a one minute incubation on ice between each round. Cell lysates were centrifuged twice until clarified and brought to 15% (w/v) trichloroacetic acid (TCA) with additional acetone for precipitation. Proteins were resuspended in 6 M urea, 2 M thiourea and 100 mM Tris-HCl pH 8.0 and then adjusted to 1 M urea with addition of ammonium bicarbonate. 15 μg of protein for each protein lysate preparation was reduced using dithiothreitol (DTT), alkylated using iodoacetamide (IAA), and digested using a combination of sequencing-grade trypsin and ProteaseMAX surfactant at a concentration of 0.01% (w/v). Digested peptides were acidified with addition of trifluoroacetic acid (TFA). C_{18} ZipTips ((Millipore® Ziptips C18)) were used to desalt 5 μg of tryptic peptides for Mass spectrometry. 750 ng of peptide mix was eluted onto a Q-Exactive (ThermoFisher Scientific, U.S.A) coupled to a Dionex RSLCnano for analysis by nano-flow liquid chromatography electro-spray ionisation tandem mass spectrometry (LC-MS/MS). LC gradients from 3-45% B were run over 110 min and data and the Top15 method used to collect data for MS/MS scans. Spectra were sorted into polypeptides by alignment to the predicted protein database of *Agaricus bisporus* var. *bisporus* (H97) v2.0 (Morin *et al.*, 2012). MaxQuant (version 1.6.2.3) with integrated Andromeda used for database searching (Cox and Mann, 2008). MaxQuant parameters are as previously described (Owens *et al.*, 2015). Removal of reverse hits and contaminant sequences, filtering of protein hits found in only a single replicate (n = 3), and Log_2 transformation of LFQ intensities was performed using Perseus (version 1.4.1.3; (Tyanova *et al.*, 2016)).

4.2.8 Functional annotation of transcriptomic and proteomic data

Transcriptomic and proteomic data were functionally annotated using BLAST2GO (version 5.2.4; Conesa *et al.*, 2005; Götz *et al.*, 2008). Sequences were queried against the NCBInr database using BLASTp (E value hit filter E^{-03}) and EMBL-EBI database using InterProScan (Altschul *et al.*, 1997; Jones *et al.*, 2014). The

CloudIPS resource was utilised for the most up-to-date databases in the dedicated computing cloud (2019.09). Independent InterproScan 5 searches were employed in parallel to assign Pfam IDs and associated Gene Ontology (GO) Term IDs. Predicted proteins were subjected to the complete GO workflow in BLAST2GO (GO cut off 55, GO weight 5, E value hit filter E^{-06} and default computational evidence codes). Significantly enriched terms were assigned using a Fisher's exact test ($P < 0.05$). Quantification of enhanced pathways for compost samples from KEGG (Kyoto Encyclopaedia of Genes and Genomes; Ogata *et al.*, 1999) terms were assigned by BlastKOALA (Kanehisa *et al*., 2016). Signal peptides were assigned to statistically significant differentially abundant SSDA *A. bisporus* proteins from compost using SignalP v5 (Almagro Armenteros *et al.*, 2019). All gene accession IDs listed in this text are preceded by the Joint Genome Institute (JGI) identifier 'jgi|Agabi_varbisH97_2'.

4.3. Results

4.3.1 *In vitro* horizontal transfer of MVX

MVX is hypothesised to primarily transfer from an infected host mycelium to non-infected hyphae via horizontal transmission (anastomosis). The transmission potential of MVX was trialled in dual-culture interactions whereby a donor (MX-1153) and acceptor (five strains of *A. bisporus*) cultures were grown together to facilitate potential transfer of viruses. Diagnostics were conducted for AbV16 (the virus linked to the brown disease-phenotype) at three time-points (T_0-T_2) in triplicate (**Figure 1C**). A total of 90 MVX assays were conducted. No virus-loss was noted in any of the donor hyphae as positive diagnostics for AbV16 were recorded for all time-points. Interestingly, acceptor hyphae in all five strains were positive for AbV16 as early as T_0 (first day of anastomosis). Temporal findings for the detection of AbV16 were also positive in T_1 and T_2, except for SCC T_2. No detection of AbV6 was recorded in any donor or acceptor strain in any time-points. The lack of AbV6 in both donor and acceptor hyphae is expected, as the source inoculum MVX-1153 did not test positive for this virus when originally sampled (not shown). Our results show that a variety of interactions can occur between the donor and acceptor strains (**Figure 1B**). The donor and A15 acceptor dual culture display high levels of interaction, this is unsurprisingly as they are vegetatively compatible strains. These findings show that the AbV16 virus can horizontally transfer from an infected mycelium to all five strains *in vitro*, even at different levels of vegetative compatibility, once an interaction zone has been established.

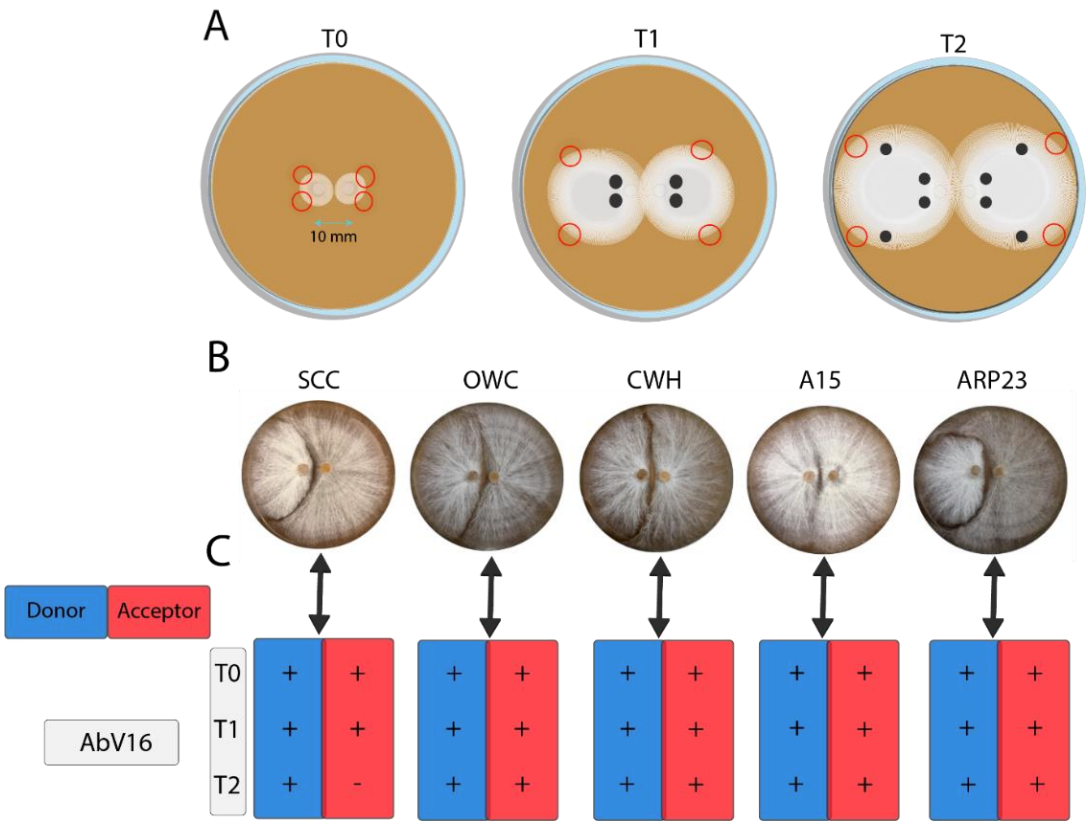

Figure 1: Overview of experimental design and main finding of *in vitro* MVX transmission experiment. (A) Diagram of the crossing culture setup and sample collection over three time-points. Red circles indicate areas where samples are taken for subsequent MVX diagnostics. Agar plugs from donor strain (MVX 1153) and acceptor strain (non-infected) are placed 10 mm apart and allowed to anastomose. Samples are taken at the first day of anastomosis (T_0), 6 days after (T_1) and 12 days after (T_2). Each sample is taken in duplicate from upper and lower areas of the growing periphery of mycelia. (B) Images of the five interactions. Headers for each plate indicate the acceptor partner, where the donor is on the left and the acceptor is on the right. Note the variety of interactions between all crossing cultures. (C) Indicates either a positive (+) or negative (-) diagnostic for AbV16 (*n* =3).

4.3.2 MVX diagnostics in fruit bodies of five strains of *A. bisporus*

RT-PCR tests for the presence of MVX were also undertaken on the fruit bodies of each of the five strain and corresponding treatment (**Figure 2**). The same inoculum used in dual-culture interactions (MVX-1153) was used to infect different plots (crates) at MS and MC time-points at a rate of 0.01 %. This inoculation rate was chosen as previous studies have shown that a greater number of off-colour and brown mushrooms were produced with the addition 0.01 % MVX inoculum compared to higher amounts, a phenotype indicative of higher viral-titres (Grogan *et al.*, 2004a; Fleming-Archibald *et al.*, 2015). As mentioned previously, MVX-1153 was isolated from a commercial mushroom crop exhibiting high frequency of the brown cap disease phenotype. When tested, the band corresponding to AbV16 was detected and the band for AbV6 was not. Results show that for the early infection (MS) plots, the A15 strain had a positive test for two of the three fruit bodies tested, the highest incidence for any strain tested (**Figure 2**). Conversely, AbV16 was not detected in MS treatments for strains SCC, OWC and ARP23. The only other strain with detection at MS was CWH (n = 1/3; **Figure 2**). A different pattern was observed for the late infection (MC) plots. AbV16 was detected in all isolates of A15 for MC (n = 3). All other strains, bar CWH (MC), showed presence of the band for AbV16 in one or more MC replicate. In terms of infectivity, MC treatments produced the highest level of AbV16 detection (**Figure 2**). CWH (MC) was the only strain that tested negative in each replicate for AbV16 and so can be considered one of the least susceptible to MVX infection. CWH cannot be considered totally MVX-resistant however as AbV16 was detected in one MS replicate (**Figure 2**).

We also tested for the presence of AbV6 in all strains and corresponding treatment time points (**Figure 2**). AbV6 was not present in the MVX-1153 inoculum and so AbV6-infection was not anticipated in any fruit body for MS or MC treatments. Furthermore, diagnostics from *in vitro* MVX assays did not detect bands corresponding to AbV6. As expected, no AbV6 bands were recorded in strains SCC, OWC, CWH or A15 (**Figure 2**). However, a AbV6 band was detected in a single MS and MC replicate for strain ARP23 (**Figure 2**). This finding is interesting as AbV6 was not present in any control ARP23 fruit bodies and these findings suggest the MVX-1153 inoculum, which does not contain detectable levels of AbV6 by standard diagnostics, is responsible for positive detection of AbV6 in these fruit body isolates. Furthermore, the one replicate

fruit body positive for AbV16 is negative for AbV6 infection. The influence of certain virus titres on the presence of other viruses in the MVX complex and mechanisms of virus loss have been suggested previously (Deakin *et al.*, 2017). In that regard, virus-virus interactions can influence changes in levels of different viruses and this may account for the findings of AbV6 in the ARP23 fruit bodies, but this requires further investigation (**Figure 2**).

It is worth noting that presence of bands for AbV16 can appear faint. This is likely a consequence of the original MVX-1153 inoculum not having a strong AbV16 band when originally sampled and so the potential for infection may be less when using this type of inoculum. Nonetheless, each strain demonstrated at least some degree of AbV16-infection from the MVX diagnostics performed here. The same mushrooms that were tested for MVX infection were used for subsequent transcriptomic and proteomic analyses detailed below.

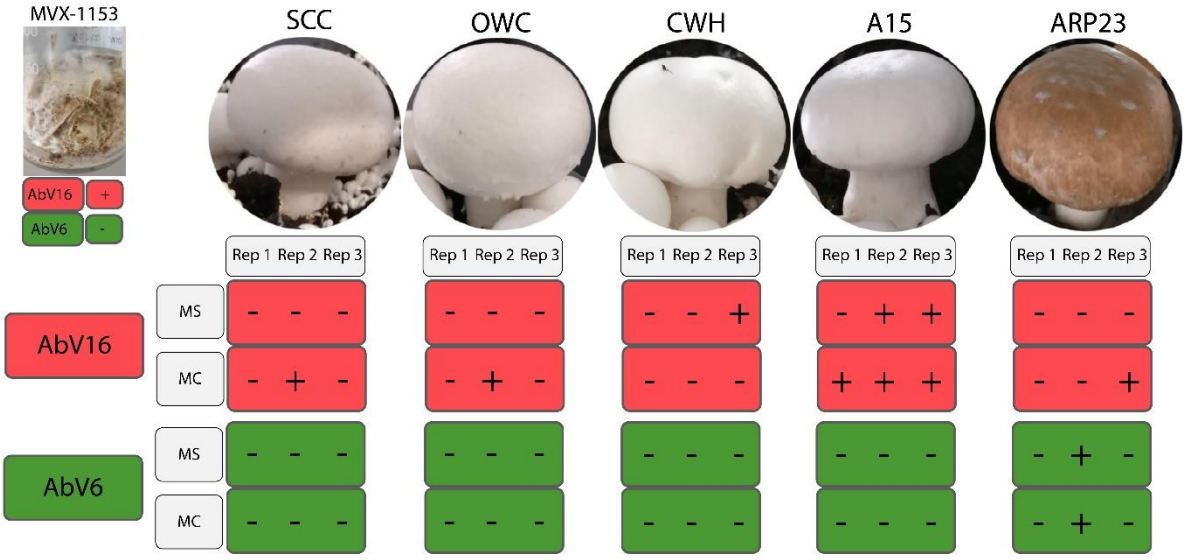

Figure 2: MVX diagnostics (RT-PCR) from the cropping experiment. Images of fruit bodies correspond to control treatments. The MVX inoculum MVX-1153 was used to infect the mycelium of five different strains of *A. bisporus* (+: band present, -: band absent). MVX-1153 was introduced at the beginning of spawn run (MS) and beginning of case run (MC) to the compost layer of individual plots. The fruit bodies were harvested, and candidates tested for the presence of AbV16 and AbV6. The highest level of susceptibility to MVX-infection was observed in A15 for AbV16, particularly in MC treatments where all tested positive. AbV16 was detected in at least one replicate plot fruit body for MC treatments for all strains bar CWH, which had only a single positive detection in an MS treatment. AbV6 was not detected in most isolates, but the wild strain ARP23 was positive for this virus once in both MS and MC treatments. MC treatments evidently produce the greatest frequency of MVX-infection. CWH seems the least susceptible to MVX-infection but cannot be considered resistant, as not all fruit bodies tested were negative.

4.3.3 MVX disease phenotypes and mushroom producing capacities

Different disease phenotypes were noted in the experimental crop (**Figure 3A-D**). The brown cap disease phenotype and off-coloured fruit bodies (detected namely via chromometric means) was the most prevalent of the phenotypes (**Figure 3A-B)**. Thickened/misshapen stipes were noted in MVX-inoculated plots of A15 (**Figure 3C**), a phenotype previously recorded in diseased crops (Grogan *et al.*, 2003). Unlike the other four strains, CWH displayed premature cap-opening of mushrooms from MVX-inoculated plots (32 incidences) (**Figure 3D**). Total fruit-body biomass was measured by weighing each fruit body harvested over two flushes (**Figure 3E and Table_S1**).

Interaction with the MVX 1153 inoculum appeared to marginally increase yield in many samples. Overall, the control treatments did not result in the highest yields per strain (bar CWH). For the remaining four strains, the MC treatment resulted in the greatest increase in yield per strain (**Figure 3E**). The MS treatment generally resulted in the lowest fruit body biomass, except for A15 where it was greater than the control and SCC where it produced the greatest yield (**Figure 3E**).

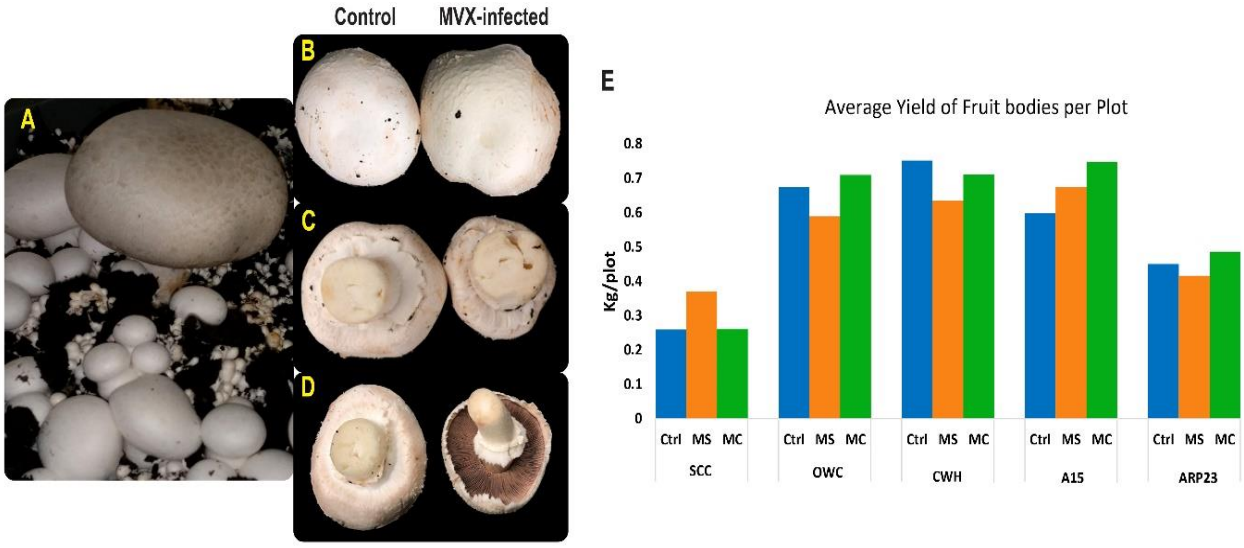

Figure 3: MVX disease phenotypes manifested in the experimental crop and impact on fruit body yield. (A) A brown mushroom growing in the casing bed next to white mushrooms. (B) A white and spherical pileus of a control mushroom compared to an irregularly shaped vaguely off-white mushroom from an MVX-infected plot. (C) Comparison of a control mushroom stipe next to an enlarged/swollen stipe of a mushroom from an MVX-infected plot. (D) Comparisons of medium sized mushrooms, where the control mushroom is closed-cap and the mushroom from an MVX-infected plot has a prematurely opened cap. (A-C) are mushrooms from the strain A15 and (D) is a mushroom from the strain CWH. (E) Comparison if fruit body biomass (KG/plot) between each strain and treatment. A total of 45 plots were used in this crop. MC most consistently results in higher yields for three of the five strains.

4.3.4 Mushroom colour measurements from the cropping experiment

The impact of MVX-inoculation was assessed through chromometric analyses of fruit bodies for MS and MC treatments in all five strains. A prominent symptom of MVX is brown cap discolouration. As such, 'whiteness' was deduced by measuring ΔE of each mushroom (**Figure 4)**. Chromometric analyses of fruit bodies were carried out over the first and second flush. A total of 1,050 mushrooms and 2,460 fruit bodies were measured for ΔE in first and second flush, respectively (note; the higher number of mushrooms in the second flush is a consequence of delayed pinning of some of the strains used, due to their optimal growth conditions differing to that of the typical commercial practices used in this experiment). An overall trend is seen in all five strains whereby the introduction of MVX inoculum at MS and MC results in higher ΔE values (**Figure 4**). The mean ΔE in all strains is higher in MS and MC compared to controls. Whiteness seems least affected in strain SCC, where mean ΔE values are very similar. Some high ΔE outliers can be seen in the 1st flush MC treatment and 2nd flush MS treatment, but these values do not result in any significant differences between controls and treatments (ANOVA, $P < 0.05$). Strain OWC MC has a significantly greater number of brown mushrooms overall in the 1st flush, a trend that switches to MS in the 2nd flush. CWH MC has a slightly higher ΔE mean compared to MS (differences of SCC MS and MC are significant; $P < 0.05$) and this difference becomes more inflated in the 2nd flush, where MS and control CWH mushrooms are not significantly different. Strain A15 had significantly higher ΔE values in 1st and 2nd flush for both MS and MC treatments compared to control, however, MS and MC were not significantly different to one another in both flushes. Unexpectedly, ARP23 showed significantly greater ΔE values in both flushes for MS and MC treatments compared to controls, where MC had a higher mean in 1st flush and MS higher in the 2nd flush. The effect of MVX-1153 inoculum on the colour of ARP23 was not anticipated, as ARP23 is a brown wild strain. As such, average ΔE for this strain (control) is between 45-50. This becomes significantly higher when exposed to MVX. In terms of overall frequency of MVX-infected brown mushrooms, the 2nd flush appears greater than the 1st flush for most strains (**Figure 4**).

Some precautions should be taken when interpreting this data; whiteness is a measurement of quality and this is particularly pertinent for the commercial A15, a strain commercially cultivated due in part to its distinctly white phenotype. Strains

CWH and OWC are ‘off-white’ varieties, and so brown outliers can be recorded for isolates that are simply more ‘off-white’ than others, a note also to be considered for MVX-inoculated treatments. Also skewed mean values and statistical differences can occur when arbitrarily low ΔE values or pure white outliers are recorded. It is therefore more informative to observe brown/high ΔE outliers when assessing the impact of the quality of a crop inoculated with MVX, as diseased crops often spontaneously produce abnormally brown mushrooms surrounded by white, yet infected fruit bodies.

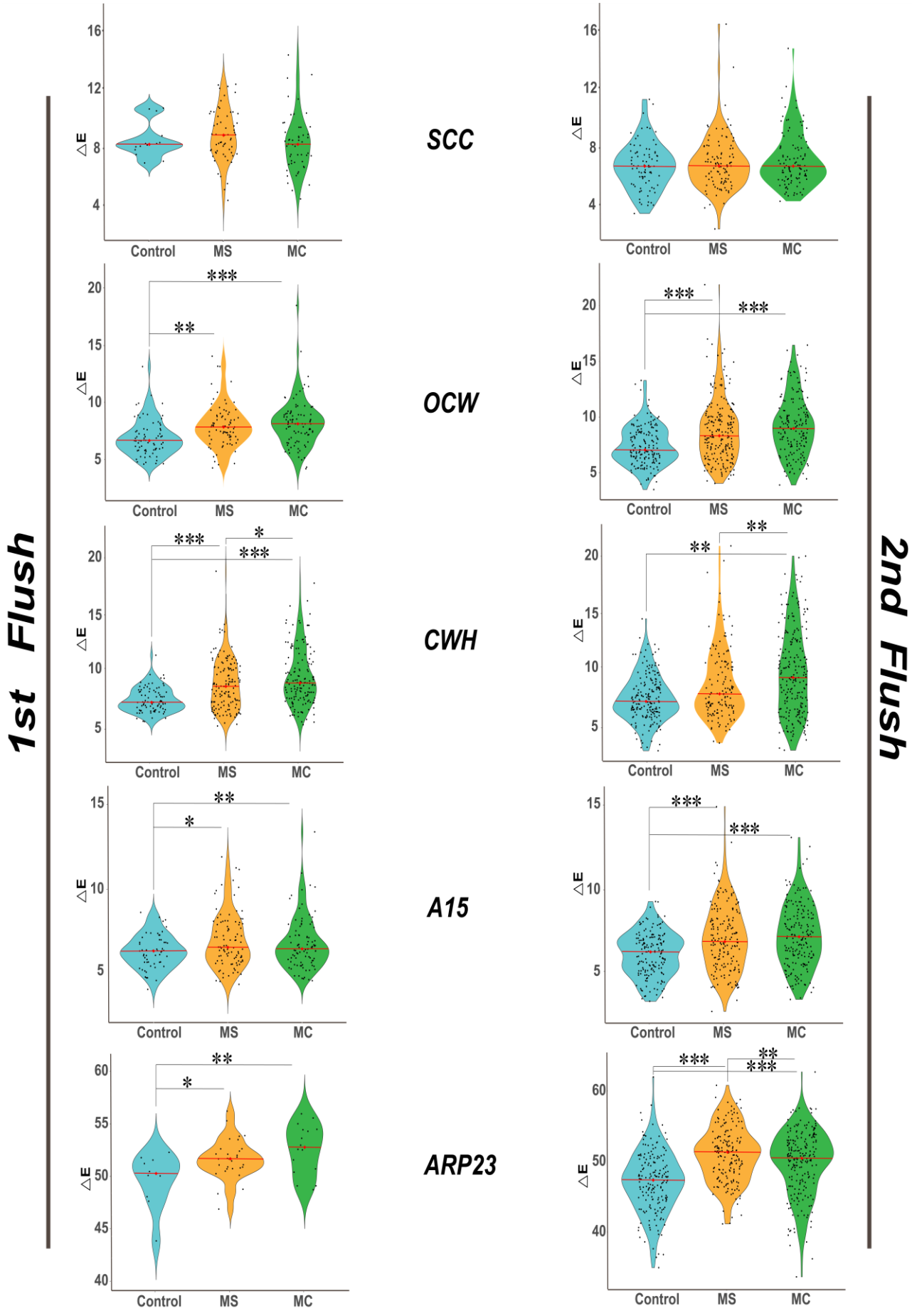
1st Flush
2nd Flush
SCC
OCW
CWH
A15
ARP23
ΔE
Control
MS
MC
***
**
*

Figure 4: Chromo metric data for 1st and 2nd flush from experimental crop. Violin plot used to compare disparity of colour data (ΔE) of control treatments to MVX-inoculated plots in the first and second flush. Low ΔE values represent pure white colours of fruit bodies. Mean values are represented by red line-centred diamonds per treatment. The width of the plot represents frequency/clustering of colour data to a given ΔE reading. Low yields account for some of the unusual distributions (e.g. SCC control). Colour readings for ARP23 are very high in comparison to the other four strains as this strain produces brown fruit bodies. Differences in all strains are evident when comparing MVX-inoculated treatment to non-infected controls. Significant differences were also observed between MVX-inoculation at spawning (MS) and MVX-inoculation at casing (MC) treatments (*****: $P < 0.05$, ******: $P < 10^{-3}$, ***: $P < 10^{-5}$)

4.3.5 Changes in the transcriptomes of strains A15, ARP23 and CWH upon MVX-inoculation

Out of the five *A. bisporus* strains in this work, strains A15, CWH and ARP23 were chosen for transcriptomic analyses. These were chosen as A15 is the MVX-susceptible commercial strain, CWH shows low susceptibility to MVX and ARP23 was included for novel discovery as it is a strain from a wild *A. bisporus* population. The strain SCC and OWC, while of interest due to their lower susceptibility to MVX-infection (**Figure 2**), are highly similar varieties to A15 and CWH already, warranting their inclusion in transcriptomic analyses unnecessary. Fruit bodies from each strain were harvested from non-infected (control; Ctrl), MVX-inoculated at the beginning of spawn run (MS), and MVX-inoculated at the beginning of case run (MC). Comparisons of early MVX-inoculation (MS) and late MVX-inoculation (MC) to non-infected (Ctrl) mushrooms were made to compare levels of differentially expressed genes (DEGs) between each strain. A liberal cut-off value of $\log_2$ fold change ± 1.5 or greater and a p-value of < 0.05 was utilised. A full list of DEGs for each strain and treatment timepoint can be found in supplementary information (**Table_S2**). For strain A15, a total of 304 upregulated and 15 downregulated DEGs and 103 upregulated and 44 downregulated DEGs were identified in MS and MC treatments respectively (**Figure 5**). CWH revealed 46 upregulated and 48 downregulated DEGs and 64 up-regulated and only 4 down-regulated DEGs in MS and MC treatments respectively (**Figure 5)**. Finally, ARP23 had

108 upregulated and 302 downregulated and 14 upregulated and 11 downregulated genes in MS and MC treatments respectively (**Figure 5**). DEGs from all strains share a trend whereby the gene expression response to MVX is greater in mushrooms formed from mycelium exposed to MVX viruses at an earlier stage (MS treatments). A15 fruit bodies show upregulation of a variety of genes when infected with MVX , whereas ARP23 primarily displays repressed regulatory mechanisms of genes when MVX-infected, with the greatest number of upregulated DEGs in A15 MS (n = 304) and the greatest number of downregulated DEGs in ARP23 MS treatments (n = 302) (**Figure 5** and **Table_S2**).

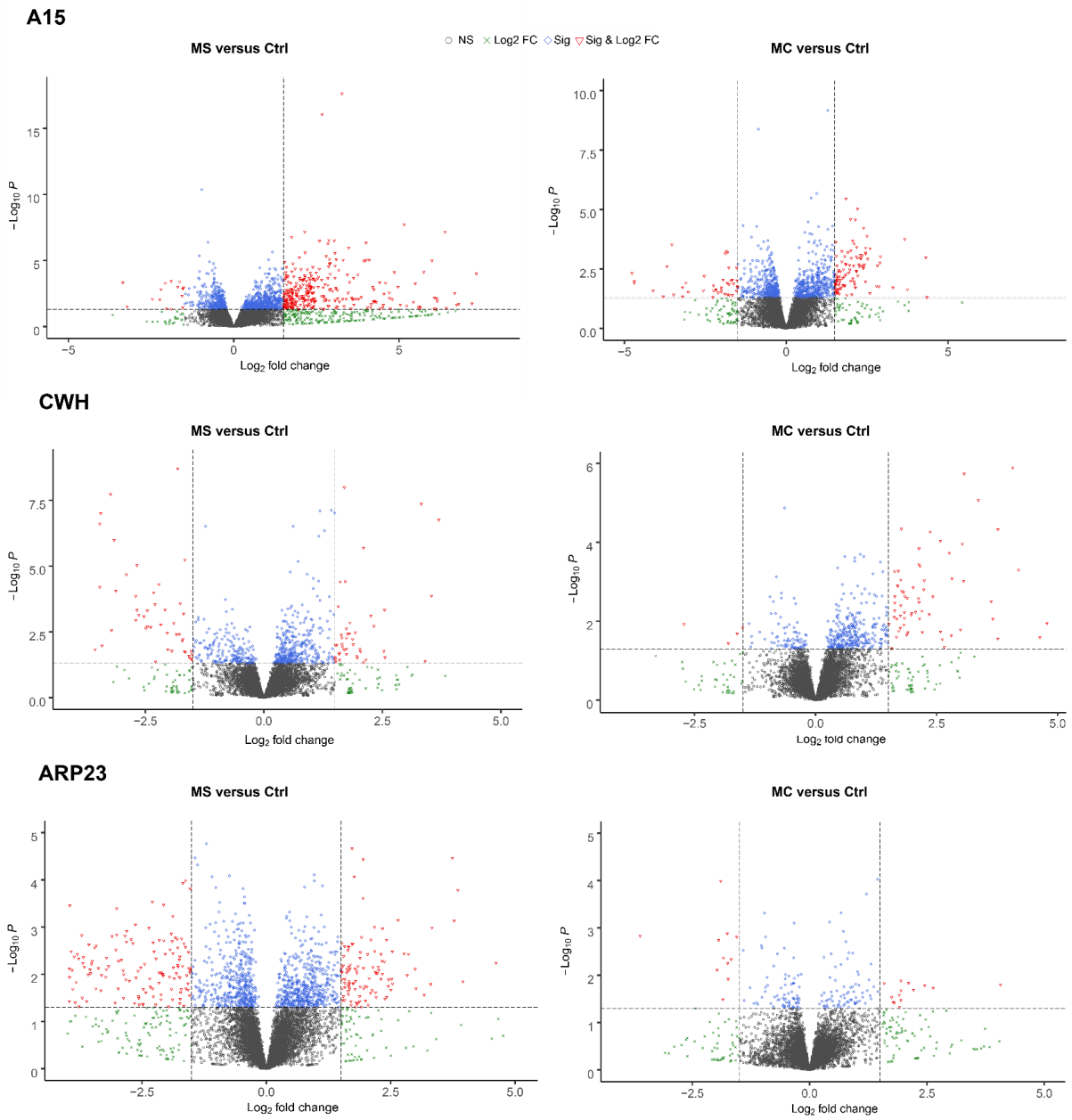

Figure 5: DEGs of strains A15, CWH and ARP23 for MS (early MVX inoculation) and MC (late MVX inoculation) treatments compared to non-inoculated control mushrooms. Data legend denotes colour coding of data labels. Note, not all statistically significant DEGs are visible within the dimensions of the volcano plot. See **Table_S2** for corresponding lists of DEGs. Values above the horizontal dotted line represent $P < 0.05$ and the values the left and to the right of the vertical dotted lines represent Log_2 fold changes < -1.5 and > 1.5, respectively. Data represents individual read counts from gene responses that are normalised against the overall means of counts from each replicate treatment within a given strain.

Looking at the A15 MS exposure to MVX our results show that 304 genes were upregulated and 15 were downregulated relative to the control (**Table_S2**). With respect to the A15 MC treatment, 103 genes were upregulated and 44 and downregulated. In terms of a shared response to MVX both A15 MS and MC treatments share 84 upregulated genes,

similarly they also share 6 downregulated genes (**Table_S2**). The CWH MS treatment displayed 46 upregulated and 48 downregulated genes with respect to the control, while 64 upregulated and 4 downregulated genes where observed in the CWH MC treatment relative to the control. The number of shared genes per CWH treatment was relatively low however, with only 7 upregulated genes being observed in both treatment time points, in the same vain only a single downregulated gene was observed between both CWH treatments. The ARP23 MS treatment resulted in 108 genes being upregulated and 302 downregulated with respect to the control while a reduced response was observed in the MC treatment with only 14 genes upregulated and 11 downregulated. In terms of a shared response between ARP23 MS and MC treatments, 8 genes were upregulated and 6 were downregulated in both.

Comparisons between DEG profiles were made between each strain and each treatment (**Figure 6A**). Apparent differences are observed between transcriptomic responses upon exposure to MVX at MS and MC, with most upregulated and downregulated DEGs being uniquely detected between treatments in each strain (**Figure 6A)**. The highest number of unique DEGs per strain were; A15 MS in terms of upregulation (n = 219), CWH MC upregulation (n = 57) and downregulation in MS for ARP23 (n = 296). The strain that shows the highest common response between different treatments is A15 MS and MC, at 84 upregulated DEGs. Only a single gene was commonly up- and down-regulated in A15 MS and MC, respectively (**Figure 6A**). This gene has no functionally annotated domains or orthologous annotation (accession:206844). *A. bisporus* demonstrates an overall strain-specific response to both early (MS) and late (MC) MVX-inoculation with regards the strains analysed. The number of DEGs common to at least two strains is generally quite low (**Figure 6B)**. In terms of similarities between individual strains, the upregulated genes of A15 MS and ARP23 MS share the highest number between any pair-wise comparison (n = 26). The only incidence of commonality between all three strains is in MS by a single upregulated gene (**Figure 6B**). This is the same unannotated transcript exclusively

common in both upregulated and downregulated DEG profile (accession:206844). All DEGs downregulated at MC are unique to each strain, suggesting MVX invokes strain-specific suppression of transcription.

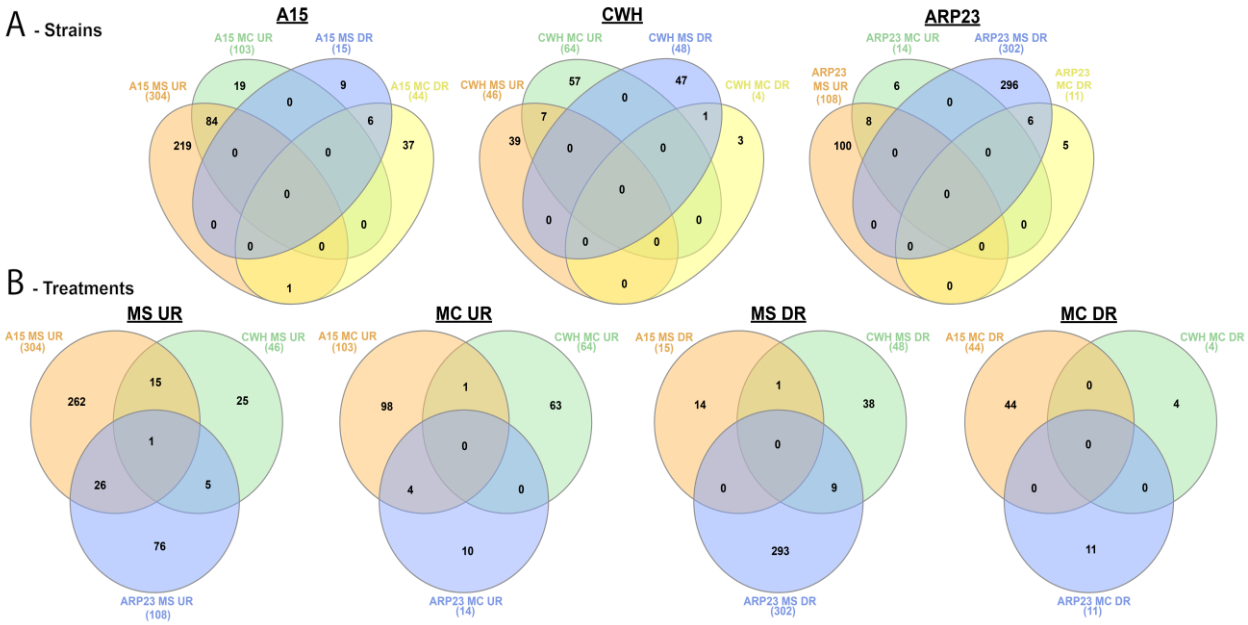

Figure 6: Common and unique significantly DEGs in strains A15, CWH and ARP23 in each treatment. A: Four set Venn diagrams represent up-regulated (UR) and down-regulated (DR) genes for MS and MC treatments for a given strain. The frequency of UR DEGS shared in MS and MC treatments for A15, CWH and ARP23 were 20.6 %, 0.1% and 6.1 %, respectively. Rates of DR DEGS common to A15, CWH and ARP23 were 10.2 %, 1.9 % and 1.9%, respectively. B: Three set Venn diagrams represent comparisons of the profiles of UR and DR DEGs by treatment. Almost no DEGs were common to any strain in any comparison. The highest degree of shared response to MVX was found in the UR of genes with an earlier inoculation of MVX (MS). Later MVX inoculation (MC) shows the lowest degree of common response between the strains, particularly in terms of DR. The greatest unique response to MVX is evident in ARP23 with the MS treatment (n = 293) by means of DR of genes followed by UR of genes of A15 with MS treatments (n = 262).

4.3.6 Differential expression of genes with putative viral-associated functions and transcription factors

Significant DEGs were examined for their putative proviral and antiviral functions (**Table 1**). RNA-interacting proteins play complex and conflicting roles depending on host capacity to recognise pathology and the class of invading virus. RNase H is a ubiquitous endonuclease involved in the processing of genetic information, mitochondrial genome replication, R-loop processing and reverse transcription of retroviruses (Moelling *et al.*, 2017). It facilitates retroviral genome replication through hydrolysis of RNA strands in RNA-DNA hybrids, accumulation of RNA primers and subsequent DNA synthesis (Racaniello *et al.*, 2015). MVX viruses are hypothesised to be ss(+)RNA viruses which replicate through RNA-dependant RNA polymerase (RdRp) (Deakin *et al.*, 2017). Therefore, it is likely that the multiple RNase H are playing a role in mitochondrial genome replication or housekeeping during DNA replication (**Table 1)**. Upregulation was noted for a RNase H genes in A15 MS (accession:121386**)** and also CWH MS (accession:58493**)** (both containing MVX-infected replicates; **Table 1**). Two RNase H genes are downregulated in ARP23 MS (accessions:121386 & 75272) along with a reverse transcriptase-RNA H-integrase gene (accession:57022**; Table 1**). A ribonuclease T2 family gene is upregulated in CWH MS (accession:62276; **Table 1**). RNase T2 have a diverse range of activities from modulation of host immune systems, breakdown of host RNA and many other functions. RNase T2 have been shown to play a role in xenophagy of viral RNA during autophagy, a process induced during viral infection (Levine, 2005; Luhtala and Parker, 2010; Wileman, 2013). Vacuolar RNase T2 cleaves the RNA sequestered there by autophagosomes (Huang *et al.*, 2015). Further evidence for the induction of autophagy and the possible connecting roles of RNase T2 is provided by CWH MS also up-regulating an autophagy-related protein 13 (accession:146937; **Table 1**). A guanyl-specific ribonuclease Po1 (accession:189342) is also up-regulated in CWH MS along with A15 MS (**Table 1**). These belong to the broad ribonuclease T1 superfamily. Another RNase T1 guanyl-specific enzyme from *Bacillus pumilus* has been investigated for its strong antiviral effect on influenza A (H1N1) virus (Shah Mahmud and Ilinskaya, 2013). Multiple DEGs related to RNA recognition motifs (RRMs) were also significantly regulated (**Table 1**). These are also known as ribonucleoprotein domain (RNP) or RNA-binding domain (RBD) and are extremely versatile domains (Maris,

Dominguez and Allain, 2005). RBDs can directly interfere with invading viruses by RNA-specific binding, preventing movement and replication or they can indirectly negatively impact in virus replication through changes in host gene expression and cellular vesicle trafficking (Musidlak, Nawrot and Goździcka-Józefiak, 2017). RBPs are also associated with stress stimuli, a topic explored in plant stress-response studies (Lorković, 2009; Woloshen, Huang and Li, 2011; Ambrosone *et al.*, 2012). Putative proviral genes are up-regulated in A15 MS including a Peptidyl-prolyl isomerase (accession:229065; **Table 1**), these isomerases have a range of functions from protein folding and transport, regulation of the cell cycle and regulatory functions in different receptors (Schiene *et al.*, 1998). They have also been implicated in viral replication (Franke, Yuan and Luban, 1994; Thali *et al.*, 1994; Sherry *et al.*, 1998). Another proviral protein (DNA damage-responsive (DDR) protein) with differential expression was located in both A15 MS & MC treatments (accession:62215; **Table 1**). RNA viruses can sequester early activators of DDR in a bid to delay incumbent apoptosis before the viruses have met full replication potential within the infected cell (Luftig, 2014). In contrast, a more prominent feature of DDR and RNA viruses is consistent recruitment of DDR pathways as a requirement for lytic replication. RNA viruses, even those non-retroviral, can cause significant genomic DNA damage and inevitable apoptosis, a vector for infecting neighbouring cells (Xiaofei and Kowalik, 2014; Luftig, 2014; Weitzman and Fradet-Turcotte, 2018).

Table 1: Presence/absence of transcripts with important associations with putative-viral activity. List of putative virus-associated functional genes taken from DEGs of each strain and treatment.

tative Virus-Associated Genes			Fold Change					
Gene Acc.	†Putative Function	Description	A15 MS vs Ctrl	A15 MC vs Ctrl	CWH MS vs Ctrl	CWH MC vs Ctrl	ARP23 MS vs Ctrl	ARP23 MC vs Ctrl
189342	Antiviral Activity	Guanyl-specific ribonuclease Po1	2.01		1.74			
62276		Ribonuclease T2 family			1.74			
146937		Autophagy-related protein 13			3.40			
117525		Antiviral protein CAP			2.10		-2.07	
177408		*HEN1*			1.8			
113810	Putative Antiviral Activity	RNA recognition motif	2.20	2.01				
144580		RNA recognition motif		1.64				
229063		RNA recognition motif		1.51				
71717		RNA Methyltransferase					1.52	
121386	Antiviral and/or Proviral Activity	RNase H	4.71				-3.50	
58493		RNase H			1.59			
75272		RNase H					-3.70	
51550		RNase H-domain containing					-3.68	
57022		Reverse transcriptase-RNase H-integrase					-6.42	
121495	Proviral Activity	Integrase zinc binding domain	2.23	2.24				
229065		Protein peptidyl-prolyl isomerization	1.96					
62215		Related to DNA damage-responsive protein 48	4.10	2.82				
178974		Hypothetical Protein - cellular response to DNA damage stimulus					-1.75	

†Functions are predicted from the literature and in some cases both proviral and antiviral activity may be assigned. The listed function is based on the one with the majority of literature support. Fold change values are from $\log_2$ transformed data.

We also examined our results to determine if the expression of transcription factors (TFs) were affected. Mycoviruses can exploit regulation of TFs for their own expansion during infection (Cho *et al.*, 2012; Lee *et al.*, 2014). Our results show that the regulation of multiple TFs (based on functional annotation) and other gene expression-regulators differ between the three strains and early and late MVX treatments (**Table 2**). Overall, 18 TFs showed altered gene expression. Some TFs (Zn_2Cys_6 for example accession:138736) displayed altered expression in multiple strains (A15, CWH and ARP23) while other TFs such as FRT1-like (accession:114425) were specific for individual strains (A15) (**Table 2**). Across all strains and treatments 29 incidences of altered expression were observed, the majority of these (18) showed upregulation of the TF. In most strains, TFs were upregulated except in the case of A15 MC and ARP23 MS. Overall, 5 TFs displayed altered expression in A15 MC and two of these were downregulated. Interestingly, of the 10 TFs that show differential expression in ARP23 MS, 9 are downregulated signifying a very different response in this strain when exposed to MVX at an early stage (**Table 2**). In terms of log fold change the greatest downregulated TF was the Zn_2Cys_6 TF in A15 MC (log_2 -6.12-fold) (accession:138736; **Table 2**). The Zn_2Cys_6 TF was also the most common DEG amongst strains and treatments with increased expression in CWH MS and MC treatments and decreased expression in A15 MC and ARP23 MS treatments (**Table 2**). Previous studies have also shown Zn_2Cys_6 are TFs most commonly regulated during mycoviral infection (Son *et al.*, 2011; Cho *et al.*, 2012; Lee *et al.*, 2014; Wang *et al.*, 2018). The C_2H_2 zinc finger TF was found upregulated in A15 MS and CWH MC (accession:122941; **Table 2**). This TF was also found upregulated in a former investigation with MVX-infected A15 mushrooms (Eastwood *et al.*, 2015).

Table 2: Presence/absence of transcription factor gene regulation. List of transcription factors in each DEG profile. Upregulation is represented by red and downregulation by green.

Transcription Factors		Fold Change					
Gene Acc.	Description	A15 MS vs Ctrl	A15 MC vs Ctrl	CWH MS vs Ctrl	CWH MC vs Ctrl	ARP23 MS vs Ctrl	ARP23 MC vs Ctrl
122941	C_2H_2 zinc finger*	3.31			2.42		
186054	Zn_2Cys_6; Fungal specific transcription factor domain*				1.76		
204206	Zn_2Cys_6; Fungal specific transcription factor domain*		-1.67				
138736	Zn_2Cys_6*		-6.12	3.54	3.77	-3.51	
201001	Fungal specific transcription factor domain					-1.93	
190401	GATA zinc finger*				1.64	1.95	
122668	Zinc finger 521	5.49				-4.56	
184667	bZIP					-1.53	
193938	Fruit-body specific gene C					-1.75	1.80
114778	BTB/POZ domain						1.80
70795	SET domain					-4.41	
120625	Putative hmg-i hmg-y DNA-binding	3.06	2.87				
135160	CBF/NF-Y					-2.22	
78143	Chromo Domain**					-2.47	
114425	FRT1-like*	1.73	2.20				
116879	*Predicted Protein****	2.22	2.16				
153600	*Predicted Protein****					-6.71	
56200	*Hypothetical Protein****	1.74			1.83		

*: Transcription factors known to play important functions in fruit body development. **: May not be annotated as transcription factors but play a strong regulatory role in gene expression. ***: Contain nucleic acid binding ontologies. Fold change values are from log_2 transformed data.

4.3.8 Regulation of A15, CWH and ARP23 gene expression when exposed to MVX

Functional annotation of genes was in the range 50-85% in each sample after Interproscan and BLAST2GO analyses. However, many of the most highly regulated genes lack any known function and could be involved in key fungus-mycovirus interactions (**Table_S2**). ARP23 MS DEGs had the greatest rate of genes with no annotation at 47 % and the lowest was found in ARP23 MC at 12 % (**Figure_S1**).

The top 15 highest and lowest fold changes of A15 from MS and MC treatments were tabulated (**Table 3** and **Table_S2)**. The only gene involved in carbohydrate-active enzymatic activity in A15 MS shows the largest log fold change (log_2 7.34) for a glycosyl hydrolase 88 (GH88; accession:212258), a d-4,5-unsaturated β-glucuronyl hydrolase involved in pectin saccharification pathways (van den Brink and de Vries, 2011). The upregulation of multiple genes in A15 MS involved in peroxidase activity, translation elongation and zinc ion binding are apparent. Genes that showed the greatest degree of downregulation included those involved in ribosome activities, xylan catabolism and serine-type endopeptidase activity (**Table 3**). The top 15 list of of upregulated DEGs in A15 MC differed to the MS treatment overall but some crossover in terms of putative function were observed, for example numerous genes involved in peroxidase activity are upregulated in both, as well a cutinase gene (accession:183005) and a nuclear envelope stress response gene (accession:187933 **Table 3**). In terms of downregulated genes a gene involved in xylan catabolism (accession:194000) was also downregulated in both A15 MC and MS treatments.

Table 3: List of top 15 annotated over-expressed and under-expressed DEGs from A15 MS and MC treatments. Lists of transcripts do not exceed 15 where applicable. Positive integer and negative integer fold change values for protein abundance are represented by ↑ and ↓, respectively

Treatment	Gene Acc.	Description*	Gene Ontology	Fold Change	P-value
MS vs Ctrl	212258	Glycosyl Hydrolase Family 88	No GO Terms	↑7.34	0.0001
	7233	*Hypothetical protein*	Zinc ion binding	↑7.21	0.018333
	186833	Peroxidase, family 2	Peroxidase activity	↑6.14	0.00761
	122668	*Zinc finger*	Nucleic acid binding	↑5.49	0.00058
	208153	*Zinc metalloproteinase*	No GO Terms	↑4.97	0.00102
	148454	Histidine phosphatase superfamily (branch 1)	No GO Terms	↑4.74	0.0455
	121386	RNase H	Nucleic acid binding, RNA-DNA hybrid ribonuclease activity	↑4.71	0.00701
	183005	Cutinase	Hydrolase activity	↑4.59	0.000486
	52638	Peroxidase, family 2	Peroxidase activity	↑4.51	0.0341
	193529	*Hypothetical protein*	RNA binding	↑4.41	0.000468
	207786	Peroxidase, family 2	Peroxidase activity	↑4.22	0.0132
	62215	*Related to DNA damage-responsive protein*	Helicase activity	↑4.10	9.19
	187933	Putative stress-responsive nuclear envelope protein	No GO Terms	↑4.00	0.000000467
	202473	*Predicted protein*	Translational elongation	↑3.77	0.008230291
	122941	Zinc finger C2H2 type	Nucleic acid binding	↑3.31	0.000009
	194000	*Carbohydrate-binding module family 13 protein*	Xylan catabolic process	↓3.36	0.000469
	205316	Protoglobin	No GO Terms	↓2.46	0.00797

	219134	Prolyl oligopeptidase family; Prolyl oligopeptidase, N-terminal beta-propeller domain	Serine-type endopeptidase activity; Proteolysis; Serine-type exopeptidase activity; Serine-type peptidase activity	↓2.20	0.00152
	180772	*Hypothetical protein*	Protein binding	↓2.07	0.034083
	45523	PH domain; P21-Rho-binding domain	No GO Terms	↓2.03	0.0431
	194402	*Toxin-like protein*	No GO Terms	↓1.89	0.000358
	191396	50S ribosome-binding GTPase	GTP binding	↓1.64	0.000393
	115967	Ricin-type beta-trefoil lectin domain	No GO Terms	↓1.56	0.00476
	191682	*Hypothetical protein*	Protein binding	↓1.55	0.036919
	200699	*Predicted protein*	RNA binding	↓1.54	0.001384
MC vs Ctrl	183005	Cutinase	Hydrolase activity	↑4.32	0.001053
	42806	Alpha/beta hydrolase family	No GO Terms	↑3.75	0.022618
	195889	*Extracellular metalloproteinase 3*	Peptidase activity	↑2.91	0.000957
	122173	*Peroxidase*	Peroxidase activity	↑2.89	0.001764
	120625	*Putative hmg-i hmg-y DNA-binding conserved site protein*	DNA binding	↑2.87	0.017534
	62215	*Related to DNA damage-responsive protein 48*	Helicase activity	↑2.82	0.002368
	198869	Domain of unknown function (DUF1929); Glyoxal oxidase N-terminus	No GO Terms	↑2.59	0.000433
	181636	HPP family	No GO Terms	↑2.58	0.033831
	211459	Alcohol dehydrogenase GroES-like domain; Zinc-binding dehydrogenase	Oxidation-reduction process	↑2.50	0.000132
	185963	Sir2 family	NAD+ binding	↑2.46	0.000716
	114455	F-box-like	Protein binding	↑2.45	0.000405
	177540	Indoleamine 2,3-dioxygenase	Heme binding	↑2.45	0.01101
	187933	Putative stress-responsive nuclear envelope protein	No GO Terms	↑2.39	0.002699
	178286	*Late embryogenesis abundant protein*	Cellular component	↑2.39	0.0000595
	189334	Fungal hydrophobin	Fungal-type cell wall; Structural constituent of cell wall	↑2.38	0.002962

	138736	Fungal Zn(2)-Cys(6) binuclear cluster domain	DNA-binding transcription factor activity, RNA polymerase II-specific; nucleus; regulation of transcription, DNA-templated; zinc ion binding	↓6.12	0.000865
	122913	Methyltransferase domain	No GO Terms	↓4.70	0.012189
	195436	Peroxidase, family 2	Peroxidase activity	↓4.70	0.010548
	211605	Fumarylacetoacetate (FAA) hydrolase family	Catalytic activity	↓3.69	0.002466
	194651	*Hypothetical protein*	Integral component of membrane	↓3.20	0.04626
	194017	Phosphopantetheine attachment site; Male sterility protein; AMP-binding enzyme	Catalytic activity	↓3.20	0.019087
	194651	*Hypothetical protein*	Integral component of membrane	↓3.20	0.04626
	194280	Glycosyl hydrolase family 12	Polysaccharide catabolic process; Cellulase activity	↓2.56	0.025416
	137057	Phosphatidylethanolamine-binding protein	No GO Terms	↓2.25	0.015795
	187070	OPT oligopeptide transporter protein	Transmembrane transport	↓2.24	0.025528
	149852	*Hypothetical protein*	Integral component of membrane	↓2.10	0.032199
	194000	*Carbohydrate-binding module family 13 protein*	Xylan catabolic process	↓2.01	0.023843
	119114	Cytochrome P450	Iron ion binding; oxidoreductase activity, acting on paired donors, with incorporation or reduction of molecular oxygen; oxidation-reduction process; heme binding	↓1.95	0.009191
	116357	NAD dependent epimerase/dehydratase family	Catalytic activity; coenzyme binding	↓1.90	0.035507
	220588	*Hypothetical protein*	Integral component of membrane; electron transport chain	↓1.85	0.000555

*Italicised descriptions represent functional annotations from top BLASTp hits. Non-italicised descriptions are derived from Pfam domain annotations. Multiple Pfam domain annotations are denoted by the separation of two descriptions by a semi-colon (;)

The transcriptomic response to MVX-inoculation evidently manifests quite a different set of DEGs in the less susceptible strains CWH (**Table 4** and **Table_S2**). Upregulated DEGs of CWH MS range in functionality from lipid metabolic processes, electron transfer via electron transport chains in the membrane and oxidation and reduction of alcohol dehydrogenases. Downregulated DEGs of CWH MS include cytochrome P450, a fruit-body specific protein A and tyrosinase-activity (**Table 4**). The later exposure to MVX (MC) shares a glutathione S-transferase gene with CWH MS and is highly represented by proteins functioning in signal transduction over the membrane and membrane components. Only three downregulated genes were found for CWH MC, a MULE transposase, a gene related to transmembrane activity and a spliceosomal snRNP complex (**Table 4**).

Table 4: List of top 15 annotated over-expressed and under-expressed DEGs from CWH MS and MC treatments. Lists of transcripts do not exceed 15 where applicable. Positive integer and negative integer fold change values for protein abundance are represented by ↑ and ↓, respectively

Treatment	Gene Acc.	Description*	Gene Ontology	Fold Change	P-value
MS vs Ctrl	46135	*Predicted protein*	Electron transfer activity; membrane; integral component of membrane; electron transport chain	↑5.23	0.005254
	138736	Fungal Zn(2)-Cys(6) binuclear cluster domain	Nucleus; zinc ion binding; regulation of transcription, DNA-templated; DNA-binding transcription factor activity, RNA polymerase II-specific	↑3.54	0.000135
	146937	Autophagy-related protein 13	Autophagy; Atg1/ULK1 kinase complex	↑3.40	0.040763
	195570	Ricin-type beta-trefoil lectin domain-like	No GO Terms	↑2.73	9.54×10^{-12}
	67334	*Hypothetical protein*	Integral component of membrane	↑2.56	0.029743
	187622	Fatty acid desaturase	Lipid metabolic process	↑2.55	0.000473
	178437	Lipase (class 3)	Lipid metabolic process	↑2.53	0.017203
	194619	Zinc-binding dehydrogenase; Alcohol dehydrogenase GroES-like domain	Oxidation-reduction process	↑2.32	0.001938
	70106	Alpha galactosidase C-terminal beta sandwich domain; Alpha galactosidase A	Hydrolase activity, hydrolyzing O-glycosyl compounds; carbohydrate metabolic process	↑2.26	0.000786
	117525	*Antiviral protein CAP*	Membrane	↑2.10	0.045206
	139552	Zinc-binding dehydrogenase; Alcohol dehydrogenase GroES-like domain	Oxidation-reduction process	↑2.10	0.00000203
	208153	*Zinc metalloproteinase*	No GO Terms	↑2.04	0.017631
	119457	*Cell envelope integrity protein TolA*	Integral component of membrane; toxin transmembrane transporter activity; bacteriocin transport; cell division; toxin transport	↑2.03	0.013925
	202658	Glutathione S-transferase, C-terminal domain; Glutathione S-transferase, N-terminal domain	Protein binding	↑1.97	0.030753

	190123	FKBP-type peptidyl-prolyl cis-trans isomerase	No GO Terms	↑1.95	4.29×10^{-19}
	59492	Phage lysozyme	Lysozyme activity; cell wall macromolecule catabolic process; peptidoglycan catabolic process	↓4.51	0.00000337
	122901	NACHT domain	No GO Terms	↓3.56	0.014738
	139293	Fungal hydrophobin	Fungal-type cell wall; structural constituent of cell wall	↓3.46	0.00000025
	194556	Glycosyltransferase family 18	Alpha-1,6-mannosylglycoprotein 6-beta-N-acetylglucosaminyltransferase activity; protein N-linked glycosylation	↓3.46	0.0000636
	136361	Cysteine-rich secretory protein family	No GO Terms	↓3.44	0.0000001
	203684	O-methyltransferase domain	O-methyltransferase activity	↓2.90	0.0000209
	191532	Common central domain of tyrosinase; Tyosinase C-terminal domain	Oxidoreductase activity	↓2.70	0.00014
	194024	Cytochrome P450	Iron ion binding; oxidoreductase activity, acting on paired donors, with incorporation or reduction of molecular oxygen; heme binding; oxidation-reduction process	↓2.68	0.000473
	120049	Common central domain of tyrosinase	Oxidoreductase activity	↓2.64	0.000721
	210159	Protein of unknown function (DUF563)	Transferase activity, transferring glycosyl groups	↓2.53	0.000828
	120050	Common central domain of tyrosinase; Tyosinase C-terminal domain	Oxidoreductase activity	↓2.49	0.002302
	114851	Fungal hydrophobin	Fungal-type cell wall; structural constituent of cell wall	↓2.45	0.000496
	194030	*Fruit-body specific protein A*	No GO Terms	↓2.32	0.000102
	122169	FAD binding domain	FAD binding	↓2.30	0.000289
	177137	FAD binding domain	FAD binding	↓2.04	0.003517
MC vs Ctrl	123463	*Lea domain-containing protein*	No GO Terms	↑4.19	0.000506
	65971	Ferritin-like domain	No GO Terms	↑4.07	0.00000129
	138736	Fungal Zn(2)-Cys(6) binuclear cluster domain	Zinc ion binding; DNA-binding transcription factor activity, RNA polymerase II-specific; regulation of transcription, DNA-templated; nucleus	↑3.77	0.0000474

	228532	*Histone gcn5 superfamily*	Hydrolase activity, hydrolyzing O-glycosyl compounds; carbohydrate metabolic process; N-acetyltransferase activity; integral component of membrane	↑3.66	0.008773
	193065	*Hypothetical protein*	Integral component of membrane	↑3.63	0.003189
	194746	*Mismatched base pair and cruciform DNA recognition protein*	NO GO Terms	↑3.36	0.00000862
	123392	*Histidine kinase*	Signal transduction; integral component of membrane	↑3.03	0.00011
	121504	*Hypothetical protein*	Integral component of membrane	↑2.99	0.016394
	63236	NADP oxidoreductase coenzyme F420-dependent; Pyrroline-5-carboxylate reductase dimerisation	No GO Terms	↑2.82	0.000834
	122941	Zinc finger, C2H2 type	Nucleic acid binding	↑2.42	0.002391
	195499	Glutathione S-transferase, C-terminal domain; Glutathione S-transferase, N-terminal domain	Protein binding	↑2.37	0.000054
	211605	Fumarylacetoacetate (FAA) hydrolase family	Catalytic activity	↑2.35	0.006783
	176453	Amino acid permease	Transmembrane transport; membrane	↑2.24	0.000948
	146117	Glycosyl Hydrolase Family 88	No GO Terms	↑2.21	0.019123
	187912	Amino acid permease	Transmembrane transport; membrane; transmembrane transporter activity	↑2.14	0.000145
	119353	MULE transposase domain	No GO Terms	↓1.80	0.036627
	183903	Sugar (and other) transporter	Integral component of membrane; transmembrane transport; transmembrane transporter activity	↓1.62	0.020794
	118335	*Sec63-domain-containing protein*	Spliceosomal conformational changes to generate catalytic conformation; spliceosomal complex; organic cyclic compound binding; spliceosomal snRNP complex; heterocyclic compound binding	↓2.72	0.012047

*Italicised descriptions represent functional annotations from top BLASTp hits. Non-italicised descriptions are derived from Pfam domain annotations. Multiple Pfam domain annotations are denoted by the separation of two descriptions by a semi-colon (;)

Finally, ARP23 mounts quite a different repertoire of DEGs in both MS and MC (**Table 5**). ARP23 MS opposingly shows upregulation of cytochrome P450 but also shares upregulation of metalloproteinase genes. Putative-stress response is upregulated (mismatched base pair and cruciform DNA recognition protein) and two genes are seen upregulated for sodium bile acid symporter families (**Table 5** and **Table_S2**). The extent of downregulation in ARP23 MS is dramatic. Examples include a membrane-type gene and a putative plant-senescence-associated protein. Contrary to A15 and CWH, ARP23 down-regulates peroxidase activity and cutinase (**Table 5**). Like ARP23 MS, MC shows upregulation of two genes encoding proteins with PQ loop repeats (**Table 5**). Metalloproteinase is also upregulated, again. Two genes with annotations for mismatched base pair and cruciform DNA recognition protein are downregulated in ARP23 MC, as well as hydrophobin (**Table 5**).

Table 5: List of top 15 annotated over-expressed and under-expressed DEGs from ARP23 MS and MC treatments. Lists of transcripts do not exceed 15 where applicable. Positive integer and negative integer fold change values for protein abundance are represented by ↑ and ↓, respectively

Treatment	Gene Acc.	Description*	Gene Ontology	Fold Change	P-value
MS vs Ctrl	195570	Ricin-type beta-trefoil lectin domain-like	No GO Terms	↑3.95	0.014201
	191563	Aldose 1-epimerase	Carbohydrate metabolic process; isomerase activity	↑3.85	0.000167
	190126	FKBP-type peptidyl-prolyl cis-trans isomerase	No GO Terms	↑3.77	0.000755
	77432	Cytochrome P450	Oxidoreductase activity, acting on paired donors, with incorporation or reduction of molecular oxygen; oxidation-reduction process; iron ion binding; heme binding	↑3.74	0.0000352
	138343	*Mismatched base pair and cruciform DNA recognition protein*	No GO Terms	↑3.33	0.001047
	194619	Zinc-binding dehydrogenase; Alcohol dehydrogenase GroES-like domain	Oxidation-reduction process	↑3.31	0.016506
	176448	Gamma-glutamyl cyclotransferase, AIG2-like	No GO Terms	↑3.17	0.027645
	194754	AMP-binding enzyme; AMP-binding enzyme C-terminal domain; Acetyl-coenzyme A synthetase N-terminus	Catalytic activity	↑2.86	0.003753
	211033	*Hypothetical protein*	DNA binding	↑2.83	0.010637
	195889	*Extracellular metalloproteinase 3*	Peptidase activity	↑2.65	0.000729
	42712	PQ loop repeat	No GO Terms	↑2.77	0.003717
	154430	PhoD-like phosphatase; PhoD-like phosphatase, N-terminal domain	No GO Terms	↑2.54	0.01608
	43781	PQ loop repeat	No GO Terms	↑2.53	0.003334
	203715	Sodium Bile acid symporter family	Membrane	↑2.52	0.012835
	220687	Sodium Bile acid symporter family	Membrane	↑2.50	0.021488
	213215	*Hypothetical protein*	Integral component of membrane	↓30	1.6×10^{-14}

	75878	*Plant senescence-associated protein, putative*	No GO Terms	↓24.24	5.5×10^{-10}
	213215	*Hypothetical protein*	Integral component of membrane	↓8.04	0.0000775
	183646	GMC oxidoreductase; GMC oxidoreductase	Oxidoreductase activity, acting on CH-OH group of donors; oxidation-reduction process; flavin adenine dinucleotide binding	↓7.80	0.016706
	209983	Hypothetical protein	Integral component of membrane	↓7.18	0.000265
	69363	Gag-polypeptide of LTR copia-type	No GO Terms	↓7.04	0.001193
	136297	*Hypothetical protein*	Integral component of membrane	↓6.71	0.0000801
	190202	Cutinase	Hydrolase activity	↓6.62	0.008346
	179594	Peroxidase, family 2	Peroxidase activity	↓6.55	0.00368
	176382	Cutinase	Hydrolase activity	↓6.46	0.004715
	207786	Peroxidase, family 2	Peroxidase activity	↓6.43	0.000132
	153600	*Predicted protein*	Nucleic acid binding	↓6.42	0.021062
	209575	Inositol polyphosphate kinase	Kinase activity; inositol phosphate biosynthetic process	↓6.22	0.000896
	57022	*Reverse transcriptase-RNase H-integrase*	Translation elongation factor activity; translational elongation	↓6.03	0.001555
	136705	*Hypothetical protein*	Nucleic acid binding	↓6.00	0.002095
MC vs Ctrl	190126	FKBP-type peptidyl-prolyl cis-trans isomerase	No GO Terms	↑2.64	0.018709
	191563	Aldose 1-epimerase	Isomerase activity; carbohydrate metabolic process	↑2.45	0.016493
	42712	PQ loop repeat	No GO Terms	↑2.21	0.020543
	43781	PQ loop repeat	No GO Terms	↑2.11	0.01457
	195889	*Extracellular metalloproteinase 3*	Peptidase Activity	↑1.95	0.013076
	200636	*Metallothionein 2*	No GO Terms	↑1.95	0.033835
	79351	Shikimate kinase	No GO Terms	↑1.95	0.020965
	190206	*Hypothetical protein*	Integral component of membrane	↑1.92	0.047354
	114778	BTB/POZ domain	protein binding	↑1.80	0.038613
	219773	Polysaccharide deacetylase	Carbohydrate metabolic process; hydrolase activity, acting on carbon-nitrogen (but not peptide) bonds	↑1.78	0.036848

	228717	Sodium/hydrogen exchanger family	Integral component of membrane; Cation transport; transmembrane transport; solute:proton antiporter activity	↑1.75	0.029278
	152717	*Mismatched base pair and cruciform DNA recognition protein*	No GO Terms	↓3.61	0.001483
	120027	*Mismatched base pair and cruciform DNA recognition protein*	No GO Terms	↓1.97	0.007856
	193938	*Fruit-body specific gene C*	Transcription corepressor activity; negative regulation of transcription, DNA-templated; metal ion binding	↓1.94	0.001827
	194160	*Aminodeoxychorismate synthase*	Biosynthetic process; membrane; integral component of membrane; hydrolase activity	↓1.89	0.000103
	224152	Glycosyl hydrolases family 43	Carbohydrate metabolic process; hydrolase activity, hydrolyzing O-glycosyl compounds	↓1.85	0.032768
	183497	Galactose mutarotase-like; Glycosyl hydrolases family 31	Carbohydrate metabolic process; hydrolase activity, hydrolyzing O-glycosyl compounds	↓1.75	0.001333
	193032	Fungal hydrophobin	Fungal-type cell wall; structural constituent of cell wall	↓1.75	0.005628
	56108	*Predicted protein*	Integral component of membrane	↓1.74	0.012147
	136361	Cysteine-rich secretory protein family	No GO Terms	↓1.67	0.00467
	209903	*Predicted protein*	Integral component of membrane	↓1.56	0.001548

*Italicised descriptions represent functional annotations from top BLASTp hits. Non-italicised descriptions are derived from Pfam domain annotations. Multiple Pfam domain annotations are denoted by the separation of two descriptions by a semi-colon (;)

4.3.9 Gene ontology enrichment of DEGs in A15, CWH and ARP23 exposed to MVX

To gain an understanding of the functional categorisation of significant genes upon MVC-inoculation, a total of 12 lists (strain, treatment, regulation) of significant genes ($P < 0.05$) were used search for enriched GO terms against the genome of *A. bisporus* (H97) (**Table_S3**).

The most statistically significant enriched term in A15 MS for downregulated genes was for vesicle-mediated transport (GO:0016192) (**Table_S3**). Additionally, terms related to mRNA processing (GO:0006397), mRNA metabolic process (GO:0016071), RNA processing (GO:0006396) and the molecular function term nucleotide binding (GO:0000166) were also downregulated in this group. The term for gene expression (GO:0010467) is enriched in A15 MS and MC upregulated genes for translation (GO:0006412). The same terms related to gene expression are not downregulated in A15 MC. However, multiple terms related to gene expression are enriched in upregulated genes of A15 MC; transcription initiation from RNA polymerase I promoter, RNA polymerase I preinitiation complex assembly, DNA-templated transcription-initiation, transcription by RNA polymerase I, transcription preinitiation complex assembly (GO:0006361, GO:0001188, GO:000635, GO:0006360, GO:0070897). MVX-infection in CWH MS reduced the expression of terms related to DNA packaging, chromatin organisation, chromatin assembly, transmembrane transport (GO:0006323, GO:0006325, GO:0031497, GO:0055085) and others. In contrast to the findings of up-regulation of specific genes related to autophagy in DEGs of CWH MS, terms related to autophagy were significantly underrepresented in CWH MC (**Table_S4**). In terms of cellular component, endoplasmic reticulum (GO:0005783) are also underrepresented in this group (**Table_S4**). The downregulation of terms relating to negative regulation of a multitude of processes in ARP23 MS and MC are numerous (**Table_S4)**. ARP23 MS contains 11 terms and ARP23 MC 16 terms for the downregulation of inhibitors of, to name a few; RNA metabolic process, gene expression, transcription, nucleobase-containing compound, nucleic acid-templated transcription, amongst others (**Table_S5**).

4.3.10 Proteomic response to MVX-inoculation in fruit bodies of A15, CWH and ARP23

As well as looking at the changes in gene expression we also set out to examine the proteomic response of strain fruitbodies to MVX infection using LFC proteomic analysis. In total 1,746, 1,607, 1,777 unique proteins were located for the CWH, A15 and ARP23 strains (**Figure_S2**). Of the 1,746 unique proteins located for the CWH treatments 1,289 were common to all three (control, MS and MS). The CWH MS treatment contained 157 unique proteins, while the CWH MC treatment contain 33. Furthermore, the CWH MC & MS treatments contained 66 shared proteins not located in the control treatment (**Figure_S2**). Of the 1,607 proteins located for the three A15 treatments 1,177 were common to all three. The A15 MS treatment contained 12 treatment specific proteins, while the MC treatment contained 33 treatment specific proteins. Furthermore, the A15 MC & MS treatments contained 46 shared proteins not located in the control treatment (**Figure_S2)**. Of the 1,777 proteins located for the three ARP23 treatments, 961 were common to all three. The MS treatment contained no treatment specific proteins, while the MC treatment contained 93 treatment specific proteins. Interestingly, the ARP23 MC & MS treatments contained 720 shared proteins not located in the control treatment (**Figure_S2**).

Our results revealed significant differences in relative abundances and unique translation of proteins between fruit-bodies of non-infected (control), early (MS) and late (MC) infection treatments. Statistically significant differentially abundant (SSDA) proteins were evaluated for their possible role in relation to MVX-infection ($P < 0.05$, $\log_2$ fold change ± 1.0, -1.0). All SSDA proteins were tabulated for A15, CWH and ARP23 treatments (**Table 6**). A list of SSDA proteins in SCC and OWC can be viewed in supplementary information (**Table_S6** and **Table_S7**, respectively). Overall, the proteomic response in terms of SSDA proteins was low. This could partly be due to the issue that MS and MC technical replicate fruit-bodies can be either MVX-infected or uninfected within a given treatment. An increase in abundance of three proteins in both A15 MS (mismatched base pair and cruciform DNA recognition protein, an unknown protein and heterokaryon incompatibility protein Het-C) and MC (myo-inositol-1phosphate synthase, lectin, DAHP synthetase I family) and decreases of four and five

proteins was detected, respectively (**Table 6**). Increased abundance in CWH was very limited at a single protein in MS (GHMP kinases), only (**Table 6**). Decreased abundance was more highly represented at nine proteins in MS and only a single protein in MC (**Table 6**). A different pattern of protein abundance was found in SSDAs of ARP23. The levels of two proteins and a single protein were reduced in ARP23 MS (amidohydrolase family protein and Thi4 family protein) and MC (phosphoglycerate mutase-like protein), respectively (**Table 6**). Increased abundance of SSDA proteins were more prevalent than the other strains for ARP23 MS and MC comparisons to control, at 16 and 15, respectively (**Table 6**). Analysis of shared and uniquely detected proteins between treatments of each strain revealed greater differences (**Figure_S3**). A consistent pattern between A15, CWH and ARP23 showed that treatments that had at least one MVX-infected replicate had the greatest number of unique proteins, particularly CWH MS (n = 157) (**Figure_S3**). Interestingly, a member of the RNAi system (ARC complex), Arb1, was found only in the A15 MC and ARP23 MS and MC treatments (**Table_S8**). The clustering of each proteome resolves into each of the five strains, though as per treatment, groupings become more mixed (**Figure 7**). This is possible due to unequal diagnostics of fruit bodies within strains, which may represent uninfected, formerly infected and infected states. Clustering of control (Ctrl), MS and MC treatments within strains revealed, bar for SCC, that Ctrl tend to cluster with MC and not MS (**Figure 7**).

Table 6: List of SSDA proteins from the proteomes of A15, CWH and ARP23 upon MVX-inoculations (MS and MC). Positive integer and negative integer fold change values for protein abundance are represented by ↑ and ↓, respectively.

Treatment	Description	GO	Fold Change
A15			
MS vs Ctrl	*Mismatched base pair and cruciform DNA recognition protein*	No GO Terms	↑1.79
	No annotation	No GO Terms	↑1.07
	Heterokaryon incompatibility protein Het-C	No GO Terms	↑1.02
	Ribosomal protein L1p/L10e family	No GO Terms	↓1.12
	Fruit-body specific protein D	No GO Terms	↓1.14
	Polysaccharide biosynthesis	No GO Terms	↓1.36
	Glutathione S-transferase	Protein binding	↓1.45
MC vs Ctrl	Myo-inositol-1-phosphate synthase	Inositol biosynthetic process	↑3.93
	Lectin	Carbohydrate binding	↑1.67
	DAHP synthetase I family	Biosynthetic process	↑1.19
	Oligosaccharyltransferase subunit Ribophorin II	Integral component of membrane	↓1.02
	Glyoxal oxidase	No GO Terms	↓1.06
	Serine aminopeptidase, S33	No GO Terms	↓1.33
	Pro-kumamolisin activation	Serine-type endopeptidase activity	↓1.50
	No annotation	No GO Terms	↓1.59
CWH			
MS vs Ctrl	GHMP kinases	ATP binding	↑1.05
	Bromodomain - transcription regulation; WD domain	Nucleic acid binding	↓1.07
	PTFIIS helical bundle-like domain; PWWP	Nucleus	↓1.16
	RNA recognition motif. (a.k.a. RRM, RBD, or RNP domain)	Nucleic acid binding	↓1.21
	Ribosomal L28e protein family	No GO Terms	↓1.24
	Ribosomal L38e protein family	Translation	↓1.50
	Ribosomal protein L36e	Translation	↓1.70
	NADH:flavin oxidoreductase / NADH oxidase family	Oxidation-reduction process	↓2.19
	Tyrosinase	Oxidoreductase activity	↓2.48
	No annotation	No GO Terms	↓3.73

MC vs Ctrl	Fatty acid desaturase	Lipid metabolic process	↓1.04
ARP23			
MS vs Ctrl	Nucleotide triphosphate	ATP binding	↑3.12
	RNA polymerase Rpb1	Transcription	↑2.44
	Insulinase	No GO Terms	↑1.98
	Protein of unknown function DUF89	No GO Terms	↑1.96
	Phospholipase	Catalytic activity	↑1.89
	Chromosome region maintenance or exportin repeat	Nuclear export signal receptor activity	↑1.78
	Dynamin	GTPase activity	↑1.57
	Epimerase/dehydratase	Coenzyme binding	↑1.45
	Thioredoxin	Cell redox homeostasis	↑1.44
	Glucosyltransferase 24	Protein glycosylation	↑1.32
	Ubiquitin-specific protease	Protein deubiquitination	↑1.20
	Mur ligase	Biosynthetic process	↑1.14
	PheRS DNA binding domain 3; tRNA synthetases class II core domain (F)	tRNA binding	↑1.02
	Glutaminyl-tRNA synthetase, non-specific RNA binding region part 2	Nucleotide binding	↑1.05
	Hexokinase	Carbohydrate metabolic process	↑1.06
	DJ-1/PfpI family	No GO Terms	↑1.07
	Amidohydrolase family	Hydrolase activity	↓1.12
	Thi4 family	No GO Terms	↓1.81
MC vs Ctrl	EF-hand	Calcium ion binding	↑4.45
	FAD binding domain	Oxidation-reduction process	↑2.23
	EF-hand	Calcium ion binding	↑2.14
	GMC oxidoreductase	Oxidation-reduction process	↑1.65
	DJ-1/PfpI family	No GO Terms	↑1.60
	UBX domain	Protein binding	↑1.60
	Carbohydrate kinase	ADP-dependent NAD(P)H-hydrate dehydratase activity	↑1.58
	Predicted Protein	Hydrolase activity	↑1.49
	Amidohydrolase	Hydrolase activity	↑1.44

	TPR-like protein	Protein binding	↑1.40
	No Pfam	No GO Terms	↑1.28
	Domain of unknown function (DUF427)	No GO Terms	↑1.17
	Cytochrome b5-like Heme/Steroid binding domain	No GO Terms	↑1.01
	NADPH-dependent FMN reductase	Oxidoreductase activity	↑1.05
	No Pfam	No GO Terms	↑1.09
	Phosphoglycerate mutase-like protein	No GO Terms	↓1.16

*Italicised descriptions represent functional annotations from top BLASTp hits. Non-italicised descriptions are derived from Pfam domain annotations. Multiple Pfam domain annotations are denoted by the separation of two descriptions by a semi-colon (;)

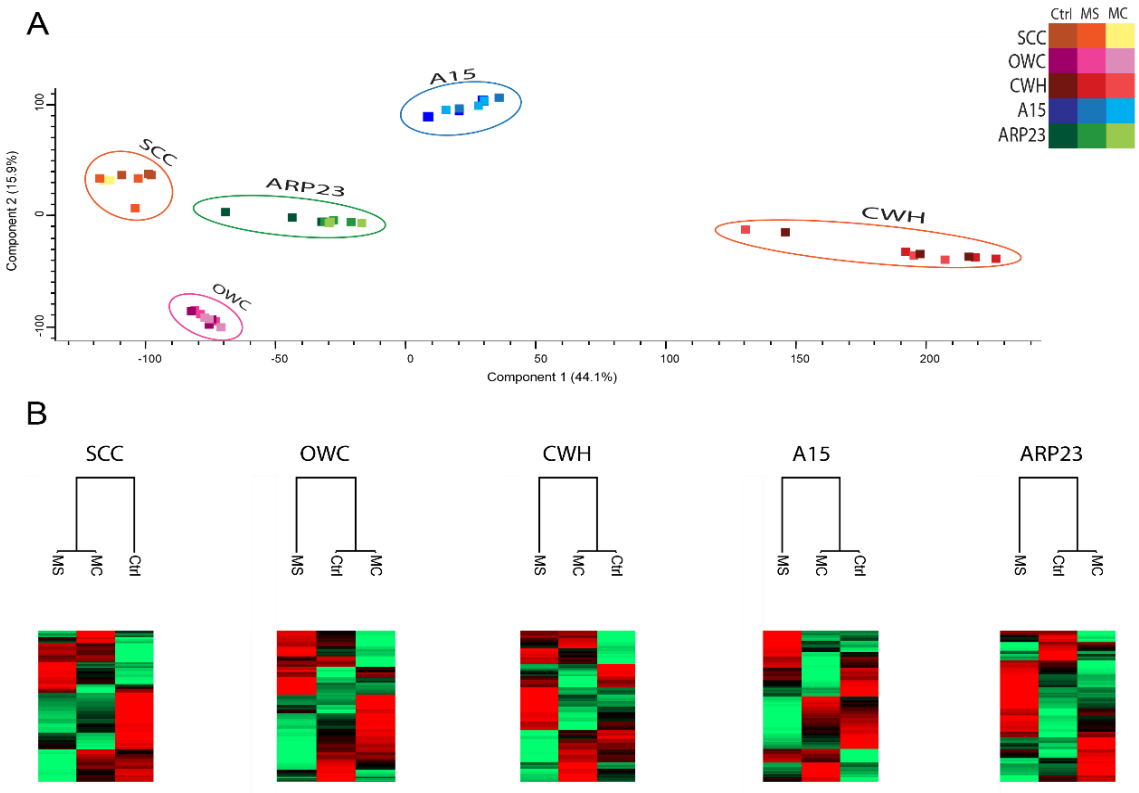

Figure 7: Clustering analysis of the proteomes of five strains *A. bisporus* control (Ctrl), MVX-inoculation at the beginning of spawn run (MS), MVX-inoculation at the beginning of case run (MC). (A) Principal component analysis shows the grouping of each strain. Individual replicates do not resolve into individual groups refelecting the individual response of fruit bodies upon MVX inoculation. (B) Hierarchical clustering of the proteomes of each strain where relative protein expression is shown in heat maps, high abundance is represented by red, average abundance by black and low abundance by green. Imputations of missing LFQ intensities for low abundance measurements were performed across all samples according to a normal distribution. Raw data was z-score normalised prior to hierarchical clustering. Clustering reveals, with the exception of SCC, that Ctrl and MC treatments consistently group with separation of MS. This may reflect the fruit bodies lack of time to respond to infection compared to MS.

A15 MS had high abundance of a mismatched base pair and cruciform DNA recognition protein (found upregulated in ARP23 MS transcriptome), a protein of unknown function (all orthologs are also annotated as hypothetical proteins) and heterokaryon incompatibility protein Het-C. Some of the underabundant proteins were specific to fruit bodies, biosynthesis of polysaccharides and certain ribosomal proteins (**Table 6**). The greatest fold change of any SSDA protein was for a myo-inositol-1-phopshate synthase in A15 MC compared to control (log_2 3.93-fold; **Table 6**). Also high in abundance in A15 MC is lectin. Dysregulation of translation is evident in MVX-infected samples of A15 and CWH via certain ribosomal proteins (**Table 6**). Membrane components and metabolism are also dysregulated in A15 MC and CWH MC (**Table 6**). The most frequent finding is down-regulation of transcription factors and more general nucleic acid binding proteins in CWH MS (**Table 5**). The highest and third highest fold-change (log_2 4.45-fold and log_2 2.14-fold, respectively) in ARP23 MC was for a protein containing an EF-hand domain involved in calcium ion binding (**Table 6**). EF-hand domain and calcium signalling are well known co-ordinators in response to biotic and abiotic stress stimuli (Day *et al.*, 2002). The lowest abundance of an SSDA protein in ARP23 MC is for phosphoglycerate mutase-like protein, involved in glycolysis (**Table 6**). An overview was made of the top GO terms found exclusively in MVX-infected replicates and counts of proteins common and unique in strain groups (**Figure_S3**).

4.3.11 Proteomes of MVX-infected vegetative mycelium in compost of strain A15

Samples of compost were extracted from plots replicating those of all fruit body analyses previously described. LC-MS/MS analyses revealed SSDA *A. bisporus* proteins of compost from MVX-inoculated at the beginning of spawning treatments (CTMS) and compost of MVX-inoculated at the beginning of casing treatments (CTMC) when compared to control, uninfected compost (CTCL) (**Table_S9**). CTMS SSDAs revealed upregulation of a total of 21 proteins and downregulation of 5 proteins when compared to CTCL (**Table_S9**). CTMC represents an earlier response of vegetative mycelia to MVX and this evident in the number of SSDAs for this treatment. upregulation of 55 proteins and downregulation of 28 proteins in this group represents the greatest variety of proteins in response to MVX-inoculation (**Table_S9**). Proteomic response of the mycelium of A15 to MVX is vastly different to that recorded in fruit

bodies (**Figure_S4**). MS fruit bodies and MS compost samples share no unique proteins between them and MC fruit bodies and MC compost exclusively share just four proteins; with functions in DNA binding (a core histone; accession: 133899), translation initiation/proteasome regulation (CSN8/PSMD8/EIF3K family protein; accession: 191954), a protein of multiple functions (a short chain dehydrogenase; accession: 149505) and a protein of unknown function found only in *A. bisporus var. bisporus* (accession: 203925) (**Figure_S4**).

Overall biological processes of significantly enriched GO terms of upregulated groups of proteins in the fruit bodies and vegetative mycelium in compost were examined (**Figure 8**). Functional categories of highly abundant proteins differ greatly between the vegetative and reproductive physiologies of A15. CTMS displays a plethora of metabolic processes form carbohydrate metabolism, glycolysis pathways for energy acquisition and nucleotide phosphorylation. Enriched terms are less prevalent in CTMC and relate to the metabolism of amino acids (**Figure 8**). However, metabolism is not represented in enriched terms of the fruit body of A15 MS. Up-regulation of endoplasmic reticulum (ER)-associated degradation (ERAD) pathways and stress response of ER dominate enrichment in A15 MS (**Figure 8**). A15 MC fruit body groups differ to MS. Oxidative stress is enriched and so too are terms for protein refolding, protein repair and the nonribosomal biosynthesis of siderophores (**Figure 8**).

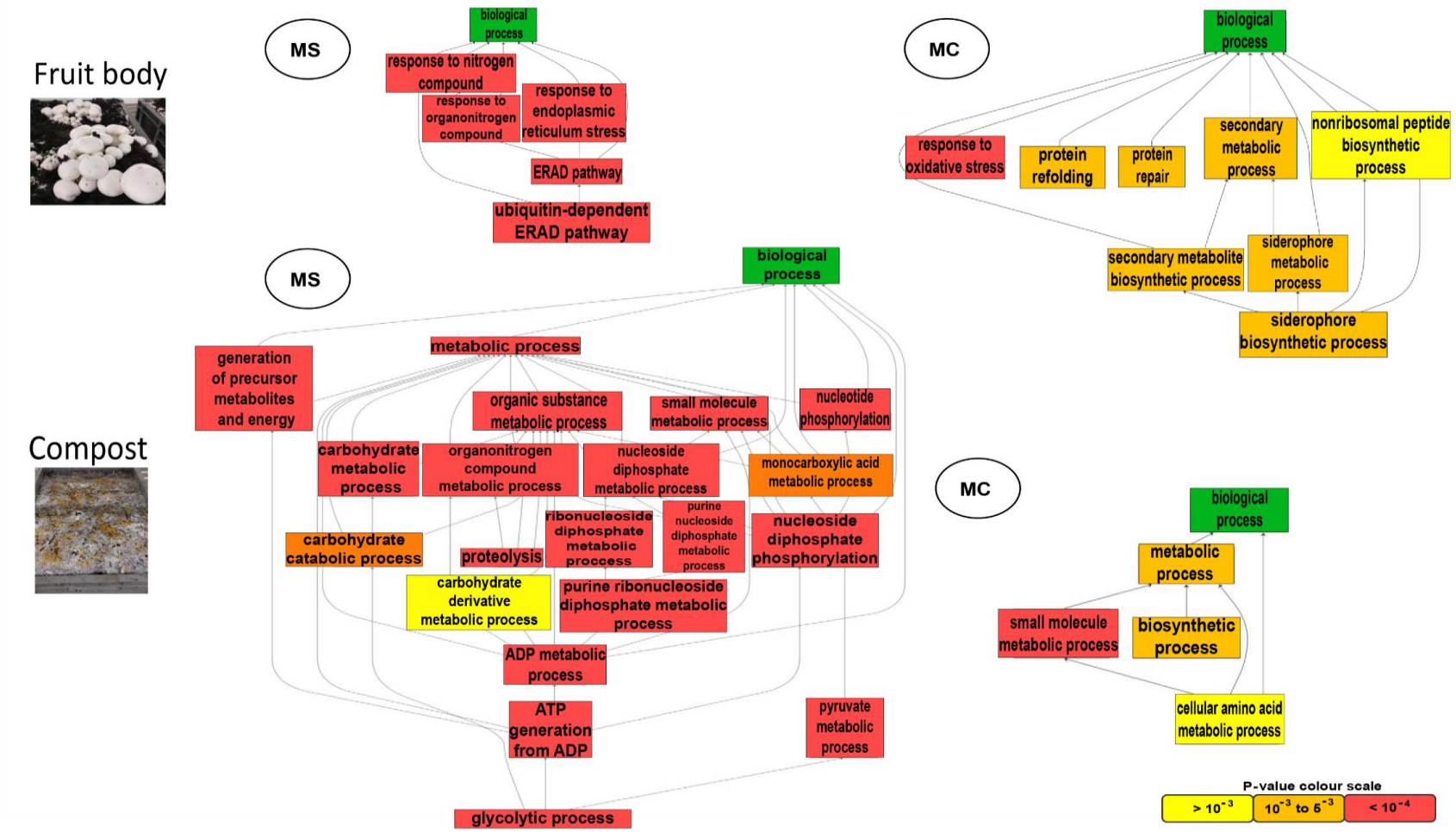

Figure 8: Hierarchy of enriched genes up-regulated in the fruit bodies and vegetative mycelium in compost upon MVX-infection. Flow diagram depicts overall organisation of biological processes significantly enriched (ranges of $P < 0.05$ to < 10-4) in MVX-infected fruit bodies and mycelium compared to the whole proteome of *A. bisporus* (H97). Lowest to highest significance ranges from terms coloured yellow, orange and red, respectively. The upper two flow diagrams relate to terms from the fruit body and the lower two flow diagrams relate to terms from the vegetative mycelium in compost.

The proteomes of CTCL, CTMS and CTMC were compared and scrutinised for the most highly enhanced KEGG pathways in in each group (**Figure 9**). As expected, carbohydrate metabolism topped the list in each proteome. This was consistently followed by genetic information processing for all. Noteworthy, the number of terms for these pathways increase in CTMS and further in CTMC. This is the case for most pathways. What differs in trends is the order of pathways with consideration of highest pathway terms to lowest. Metabolism of cofactors and vitamins are represented in CTCL, but absent in CTMS and CTMC. Signalling and cellular processing KEGG terms are evident in the MVX-infected groups, but not CTCL. Interestingly, pathways related to nucleotide metabolism increase from CTCL (n = 5), CTMS (n = 7), to CTMC (n = 12) (**Figure 9**).

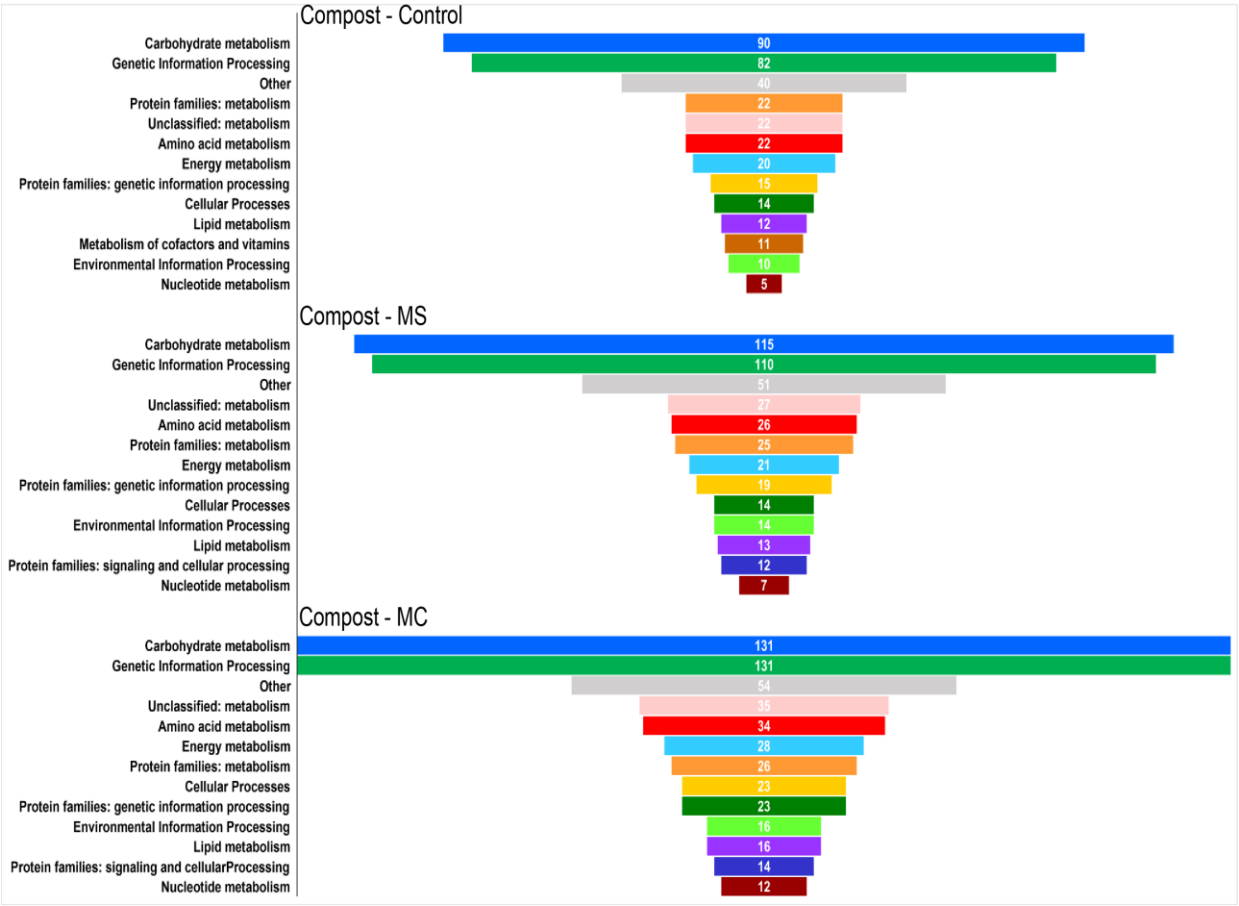

Figure 9: Overview of KEGG pathways in the proteomes of A15 compost. Proteomes for control (uninfected) early infection (MS) and late infection (MC) in terms of KEGG pathway annotation. Note; the largest differences were observed between pathways related to carbohydrate metabolism and genetic information processing. These differences increase from control, to MS, to MC. Greatest numbers of KO terms relating to nucleotide metabolism are also evident upon MC treatments.

4.4 Discussion

In this study, a model system was established to study a fungal-mycoviral interaction in a semi commercial-scale crop. Many studies focus on fungal-viral interactions in the context of the biocontrol of pathogenic fungi (Nuss, 2005; Xie and Jiang, 2014). Here, the interface of mycovirus and fungus is in the context of an economically important, globally cultivated food source. As such, the response of different strains of *A. bisporus* to MVX-inoculation was analysed through *in vitro* transmission assays in the mycelium, diagnostics of fruit bodies, transcriptomic characterisation of three key strain fruit bodies, proteomics of five strain fruit bodies and finally, proteomics of A15 mycelium in compost.

Mycoviruses are intracellular with little documented extracellular route of transmission. Instead, vectors of mycoviral infection consist of systems of vertical and horizontal transmission (Pearson *et al.*, 2009). Vertical transmission refers to the release of spores from the basidia of virus-infected fruit bodies harbouring viruses/virus elements as noted, for example, in La France Isometric virus (Romaine *et al*., 1993). Horizontal transmission involves the transfer of viruses via anastomosis between infected and non-infected mycelia, the primary mode of transmission of MVX (Grogan *et al.*, 2003). The transmission potential of MVX was investigated over a time-course totalling 12 days from initial anastomosis of a donor strain (MVX-1153) to a variety of five different acceptor strains (**Figure 1A**). MVX-1153 was isolated from a commercial crop and so exhibits full vegetative compatibility with A15. In contrast, vegetative compatibility is visibly lower in the four other strains (**Figure 1B**). Vegetative incompatibility is a known barrier to mycoviral transmission due to the inhibition of plasmogamy between differing hyphae (Romaine *et al*., 1993; van Diepeningen, Debets and Hoekstra, 1998; Chu *et al.*, 2002; Grogan *et al.*, 2004b; Kashif *et al.*, 2019). The lack of interaction between the donor and four of the acceptors lead to the hypothesis that complete restriction or latent transmission of MVX may be evident in comparison to full transmission expected in A15. In contrast, positive detection of AbV16 was found in all strains at each time-point, with the exception of SCC T2 (**Figure 1C**). This reveals that all interfaces of MVX-1153 and the five acceptor strains facilitate transfer of symptomatic viruses of MVX. However, this does not rule out the potential for different varieties of *A. bisporus* to be used as low susceptibility strains to MVX. *In vitro* transmission assays cannot replicate the complexity of the mycelial network

formed in compost beds. *In vitro* assays are effective for demonstrating transmissibility of mycoviruses between hyphae at the most basic level, though studies in the past have shown these types of experiments are not robust enough to draw grand conclusions on these biological processes, recommending a more comprehensive experimental design closer to the biological system to which mycoviruses occur *in vivo* (Brusini and Robin, 2013). To this end, the need for a broad temporal experiment of a commercial-scale crop is needed to fully assess potential vegetative incompatibility-borne resistance in different strains of *A. bisporus*. The findings from the *in vitro* transmission experiment performed here reveals that a seemingly minimal level of interaction between infected and non-infected hyphae is enough for transmission of MVX. This is an issue both for the potential of viruses to transfer to fruit bodies where commercially undesirable phenotypes can manifest and for the hyphae of newly infected mycelium residing in growing houses, acting as potential future MVX inocula for the infection of new crops.

MVX-diagnostics of fruit bodies revealed differences in the detection of MVX between different strains (**Figure 2**). A15, as anticipated, showed the highest degree of AbV16 detection of any strain, with MC giving positives in all replicates. SCC, OWC and ARP23 did not show bands for AbV16 at MS, but each showed detection in a single MC treatment (**Figure 2**). On the other hand, CWH had only one AbV16-positive fruit body in the MS setup. Based on the MVX frequency of MC, CWH is arguably the least susceptible strain to MVX-infection of the five, but not enough to be assigned as a completely resistant strain. The finding of AbV6 in the ARP23 MS and MC treatments was unusual (**Figure 2**). The AbV6 virus is more associated with the bare patch disease phenotype and does not tend to co-occur with the brown disease phenotype (Grogan *et al.*, 2003). As AbV6 was not detected in the control ARP23 fruit bodies, this suggests the introduction of an MVX inoculum for AbV16 is somehow responsible. Moreover, the transmission experiments show that the vegetative mycelium of ARP23 did not contain detectable levels of Ab6 (**Figure 1C**), pointing to an origin of AbV6 replication specifically in the fruit bodies. The presence of small numbers of AbV6 has been shown in uninfected mushrooms (Deakin *et al.*, 2017), perhaps the introduction of AbV16 initiates unknown virus-virus interactions in ARP23 fruit bodies which results in replication of AbV6 that didn't occur in the commercial strain fruit bodies. This implication warrants further study.

The delayed introduction of MVX inoculation to a crop has been previously shown to create the greatest level of symptom expression in a crop (Grogan *et al.*, 2003; Fleming-Archibald *et al*., 2015). This was also evident in the chromometric analysis of our experimental crop, where the later inoculation time resulted in the greater number of off/white and brown fruit bodies, except for first and second flush SCC and second flush ARP23 (**Figure 4**). Although, the severity of browning did not differ greatly between MVX treatments, as it has in previous work (Fleming-Archibald *et al*., 2015). This could be due to discrepancies between MVX inocula.

Yield data showed an unusual trend between the total weight of fruit body biomass and MVX-inoculation over the two flushes. MS treatments produced lower yields than the control, except for A15 and SCC where it was highest. MC treatments tended to produce highest fruit body yields in each strain, but the highest yield recorded in CWH was in a control treatment (**Figure 3E**). This is contrary to previous findings on the impact of MVX upon yield. Inoculum affiliated with AbV6 (bare patch phenotype) is known to significantly reduce yield (Grogan *et al.*, 2003). Whereas inoculum affiliated with AbV16, where symptomatic browning is strongest, has been shown to reduce yield in certain inocula (Fleming-Archibald, Ruggiero and Grogan, 2015). Additionally, other inocula were noted as showing similar or slightly higher yields than controls (Fleming-Archibald, Ruggiero and Grogan, 2015). It is worth considering that the action of inoculating at the beginning of casing (MC) creates a disturbance to the mycelium that would elicit regeneration of damaged hyphae, ultimately spiking hyphal activity and resulting in a greater number of fruit bodies to form. This however does not accommodate higher yields recorded in MS treatments also. This adds a layer of complexity when studying MVX in commercial crops. Even inocula associated with the same disease phenotypes (e.g. browning of caps), seemingly effects other elements of the crop such as yield.

The transcriptomic response of A15, CWH and ARP23 fruit bodies revealed highly distinct gene expression responses when grown from mycelium inoculated with MVX. Additionally, different times of MVX inoculation revealed disparate regulation of genes in each strain. More genes are upregulated in A15 when inoculated early in the crop (MS), whereas more are downregulated as inoculation occurs later (**Figure 6**). As many of the most highly upregulated genes relate to nucleic acid binding, oxidative stress response, and DNA-damage responses (**Table 3**). Additionally, A15 MS show

down-regulation of vesicle transport and multiple RNA metabolic processes (**Table_S3**). The knowledge of where MVX localises in the cells of infected mycelium and fruit bodies and how viruses move from cell to cell is lacking, but it is hypothesised that vesicles and vesicle-transport is implicated in virus movement through the discovery of virus packaging in membrane vesicles (Romaine *et al*., 1994) . The results suggest that when the mycelium is inoculated at an earlier point, A15 attempts to curtail infection through downregulation of vesicle transporting activities and gene expression. DEGS of A15 MC show similarities in terms of stress response, though additional DNA binding activities are apparent when compared to MS (**Table_S3**). This is reinforced when taking into account enrichment of biological processes. A15 MC is enriched for multiple terms related to gene expression (**Table_S3)**.

DEGs of CWH also show a lack of commonality between the two inoculation times (**Figure 6**). As no MVX-infection was found in CWH MC (**Figure 2**), CWH MS is more indicative of how CWH actively responds to pathology of MVX. Although, regulation of certain antiviral and stress-response genes in CWH MC point to evidence of prior MVX-infection which may have occurred in fruit bodies before harvesting. For example, intracellular stress is implicated through high levels of glutathione-S-transferase (GST) in CWH MS and CWH MC (**Table 4**). GST has a broad range of functions depending on the biological system and enzymatic class, but both biotic and abiotic stressors are know to induce GST genes (Nianiou-Obeidat *et al.*, 2017). Some of the highest transcript levels observed in CWH MS related to lipid metabolism and antiviral proteins. Autophagy is active in these groups, a process known for its antiviral and proviral potential (Chiramel, Brady and Bartenschlager, 2013) (**Table 1** and **Table 4**). Although, it is less likely that MVX elicits autophagy for proviral purposes, as this process is not upregulated in the more susceptible strain A15, where relatively high levels of MVX infection were observed (**Figure 2** and **Table_S2**). this points to the possibility that CWH utilizes this system as a mechanism for antiviral defence. Interestingly, downregulation of terms related to autophagy were enriched for CWH MC (**Table_S4**). If MVX-infected treatments of CWH upregulate genes related to autophagy, perhaps downregulation of these processes in CWH MC might reflect the ‘aftermath’ of MVX infection and return to cellular homeostasis in these fruit bodies. Although, further investigation is needed to reinforce this hypothesis. The phenomenon of autophagy induction is also closely tied to arrested cell growth (Neufeld, 2012). This

may help account for the loss in yield recorded in CWH MS, if autophagy was induced in multiple MVX-infected fruit bodies (**Figure 3D**).

Early MVX-inoculation (MS) elicited a considerably larger transcriptomic response in ARP23 than the later inoculation (MC), with downregulation of genes at MS dominating (**Figure 6**). Certain reoccurring patterns of upregulation of genes are evident in ARP23 MS and MC such as metalloproteinases, csbd-like and genes related to lipid metabolism (**Table 4**). Cellular component terms are enriched in the plasma membrane of ARP23 MS (**Table_S5**). A large variety or negative regulatory terms are down regulated in MS and MC of ARP23. Examples in MS include gene expression, macromolecule metabolism and biosynthesis processes and some examples in MC include RNA biosynthetic process, nucleic acid and DNA-templated transcription. However, GO enrichment analysis of DEGs reveals downregulation of terms found in MS and absent in MC that would putatively inhibit viral transport and replication, such as mRNA processing, protein maturation, vesicle-mediated transport and gene expression (**Table_S5**). Downregulation of both gene expression and inhibition of gene expression may suggest somewhat of an 'arms race' situation between virus and host in ARP23. The large amount of suppression of negative regulation of fundamental biological processes may be a consequence of ARP23 also having detectable levels of AbV6 in the tested fruit bodies (**Figure 2**).

Mycoviruses are known to promote up-regulation of host TFs for their own replication (Lee *et al.*, 2014). Upregulation of at least one known TF was documented in every strain and treatment tested here (**Table 2**). Early MVX-infection of A15 mycelia elicits the upregulation of a higher number of TFs compared to late inoculation (**Table 2**). RNA recognition motifs (RRMs) are identified in MC treatments and two genes with possible proviral activity (**Table 1**). However, more TFs were upregulated in MS treatments. The group with the highest degree of MVX infection, A15 MC, though showing upregulation of certain TFs, also downregulation of two TFs (**Table 2**). Notably, Zn_2Cys_6 was strongly downregulated in A15 MC (**Table 2**). This is contrary to CWH, where upregulation was noted in MS and even MVX-free MC fruit bodies. It is unclear if expression of Zn_2Cys_6 is being controlled by virus or host in response to MVX, but it is more significantly regulated than any other TF (**Table 2**). High frequency of TF regulation for Zn_2Cys_6 has been shown in other studies (Lee *et al.*, 2014). Upregulation of TFs in ARP23 was comparably low to the other two strains

(**Table 2**). Indeed, nine TFs were downregulated in ARP23 MS. As ARP23 MS is the only group with an AbV6-only and AbV6 and AbV16-infected fruit body, the high level of downregulation may be a consequence of AbV6 virus influence on the fruit body. The regulation of many virus-associated genes are supressed (**Table 1)**. The effect on the regulation of TFs upon MVX-infection is clear and this may indicate why infection is more extreme when inoculum is added closer to primordia formation (this work; Grogan *et al.*, 2003, 2004b; Fleming-Archibald et al., 2015). Stages of fungal morphogenesis are linked to the greatest levels of gene expression and therefore, to TFs (Riquelme *et al.*, 2018). Some work has even taken an in-depth look at the importance of a particular TF, C_2H_2 (also captured as differentially regulated upon MVX-infection in this study) and its crucial role in fruit body formation in *A. bisporus* (Pelkmans *et al.*, 2016). As MVX likely commandeers host gene expression for virus-replicative processes, later MVX-inoculations provides the mycelium of *A. bisporus* less opportunity to recognise and mount a response to MVX approaching the crucial point from the transition of vegetative growth to reproductive growth and this may account for the higher susceptibility to virus infection captured in later inoculations of infected fruit bodies. Yet overall, the genes identified in DEGs as putatively associated with viruses have a large repertoire of known and likely unknown functions to date. Therefore, the roles they play in MVX might not directly apply to defence of host or replication of virus. Rather, the regulation of these genes is important in understanding the dynamic relationship between *A. bisporus* and MVX-infection, one which warrants further investigation.

The proteomes of the five strains used in this study revealed an interesting clustering pattern with respect to the treatment of plots, where MS and MC did not cluster, except for SCC (**Figure 8B**). This hierarchical clustering suggests the proteomes of control uninfected and late MVX inoculation (of which four out of the five strains contain at least one MVX-infected replicate) are more similar than the earlier MVX-inoculation. This is may show how responsive genes are not induced as highly as those in MS treatments, reflecting the greater impact of later infections on crops and the important role played by the mycelium in terms of the fruit bodies outcome to infection. Of SSDA proteins, the greatest fold change was for a myo-inositol-1-phosphate synthase in A15 MC compared to control (log_2 3.93-fold; **Table 5**). Myo-inositol-1-phosphate synthase catalyses the biosynthesis of inositol, essential

precursors of structures integral to lipid membrane (Lohia *et al*., 1999). Many roles are attributed to inositol phosphates including cytoskeletal architecture organisation, control of membrane trafficking, regulation of gene expression and mRNA export (York *et al.*, 2001). Previous studies examined the metabolome of commercial white mushrooms upon mechanical damage-induced browning (O'Gorman *et al*., 2012). Myo-inositol was identified as one of the most important markers in post-harvest mechanical damage (O'Gorman *et* al., 2012). This may provide evidence for a correlation between the browning ensued by mechanical damage and the browning disease phenotype induced by MVX, through biosynthesis of myo-inositol. Also high in abundance in A15 MC is lectin (**Table 5**). The range of processes known for fungal lectins are unclear (Kobayashi and Kawagishi, 2014). Certain lectins are known for their defence-response roles, though characterisation of these defences is limited (Bleuler-Martinez *et al.*, 2017; Tayyrov *et al.*, 2018). SSDA of a mismatched base pair and cruciform DNA recognition protein was also detected in A15 MS (also present as a DEG of ARP23 MS). Detailed functional characterisation of this protein is limited except that it contains a Pfam domain for csbd-like (PF05532). Csbd-like protein is known in bacteria for its role in stress response (Prágai and Harwood, 2002). Abundance of ribosomal proteins is significantly lower in A15 MS and CWH MS, whereas no SSDA ribosomes are evident in MVX-inoculated ARP23 groups (**Table 5**). Viruses are well known for their capacity to recruit host ribosomes for viral protein biosynthesis and so a host response may lead to inhibition of ribosomal activity to curtail virus replication (Li, 2019). CWH MS also reveals low levels of SSDA proteins of three transcription factor/DNA binding proteins (**Table 5**). This is more evidence to the capability of CWH to repress translation of proteins that may be otherwise commandeered by MVX. The SSDA proteins in the proteomes of ARP23 MS and MC consisted of high abundance SSDAs over low abundance for an array of proteins (**Table 5**). The biological processes of these proteins vary from nucleotide binding, post-translational modifications, nuclear exportation activities, transcription and carbohydrate metabolism (**Table 5**).

The compost of A15 control, MS and MC plots were harvested to assess the proteomic response in the vegetative mycelium to MVX. In contrast to A15 fruit bodies, MVX resulted in greater numbers of heightened abundance SSDA proteins over low abundance SSDA proteins (**Table_S9**). As one would expect, very minimal overlap was apparent between MVX-infected fruit-bodies and vegetative mycelium (**Figure_S4**).

However, MC proteomes of fruit bodies and mycelium shared four proteins relating to DNA binding, translation, a multi-functional protein and an *A. bisporus* specific protein (**Figure_S4**). The major biological processes of carbohydrate metabolism and genetic information processing are found in the greatest number of proteins in response to MVX, particularly in the later MC inoculation (**Figure 9**). Signalling and cellular processing are also more highly represented during MVX infection (**Figure 9)**. Overall, no distinct viral-defence or stress-response was noted in the mycelium from compost. Rather, upregulation of multiple metabolic processes was noted (**Figure 8**). This was greater in the MS infection, which may suggest the more established MVX-infected compost spikes metabolic activity and energy acquisition. Whether this is mechanistically introduced by MVX or pre-empted defence strategy to heighten vigour as fruit bodies rapidly grow from the mycelium network is unknown. As the compost was harvested at the time of first flush and given the fruit bodies tested from these plots were positive for AbV16, the molecular activities of the vegetative mycelium would not reflect effective antiviral strategy. Additionally, ERAD pathways (normally attributed to protein misfolding) and ER stress was enriched in A15 MS fruit bodies (**Figure 8**). Viruses are known to both cause ER stress during infection via synthesis of viral proteins and also intentionally trigger or manipulate ER stress response for their own replication (He, 2006). Certain ss(+)RNA are also known for forming viral replication organelles by physically manipulating the ER (Paul, 2013; Romero-Brey and Bartenschlager, 2016). A similar pattern is observed when comparisons of A15 MC mycelium are made against A15 MC fruit bodies, where upregulation is only indicative of heightened metabolism and fruit bodies are enriched in terms relating to protein repair, protein repair and oxidative stress (**Figure 8**). MVX is causing intracellular stresses to A15 fruit bodies but not in the mycelium. Virus transcripts have been documented as being as high as 4,000-fold in brown symptomatic mushrooms (Eastwood *et al.*, 2015). The viral titre in the mycelium in compared to symptomatic brown mushrooms may explain the difference in response between these two phases.

RNA silencing/interference (RNAi) components and yeast SuperKiller (SKI) components have been identified in the genome of *A. bisporus* (Morin *et al.*, 2012). This processes have been implicated ias antiviral defences in fungi (Son, Yu and Kim, 2015). These systems were not been previously identified in the defensive response to MVX, contrarily, RNAi suppression was induced in MVX-infected fruit bodies (Deakin

et al., 2015). This study also suggests these systems are not adopted in response to MVX.

5. Conclusion

This work has demonstrated that a variety of strains of *A. bisporus* can become infected by the causal virus for brown cap disease phenotypes through early interaction/anastomosis with MVX-infected mycelium. Infection impacts fruit bodies by altering yields, producing abnormal phenotypes and causing a browning to occur. AbV16 is detected at different frequencies in fruit bodies depending on strain susceptibility and the timing of inoculation, where introducing MVX closer to primordia formation (pinning) results in more disease. MVX induces distinct transcriptomic and proteomic response between strains and point of inoculation. A15 is most susceptible to infection, likely due to the vegetative compatibility of sources of MVX. This is reflected in cellular stress responses, notably ER stress, manipulation of TF regulated gene expression and putative mechanical damage via myo-inositol biosynthesis. Proteomes of MVX-infected compost of A15 did not reveal any defensive strategy, rather heightened activity in a variety of biological processes. CWH fruit bodies are less susceptible to MVX and demonstrated a variety of antiviral activity when AbV16 was detected, including high levels of ribonucleases, antiviral proteins, stress responses and autophagy. CWH fruit bodies testing negative for MVX still showed evidence of viral activity (though much less than infected individual), possibly indicating eradication of viruses over the prevention of initial entry from the mycelium. ARP23, though almost as unsusceptible to MVX as CWH, mounted an entirely different transcriptomic and proteomic response. This could be due in part to detectable levels of AbV6 in ARP23 fruit bodies. Antiviral strategies of this strain amounted to downregulation of a plethora of processes, namely gene expression.

This work is the first to detail the host response from fruit bodies of a variety of *A. bisporus* strains to MVX-inoculation. This work will add to our understanding of the how MVX impacts the fruit bodies of *A. bisporus* and the processes mounted by host and induced by pathogen.

Literature Cited

Almagro Armenteros, J. J. *et al.* (2019) 'SignalP 5.0 improves signal peptide predictions using deep neural networks', *Nature Biotechnology*, 37(4), pp. 420–423.

Altschul, S. F. *et al.* (1997) 'Gapped BLAST and PSI-BLAST: A new generation of protein database search programs', *Nucleic Acids Research*, pp. 3389–3402.

Ambrosone, A. *et al.* (2012) 'Beyond transcription: RNA-binding proteins as emerging regulators of plant response to environmental constraints', *Plant Science*, 182, pp. 12–18.

Bleuler-Martinez, S. *et al.* (2017) 'Dimerization of the fungal defense lectin CCL2 is essential for its toxicity against nematodes.', *Glycobiology*, 27(5), pp. 486–500.

van den Brink, J. and de Vries, R. P. (2011) 'Fungal enzyme sets for plant polysaccharide degradation', *Applied Microbiology and Biotechnology*, 91(6), pp. 1477–1492.

Brusini, J. and Robin, C. (2013) 'Mycovirus transmission revisited by in situ pairings of vegetatively incompatible isolates of Cryphonectria parasitica', *Journal of Virological Methods*, 187(2), pp. 435–442.

Burton, K. *et al.* (2011) 'Mushroom Virus X – the Identification of Brown Cap Mushroom Virus and a New Highly Sensitive Diagnostic Test for Phase Iii Compost', *Proceedings of the 7th International Conference on Mushroom Biology and Mushroom Products*, pp. 466–473.

Chiramel, A., Brady, N. and Bartenschlager, R. (2013) 'Divergent Roles of Autophagy in Virus Infection', *Cells*, 2(1), pp. 83–104.

Cho, W. *et al.* (2012) 'Genome-wide expression profiling shows transcriptional reprogramming in Fusarium graminearum by Fusarium graminearum virus 1-DK21 infection', *BMC Genomics*, 13(1), p. 173.

Chu, Y.-M. *et al.* (2002) 'Double-Stranded RNA Mycovirus from Fusarium graminearum', *Applied and Environmental Microbiology*, 68(5), pp. 2529–2534.

Conesa, A. *et al.* (2005) 'Blast2GO: a universal tool for annotation, visualization and analysis in functional genomics research', *Bioinformatics*, 21(18), pp. 3674–3676.

Cox, J. and Mann, M. (2008) 'MaxQuant enables high peptide identification rates, individualized p.p.b.-range mass accuracies and proteome-wide protein quantification', *Nature Biotechnology*, 26(12), pp. 1367–1372.

Day, I. S. *et al.* (2002) 'Analysis of EF-hand-containing proteins in Arabidopsis.', *Genome biology*, 3(10), p. RESEARCH0056.

Deakin, G. *et al.* (2017) 'Multiple viral infections in Agaricus bisporus - Characterisation of 18 unique RNA viruses and 8 ORFans identified by deep sequencing', *Scientific Reports*, 7(1), p. 2469.

Deakin G, 2015. Understanding the Biology of Mushroom Virus X by Molecular Characterisation of Viral RNAs and their Role in Disease Epidemiology. PhD dissertation, East Malling Research.

van Diepeningen, A. D., Debets, A. J. M. and Hoekstra, R. F. (1998) 'Intra- and Interspecies

Virus Transfer in Aspergilli via Protoplast Fusion', *Fungal Genetics and Biology*, 25(3), pp. 171–180..

E, X. and Kowalik, T. (2014) 'The DNA Damage Response Induced by Infection with Human Cytomegalovirus and Other Viruses', *Viruses*, 6(5), pp. 2155–2185.

Eastwood, D. *et al.* (2015) 'Viral Agents Causing Brown Cap Mushroom Disease of Agaricus bisporus', *Applied and Environmental Microbiology*, 81(20), pp. 7125–7134.

Fleming-Archibald, C., Ruggiero, A. and Grogan, H. M. (2015) 'Brown mushroom symptom expression following infection of an Agaricus bisporus crop with MVX associated dsRNAs', *Fungal Biology*, 119(12), pp. 1237–1245.

Franke, E. K., Yuan, H. E. H. and Luban, J. (1994) 'Specific incorporation of cyclophilin A into HIV-1 virions', *Nature*, 372(6504), pp. 359–362.

Gotz, S. *et al.* (2008) 'High-throughput functional annotation and data mining with the Blast2GO suite', *Nucleic Acids Research*, 36(10), pp. 3420–3435.

Grogan, H. M. *et al.* (2003) 'Double-stranded RNA elements associated with the MVX disease of Agaricus bisporus', *Mycological Research*, 107(2), pp. 147–154.

Grogan, H. M. *et al.* (2004a) 'Transmission of Mushroom Virus X Disease in crops', *Mushroom Science XVI - Science and Cultivation of Edible Medicinal Fungi (eds Romaine, C. P., Keil, C. B., Rinker, D. J. & Royse, D. J.)*, pp. 489–498.

Grogan, H. M. *et al.* (2004b) 'Transmission of Mushroom Virus X Disease in crops', *Mushroom Science*, 16, pp. 489–498.

He, B. (2006) 'Viruses, endoplasmic reticulum stress, and interferon responses', *Cell Death & Differentiation*, 13(3), pp. 393–403.

Huang, H. *et al.* (2015) 'Bulk RNA degradation by nitrogen starvation-induced autophagy in yeast', *The EMBO Journal*, 34(2), pp. 154–168.

Jones, P. *et al.* (2014) 'InterProScan 5: genome-scale protein function classification', *Bioinformatics*, 30(9), pp. 1236–1240.

Kanehisa, M., Sato, Y. and Morishima, K. (2016) 'BlastKOALA and GhostKOALA: KEGG Tools for Functional Characterization of Genome and Metagenome Sequences', *Journal of Molecular Biology*, 428(4), pp. 726–731.

Kashif, M. *et al.* (2019) 'Alphapartitiviruses of Heterobasidion Wood Decay Fungi Affect Each Other's Transmission and Host Growth.', *Frontiers in cellular and infection microbiology*, 9, p. 64.

Kim, D., Langmead, B. and Salzberg, S. L. (2015) 'HISAT: a fast spliced aligner with low memory requirements.', *Nature methods*, 12(4), pp. 357–60. doi: 10.1038/nmeth.3317.

Kim, J.-M. *et al.* (2013) 'Occurrence of dsRNA Mycovirus (LeV-FMRI0339) in the Edible Mushroom Lentinula edodes and Meiotic Stability of LeV-FMRI0339 among Monokaryotic Progeny', *The Plant Pathology Journal*, 29(4), pp. 460–464.

Kim, S.-W. *et al.* (2008) 'Detection of the mycovirus OMSV in the edible mushroom, Pleurotus ostreatus, using an SPR biosensor chip', *Journal of Virological Methods*, 148(1–2), pp. 120–124.

Kobayashi, Y. and Kawagishi, H. (2014) 'Fungal Lectins: A Growing Family', in *Methods in Molecular Biology*, pp. 15–38.

Lee, K.-M. *et al.* (2014) 'A comparison of transcriptional patterns and mycological phenotypes following infection of Fusarium graminearum by four mycoviruses.', *PloS one*. Edited by J.-H. Yu, 9(6), p. e100989.

Levine, B. (2005) 'Eating Oneself and Uninvited Guests', *Cell*, 120(2), pp. 159–162.

Li, S. (2019) 'Regulation of Ribosomal Proteins on Viral Infection', *Cells*, 8(5), p. 508.

Lohia, A., C. Hait, N. and Lahiri Majumder, A. (1999) 'l-myo-Inositol 1-phosphate synthase from Entamoeba histolytica', *Molecular and Biochemical Parasitology*, 98(1), pp. 67–79.

Lorković, Z. J. (2009) 'Role of plant RNA-binding proteins in development, stress response and genome organization', *Trends in Plant Science*, 14(4), pp. 229–236.

Love, M. I., Huber, W. and Anders, S. (2014) 'Moderated estimation of fold change and dispersion for RNA-seq data with DESeq2.', *Genome biology*, 15(12), p. 550.

Luftig, M. A. (2014) 'Viruses and the DNA Damage Response: Activation and Antagonism', *Annual Review of Virology*, 1(1), pp. 605–625.

Luhtala, N. and Parker, R. (2010) 'T2 Family ribonucleases: ancient enzymes with diverse roles', *Trends in Biochemical Sciences*, 35(5), pp. 253–259.

Luo, M. R. (2015) 'CIELAB', in *Encyclopedia of Color Science and Technology*. Berlin, Heidelberg: Springer Berlin Heidelberg, pp. 1–7.

Magae, Y. (2012) 'Molecular characterization of a novel mycovirus in the cultivated mushroom, Lentinula edodes', *Virology Journal*, 9(1), p. 60.

Magae, Y. and Sunagawa, M. (2010) 'Characterization of a mycovirus associated with the brown discoloration of edible mushroom, Flammulina velutipes', *Virology Journal*, 7(1), p. 342.

Maris, C., Dominguez, C. and Allain, F. H. T. (2005) 'The RNA recognition motif, a plastic RNA-binding platform to regulate post-transcriptional gene expression', *FEBS Journal*, 272(9), pp. 2118–2131.

Martin, M. (2011) 'Cutadapt removes adapter sequences from high-throughput sequencing reads', *EMBnet.journal*, 17(1), p. 10.

Moelling, K. *et al.* (2017) 'RNase H As Gene Modifier, Driver of Evolution and Antiviral Defense.', *Frontiers in microbiology*, 8, p. 1745.

Morin, E. *et al.* (2012) 'Genome sequence of the button mushroom Agaricus bisporus reveals mechanisms governing adaptation to a humic-rich ecological niche', *Proceedings of the National Academy of Sciences*, 109(43), pp. 17501–17506. d

Musidlak, O., Nawrot, R. and Goździcka-Józefiak, A. (2017) 'Which Plant Proteins Are Involved in Antiviral Defense? Review on In Vivo and In Vitro Activities of Selected Plant Proteins against Viruses', *International Journal of Molecular Sciences*, 18(11), p. 2300.

Neufeld, T. P. (2012) 'Autophagy and cell growth - the yin and yang of nutrient responses',

Journal of Cell Science, 125(10), pp. 2359–2368.

Nianiou-Obeidat, I. *et al.* (2017) 'Plant glutathione transferase-mediated stress tolerance: functions and biotechnological applications', *Plant Cell Reports*, 36(6), pp. 791–805.

Nuss, D. L. (2005) 'Hypovirulence: Mycoviruses at the fungal–plant interface', *Nature Reviews Microbiology*, 3(8), pp. 632–642.

O'Connor, E. *et al.* (2019) 'Whole Genome Sequence of the Commercially Relevant Mushroom Strain Agaricus bisporus var. bisporus ARP23.', *G3 (Bethesda, Md.)*, p. g3.400563.2019.

O'Gorman, A., Barry-Ryan, C. and Frias, J. M. (2012) 'Evaluation and identification of markers of damage in mushrooms (Agaricus bisporus) postharvest using a GC/MS metabolic profiling approach', *Metabolomics*, 8(1), pp. 120–132.

Ogata, H. *et al.* (1999) 'KEGG: Kyoto Encyclopedia of Genes and Genomes', *Nucleic Acids Research*, 27(1), pp. 29–34.

Owens, R. A. *et al.* (2015) 'Interplay between Gliotoxin Resistance, Secretion, and the Methyl/Methionine Cycle in Aspergillus fumigatus', *Eukaryotic Cell*, 14(9), pp. 941–957.

Patro, R. *et al.* (2017) 'Salmon provides fast and bias-aware quantification of transcript expression', *Nature Methods*, 14(4), pp. 417–419.

Paul, D. (2013) 'Architecture and biogenesis of plus-strand RNA virus replication factories', *World Journal of Virology*, 2(2), p. 32.

PEARSON, M. N. *et al.* (2009) 'Mycoviruses of filamentous fungi and their relevance to plant pathology', *Molecular Plant Pathology*, 10(1), pp. 115–128.

Pelkmans, J. F. *et al.* (2016) 'The transcriptional regulator c2h2 accelerates mushroom formation in Agaricus bisporus', *Applied Microbiology and Biotechnology*, 100(16), pp. 7151–7159.

Prágai, Z. and Harwood, C. R. (2002) 'Regulatory interactions between the Pho and σB-dependent general stress regulons of Bacillus subtilis', *Microbiology*, 148(5), pp. 1593–1602.

Racaniello, V. R. *et al.* (2015) *Principles of Virology, Bundle, Principles of Virology, Bundle*. American Society of Microbiology.

Riquelme, M. *et al.* (2018) 'Fungal Morphogenesis, from the Polarized Growth of Hyphae to Complex Reproduction and Infection Structures', *Microbiology and Molecular Biology Reviews*, 82(2).

Romaine, C. P., Schlagnhaufer, B. and Goodin, M. M. (1994) 'Vesicle-associated double-stranded ribonucleic acid genetic elements in Agaricus bisporus', *Current Genetics*, 25(2), pp. 128–134.

Romaine, C. P., Ulhrich, P. and Schlagnhaufer, B. (1993) 'Transmission of La France Isometric Virus during Basidiosporogenesis in Agaricus bisporus', *Mycologia*, 85(2), p. 175.

Romero-Brey, I. and Bartenschlager, R. (2016) 'Endoplasmic Reticulum: The Favorite Intracellular Niche for Viral Replication and Assembly', *Viruses*, 8(6), p. 160.

Schiene, C. *et al.* (1998) 'Mapping the stereospecificity of peptidyl prolyl cis/trans isomerases', *FEBS Letters*, 432(3), pp. 202–206.

Shah Mahmud, R. and Ilinskaya, O. N. (2013) 'Antiviral Activity of Binase against the Pandemic Influenza A (H1N1) Virus.', *Acta naturae*, 5(4), pp. 44–51.

Sherry, B. *et al.* (1998) 'Role of cyclophilin A in the uptake of HIV-1 by macrophages and T lymphocytes', *Proceedings of the National Academy of Sciences*, 95(4), pp. 1758–1763.

Son, H. *et al.* (2011) 'A Phenome-Based Functional Analysis of Transcription Factors in the Cereal Head Blight Fungus, Fusarium graminearum', *PLoS Pathogens*. Edited by J.-R. Xu, 7(10), p. e1002310.

Son, M., Yu, J. and Kim, K.-H. (2015) 'Five Questions about Mycoviruses', *PLOS Pathogens*. Edited by J. Heitman, 11(11), p. e1005172.

Sonnenberg, A. S. M. *et al.* (2017) 'Developments in breeding of Agaricus bisporus var. bisporus: progress made and technical and legal hurdles to take', *Applied Microbiology and Biotechnology*, 101(5), pp. 1819–1829.

Suzuki, N. *et al.* (2018) 'ICTV Virus Taxonomy Profile: Hypoviridae', *Journal of General Virology*, 99(5), pp. 615–616.

T. Fletcher, J. and H. Gaze, R. (2007) *Mushroom Pest and Disease Control*, *Mycological Research*. CRC Press.

Tayyrov, A. *et al.* (2018) 'Toxicity of Potential Fungal Defense Proteins towards the Fungivorous Nematodes Aphelenchus avenae and Bursaphelenchus okinawaensis', *Applied and Environmental Microbiology*. Edited by H. L. Drake, 84(23).

Thali, M. *et al.* (1994) 'Functional association of cyclophilin A with HIV-1 virions', *Nature*, 372(6504), pp. 363–365.

Tyanova, S. *et al.* (2016) 'The Perseus computational platform for comprehensive analysis of (prote)omics data', *Nature Methods*, 13(9), pp. 731–740.

Wang, L. *et al.* (2018) 'De novo transcriptomic assembly and mRNA expression patterns of Botryosphaeria dothidea infection with mycoviruses chrysovirus 1 (BdCV1) and partitivirus 1 (BdPV1)', *Virology Journal*, 15(1), p. 126.

Weitzman, M. D. and Fradet-Turcotte, A. (2018) 'Virus DNA Replication and the Host DNA Damage Response', *Annual Review of Virology*, 5(1), pp. 141–164.

Wileman, T. (2013) 'Autophagy as a defence against intracellular pathogens', *Essays In Biochemistry*, 55, pp. 153–163.

Woloshen, V., Huang, S. and Li, X. (2011) 'RNA-Binding Proteins in Plant Immunity', *Journal of Pathogens*, 2011, pp. 1–11.

Xie, J. and Jiang, D. (2014) 'New Insights into Mycoviruses and Exploration for the Biological Control of Crop Fungal Diseases', *Annual Review of Phytopathology*, 52(1), pp. 45–68.

York, J. D. *et al.* (2001) 'An expanded view of inositol signaling', *Advances in Enzyme Regulation*, 41(1), pp. 57–71.

Yu, X. *et al.* (2010) 'A geminivirus-related DNA mycovirus that confers hypovirulence to a

plant pathogenic fungus', *Proceedings of the National Academy of Sciences*, 107(18), pp. 8387–8392.

Chapter 5:

FISHing in fungi: Visualisation of mushroom virus X in the mycelium of *Agaricus bisporus* by fluorescence *in situ* hybridisation

5.0 FISHing in fungi: Visualisation of mushroom virus X in the mycelium of *Agaricus bisporus* by fluorescence *in situ* hybridisation

Eoin O'Connor[1,3], Christopher J. Coates[2], Dan C. Eastwood[2], David A. Fitzpatrick[1,4] & Helen Grogan[3]

[1] Department of Biology, Maynooth University, Maynooth, Co. Kildare, Ireland

[2] School of Biosciences, Swansea University, Swansea, United Kingdom

[3] Horticulture Development Department, Teagasc Food Research Centre, Ashtown, Dublin 15, D15 KN3K, Ireland

[4] Kathleen Lonsdale Institute for Human Health Research, Maynooth University, Maynooth, Co. Kildare, Ireland

This paper was accepted for publication in the Journal of Microbiological Methods (April 2020)

Citation:

O'Connor, E., Coates, C.J., Eastwood, D.C., Fitzpatrick, D.A. and Grogan, H., 2020. FISHing in fungi: Visualisation of mushroom virus X in the mycelium of *Agaricus bisporus* by fluorescence *in situ* hybridisation. *Journal of Microbiological Methods*, p.105913.

Keywords: *Agaricus bisporus,* fluorescence *in situ* hybridisation, FISH, mushroom virus X, MVX, mycovirology, mycovirus

Abstract

Agaricus bisporus is a commercial mushroom crop susceptible to a disease caused by a complex of viruses known collectively as mushroom virus X (MVX). Symptoms of MVX include bare patches and mushroom cap discolouration (browning) in the fruiting bodies, phenotypes associated with the viruses AbV6 and AbV16, respectively. Limited understanding exists of the localisation and mobilisation of these viruses within the mycelium of *A. bisporus*. To this end, a non-destructive fluorescence *in situ* hybridisation (FISH) method was developed for *in situ* targeting of AbV6 and AbV16 in *A. bisporus* mycelium. An MVX strain associated with the bare patch disease phenotype revealed predominantly high signal towards the growing edges of cultures when probed for AbV6, with a 'halo-effect' of high signal intensity around putative vacuoles. An MVX strain associated with the browning disease phenotype showed high signal intensities within reticulating networks of hyphae in a highly compartmentalised manner when probed for AbV16. Localisation of the two viruses in MVX-infected cultures appears independent, as both viruses were found in completely discrete areas of the mycelium in differential patterns. FISH detected low level presence of the two viruses, AbV6 and AbV16 in a number of cultures which had tested negative for the viruses by RT-PCR. This suggests that FISH may be more sensitive at detecting viruses at low levels than molecular methods. This study demonstrates that FISH is a powerful tool in the field of mycovirology.

5.1 Introduction

Fluorescence *in situ* hybridisation (FISH) is a method for the hybridisation of targeted nucleic acid sequences using bespoke fluorophore-conjugated nucleic acid probes. A technique developed in the 1980's, the initial intricacies of the technique led to its use being considered challenging and difficult. Innovations in subsequent years have resulted in FISH becoming a more accessible method, with a wide breadth of applications (Huber et al., 2018), with cytogenics arguably reaping the greatest degree in advances (Jiang, 2019).

FISH is a powerful tool in microbiology. For example, it has been used in the detection of community structures in biofilms (Almeida et al., 2011; Aoi, 2002), aquatic microbiome sampling (Dawson et al., 2012; Kurisu et al., 2015; Medlin and Orozco, 2017), cultural heritage conservation (La Cono and Urzì, 2003; Urzì and De Leo, 2001), in clinical samples of blood sera (Da Silva et al., 2015) and many other uses. FISH has been used for the localisation of bacteria, fungi and viruses within respective hosts (reviewed in (Kliot and Ghanim, 2016)). The first use of FISH targeting fungi was in the yeast-like fungus *Aureobasidium pullulans* (Li et al., 1997). The greatest hurdle in applications of FISH in localisation studies is commonly the issue of probe penetration (Kliot and Ghanim, 2016). This is particularly relevant to fungi, as the fungal cell wall is a complex structure of hydrophobic scaffolds of α-1,3-glucan and chitin encased in layers of convoluted linkages of β-glucans, glycoproteins and α-1,3-glucan (Kang et al., 2018). The lack of or complete absence of permeability of the fungal cell wall, can act as a barrier to probe penetration (Brul et al., 1997; Teertstra et al., 2004). Due to the hydrophobicity and varying degrees of negative charge observed in the fungal cell walls (Free, 2013), non-charged semi-synthetic hybridisation probe alternates may be used, known as peptide nucleic acid (PNA) probes (Nielsen and Egholm, 1999). PNA probes have seen many uses of FISH in fungi (Da Silva et al., 2015; Ferreira et al., 2017; Nakada et al., 2013; Reller et al., 2007; Teertstra et al., 2004). Although, PNA probes are expensive and their use can be highly cost prohibitive. The process or permeabilising the cells of fixed fungal mycelium, without destructive proteases and chitinases, is an effective way of allowing access of DNA probes to their targets and minimizing the dependency on use of PNA technology (Villa et al., 2009).

To date, mycovirology has yet to fully harness the application of FISH. A single study probed a DNA mycovirus in the mycelium of *Sclerotinia sclerotiorum*, but this was achieved using methods incorporating lytic enzymes (which were avoided in this study) and the resolution of nucleus fluorescence and probed virus fluorescence was limited (Yu et al., 2013).

In this study, the technique of FISH was applied for the investigation of two viruses in the mushroom virus X (MVX) complex. The application of FISH was used to assess whether both viruses could be probed for their detection and for the understanding of their spatial distributions within the mycelium of *A. bisporus*. The targets were AbV6 and AbV16, which are multipartite and bipartite viruses, respectively (Deakin et al., 2017). As such, the probes designed specifically targeted AbV16 RNA 1(^{MVX} 1.8 kbp) and AbV6 RNA 2 (^{MVX} 3.6 kbp) (Grogan et al., 2003). AbV16 RNA 1 is causal for the brown disease phenotype, and present particularly in MVX-infected crops in Ireland (Eastwood et al., 2015; Fleming-Archibald et al., 2015; Grogan et al., 2003). AbV6 was associated with the bare patch disease phenotype, prevalent in diseased crops in the UK in some of the earliest reports of MVX (Grogan et al., 2003) although a definitive correlation with symptoms has not been established. It has been detected in high abundance in AbV16 infected crops with no bare patch symptoms (unpublished data). Low levels were also reported in a 'non-diseased commercial culture' (Deakin et al., 2017). The work reported here involves an adapted method of FISH, whereby *A. bisporus* cultures (with and without MVX viruses) are grown, permeabilised, hybridised and visualised *in situ*, so as to negate any disturbance to the mycelium. This technique uses non-destructive permeabilization methods (Villa et al., 2009) which allow the use of DNA probes, making the method cost-effective and reproducible. This is the first robust application of FISH on mycoviruses within the mycelium of a fungal host.

5.2 Methods

5.2.1 Strains and culture conditions

MVX-infected *A. bisporus* cultures MVX-1283, MVX-2735, and MVX-1153 were derived from mushroom samples that were taken from symptomatic crops in the UK and Ireland between 2000- and 2016 (**Table 1**). Presence of AbV16 RNA 1 was confirmed by RT-PCR according to (Fleming-Archibald et al., 2015). Presence of AbV6 RNA 2 was confirmed using the same methodology, and PCR primers designed specifically for AbV6 RNA 2 (F: GGCAGGAGCAGATGAACATT R: ACCTGGAACAGCAGCAAAAC; product size 305 bp; Fleming-Archibald, unpublished) based on the published sequence (Genbank KY357490). MVX cultures were retrieved from liquid nitrogen storage and grown on complete yeast medium (CYM) containing 2 g proteose peptone, 2 g yeast extract, 20 g glucose, 0.5 g $MgSO_4$, 0.46 g KH_2PO_4, 1 g K_2HPO_4, 10 g agar in 500 ml dH_20. Cultures were incubated at 25°C for two weeks, in the dark prior to use. A commercial strain of *A. bisporus* (Sylvan A15; www.sylvaninc.com) was used as a non-MVX control strain in this study. A culture was derived from a spawn grain, taken from a new bag of commercial spawn and grown on CYM and incubated at 25°C for two weeks, in the dark prior to use.

Table 1. Information on the *A. bisporus* strains used for FISH. MVX cultures were derived from mushrooms collected at different locations from crops displaying MVX symptoms and which were shown to contain AbV6 or AbV16 at the time of collection. The results of RT-PCR tests (+ = positive; - = negative) on the cultures used in these studies in 2017 are also shown.

***A. bisporus* Strain**	**Disease Phenotype**	**MVX in original culture**	**Year Collected**	**Country of origin**	**RT-PCR 2017 AbV6**	**RT-PCR 2017 AbV16**
MVX-1283	Bare patches on crop bed	AbV6	2000	UK	+	-
MVX-2735*	Brown caps	AbV16	2002	Ireland	-	-
MVX-1153	Brown caps	AbV16	2016	Ireland	-	+
Non-MVX (A15)	None (control)	None	2017	France	-	-

* MVX 2735 had originally contained AbV16 and had originally tested positive by RT-PCR but in recent years the culture is frequently negative by RT-PCR for AbV16

5.2.2 Slide culture preparations

Microscope slides (75 mm × 25 mm) were sterilised by autoclaving. To obtain a thin solid layer of medium, 600 µl of molten CYM was carefully pipetted to the centre of a microscope slide and immediately covered by another microscope slide. The medium was left to solidify for 1 min and the slide placed on top was carefully separated and removed with sterile forceps. The slide with the adhered CYM layer was added to a Petri dish containing a sterile, dH_2O-moistened filter paper to act as a humidity chamber (**Figure 1A**). Agar plugs of *A. bisporus* cultures were placed on top of the thin, flat layer of solid media and incubated at 25°C for one week, in the dark. CYM was considered a suitable medium to use in this study as it is commonly used to cultivate *A. bisporus* mycelium *in vitro* (De La Bastide et al., 1997; Kaur et al., 2011; Li et al., 1994; Masoumi et al., 2015) . Control steps were taken to ensure CYM did not harbour problematic levels of nascent autofluorescence that would impede fluorescence observations (data not shown).

5.2.3 Fixation, permeabilisation and hybridisation of DNA probes

Slide cultures of *A. bisporus* were fixed for 1 h on ice with freshly prepared 4% formaldehyde in PBS, pH 7.4. The agar plugs were gently removed with sterile forceps, leaving a flat layer of hyphae on the medium. Cultures were washed twice in PBS and then dehydrated by submerging in 50% ethanol (v/v) and stored overnight at -20°C. Cultures were rinsed once and submerged in PBS for 20 min then washed in pre-hybridisation wash buffer (0.5% Tween-20, 0.2% BSA in PBS) for 1 h 30 min followed by thorough rinsing in dH_2O. Permeabilisation of hyphae was carried out by soaking in permeabilisation buffer (1% Triton X-100 in 0.05 M Tris-HCl, 0.04 M EDTA, 0.1 M β-mercaptoethanol) at 30°C for 30 min and at 40°C for an additional 15 min (Villa et al., 2009). Osmotic pressure was applied through submerging cultures in glycerol solution (31.75 ml glycerol (Sigma-Aldrich) and 68.25 ml dH_2O) on ice (**Figure 1B**) for 30 min (Villa et al., 2009). Dry filter paper was dabbed near the edges of cultures to facilitate the removal of permeabilising agents and allowed to air-dry, briefly. Hybridisation buffer (0.9 M NaCl, 0.02 M tris-HCl pH 7.2, 0.01% w/v SDS, 20% v/v deionised

formamide, 50 ng/µl DNA probe and 1 mg/ml 1× RNase-free BSA) was pre-warmed and 20 µl slowly added to the surface of hyphae. A HybriSlip™ (22 mm × 22 mm; Sigma-Aldrich) was placed over the hybridisation buffer carefully to avoid bubbles forming in the culture/cover slip interface. Latex glue was applied around the entire circumference of the HybriSlip to seal in the hybridisation buffer (**Figure 1C**). Cultures were added to a hybridisation chamber (high humidity) and incubated at 52.8°C for 14 h in the dark. The hybridisation chamber was allowed to cool to room temperature over 5 min before proceeding further. Latex glue and cover slip were carefully removed and cultures were rinsed with dH_2O. Cultures were washed by submerging slides in post-hybridisation wash buffer (0.2 M NaCl, 0.02 M tris-HCl pH 7.2, 0.01% w/v SDS) at 47°C for 20 min on a rocking platform. Cultures were further rinsed in dH_2O and air-dried for 5 min. 15 µl of Vectashield Mounting Medium containing 4',6-diamidino-2-phenylindole (DAPI) stain (Vector Labs, Burlingame, CA, USA) was added to cultures and incubated at 4°C for 30 min, in the dark. ssRNA target specificity of hybridisation was assessed by flushing cultures with and without the presence of RNase cocktails, as detailed in previous work (Teertstra et al., 2004). RNase-treated slides functioned as negative controls.

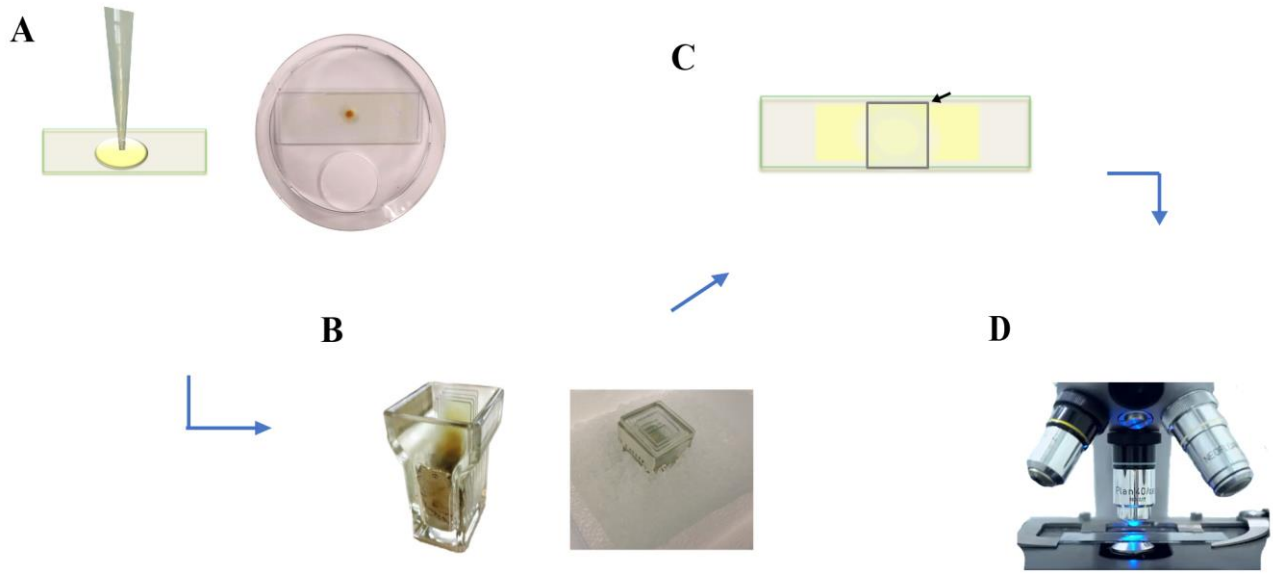

Figure 1: Schematic of the MVX-FISH workflow. (**A-D**) Represents the order of the main aspects of the method. **A: Slide cultures**. A slide is coated in CYM by pipetting, then it is added to a petri dish containing a moist filter paper to facilitate humid environment. An agar plug colonised with *A. bisporus* hyphae is added to the slide. **B: Pre-treatments.** Coplin jars are used to submerge cultures in solutions for fixation, washing and permeabilisation. Jars can be imbedded in ice, heated and agitated when necessary. **C: Hybridisation**. For hybridisation, a cover slip (black arrow) is glued over the preparation with a latex glue. **D: Visualisation**. A fluorescence microscope is used to visualise cultures on the same slide used from **A**.

5.2.4 MVX FISH probes

FISH probes were made by designing oligonucleotide DNA probes (Eurofins Genomics, Ebersberg, Germany) complementary to the sequences of AbV16 RNA 1 and AbV6 RNA 2 (Deakin et al., 2017). The two FISH probes (5'-TGTTATGTGGGTGTAGTTAG-3' for AbV16 RNA 1, designed from GenBank accession: KY357502.1 and 5'-TGTCAGGTGTTCAACCAGC-3' for AbV6 RNA 2, designed from GenBank accession: KY357490.1) were 5'-end fluorescein

isothiocyanate (FITC) labelled (Eurofins Genomics, Ebersberg, Germany). At the concentrations used, the DNA probes for AbV16 RNA 1 and AbV6 RNA 2 had a Tm of 52.4°C and 62.5°C, respectively.

5.2.5 Fluorescence microscopy

Fluorescein and UV fluorescence were monitored using a FITC and DAPI filter set, respectively. Fluorescence light microscopy was conducted with an Olympus BX43 system microscope coupled with a CoolLED pE-300 Illuminator. Images were capture by an Olympus SZX16 camera mounted on the microscope, connected to a computer.

5.3 Results

5.3.1 Permeabilisation of *A. bisporus* hyphae and FISH controls

Permeabilisation was necessary to facilitate FISH probe penetration of fungal cell walls. Porousness of cells was achieved using the nuclear stain DAPI (**Figure 2**). DAPI was added to every culture preparation as quality control to reduce the likelihood of false negatives i.e. where no fluorescent signal is a result of inefficient cell permeabilisation and not the absence of the target virus. Additionally, RNase-cocktails were used to introduce negative controls. Specificity of probes to bind to target RNA was evaluated by flushing permeabilised hyphae with RNase, which can be confirmed by a loss in signal due to the destruction of virus RNA (**Figure_S1**). Non-specific binding of DNA probes and nuclei can occur by affinities of probe nucleotide sequences to chromosomal regions. To ensure DNA probes were not non-specifically binding to nuclei within cells, DAPI stain fluorescence was compared to FITC fluorescence to ensure no superimposable signal intensity was captured (**Figure_S2**). These measures provide confidence that the observed fluorescence is as a result of the hybridisation of the probes to viruses within the mycelium.

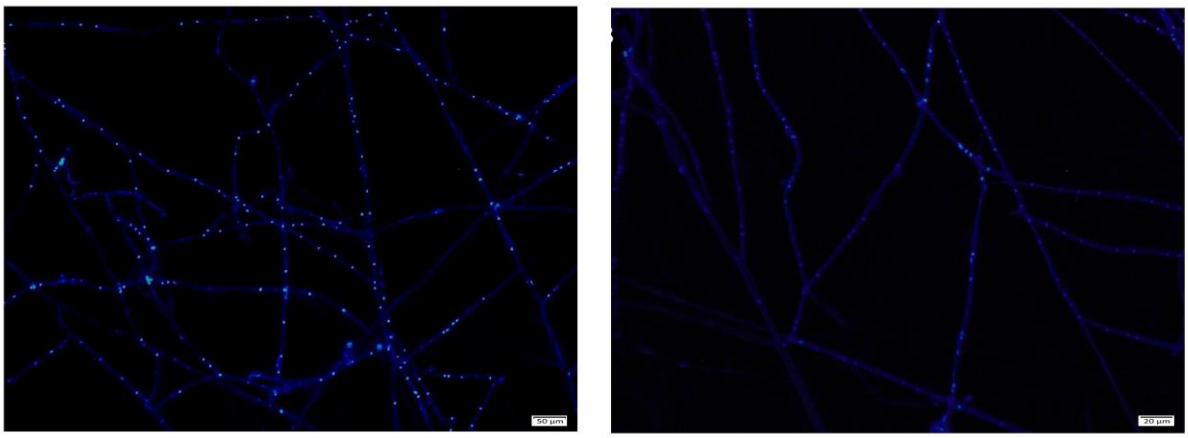

Figure 2: **Assessment of permeabilisation of hyphae with DAPI.** DAPI nuclear stain is added to porous hyphae and viewed with a fluorescence microscope under a UV filter set. Bright dotted areas represent fluorescence from stained nuclei. Fluorescence was monitored using a fluorescence light microscope. Images represent replicates of DAPI stained nuclei at two magnification, where scale bars are provided for measure.

5.3.2 FISH detection of AbV6 in *A. bisporus* strains

Each strain was hybridised with AbV6 probes. MVX-1283 was positive for AbV6 infection upon original testing and also when tested by RT-PCR in 2017 (**Table 1**) and was the only strain that showed high levels of fluorescence when probed for AbV6 (**Figure 3**). Localisation of AbV6 was observed primarily at the margins of the colony. The intensity of fluorescence was high, occurring throughout the length of the hyphae. The fluorescence was strong enough in certain hyphae that a particular pattern was observed, whereby negative staining zones (possibly vacuoles) were surrounded by very high fluorescence (**Figure 3B, 3D**), giving an apparent 'halo-effect'.

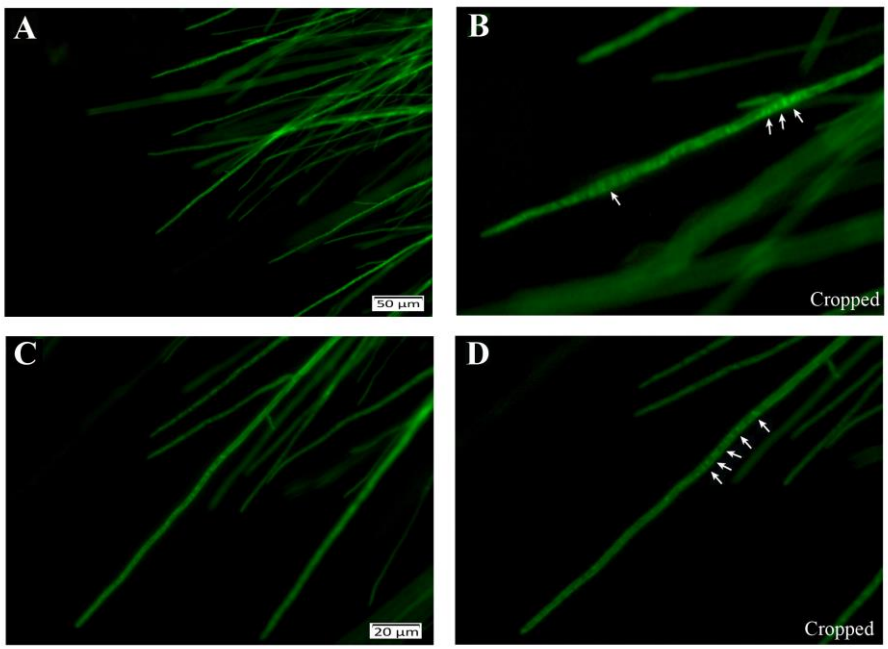

Figure 3: **FISH of MVX-1283 with a FITC-labelled AbV6 probe**. High degree of fluorescence is detected in hyphae towards the periphery of the cultures. **A** and **C**: Images taken of MVX-1283 culture in different areas and at different magnification. **B** and **D**: Close up of area shown with arrows in images **A** and **C**, respectively. White arrows point to areas where a halo-effect is seen whereby vacuoles have low fluorescent signal but are surrounded by strong circles of fluorescent signal. Fluorescence was monitored using a fluorescence light microscope. Scale bars are provided in original images for measure.

Although the non-MVX control strain had tested negative by RT-PCR for AbV6 (**Table 1**), some fluorescence was recorded in all replicate preparations (n = 25) when AbV6 was the target. The extent of probe fluorescence was low, but still easily discernible at the extreme apices of hyphae on the growing periphery of cultures (**Figure 4**). A fluorescent gradient, brightest at the apex and lessening down the hypha, was apparent (**Figure 4**). Additionally, branching hyphae were found to contain fluorescent signal, where the primary hypha, at the point of origin of the branching, did not (**Figure 4**). High fluorescent signal was also captured in a swelling that was beginning to, but had not yet formed, a new hyphal branch (**Figure 4).** MVX-1153 and MVX 2735 which had tested negative for AbV6 by RT-PCR (**Table 1**), also showed very low fluorescent signal for AbV6 detection at levels similar to the non-MVX control strain in all replicate preparations (n = 25) (**Figure_S3**). The negative control (RNase-treated) is the only culture that did not display any level of AbV6 detection using FISH (**Table 2**).

Table 2: **FISH detection of MVX in each strain of *A. bisporus* tested.** Fluorescence detection is rated as follows; (++), High levels of fluorescence; (+), Low levels of fluorescence and (-), no fluorescence detected.

Strain	Untreated		RNase-Treated	
	AbV6	AbV16	AbV6	AbV16
Non-MVX (A15)	+	-	-	-
MVX-1283	++	-	-	-
MVX-2735	+	+	-	-
MVX-1153	+	++	-	-

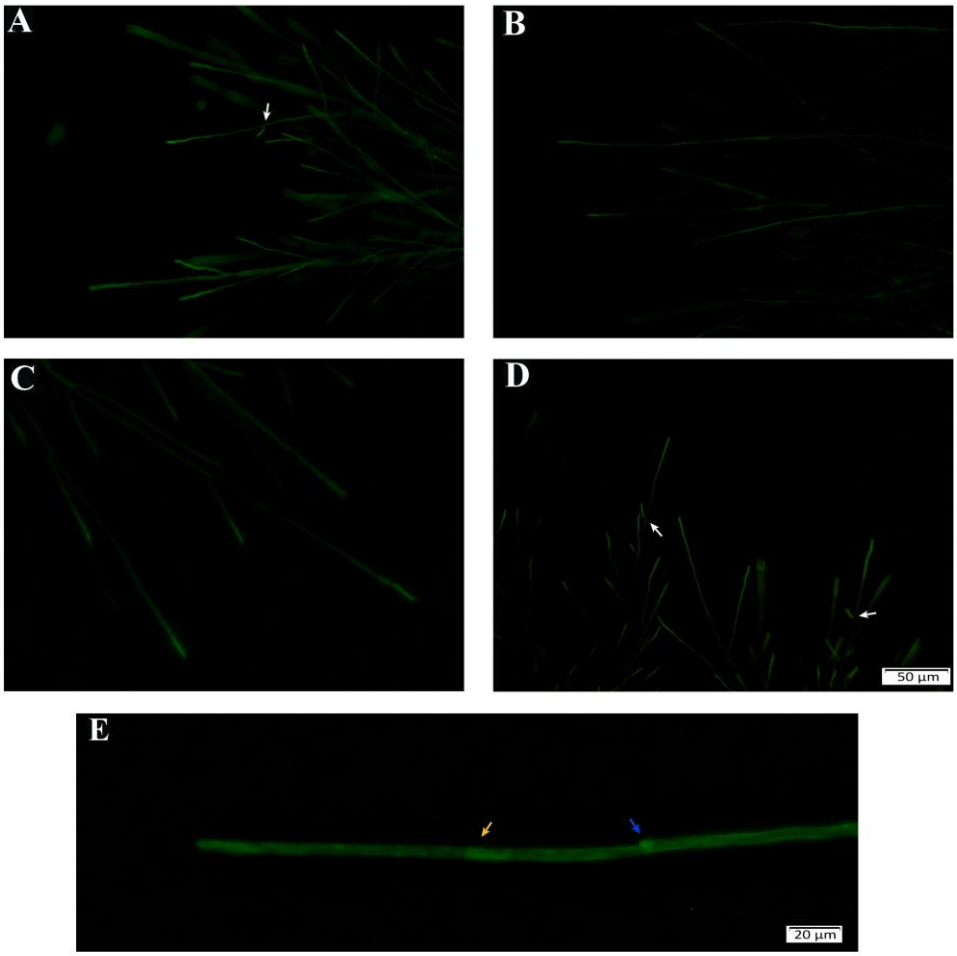

Figure 4: **FISH of non-MVX hyphae with a FITC-labelled AbV6 probe.** Fluorescence was observed for AbV6 most intensely at the extreme apices of the hyphae (**A-D**). **A-D** represent different replicates of the non-MVX strain probed for AbV6 all with similar patterns of AbV6 detection. White arrows in **A** & **D** point to areas where hyphal branches exhibiting fluorescent signal can be seen developing from a point on the primary hypha where there is no signal. (**E**) Image of a hypha where the right arrow shows a newly forming branch (swelling) where fluorescence is notably high. The left arrow highlights a cellular compartment where AbV6 is congregating at the septum in the direction of the hyphal apex. Fluorescence was monitored using a fluorescence light microscope. Scale bars are provided for measure (**A**-**D** scale: 50 µm).

5.3.3 FISH of AbV16 in *A. bisporus* strains

FISH was used to localise AbV16 in the mycelium of all strains but was detected in only MVX-2735 and MVX-1153 (**Figure 5A, B**). MVX-1153, which was positive for AbV16 on original testing and also by RT-PCR in 2017, showed high fluorescent signal when probed for AbV16 (**Figure 5B**). Signals were found in the reticulating network of mycelium towards the centre of cultures and not at the growing edges/hyphal apices. AbV16 showed a highly compartmentalised sequential pattern of signal distribution in the hyphae (**Figure 5B**). FISH did not reveal any fluorescence in any replicate (n = 25) of the non-MVX control strain. A very faint fluorescent signal was detected in replicates of MVX-2735 (**Figure 5A**), which had been positive for AbV16 when originally collected but it appeared to have lost this virus when tested by RT-PCR in 2017. MVX 1283 and the non-MVX control did not display any level of AbV16 detection using FISH (**Table 2**).

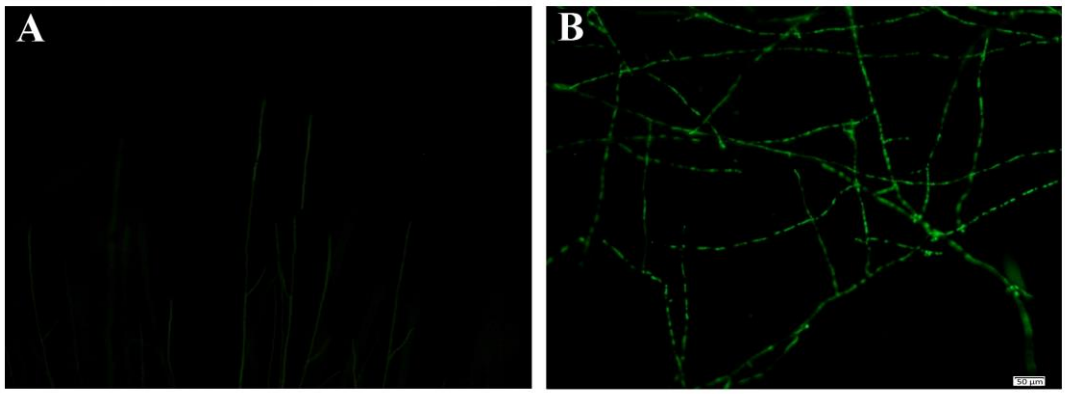

Figure 5: **FISH of MVX strains with a FITC-labelled AbV16 probe**. (**A**) MVX-2735 showing low amounts of fluorescent signal. (**B**) MVX-1153 showing a high amount of fluorescent signal. AbV16 can be seen in a compartmentalised manner throughout the interconnecting hyphae. Localisation of signal was found at a distance from hyphal apices towards the centre of the culture mycelium. Fluorescence was monitored using a fluorescence light microscope. Scale bars are provided for measure (**A** and **B**: 50 µm).

5.4 Discussion

The method for FISH was adapted from previous studies involving this technique on filamentous fungi (Teertstra et al., 2004; Villa et al., 2009), and was used in a novel application to target two disease phenotype-associated viruses of MVX in *A. bisporus* mycelium. This approach facilitated *in situ* cultivation, permeabilisation, hybridisation of FISH probes and visualization by fluorescence light microscopy of mycelium on a singular platform, without the need for cutting, embedding, or any form of translocation of material (**Figure 1**). As such, this technique allows for *in vitro* growth of hyphae and FISH of nucleic acid targets with minimal disturbance to the mycelium architecture. Furthermore, by adapting methods previously evaluated for non-destructive permeabilisation of hyphal cell walls (Villa et al., 2009), the need for lytic enzymes to facilitate DNA probe penetration into fungal hyphae was avoided (**Figure 2**). This is highly beneficial as destructive methods delocalise fluorescence signals (Teertstra et al., 2004).

Using the FISH technique described above, and an AbV6 specific probe, a very strong signal was obtained in the peripheral hyphae of the AbV6-positive strain, MVX-1283 (**Figure 3**). The RNase-treated negative control produced no fluorescence, giving confidence that the observed fluorescent signal was an accurate reflection of where the AbV6 virus was located in the mycelium, and clearly showing it to be concentrated in the growing edge of the colony. The level of fluorescence was strong enough to reveal a pattern whereby putative vacuoles (visible as sequentially arranged, equally sized and circular structures in hyphae) appeared to lack fluorescence, but the circumference of these putative vacuoles showed peaks in fluorescent signal, suggesting a possible 'halo-effect' (**Figure 3B, D**). However, greater resolution of cellular compartments is needed to better characterise the observed pattern of signal. If a halo-effect on vacuoles was confirmed, it could suggest that the fluorescence is due the congregation of vesicles surrounding the tonoplast of the vacuole (Klionsky et al., 1990).

Contrary to what was expected, AbV6 signal was also detected in the non-MVX control (**Figure 4**) as well as in MVX 1153 (**Figure_S3**) and MVX 2735 (**Table 2**) , all of which had tested negative by RT-PCR in 2017 and had not been shown to contain AbV6 when they were originally collected (**Table 1**). The signal of AbV6 in these strains was much weaker than that in MVX 1283, and was confined to the apical

compartments of hyphae, with signal intensity highest at the extreme apex and lessening in a gradient pattern down the length of the hypha (**Figure 4A-D**). Sub-apical regions in hyphae are areas of high pressure where a variety of molecules congregate such as ribosomes, actin and vesicles. Endomembrane processes feed vesicles from these areas into the extreme apex and surround the Spitzenkörper, during the process of apical growth (Grove and Bracker, 1970). As such, FISH of non-MVX hyphae also suggests synchronous virus localisation with vesicle transport, although this hypothesis warrants further study for validation.

In a study of MVX viruses using a deep sequencing approach, Deakin et al. (2017) detected low levels of AbV6 in mushrooms from a 'non-diseased commercial culture' grown as a control crop and thus, low level presence of this virus may be 'normal'. Similarly, a low-level presence of AbV6 was detected in 'sample 2735' (MVX-2735) by Deakin et al. (2017), similar to the FISH results presented here (**Table 2**). Other dsRNA elements and virus-like particles have been reported in healthy *A. bisporus* fruitbodies in the past (Akarapisan, 2000; Grogan et al., 2003; Romaine and Schlagnhaufer, 1989; Romaine et al., 2004), but most testing has been on mushrooms rather than mycelium. Virus presence may vary between mushroom fruitbodies and the vegetative mycelium giving rise to them. The FISH method may be useful to visualise viruses *in situ* in different tissues to explore virus dynamics at whole organism level.

The second virus targeted for observation by FISH was AbV16, which is associated with the brown cap symptom (Eastwood et al, 2015; Fleming-Archibald et al, 2015). Neither the RNase-treated control cultures nor the non-MVX strain produced fluorescence when probed for AbV16. High levels of AbV16 were detected in MVX-1153 (**Figure 5B**). In contrast to the results for AbV6, AbV16 fluorescence signals were found at high levels within the central areas of the colony at a distance from the culture peripheries (**Figure 5B**). Patterns of signal distribution suggest that AbV16 is highly compartmentalised and packaged within the mycelium of MVX-1153 (**Figure 5B**). RNA virus packaging in vesicles of *A. bisporus* has been reported previously (Romaine et al., 1994).

MVX-2735 cultures showed very low levels of fluorescence for AbV16, with very localised occurrence (**Figure 5A**). Recent studies also suggest that AbV16 was 'lost' from this inoculum (Deakin et al., 2017) and by RT-PCR (this study). The loss of

the virus could be due to long-term culture maintenance of the strain as the more recently isolated strain MVX-1153 had much greater AbV16 signal intensity. The FISH technique highlights how, although AbV16 was not recently detected in MVX-2735 by either deep sequencing (Deakin et al., 2017) or by RT-PCR (this study), the AbV16 virus was still present within the MVX-2735 mycelium, but at a very low level. This highlights the benefits of the FISH technique in detecting virus presence at low levels and could be a very useful tool in studying viral dynamics in cultures where many viruses may be present in the same mycelium.

The characterisation and localisation of AbV6 and AbV16 within host *A. bisporus* mycelium is ground-breaking and would not be possible with typical molecular techniques. These results validate the application of FISH to study MVX. Furthermore, the reproducible and non-destructive methods described provide an application for use in other species of filamentous fungi for the study of intracellular mycoviruses.

5. Conclusion

In this work, FISH was successfully adapted to target two viruses within the mycelium of *A. bisporus*. The full FISH workflow was achieved on singular microscope slides, with a reproducible, cost-effective and non-destructive method. The detection, localisation and patterns of distribution of two different mycoviruses, AbV6 and AbV16, at both high and low levels of presence within the host mycelium, were characterised. The localisation patterns observed may suggest movement of viruses through vesicle-hijacking mechanisms, in particular the observed congregation of AbV6 at hyphal apices and putatively surrounding vacuoles. This work demonstrates how FISH can be applied to studies of mycoviruses within fungal host mycelium.

Acknowledgments

EOC is funded by a Teagasc Walsh Scholarship Scheme (grant reference number 10564231). This work was also funded by the Teagasc Overseas Travel Award (2017).

Literature Cited

Akarapisan, A., 2000. Molecular analysis of double-stranded RNA viruses in Agaricus bisporus and associated fungi. PQDT - Glob.

Almeida, C., Azevedo, N.F., Santos, S., Keevil, C.W., Vieira, M.J., 2011. Discriminating Multi-Species Populations in Biofilms with Peptide Nucleic Acid Fluorescence In Situ Hybridization (PNA FISH). PLoS One 6, e14786.

Aoi, Y., 2002. In situ identification of microorganisms in biofilm communities. J. Biosci. Bioeng. 94, 552–556.

Brul, S., Nussbaum, J., Dielbandhoesing, S.., 1997. Fluorescent probes for wall porosity and membrane integrity in filamentous fungi. J. Microbiol. Methods 28, 169–178.

Da Silva, R., Da Silva Neto, J., Santos, C., Frickmann, H., Poppert, S., Cruz, K., Koshikene, D., De Souza, J., 2015. Evaluation of fluorescence in situ hybridisation (FISH) for the detection of fungi directly from blood cultures and cerebrospinal fluid from patients with suspected invasive mycoses. Ann. Clin. Microbiol. Antimicrob. 14, 6.

Dawson, K.S., Strąpoć, D., Huizinga, B., Lidstrom, U., Ashby, M., Macalady, J.L., 2012. Quantitative Fluorescence In Situ Hybridization Analysis of Microbial Consortia from a Biogenic Gas Field in Alaska's Cook Inlet Basin. Appl. Environ. Microbiol. 78, 3599–3605.

Deakin, G., Dobbs, E., Bennett, J.M., Jones, I.M., Grogan, H.M., Burton, K.S., 2017. Multiple viral infections in Agaricus bisporus - Characterisation of 18 unique RNA viruses and 8 ORFans identified by deep sequencing. Sci. Rep. 7, 2469.

Eastwood, D., Green, J., Grogan, H., Burton, K., 2015. Viral Agents Causing Brown Cap Mushroom Disease of Agaricus bisporus. Appl. Environ. Microbiol. 81, 7125–7134.

Ferreira, A.M., Cruz-Moreira, D., Cerqueira, L., Miranda, J.M., Azevedo, N.F., 2017. Yeasts identification in microfluidic devices using peptide nucleic acid fluorescence in situ hybridization (PNA-FISH). Biomed. Microdevices 19, 11.

Fleming-Archibald, C., Ruggiero, A., Grogan, H.M., 2015. Brown mushroom symptom expression following infection of an Agaricus bisporus crop with MVX associated dsRNAs. Fungal Biol. 119, 1237–1245.

Free, S.J., 2013. Fungal Cell Wall Organization and Biosynthesis, in: Advances in Genetics. pp. 33–82.

Grogan, H.M., Adie, B.A.T., Gaze, R.H., Challen, M.P., Mills, P.R., 2003. Double-stranded RNA elements associated with the MVX disease of Agaricus bisporus. Mycol. Res. 107, 147–154.

Grove, S.N., Bracker, C.E., 1970. Protoplasmic organization of hyphal tips among fungi: vesicles and Spitzenkörper. J. Bacteriol. 104, 989–1009.

Huber, D., Voith von Voithenberg, L., Kaigala, G.V., 2018. Fluorescence in situ

hybridization (FISH): History, limitations and what to expect from micro-scale FISH? Micro Nano Eng. 1, 15–24.

Jiang, J., 2019. Fluorescence in situ hybridization in plants: recent developments and future applications. Chromosom. Res. 27, 153–165.

Kang, X., Kirui, A., Muszyński, A., Widanage, M.C.D., Chen, A., Azadi, P., Wang, P., Mentink-Vigier, F., Wang, T., 2018. Molecular architecture of fungal cell walls revealed by solid-state NMR. Nat. Commun. 9, 2747.

Kaur, L., Dhanda, S., Sodhi, H.S., Kapoor, S., Khanna, P.K., 2011. Storage and Preservation of Temperate Mushroom Cultures, Agaricus Bisporus and Pleurotus Florida. Indian J. Microbiol. 51, 234–238.

Klionsky, D.J., Herman, P.K., Emr, S.D., 1990. The fungal vacuole: composition, function, and biogenesis. Microbiol. Rev. 54, 266–92.

Kliot, A., Ghanim, M., 2016. Fluorescent in situ hybridization for the localization of viruses, bacteria and other microorganisms in insect and plant tissues. Methods 98, 74–81.

Kurisu, F., Zang, K., Kasuga, I., Furumai, H., Yagi, O., 2015. Identification of estrone-degrading Betaproteobacteria in activated sludge by microautoradiography fluorescent in situ hybridization. Lett. Appl. Microbiol. 61, 28–35.

La Cono, V., Urzì, C., 2003. Fluorescent in situ hybridization applied on samples taken with adhesive tape strips. J. Microbiol. Methods 55, 65–71.

Li, A., Begin, M., Kokurewicz, K., Bowden, C., Horgen, P.A., 1994. Inheritance of Strain Instability (Sectoring) in the Commercial Button Mushroom, Agaricus bisporus. Appl. Environ. Microbiol. 60, 2384–8.

Li, S., Spear, R.N., Andrews, J.H., 1997. Quantitative fluorescence in situ hybridization of Aureobasidium pullulans on microscope slides and leaf surfaces. Appl. Environ. Microbiol. 63, 3261–7.

Masoumi, F., Pourianfar, H.R., Masoumi, A., Mendi, E.M., 2015. A study of mycelium characterization of several wild genotypes of the button mushroom from Iran. Int. J. Adv. Res. Journalwww.journalijar.com Int. J. Adv. Res. 3, 236–246.

Medlin, L., Orozco, J., 2017. Molecular Techniques for the Detection of Organisms in Aquatic Environments, with Emphasis on Harmful Algal Bloom Species. Sensors 17, 1184.

Nakada, Y., Nakaba, S., Matsunaga, H., Funada, R., Yoshida, M., 2013. Visualization of the Mycelia of Wood-Rotting Fungi by Fluorescence *in Situ* Hybridization Using a Peptide Nucleic Acid Probe. Biosci. Biotechnol. Biochem. 77, 405–408.

Nielsen, P.E., Egholm, M., 1999. An introduction to peptide nucleic acid. Curr. Issues Mol. Biol.

Reller, M.E., Mallonee, A.B., Kwiatkowski, N.P., Merz, W.G., 2007. Use of Peptide Nucleic Acid-Fluorescence In Situ Hybridization for Definitive, Rapid Identification of Five Common Candida Species. J. Clin. Microbiol. 45, 3802–

3803.

Romaine, C.P., Schlagnhaufer, B., 1989. Prevalence of Double-Stranded RNAs in Healthy and La France Disease-Affected Basidiocarps of Agaricus bisporus. Mycologia 81, 822.

Romaine, C.P., Schlagnhaufer, B., Goodin, M.M., 1994. Vesicle-associated double-stranded ribonucleic acid genetic elements in Agaricus bisporus. Curr. Genet. 25, 128–134.

Teertstra, W.R., Lugones, L.G., Wösten, H.A.B., 2004. In situ hybridisation in filamentous fungi using peptide nucleic acid probes. Fungal Genet. Biol. 41, 1099–1103.

Urzi, C., La Cono, V., Stackebrandt, E., 2004. Design and application of two oligonucleotide probes for the identification of Geodermatophilaceae strains using fluorescence in situ hybridization (FISH). Environ. Microbiol. 6, 678–685.

Urzì, C., De Leo, F., 2001. Sampling with adhesive tape strips: an easy and rapid method to monitor microbial colonization on monument surfaces. J. Microbiol. Methods 44, 1–11.

Villa, F., Cappitelli, F., Principi, P., Polo, A., Sorlini, C., 2009. Permeabilization method for in-situ investigation of fungal conidia on surfaces. Lett. Appl. Microbiol. 48, 234–240.

Yu, X., Li, B., Fu, Y., Xie, J., Cheng, J., Ghabrial, S.A., Li, G., Yi, X., Jiang, D., 2013. Extracellular transmission of a DNA mycovirus and its use as a natural fungicide. Proc. Natl. Acad. Sci. 110, 1452–1457.

Chapter 6:

Synthesis and Future Directions

6.0 Synthesis and Future Directions

6.1 Synthesis

Prior to the results presented within this thesis, the molecular response of *A. bisporus* to MVX was limited to the differential expression of a small number of genes in the commercial A15 strain (Eastwood et al., 2015). Thus, the findings in the main results chapter of this thesis represents the first transcriptomic and proteomic study of the globally cultivated button mushroom *A. bisporus* in response to MVX infection (**Chapter 4**). Additionally, a process pivotal to the transmission of MVX, anastomosis, was characterised using an untargeted proteomic approach (**Chapter 3**). A pioneer study in the use of FISH was also developed to gain novel understanding into the behaviour of viruses in a range of MVX inocula (**Chapter 5**). This thesis also describes the first whole genome sequence and analysis of a wild *A. bisporus* var. *bisporus* strain (**Chapter 2**).

The work presented in this thesis adds substantially to the current knowledge pertaining to the dynamics of *A. bisporus* and MVX. Outbreaks of MVX were first reported just over two decades prior to the studies presented in this thesis and so in relative terms, MVX may still be considered a novel disease in commercial mushroom production. The viruses of MVX and the collective symptomologies and outbreaks in mushroom crops have been well documented (Adie et al., 2004; Burton et al., 2011; Deakin et al., 2017; Eastwood et al., 2015; Fleming-Archibald et al., 2015; Grogan et al., 2004, 2003; Sonnenberg and Larvrijssen, 2004; Gaze *et al*., 2000; Deakin, 2015; Green, 2010; Maffettone, 2007). However, insight into the molecular response of *A. bisporus* to MVX infection is scant. Moreover, to the best of the author's knowledge, genome-wide expression (beyond suppression-subtractive hybridisation) and proteomic analyses had never been applied to MVX-infected fruit bodies of any strain.

The central aim of this thesis was to elucidate the host response to MVX by examining the fruit bodies of different strains of *A. bisporus*. The experimental design of these studies was purposely modelled to best reflect commercial cultivation settings as MVX is solely problematic in industry and has not yet been reported in the wild. This model is multifactorial such that it represents (1) the host response of strains ranging from high susceptibly to lower susceptibilities to infection, (2) the response of non-

infected, MVX-challenged non-infected and MVX-infected fruit bodies (3) the transcriptomes and proteomes of fruit bodies produced from hyphae exposed to MVX at two different points crucial to the cultivation process.

Initial studies examining the *in vitro* transmission potential of MVX in the hyphae of each strain were carried out to assess each strain's potential as MVX-resistant candidates. The variety of interactions observed between these strains led to the examination of mechanisms underpinning anastomosis. This was the first study to characterise the proteome of a range of vegetative compatibilities in a filamentous fungus and only the second proteomic investigation of anastomosing fungi (Zhong et al., 2018). Finally, a first glimpse into the spatial distribution of viruses of MVX was provided in this work, including their localisation and intracellular movement and these may help inform about their behaviour within host mycelium.

This chapter revisits some of the primary concepts outlined in **Chapter 1** and hypotheses borne from these concepts and collaborative efforts of the industry and affiliated researchers. I will then provide the synthesises of key findings of the experimental work from **Chapters 2-5** in the context of those concepts. New hypotheses are offered in light of new findings and proposals for the direction of future work.

6.1.1 Hypothesis 1: Vegetative incompatibility acts as a barrier to virus transmission. Therefore, the key to MVX-resistance is cultivation of strains which do not readily anastomose with the susceptible commercial strain A15.

Mycoviruses predominantly lack any independent exogenous route of transmission and function as obligate intracellular parasites (Ghabrial, 1998; Ghabrial et al., 2015; Ghabrial and Suzuki, 2009). The most frequently reported mechanism that mycoviruses annex for transmission between their fungal hosts is anastomosis, followed by sporulation (vertical transmission) (Thapa and Roossinck, 2019). MVX does not differ in this regard as it has been shown to readily transmit between the fusion of hyphae of two separate colonies (Grogan et al., 2004b) but only partially in spores (data unpublished). As much commercial cultivation avoids mature mushrooms with open veils (portobello), this would go a long way to explain the persistent nature of disease in

an afflicted growing house. Just a few fragments of infected substrate from a diseased crop making physical contact with an incumbent batch of phase II or III compost may reintroduce the disease to the new crop cycle. In a hypothetical regard, if the bulk phase III compost were to harbour a vegetatively incompatible variety of *A. bisporus* to the previous crop, the opportunity for reintroduction of disease from fragments that escaped the cleaning process would be much lower.

This assumption was challenged in **Chapter 4** by *in vitro* assays of dual-culture interactions of an MVX-infected hyphae with the hyphae of five diverse strains, one of which matched the MVX-infected strain. Incompatibility of the four other strains was apparent through observation of colonies and microscopically, although accurately documenting the precise frequency of anastomosis with brightfield microscopy proved too difficult for these interactions. Temporal findings from as early as initial anastomosis of infected and healthy hyphae revealed MVX infection in all strains. This demonstrated that these distinct varieties of *A. bisporus* engage in anastomosis, therefore MVX can traverse the incompatibility barrier. As these viruses do not form virions and are unencapsidated, this transfer can only be facilitated by whatever degree of somatic fusion occurs between discrete colony hyphae. On this basis, *Hypothesis 1* is rejected. However, the vegetative incompatibility is still a powerful process to exploit for the control or sequestration of the impact of MVX. The investigation described above cannot replicate the complex architecture of interactions in the fungal mycelium that occurs in the substrate of commercial crops. The process of anastomosis and vegetative incompatibility has been an area of intense study but predominantly from a genetic perspective in model filamentous fungi (Bégueret et al., 1994; Glass et al., 2000; Kauserud et al., 2006; Paoletti, 2016; Saupe, 2000; van der Nest et al., 2011). The results presented in **Chapter 3** characterise, for the first time, the proteome of anastomosing strains of *A. bisporus.* Enzymes participating in extension of hyphae through breakdown processes of chitins, glucans and other cell wall architectural proteins were highly expressed in interactions where anastomosis was most prevalent (vegetative compatible). The use of a strain with hybrid commercial and wild type parentage (CWH) was not genetically distant enough from A15 to trigger the synthesis of categorised proteins involved in *vic* systems and so no evidence of vegetative incompatible response was found, whereas substrate starvation and high levels ROS producing enzymes were captured. Evidence of vegetative incompatibility systems were

found for interactions with the wild strain (ARP23) and stress-induced antagonism. As the proteomes of interacting cultures did not elicit strong responses relating to vegetative incompatibility (**Chapter 3**) and virus transmission was detected between the interactions of these strain (**Chapter 4**), it is unsurprising that these conspecific interactions facilitated full transmission of MVX. This may represent less of an argument against the efficacy of supposedly vegetative incompatible barriers against virus transmission and more the need for interactions of different species of *Agaricus* (for example *Agricus bitorquis*) to achieve a consistent prevention of infection. This is further reason to reject *Hypothesis 1*.

6.1.2 Hypothesis 2: The introduction of infectious MVX material at a later point in the cropping cycle results in a greater level of disease in the fruit bodies. This is due to an inability of the host to mount a response to infection whilst undergoing the morphogenic switch from vegetative growth to reproductive growth.

The symptom expression of MVX is dynamic and sporadic. The underlying events leading to isolated fruit bodies exhibiting disease symptom expression (most conspicuously the brown cap phenotype) in close proximity to symptomless fruit bodies, at times from stipes clustered from an adjoining base, is still not understood. Frequency of browning has been linked to the timing of MVX inoculation in the mycelium of growing trays/crates (Fleming-Archibald et al., 2015; Grogan et al., 2003). This has been suggested as an adaptive strategy by the viruses to proliferate during high levels of cell division (Eastwood et al., 2015). The results documented in **Chapter 4** provide novel insight into this phenomenon. Symptom expression (the brownness of the fruit body) was not as differentiated between early and later inoculation of MVX as in the aforementioned studies (Fleming-Archibald et al., 2015; Grogan et al., 2003). However, average mean value related to high quality mushrooms were more frequent in the non-inoculated treatments compared to inoculated treatments and where MVX was introduced at a later point in the crop, symptom expression was marginally the most severe. Stochastic sampling of fruit bodies revealed levels of AbV16 to be most prevalent in the susceptible A15 strain. The other strains in this study each revealed a single isolate positive for the presence of this virus, but only in the later infection with the exception of CWH. These findings correlate with those previously published on the

impact of timing of infection on symptom expression in fruit bodies. The browning of mushrooms has been hypothesised as a consequence of the mixing of cellular contents that triggers the oxidation of phenolic substrates into quinones and subsequent melanogenesis (Eastwood et al., 2015; Weijn et al., 2013). Yet to date, no corroboration of virus infected fruit bodies with higher concentrations of polyphenol oxidases have been demonstrated (Green, 2010; Deakin, 2015). The transcriptomic and proteomic data from this thesis also bares no support for this hypothesis of virus-induced browning. However, a mechanical-damage marker (myo-inositol) was reported in the proteomes of fruit bodies with the highest frequency of infection. Support for post-harvest tissue damage and this carbocyclic sugar exist for *A. bisporus* (O'Gorman et al., 2012), but its links to virus infection and browning warrants further investigation. The proteomes of these fruit bodies also revealed vesicle-induced damage and ER-stress, protein misfolding and repair responses. These types of ER-stresses have been shown to cause extensive cell wall damage in *S. cerevisiae* (Scrimale et al., 2009). To what end the lateness of infection relates to disease expression, may be better understood in light of transcriptomic analyses of the fruit bodies also presented in **Chapter 4**. Genes related to transcription factors, genes with putative transcription factor activity and more general promotors of gene expression were up-regulated in MVX-infected A15 fruit bodies, but primarily when MVX was introduced early i.e. has established in the mycelium prior to fruitification. If the viruses promote the up-regulation of genes that augment gene expression, this could represent an adaptive strategy to exploit the host for their own replication. This also fits with the observation that viral titre is significantly higher in fruit bodies (Eastwood et al., 2015), as these cells are under mass cell division Conversely, later inoculation of MVX with A15 showed down-regulation of some transcription factors. This may be an early response by the host to curtail further proliferation of the viruses, as these particular fruit bodies all tested positive for disease. Virus-infected CWH revealed that viruses did not elicit the upregulation of transcription factors, however, in the later infection where the levels of virus related to disease were not found, transcription factors were up-regulated in CWH. This may represent the outcome after viruses have been eradicated, but this explanation is merely speculative as the mechanisms behind this result are unknown. **Chapter 4** clearly highlights, the presence of these viruses at elevated levels in fruit bodies and even their incidence in the mycelium elicits the regulation of an array of transcription factors. The ability of

mycoviruses to promote the expression of genes for transcription factors has been demonstrated in separate studies (Lee et al., 2014; Wang et al., 2018). As transcription factors play pivotal role in fruit body formation, this helps expound the link between later infection time and severity of symptom expression. Based on the results presented here we accept hypothesis 2 i.e. The introduction of infectious MVX material at a later point in the cropping cycle results in a greater level of disease in the fruit bodies.

6.1.3 Hypothesis 3: The current commercially cultivated monoculture (strain A15) is susceptible to infection by MVX. The establishment of wild germ plasm into commercial breeding may be a valuable reservoir of resistance attributes to MVX.

The vegetative clonal propagation and difficulty in deriving novel varieties harbouring commercially viable traits from wild germplasms has hindered *A. bisporus* breeding progress and created a monoculture crop susceptible to a variety of pathogens. The core focus of this thesis revolved around three *A. bisporus* strains; A15, CWH and ARP23. The pedigree of CWH and ARP23 makes them obvious candidates for novel molecular discoveries that could be incorporated in cultivation and breeding programs. CWH is the progeny of U1 (a progenitor shared with A15) and *A. bisporus* var. *burnettii.* Therefore it derives one of its heterologous nuclei originally from a wild strain. *A. bisporus* var. *burnettii* is a well suited candidate for breeding due to its resistance attributes to certain commercial pathogens (Foulongne-Oriol et al., 2011) and its also has a genome available for genetic mining (Morin et al., 2012). ARP23 on the other hand is not a hybrid variety and was sourced directly from the wild. Prior to the work of this thesis, no focused studies on capacity of ARP23 to resist MVX infection existed. Investigations from **Chapter 3** revealed that ARP23 is distant enough to elicit the *vic* system with A15 and furthermore, showed low incidence of infection in fruit bodies **Chapter 4**. The greatest variety of downregulated transcription factors was documented in MVX-challenged ARP23 fruit bodies. The potential of ARP23 as a strain that shows lower susceptibilities to MVX led to whole genome sequencing of this strain **Chapter 2**. Phylogenomic reconstruction of candidate fungi with the newly sequenced genome of ARP23, H97 (commercial hybrid) and var. *burnettii* grouped ARP23 and H97 as sister taxa revealing that ARP23 represents a wild *Agaricus* more closely related to the commercially cultivated white hybrid. The pangenome of *A.*

bisporus revealed that over 40% of the ARP23 is considered accessory in relation to the genomes of H97, H39 and var *burnettii* (**Chapter 2**). **Chapter 2** also presents the detailed analysis of the *A. bisporus* mating loci and confirmed it to be unifactorial and unsurprisingly it is highly conserved between different *A. bisporus* strains. This unique gene repertoire qualifies ARP23 as an important gene library for mining of disease resistant attributes.

From **Chapter 4**, the transcriptome of CWH reveals key antiviral responses to MVX. Infected fruit bodies of CWH induced the greatest array of antiviral responses most of which were found only in this strain and exclusively where fruit bodies were diseased. The proteomes of CWH also showed down regulation of translational machinery. Downregulation was the dominant response of ARP23. ARP23 fruit bodies showed proficient virus recognition when exposed to MVX at an early point in the crop vis-à-vis the negative regulation of transcription factors, translational machinery, RNA metabolism, macromolecule biosynthesis pathways. ARP23 transcriptomic and proteomic strategies suggests that infection of these fruit bodies manifests as negative regulation of a variety of processes. These findings result in the acceptance of *Hypothesis* 3 i.e the current commercially cultivated monoculture (strain A15) is susceptible to infection by MVX.

6.2 Novel insights of virus strategy

Many mycoviruses have pressumed adaptive strategies to traverse mycelia through cell-to-cell movement necessitated by the lack of an extracellular phase (Ghabrial et al., 2015). Numerous studies have shown these intercellular events in mycovirus transmission, but few can demonstrate the intracellular movement. **Chapter 5** of this thesis offers a novel approach to characterise the spatial distribution, discrete localisation and possible behaviours of two crucial viruses related to disease in MVX within the mycelium of non-infected and infected individuals. This approach may elucidate the persistent nature of MVX through localisation strategies related to infection and protection. The association of virus transport and vesicles has been alluded to in previous work (Deakin et al., 2017; Eastwood et al., 2015; Mafettonne, 2007; Deakin, 2015; Green, 2010) based off of prior findings of dsRNA molecules within vesicle-associated elements (Romaine et al., 1994). Visualisation of these viruses

revealed local patterns also linked to vesicle transport, supporting the findings of Romaine *et al.* (1994). Furthermore, vesicle-mediated transport was consistently downregulated in the transcriptomes of diseased fruit bodies which could relate to a defensive strategy of cells (**Chapter 4**). The proteomes also revealed vesicle-associated ER-stress in the presence of MVX (**Chapter 4**).

6.3 Summary

The research presented in this thesis includes the first whole genome sequence of a commercially relevant strain of *A. bisporus* from a wild population, revealed to be more closely related to the commercial white hybrid yet with a large accessory genome (**Chapter 2**). The process crucial to virus transmission was characterised using an untargeted proteomic approach comparing the vegetative mycelium of monocultures to diverse interactions of co-cultures with the cultivated A15 strain revealing diverse strategies of hypha remodelling, competitive strategies and antagonism between strains (**Chapter 3**). The molecular host response to MVX was characterised with a robust methodology incorporating the transmission of viruses in five strains, symptom expression in fruit bodies, genome-wide transcriptional patterns of fruit bodies, proteomic responses of fruit bodies and the proteomic response of commercial strain mycelium in the compost substrate. The results from this thesis help form an understanding of virus infection in fruit bodies where vegetative incompatibility and antiviral responses are believed to aid *A. bisporus* in the defence against MVX (**Figure 6.1**). The diverse molecular responses from the commercial susceptible strain, the less susceptible strains with hybrid commercial and wild parentage and a wild strain have been characterised (**Figure 6.2**).

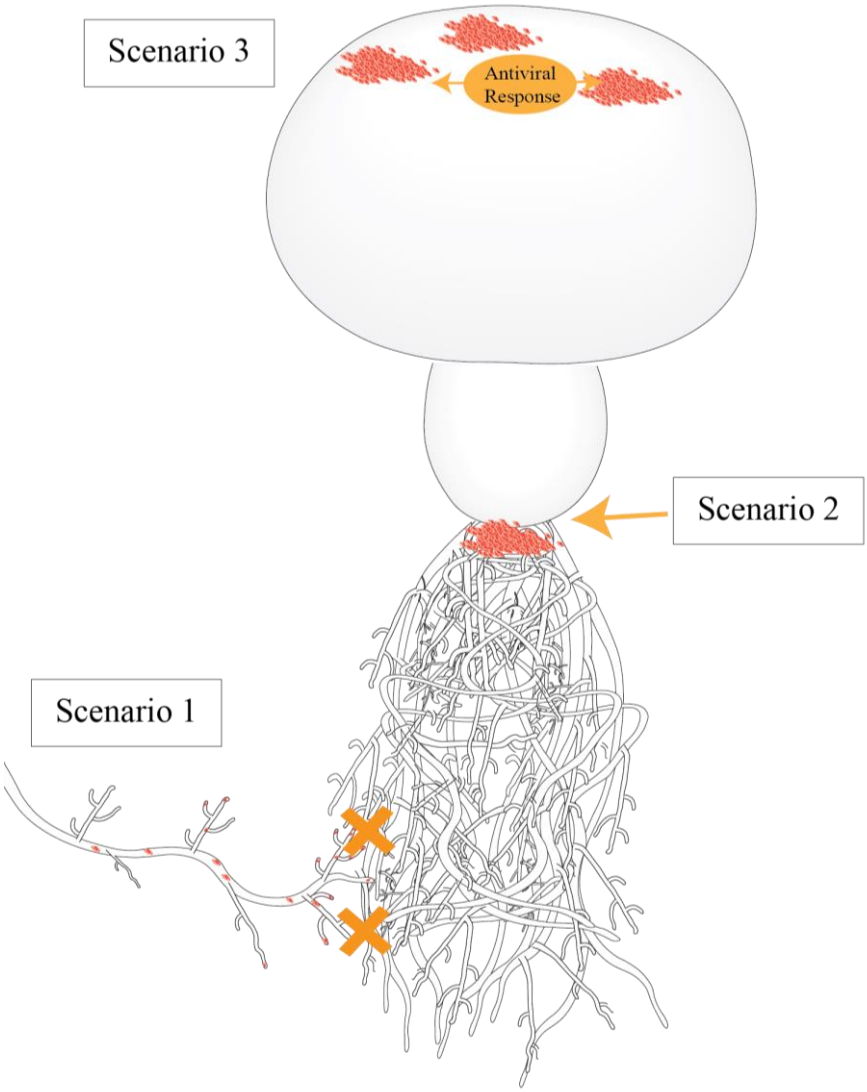

Figure 6.1: Schematic of *A. bisporus* fruit body and vegetative mycelium and the possible scenarios where resistance to MVX infection may arise. Viruses are illustrated in red. Structures are not to scale. (**Scenario 1**) Hyphae from a separate mycelium infected with MVX is vegetatively incompatible with the hyphae of non-infected mycelium. (**Scenario 2**) Hyphae of vegetative mycelium harbours MVX but the viruses are partitioned from the fruit body at the point of original primordia formation/switch from vegetative cells to reproductive cells. (**Scenario 3**) Fruit body is infected with MVX whereby the host regulates genes to induce an antiviral response. The findings of this these do not support **Scenario 1**; however, they do not oppose it either. Although MVX can transmit in *in vitro* conspecific interactions, this does not reflect the role of vegetative compatibility in the substrate of crops. **Scenario 2** is rejected by the results of this thesis, as even fruit bodies negative for MVX still showed evidence for the activation of an antiviral response and viruses evidently benefit from the host morphogenic switch to reproductive growth. **Scenario 3** is supported by this thesis, as every infected strain mounted some level of antiviral response, with the less susceptible strains showing regulation of genes with offensive strategies towards viruses or a defence to their pathologies.

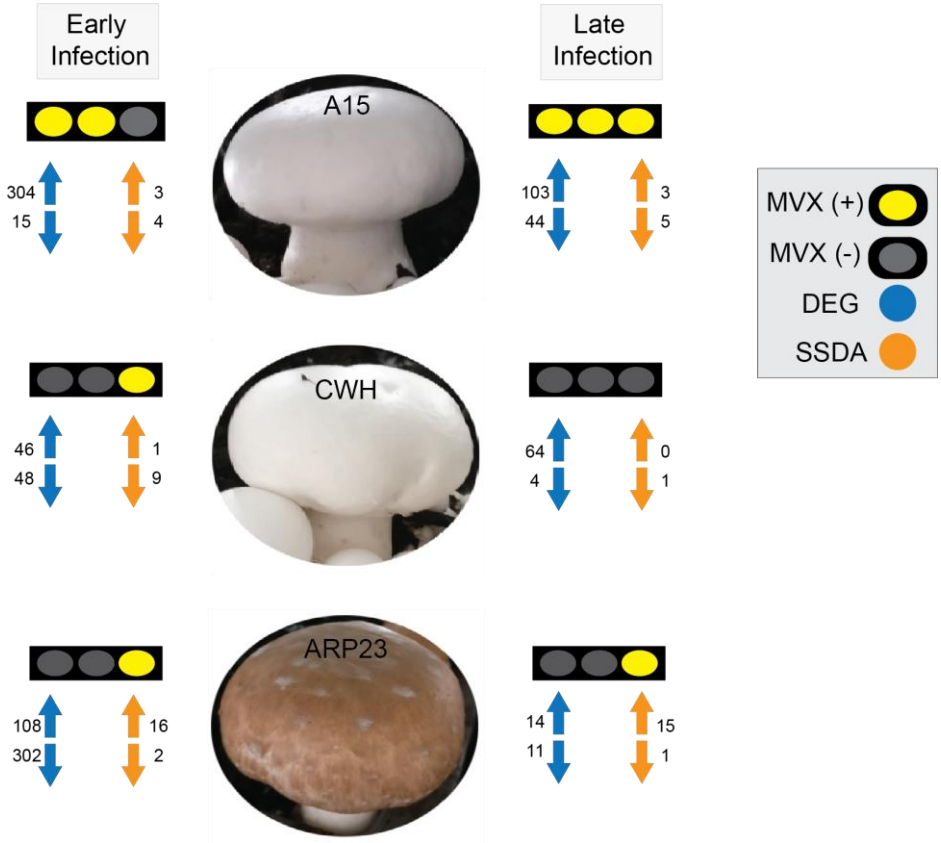

Figure 6.2: Overview of the changes in the transcriptomes (blue) and proteomes (orange) of early and late MVX infection on the fruit bodies of A15. CWH and ARP23. Direction of arrows represents high abundance (up) and low abundance (down) of differentially expressed genes (DEGs) and statistically significant differentially abundant (SSDA) proteins. Information derived from **Chapter 4**.

6.4 Future Perspectives

The results presented here of the molecular response of diverse strains of *A. bisporus* to MVX is now better understood. The antiviral strategies of a strain that is a progeny of a wild parent and a strain originating from a wild population have been demonstrated. It is recommended that breeders of button mushroom continue to try and incorporate wild germ plasms into commercially viable strains to widen the genetic bottleneck currently impacting the industry. The transmission of MVX within fully cultivated compost beds should be a focus of future studies examining putative resistant strains of *A. bisporus. In vitro* assays do not fully represent the capacity of different levels of vegetative incompatibility *in vivo*, as a representative method of inhibition of virus transmission in growing houses.

It is recommended that closer examination be taken in the infection model of MVX in commercial crops. The work presented here has examined the response of fruit bodies and the proteomes of MVX infected compost, this molecular response is not yet understood between the fine transition of viruses from vegetative mycelium, to primordia formation and into mature fruit bodies. As transcription factor and host gene expression has been shown to correlate to the activities of MVX infection, acute focus of the primordia should elucidate the narrow frame of time where MVX proliferates into fruit bodies, causing cellular stresses to the tissue and possible mechanical damage.

The new methodology of FISH can be applied for novel interaction studies of fungus-virus and even virus-virus platforms in *A. bisporus* and MVX. Future work could apply the newly developed FISH to map the transfer of MVX from healthy and infected interacting hyphae. FISH could also provide a new method for detection of viruses in commercial settings. This method also has the potential to be adapted to real-time imaging of virus.

6.5 Concluding remarks

The first molecular characterisation on a genome-wide and proteomic scale study has been described for the globally button mushroom (*A. bisporus*) in response to infection by the commercially damaging MVX disease. This work has shed new light

on the transmission and host response biology of this basidiomycete-mycovirus system that will add to the growing field of mycovirology. Additional contributions to the field of *A. bisporus* research are vast, with the addition of a newly sequenced wild strain genome, characterisation of the proteomic response of interacting hyphae and a new method to fluorescently tag and visualise mycoviruses with the mycelium of their host. The findings lend credence to the complexity of *A. bisporus* strains upon exposure to this disease and provides new understanding for the challenges facing the mushroom industry in the face of MVX.

Literature Cited

Adie, B., Choi, I., Soares, A., Holcroft, S., Eastwood, D.C., Mead, A., Grogan, H., Kerrigan, R.W., Challen, M., Mills, P.R., 2004. MVX disease and double-stranded RNA elements in Agaricus bisporus. Mushroom Sci. 16 Proc. 16th Int. Congr. Sci. Cultiv. Edible Fungi.

Bégueret, J., Turcq, B., Clavé, C., 1994. Vegetative incompatibility in filamentous fungi: het genes begin to talk. Trends Genet. 10, 441–446.

Burton, K., Green, J., Baker, A., Eastwood, D. a N., Grogan, H., 2011. Mushroom Virus X – the Identification of Brown Cap Mushroom Virus and a New Highly Sensitive Diagnostic Test for Phase Iii Compost. Proc. 7th Int. Conf. Mushroom Biol. Mushroom Prod. 466–473.

Deakin, G., Dobbs, E., Bennett, J.M., Jones, I.M., Grogan, H.M., Burton, K.S., 2017. Multiple viral infections in Agaricus bisporus - Characterisation of 18 unique RNA viruses and 8 ORFans identified by deep sequencing. Sci. Rep. 7, 2469.

Eastwood, D., Green, J., Grogan, H., Burton, K., 2015. Viral Agents Causing Brown Cap Mushroom Disease of Agaricus bisporus. Appl. Environ. Microbiol. 81, 7125–7134.

Fleming-Archibald, C., Ruggiero, A., Grogan, H.M., 2015. Brown mushroom symptom expression following infection of an Agaricus bisporus crop with MVX associated dsRNAs. Fungal Biol. 119, 1237–1245.

Foulongne-Oriol, M., Rodier, A., Rousseau, T., Largeteau, M., Savoie, J.-M., 2011. Quantitative genetics to dissect the fungal–fungal interaction between Lecanicillium verticillium and the white button mushroom Agaricus bisporus. Fungal Biol. 115, 421–431.

Ghabrial, S.A., 1998. Origin, adaptation and evolutionary pathways of fungal viruses. Virus Genes.

Ghabrial, S.A., Castón, J.R., Jiang, D., Nibert, M.L., Suzuki, N., 2015. 50-plus years of fungal viruses. Virology 479–480, 356–368. https://doi.org/10.1016/j.virol.2015.02.034

Ghabrial, S.A., Suzuki, N., 2009. Viruses of Plant Pathogenic Fungi. Annu. Rev. Phytopathol. 47, 353–384.

Glass, N.L., Jacobson, D.J., Shiu, P.K.T., 2000. The Genetics of Hyphal Fusion and Vegetative Incompatibility in Filamentous Ascomycete Fungi. Annu. Rev. Genet. 34, 165–186.

Grogan, H.M., Adie, B.A.T., Gaze, R.H., Challen, M.P., Mills, P.R., 2003. Double-stranded RNA elements associated with the MVX disease of Agaricus bisporus. Mycol. Res. 107, 147–154.

Grogan, H.M., Tomprefa, N., J., M., Holcroft, S., Gaze, R., 2004a. Transmission of Mushroom Virus X Disease in crops. Mushroom Sci. XVI - Sci. Cultiv. Edible Med. Fungi (eds Romaine, C. P., Keil, C. B., Rinker, D. J. Royse, D. J.) 489–498.

Grogan, H.M., Tomprefa, N., J., M., Holcroft, S., Gaze, R., 2004b. Transmission of Mushroom Virus X Disease in crops. Mushroom Sci. 16, 489–498.

Kauserud, H., Sætre, G.-P., Schmidt, O., Decock, C., Schumacher, T., 2006. Genetics of self/nonself recognition in Serpula lacrymans. Fungal Genet. Biol. 43, 503–510. https://doi.org/10.1016/j.fgb.2006.02.004

Lee, K.-M., Cho, W.K., Yu, J., Son, M., Choi, H., Min, K., Lee, Y.-W., Kim, K.-H., 2014. A comparison of transcriptional patterns and mycological phenotypes following infection of Fusarium graminearum by four mycoviruses. PLoS One 9, e100989.

Morin, E., Kohler, A., Baker, A.R., Foulongne-Oriol, M., Lombard, V., Nagye, L.G., Ohm, R. a., Patyshakuliyeva, A., Brun, A., Aerts, A.L., Bailey, A.M., Billette, C., Coutinho, P.M., Deakin, G., Doddapaneni, H., Floudas, D., Grimwood, J., Hilden, K., Kues, U., LaButti, K.M., Lapidus, A., Lindquist, E.A., Lucas, S.M., Murat, C., Riley, R.W., Salamov, A. a., Schmutz, J., Subramanian, V., Wosten, H. a. B., Xu, J., Eastwood, D.C., Foster, G.D., Sonnenberg, A.S.M., Cullen, D., de Vries, R.P., Lundell, T., Hibbett, D.S., Henrissat, B., Burton, K.S., Kerrigan, R.W., Challen, M.P., Grigoriev, I. V., Martin, F., 2012. Genome sequence of the button mushroom Agaricus bisporus reveals mechanisms governing adaptation to a humic-rich ecological niche. Proc. Natl. Acad. Sci. 109, 17501–17506.

O'Gorman, A., Barry-Ryan, C., Frias, J.M., 2012. Evaluation and identification of markers of damage in mushrooms (Agaricus bisporus) postharvest using a GC/MS metabolic profiling approach. Metabolomics 8, 120–132.

Paoletti, M., 2016. Vegetative incompatibility in fungi: From recognition to cell death, whatever does the trick. Fungal Biol. Rev. 30, 152–162.

Romaine, C.P., Schlagnhaufer, B., Goodin, M.M., 1994. Vesicle-associated double-stranded ribonucleic acid genetic elements in Agaricus bisporus. Curr. Genet. 25, 128–134.

Saupe, S.J., 2000. Molecular Genetics of Heterokaryon Incompatibility in Filamentous Ascomycetes. Microbiol. Mol. Biol. Rev. 64, 489–502.

Scrimale, T., Didone, L., de Mesy Bentley, K.L., Krysan, D.J., 2009. The Unfolded Protein Response Is Induced by the Cell Wall Integrity Mitogen-activated Protein Kinase Signaling Cascade and Is Required for Cell Wall Integrity in Saccharomyces cerevisiae. Mol. Biol. Cell 20, 164–175.

Thapa, V., Roossinck, M.J., 2019. Determinants of Coinfection in the Mycoviruses. Front. Cell. Infect. Microbiol. 9, 169.

van der Nest, M.A., Steenkamp, E.T., Slippers, B., Mongae, A., van Zyl, K., Stenlid, J., Wingfield, M.J., Wingfield, B.D., 2011. Gene expression associated with vegetative incompatibility in Amylostereum areolatum. Fungal Genet. Biol. 48, 1034–1043.

Wang, L., Luo, H., Hu, W., Yang, Y., Hong, N., Wang, G., Wang, A., Wang, L., 2018. De novo transcriptomic assembly and mRNA expression patterns of Botryosphaeria dothidea infection with mycoviruses chrysovirus 1 (BdCV1) and partitivirus 1 (BdPV1). Virol. J. 15, 126.

Weijn, A., Bastiaan-Net, S., Wichers, H.J., Mes, J.J., 2013. Melanin biosynthesis pathway in Agaricus bisporus mushrooms. Fungal Genet. Biol. 55, 42–53.

Zhong, Z., Li, N., Liu, L., He, B., Igarashi, Y., Luo, F., 2018. Label-free differentially proteomic analysis of interspecific interaction between white-rot fungi highlights oxidative stress response and high metabolic activity. Fungal Biol. 122, 774–784.

Supplementary Information

All supplementary information can be found on the accompanying CD with this thesis.

Chapter 2

Table S1: Shows the genomes, taxonomy and download links for the 32 genomes used in the phylogenomic and CAZy studies.

Table S2: Shows the presence of lignocellulolytic genes in the 32 fungal genomes.

Figure S1: Macrosynteny between A. bisporus H97 chromosomes and all A. bisporus ARP23 scaffolds.

Chapter 3

Table S1: All secreted and extracellular SSDA proteins.

Table S2: SSDA proteins for whole proteomes from each sample.

Table S3: Cazys from DBCann.

Table S4: Comparisons of SSDA proteins between all co-cultures .

Chapter 4:

Figure S1: Statistics for the functional annotations of DEG of A15, CWH and ARRP23 Ctrl versus MS and MC treatments.

Figure S2: Comparisons of shared and unique proteins from the proteomes of SCC, OWC, CWH, A15 and ARP23 strains under Ctrl, MS and MC treatments.

Figure S3: Comparisons of the most abundant biological processes in MVX-infected SCC, OWC, CWH, A15 and ARP23 strains.

Figure S4: Comparisons of the proteomes of A15 fruit bodies and vegetative *A. bisoprus* mycelium in compost under Ctrl, MS and MC treatments.

Table S1: Yield data recorded in Kg/plot for each treatment in five *A. bisporus* strain.

Table S2: Full list of DEGs in the fruit bodies of strains A15, CWH and ARP23 with MS and MC treatments. Columns labelled with B2GO are outputs from Blast2GO, where functional annotation is based on BLASTp analyses.

Table S3: Lists of Gene Ontologies of genes with significantly differential expression (UR and DR) in MS and MC transcriptomes compared to control in A15. BP: Biological process. MF: Molecular function. CC: Cellular component.

Table S4: Lists of Gene Ontologies of genes with significantly different expression (UR and DR) in MS and MC transcriptomes compared to control in CWH. BP: Biological process. MF: Molecular function. CC: Cellular component.

Table S5: Lists of Gene Ontologies of genes with significantly different expression (UR and DR) in MS and MC transcriptomes compared to control in ARP23. BP: Biological process. MF: Molecular function. CC: Cellular component.

Table S6: Table of SSDA proteins in MS and MC treatments compared to control of strain SCC.

Table S7: Table of SSDA proteins in MS and MC treatments compared to control of strain OWC.

Table S8: Table of proteins uniquely detected in control, MS and MC fruit bodies in strains A15, CWH and ARP23.

Table S9: List of SSDA proteins of vegetative mycelium of A15 in compost at MS and MC compared to control. Additional columns for proteins with signal peptides appended to last column.

Chapter 5

Figure S1: RNase treatment following hybridisation.

Figure S2: Test for non-specific binding of FISH probe to nuclei in hyphae.

Figure S3: FISH of MVX-1153 with a FITC-labelled AbV6 probe.